REPORT NO. FRA/ORD-80/20

DESIGN, FABRICATION AND EVALUATION OF PROTOTYPE WAYSIDE BRAKE INSPECTION SENSORS

David B. Spaulding
Kendrick W. Lentz, Jr.
Gilbert G. Fryklund
John R. Gillespie

NOVATEK, INC.
79 Terrace Hall Avenue
Burlington MA 01803

JUNE 1980

FINAL REPORT

DOCUMENT IS AVAILABLE TO THE PUBLIC THROUGH THE NATIONAL TECHNICAL INFORMATION SERVICE, SPRINGFIELD, VIRGINIA 22161

Prepared for

U.S. DEPARTMENT OF TRANSPORTATION
FEDERAL RAILROAD ADMINISTRATION
Office of Research and Development
Washington DC 20590

NOTICE

This document is disseminated under the sponsorship of the Department of Transportation in the interest of information exchange. The United States Government assumes no liability for its contents or use thereof.

NOTICE

The United States Government does not endorse products or manufacturers. Trade or manufacturers' names appear herein solely because they are considered essential to the object of this report.

Technical Report Documentation Page

1. Report No.	2. Government Accession No.	3. Recipient's Catalog No.
FRA/ORD-80/20		

4. Title and Subtitle	5. Report Date
DESIGN, FABRICATION AND EVALUATION OF PROTOTYPE WAYSIDE BRAKE INSPECTION SENSORS	June 1980
	6. Performing Organization Code
7. Author(s) D.B. Spaulding, K.W. Lentz, Jr. G.G. Fryklund, J.R. Gillespie	8. Performing Organization Report No. DOT-TSC-FRA-80-8
9. Performing Organization Name and Address NOVATEK, INC.* 79 Terrace Hall Avenue Burlington MA 01803	10. Work Unit No. (TRAIS) RR031/R0312 11. Contract or Grant No. DOT-TSC-1323
12. Sponsoring Agency Name and Address U.S. Department of Transportation Federal Railroad Administration Office of Research and Development Washington DC 20590	13. Type of Report and Period Covered Final Report December 1977- August 1978 14. Sponsoring Agency Code

15. Supplementary Notes
*Under Contract to: U.S. Department of Transportation
Research and Special Programs Administration
Transportation Systems Center
Cambridge MA 02142

16. Abstract

Prototype Wayside instrumentation has been designed, developed, and tested that proves the feasibility of measuring braking system effectiveness on moving rail cars. The instrumentation system includes a specially designed short section of instrumented rail and two infrared detectors. The rail section deflects elastically under each passing wheel load, and two orthogonally placed transducers discriminate between rail reaction to braking and to weight. A pair of infrared detectors viewing the rims on both wheels of each axle provide thermal data useful in determining the side to side ratio of total axle braking effort. Together these sensors can generate data to evaluate the braking performance of each wheel.

Field tests to evaluate the system were conducted on a commercial rail line and at the U. S. Department of Transportation's Transportation Test Center at Pueblo CO. Test results showed that the sensors were able to indicate normal and abnormal braking conditions.

Also included in the report are a railcar brake system fault and malfunction analysis, structural analysis of the instrumented rail, design analysis of the infrared sensor, detail specifications of the rail and infrared sensors, and recommendations for further system development and testing.

17. Key Words	18. Distribution Statement
Brake malfunction detection, Infrared detection, Rail car braking measurement, Reaction measurement, Wayside instrumentation, Weight measurement	DOCUMENT IS AVAILABLE TO THE PUBLIC THROUGH THE NATIONAL TECHNICAL INFORMATION SERVICE, SPRINGFIELD, VIRGINIA 22161

19. Security Classif. (of this report)	20. Security Classif. (of this page)	21. No. of Pages	22. Price
Unclassified	Unclassified		

Form DOT F 1700.7 (8-72) Reproduction of completed page authorized

PREFACE

The work described in this report was performed by Novatek, Inc., for the Transportation Systems Center, Cambridge, Massachusetts under Contract Number DOT-TSC-1323. This project is part of the Track/Equipment Inspection Program sponsored by the Federal Railroad Administration.

The authors are grateful to the TSC Technical Monitor, Kevin W. Yearwood, for his overall assistance in the project. A great deal of thanks are also due to the staff of the Transportation Test Center for their assistance and cooperation in conducting field tests.

The authors would also like to acknowledge the contributions in the area of railroad engineering of Thomas K. Dyer, Inc., Consulting Engineers (subcontractors on this project).

Appreciation is extended also to the Air Brake Association, Chicago, for permission to reprint some of their brake system data; and the Boston and Maine Corporation for permission to test the IR sensor on their property.

METRIC CONVERSION FACTORS

Approximate Conversions to Metric Measures

Symbol	When You Know	Multiply by	To Find	Symbol
		LENGTH		
in	inches	2.5	centimeters	cm
ft	feet	30	centimeters	cm
yd	yards	0.9	meters	m
mi	miles	1.6	kilometers	km
		AREA		
in^2	square inches	6.5	square centimeters	cm^2
ft^2	square feet	0.09	square meters	m^2
yd^2	square yards	0.8	square meters	m^2
mi^2	square miles	2.6	square kilometers	km^2
	acres	0.4	hectares	ha
		MASS (weight)		
oz	ounces	28	grams	g
lb	pounds	0.45	kilograms	kg
	short tons (2000 lb)	0.9	tonnes	t
		VOLUME		
tsp	teaspoons	5	milliliters	ml
Tbsp	tablespoons	15	milliliters	ml
fl oz	fluid ounces	30	milliliters	ml
c	cups	0.24	liters	l
pt	pints	0.47	liters	l
qt	quarts	0.95	liters	l
gal	gallons	3.8	liters	l
ft^3	cubic feet	0.03	cubic meters	m^3
yd^3	cubic yards	0.76	cubic meters	m^3
		TEMPERATURE (exact)		
°F	Fahrenheit temperature	5/9 (after subtracting 32)	Celsius temperature	°C

Approximate Conversions from Metric Measures

Symbol	When You Know	Multiply by	To Find	Symbol
		LENGTH		
mm	millimeters	0.04	inches	in
cm	centimeters	0.4	inches	in
m	meters	3.3	feet	ft
m	meters	1.1	yards	yd
km	kilometers	0.6	miles	mi
		AREA		
cm^2	square centimeters	0.16	square inches	in^2
m^2	square meters	1.2	square yards	yd^2
km^2	square kilometers	0.4	square miles	mi^2
ha	hectares (10,000 m^2)	2.5	acres	
		MASS (weight)		
g	grams	0.035	ounces	oz
kg	kilograms	2.2	pounds	lb
t	tonnes (1000 kg)	1.1	short tons	
		VOLUME		
ml	milliliters	0.03	fluid ounces	fl oz
l	liters	2.1	pints	pt
l	liters	1.06	quarts	qt
l	liters	0.26	gallons	gal
m^3	cubic meters	35	cubic feet	ft^3
m^3	cubic meters	1.3	cubic yards	yd^3
		TEMPERATURE (exact)		
°C	Celsius temperature	9/5 (then add 32)	Fahrenheit temperature	°F

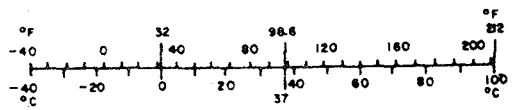

TABLE OF CONTENTS

TABLE OF CONTENTS (CONT'D)

TABLE OF CONTENTS (CONT'D)

LIST OF ILLUSTRATIONS

LIST OF ILLUSTRATIONS (CONT'D)

LIST OF TABLES

1. INTRODUCTION

1.1 Scope of Project

The Transportation Systems Center (TSC) of the U.S. Department of Transportation (DOT) initiated a project in 1976 to develop concepts for a wayside brake inspection system capable of evaluating railcar braking performance in a dynamic mode. The system would be designed to complement existing static, visual and manual inspection techniques and to increase both the speed and quality of inspection. An effective brake inspection system, if widely deployed, should result in a significant decrease in railway accidents due to brake failures.

The brake inspection system was envisioned as being installed at the receiving end of classification yards. Inspection and diagnostic evaluation would be achieved as the consist rolled over, past or through the wayside brake inspection system. In terms of the level of inspection and diagnosis, it would be desirable to differentiate between normal and abnormal braking performance:

1. For both wheels on the same axle.

2. For each wheel relative to the remainder of the wheels on that car.

3. Between cars of a consist.

From a practical point of view, utilization of the brake inspection system should have minimum impact on normal yard operations. In addition, the system should be accurate, reliable, maintainable and cost effective.

A two phase project was undertaken to study the feasibility of one particular brake inspection concept. The concept developed and evaluated consisted of the following components:

1. Reaction Rail: A specially designed 18 inch section of rail used to indicate horizontal (braking) and vertical (weight) reaction forces would be inserted into one rail at the inspection site. This device would produce signals proportional to the absolute braking force (horizontal reaction) and weight (vertical reaction) as the wheel of a consist passed over the sensor.

2. Infrared Detectors: Two infrared sensors would be used to indicate the temperatures of the right and left wheels of a single axle passing over the reaction rail. The wheel temperatures (postulated to be proportional to braking effort) would be used along with the horizontal reaction force measurement to calculate actual right and left wheel braking performance.

3. Car Counter: A photoelectric sensor for counting cars would be used to identify the start and finish of each passing car, and its output used to calculate consist velocity.

4. Support Electronics and Hardware: Electronics would include a power source, signal conditioning device, and data recorder. Hardware would be required to position and support the sensors, and to protect them from adverse environmental conditions.

The decision to study this particular concept further instead of other alternatives was made with due consideration of the stated objectives of cost-effectiveness, reliability and maintainability. The use of two reaction rail sensors to measure right and left wheel reaction forces simultaneously was considered but was rejected for reasons of cost and reliability due to funding limitations.

Phase I of the project to develop and demonstrate feasibility of the wayside brake inspection concept described above included the following objectives:

1. Analyze general railcar and braking characteristics to determine measurement requirements and predicted performance of the proposed inspection system.

2. Prepare and execute a plan of laboratory testing to verify analytical findings.

3. Perform an analysis of brake system malfunctions potentially detectable by the proposed inspection system.

4. Prepare hardware design specifications for fabricating a prototype wayside brake inspection system.

Phase II of the project had as objectives:

1. Fabricate, deliver, and install the prototype system at the Transportation Test Center.

2. Plan and execute a field test program to evaluate the prototype brake inspection system.

3. Analyze and evaluate the field test results.

Section 2 of this report describes the analysis, design, fabrication and laboratory calibration of the components of the prototype brake inspection system. Section 3 describes the field tests performed at the Transportation Test Center on December 7, 1977. Section 3 also presents the test results and uses that data to evaluate overall prototype brake inspection system performance.

The project undertaken was considered to be one primarily of hardware design, fabrication and testing. Analysis was performed only to the depth required to assure hardware functionability and reliability. The hardware developed during the project was shown to indicate both wheel weight and wheel braking reaction forces in a consistent, repeatable manner. In retrospect, the verification field test program was not extensive enough to provide understanding of all the effects of the many variables which contribute to rail/wheel force interactions. While it was highly successful in proving the viability of the basic inspection concept, it is felt that there is a great deal more diagnostic capability inherent in the hardware as it is currently designed. A more detailed description of the conclusions drawn from these tests is presented in Section 4. Recommendations for further testing required to conclusively establish other possible diagnostic relationships are presented in Section 5.

1.2 Background - Railcar Brake Inspection

Air braking systems on railway cars have traditionally been inspected by trainmen walking the length of a consist while visually and/or manually checking the performance, adjustment and condition of the braking components. The inspection consists of determining whether or not the brake system is "Operative" according to the following FRA and AAR criteria: (1)(2)

(1) Numbers in parentheses designate references at the end of report

1. Brake applies when service pressure reduction is made.

2. Brake cylinder piston travel is within specified limits.

3. Brake shoes exceed a minimum specified thickness. (3/8" for composition shoes; 1/2" for cast iron shoes).

4. Brake rigging has free, non-binding motion.

5. Brake remains applied until pipe pressure is restored. (Maximum leak rate is 5 psi/min.)

Brake system operation is inspected in a static condition, with the train at the initial terminal (3). The system is charged and an initial 15 psi reduction made. All brakes must be operative.

"A further brake pipe reduction to full service is then made, and the entire train is inspected to determine that:

1. All angle cocks are properly positioned.

2. Brakes are applied on each car.

3. Piston travel is correct.

4. Brake rigging does not bind or foul.

5. All parts of the brake equipment are properly secured.

Following this thorough inspection.....a roll-by inspection is made to determine that all brakes have released..." (3)

1.3 Background - Weighing in Motion

The reaction rail described above (Section 1.1) is capable of measuring vertical wheel loads as well as horizontal (braking) loads. Wheel weight must be used to determine the Net Braking Ratio (NBR), which is a measure of the tendency of the braked wheel to "lock-up". Weight is thus a necessary measurement requirement of the wayside brake inspection system.

The capability to "weigh" passing railcars on a wheel-by-wheel basis suggests the use of the reaction rail as a weigh-in-motion scale. The reaction rail as designed offers a low cost alternative to the more complex weigh-in-motion truck scales in use today, if the compromise in accuracy can be accepted. The wayside brake inspection system might then serve the dual purpose of brake inspection and car weight surveillance.

Mechanical lever scales were used to weigh railcars as early as 1850 (4). In-motion weighing using mechanical scales and recording systems were in existence by 1890. The first electro-mechanical in-motion scale (using strain gages as sensing elements) was introduced in 1953 and the first fully electronic system used in 1959. (4)

In-motion scales accommodate one complete truck at a time, thus side-to-side variations (roll) are not a significant source of error. According to Fisher (4), the main source of in-motion weighing error is car coupler interaction. The true weight of a car truck is influenced through bound couplers by the adjacent truck. Coupler adjusting track sections are thus used prior to weighing to relieve these influences.

2. PROTOTYPE WAYSIDE BRAKE INSPECTION SYSTEM ANALYSIS AND DESIGN

2.1 Analysis of Measurement Requirements

The measurement objective of the proposed brake inspection system is to sense, accurately and repeatably, physical quantities indicative of the integrity of the railcar braking system. The proposed reaction rail will measure braking effort by sensing horizontal forces exerted on the rail by a passing wheel. In addition, the reaction rail will sense vertical forces thus providing a measurement of wheel weight. The proposed infrared sensors provide an indirect measurement of wheel braking forces by sensing wheel temperature.

It is the objective of this section to analyze the measurement requirements of both the reaction rail and the infrared sensors such that expected air brake system malfunctions may be detected. Section 2.1.1 considers the basic force interactions between wheels and rails. Included are analyses of the horizontal, vertical and lateral forces exerted by the wheel on the rail as well as considerations of car dynamics and impact loads due to track misalignments. Section 2.1.2 describes the assumptions made regarding wheel temperature rise and temperature distribution resulting from brake application. Section 2.1.3 discusses the probable manifestation of various brake system malfunctions as wheel/rail reactions and as wheel temperature increases.

2.1.1. Wheel Rail Interactions

The instrumented rail sub-system of the wayside brake inspection system was designed to sense vertical and longitudinal forces exerted on the rail by each passing wheel. The instrumented rail was originally constructed to measure these two basic forces, but was later modified to sense applied side loads. The side load measurement capability was added for initial prototype tests so that a complete (3-dimensional) wheel/rail force interaction picture could be established. The following subsections utilize a simplified wheel/rail model to predict the static and dynamic forces to be sensed by the reaction rail.

Actual field tests resulted in some observations not anticipated by the following analyses. These results are discussed and analyzed in Section 3.5 of this report.

2.1.1.1 Rail Reaction to Braking Forces

The development of air brake retarding force at the wheel/rail interface is shown schematically in Figure 1. Notation used in the analysis that follows is also defined in the Figure.

The ratio of actual braking force (F_B) to wheel weight (W) is often referred to as net braking ratio (NBR) and is usually expressed as a percent. Since brake force depends on cylinder pressure, the pressure at which the NBR is taken must be stated. Traditionally, this has been 50 psi for freight cars and locomotives and 60 psi for passenger cars. NBR is a measure of the relative tendency of a wheel to "lock up" and begin to slip. High NBR indicates high braking capacity relative to weight, thus a tendency to slip.

Figures 2 and 3 show typical values of brake shoe friction (f_b) and adhesion (f_a) as functions of speed.

Figure 4a shows a free-body diagram of a single wheel, rolling without slip, and proceeding at a constant linear velocity to the right. The wheel is assumed to have a rolling resistance due to wheel-rail deformation, axle bearing friction, etc. This apparent retarding force, even though the air brakes are not applied, is shown as a frictional torque, M_o, about the wheel (axle) center. A summation of the moments about the wheel center (M_c) then yields:

$$\sum M_c = M_o + F_R\,(r) - F_A\,(r) \qquad (1)$$

where "r" is the wheel radius. Since the wheel is moving with constant linear as well as angular velocity, there is no acceleration, thus the sum of moments about wheel center (Equation 1) must equal zero. Solution of Equation 1 for this case shows the relation between F_A and F_R:

$$F_A = F_R + \frac{M_o}{r} \qquad (2)$$

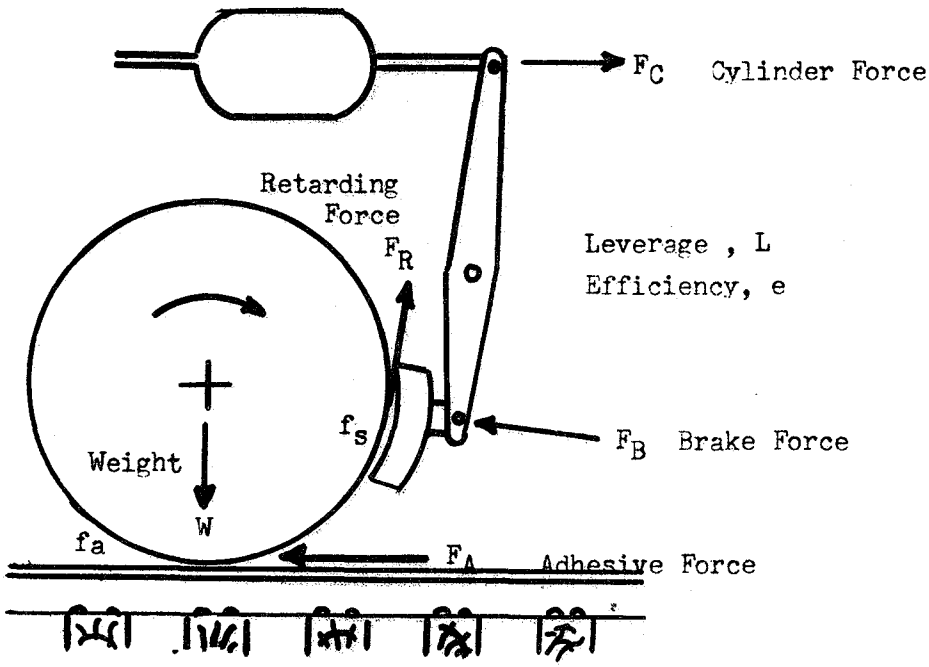

Reprinted from Engineering and Design of Railway Brake Systems by permission of the Air Brake Association. Year of first publication, 1975.

Definition of Variables:

F_C = Force exerted by the brake cylinder push rod on the input to the brake shoe leverage system. This force is the product of cylinder pressure and effective cylinder area.

L = Leverage ratio of the brake shoe lever system.

F_B = Brake force. Force pressing the brake shoes against the wheel tread. Unless otherwise designated, refers to the "actual" applied force.

FIGURE 1

STANDARD NOMENCLATURE FOR BRAKING FORCES

$F_{B_{th}}$ = Theoretical brake force as calculated from the cylinder force (F_C) and leverage (L). $F_{B_{th}} = F_C \times L$.

e = Rigging or linkage "efficiency". $e = F_B / F_{B_{th}}$

f_s = Coefficient or friction between brake shoe and wheel tread. Varies with: brake shoe material and condition, wheel tread material and condition, wheel speed, temperature, applied shoe force (F_B), and length of time brakes have been applied.

F_R = Retarding force. Tangential force exerted on wheel tending to retard wheel rotation. $F_R = F_B \times f_s$

W = Wheel weight.

F_A = Wheel/rail adhesive force exerted by the rail on the wheel, in such a way as to retard car motion. For a wheel passing at constant velocity, $F_A = F_R$.

f_a = Coefficient of friction between the wheel and rail. Varies with cleanliness, type, and condition of materials used. Expressed as a percentage, is commonly called "adhesion".

F_{Amax} = Maximum available adhesive force = $W \times f_a$. If the brake retarding force (F_R) exceeds this value, the wheel begins to slip on the rail.

FIGURE 1 (cont.)

STANDARD NOMENCLATURE FOR BRAKING FORCES

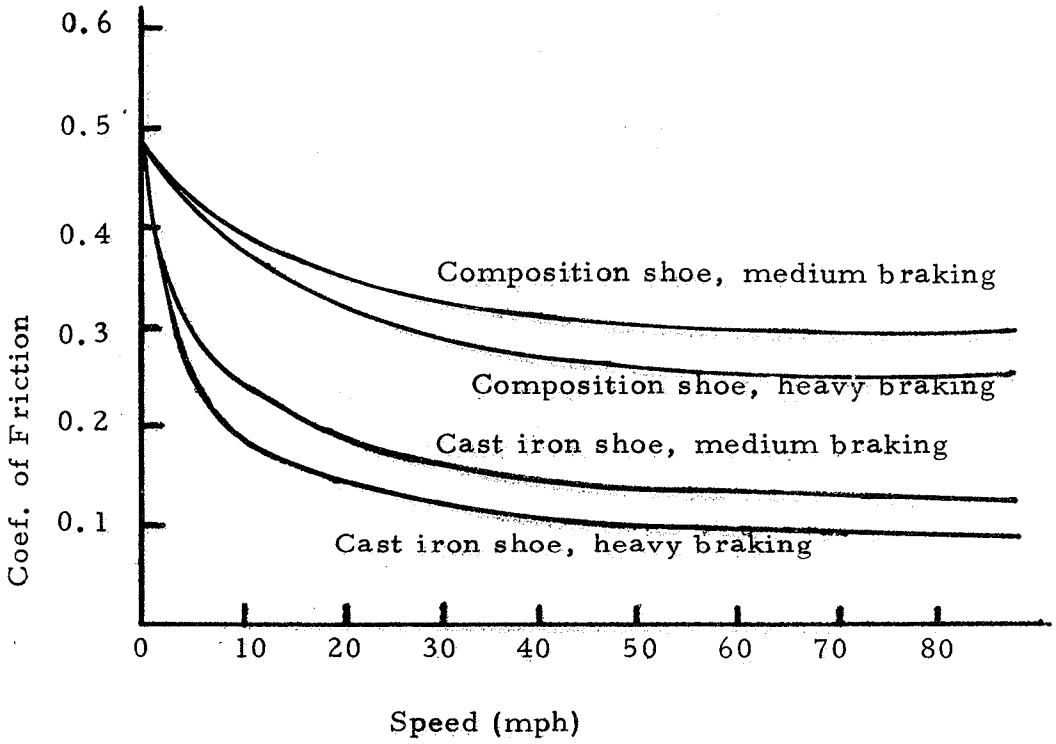

Reprinted from Engineering and Design of Railway Brake Systems by permission of the Air Brake Association. Year of first publication, 1975.

FIGURE 2

TYPICAL BRAKE SHOE FRICTION VS. SPEED

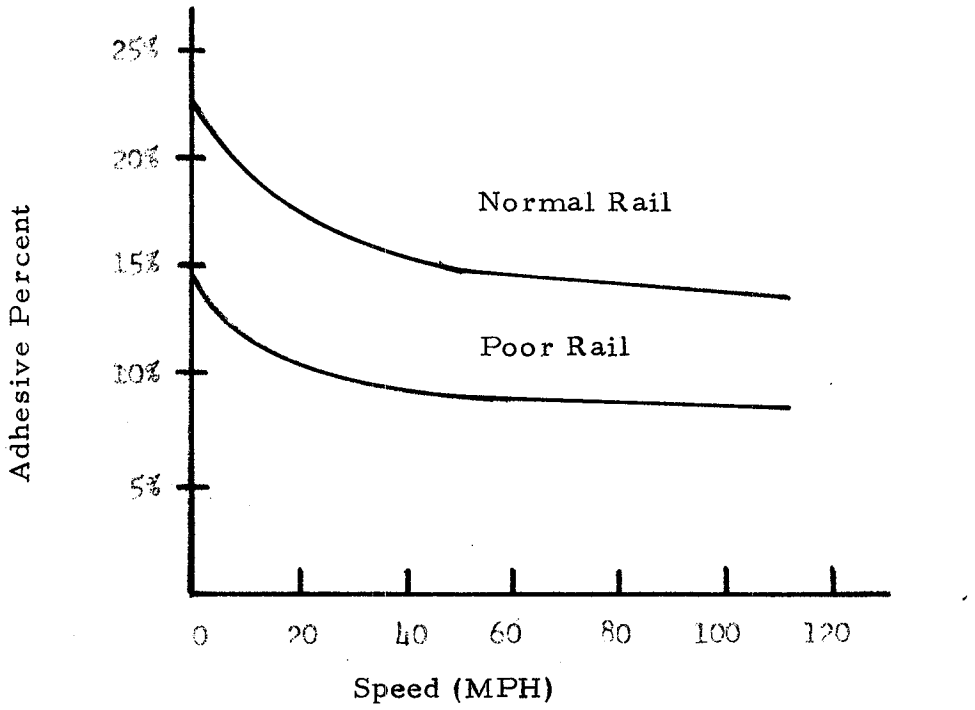

Reprinted from Engineering and Design of Railway Brake Systems by permission of the Air Brake Association. Year of first publication, 1975.

FIGURE 3

TYPICAL WHEEL/RAIL ADHESION AS A FUNCTION OF SPEED

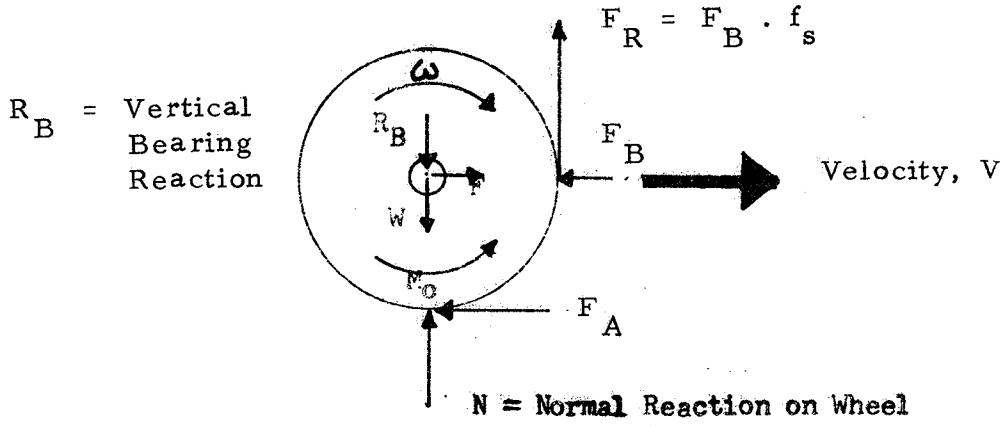

FIGURE 4a

FREE-BODY DIAGRAM OF WHEEL

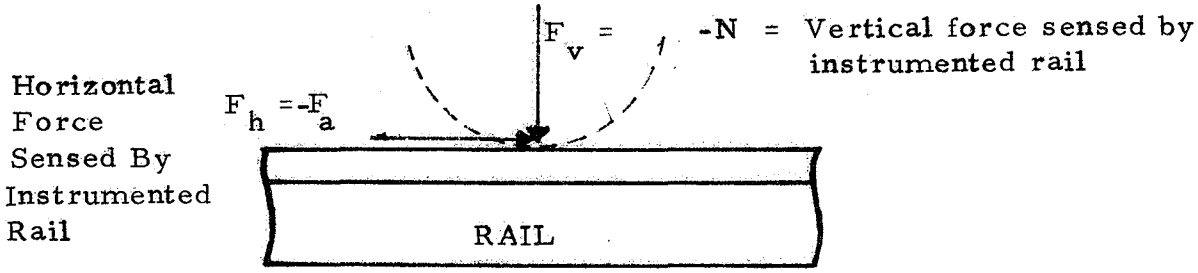

FIGURE 4b

FREE-BODY DIAGRAM OF RAIL

This linear relation holds until the adhesive force increases to the point where

$$F_A = F_R + \frac{M_o}{r} = W \times f_a \qquad (3)$$

at which point the wheel begins to slide on the rail. If sliding does occur, there will be a significant drop in the force, F_A, exerted on the wheel by the rail and conversely in the reaction force exerted on the rail by the wheel. Sliding adhesion is typically 10 - 20% of rolling adhesion (5).

The instrumented rail is designed to measure vertical and horizontal forces exerted by the wheel on the rail. Figure 4b is a free-body diagram of the rail segment indicating the measured forces, (F_v vertical) and F_h (horizontal). The horizontal force F_h, will be equal in magnitude but opposite in sign to the adhesive force, F_a. Figure 5 shows the expected reaction rail indication (F_h) of braking force as a function of actual brake force, F_B. Note that the measured reaction drops by approximately 80% when F_B becomes large enough to "lock" the wheel. A typical value for maximum adhesive force for a 100,000 lb. car, (12,500 lbs./wheel) passing at 60 mph on normal track would be 1875 lbs. If the wheel were to then slide, the measured force would drop to roughly 20% of the peak value, or 375 lbs.

2.1.1.2 Rail Reaction to Vertical Forces

A summation of forces acting on the wheel (Figure 4a) in the vertical direction will yield an expression for the normal force, N, the negative of which is the measured vertical force reaction. Since equilibrium is achieved in the vertical direction, this sum is equal to zero, and F_v can be written as:

$$F_v = -N = -W + F_R - R_B, \qquad (4)$$

where R_B is the vertical reaction force transmitted to the wheel axle through its bearing. If the truck under consideration is exactly symmetrical in terms of both braking performance and dynamic performance (springs, damping, mass) then the retarding force F_R which is transmitted back into the truck structure through the brake leverage system will be re-transmitted to the wheel in terms of a bearing reaction. In this case, $F_R = R_B$, so Equation 4 reduces to $F_v = -W$, which is the desired wheel

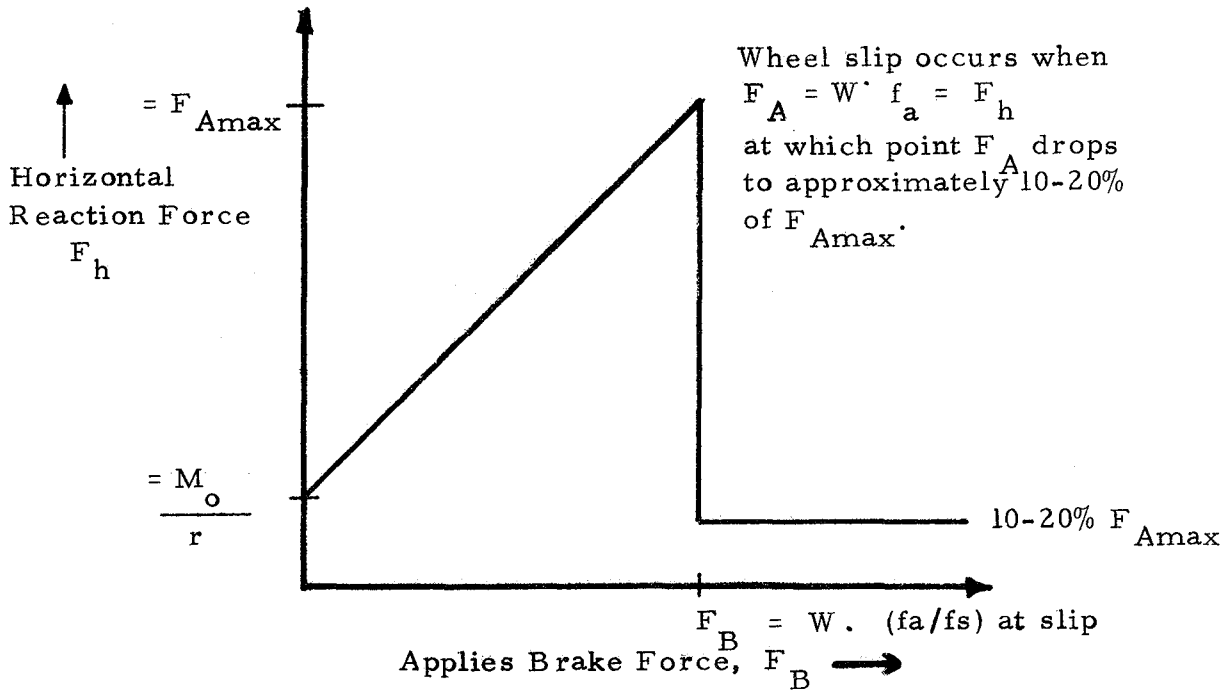

FIGURE 5

IDEALIZED HORIZONTAL REACTION F_h

AS A FUNCTION OF APPLIED BRAKE FORCE, F_B

weighing capability. See Section 2.1.1.4 for consideration of car dynamics on the indicated wheel weight.

2.1.1.3 Rail Reaction to Lateral Forces

Lateral forces exerted on a straight section of rail by individual wheels originate because:

1. The contact force, F_c, between a tapered wheel and the rail is not generally normal to the rail head top surface, (See Figure 6-a). The reaction rail will sense both the vertical component, F_V, and the lateral component, F_L in response to the contact force, F_c.

2. The vertical component of the wheel/rail contact force, F_V, is generally not coincident with the centerline of the rail cross-section. (See Figure 6-b). The eccentric vertical force, offset by a distance e from the rail section centerline produces a torsional moment about the longitudinal rail axis (6). This moment, M_T, produces an indicated lateral force, F_L:

$$F_L = \frac{M_T}{y} = \frac{F_V e}{y} \qquad (5)$$

Where: e = Distance vertical force is offset laterally from rail centerline.

y = Distance from rail cross-section torsional axis (centroid) to point of force application.

F_V = Vertical component of wheel-rail force.

3. When the wheels of a truck are braked, the truck will tend to rotate about its vertical axis if all four wheels do not brake equally. The moment, M, tending to turn the truck will be equal to the sum of the individual wheel moments as shown in Figure 6-c.

$$M = \left(F_{A1}^{+} \quad F_{A2}^{-} \quad F_{A3}^{-} \quad F_{A4}\right) \cdot a \qquad (6)$$

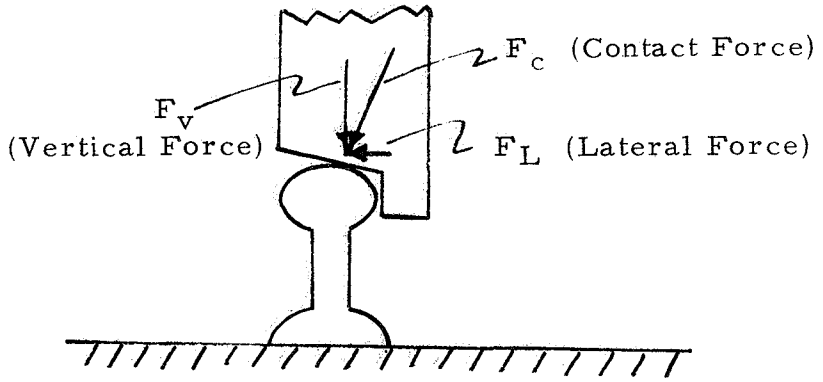

FIGURE 6a - Lateral Force Due to Static Load

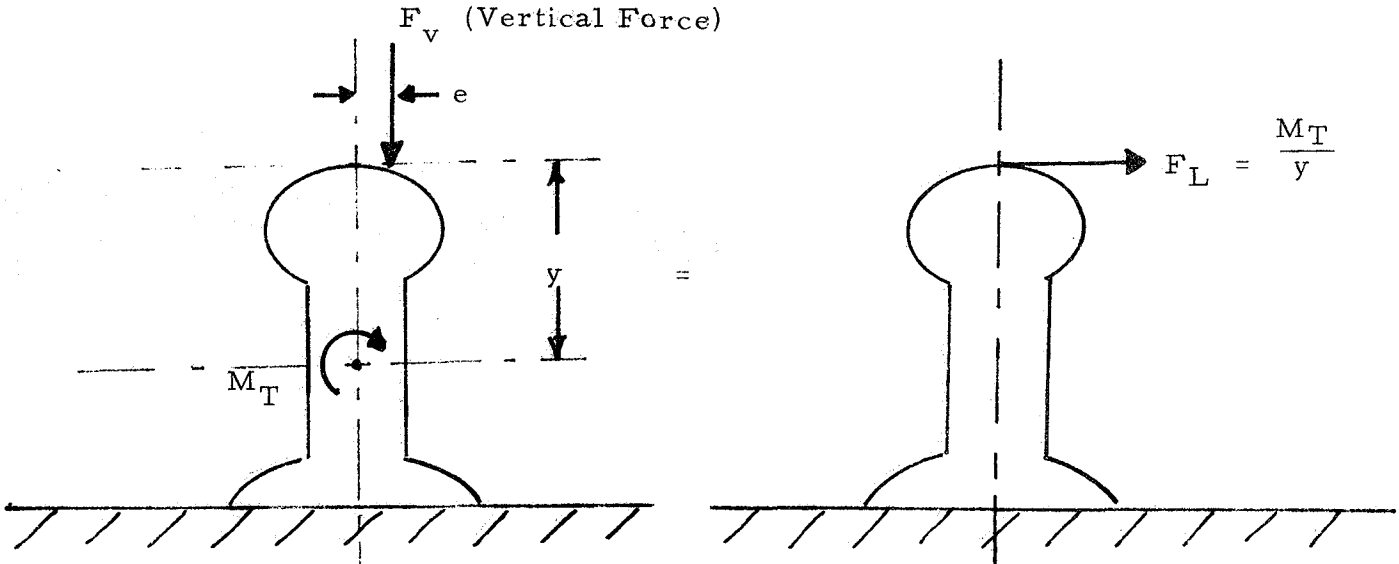

FIGURE 6b - Equivalent Lateral Force Due to Off-Center Vertical Force

FIGURE 6

SOURCES OF LATERAL LOADING
OF RAIL BY PASSING WHEEL

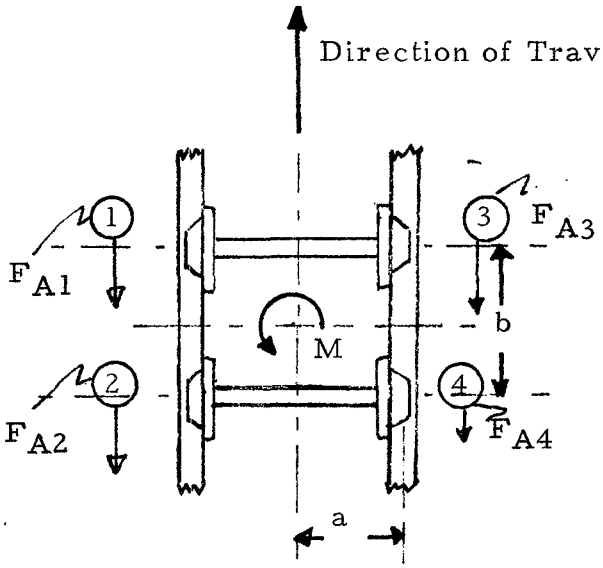

Where:

$$F_{A1} + F_{A2} > F_{A3} + F_{A4}$$

F_{A1}, F_{A2}, F_{A3}, F_{A4} are the braking forces due to each wheel of the truck under consideration.

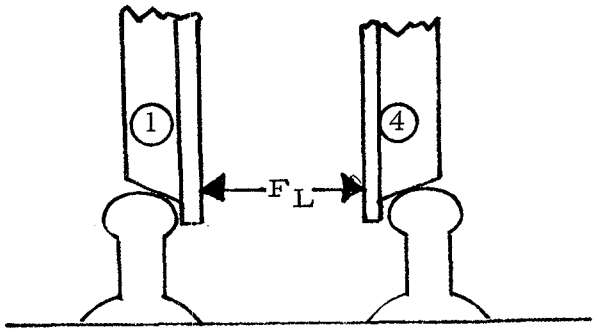

FIGURE 6c
Lateral Rail Forces Due to the Moment
Resulting from Uneven Braking of a Truck

This moment will not vanish if $F_{A1} + F_{A2}$ is not equal to $F_{A3} + F_{A4}$. The indicated lateral force component, F_L, measured by the reaction rail will be:

$$F_L = \frac{M}{b} = \left(F_{A1} + F_{A2} - F_{A3} - F_{A4}\right) \frac{a}{b} \qquad (7)$$

Where: a = Lateral distance from truck center to wheel contact point = 30 inches.

b = Longitudinal distance from truck center to axle centerline = 35 inches.

For the case shown in Figure 6-c, the total adhesive force of wheels 1 and 2 exceed that of wheels 3 and 4, thus a net counterclockwise moment is generated. This results in lateral forces exerted outward by wheels 1 and 4.

The reaction rail was originally designed and built to be sensitive to only vertical and longitudinal wheel loads, and to be insensitive to lateral forces. The lateral forces described in cases 1 and 2 above are not due to braking thus are not of diagnostic value. It was recognized that the lateral force effects of cases 1 and 2 would be included in the total lateral force measurement. Subsequent data reduction could, however, eliminate case 1 and 2 effects which are theoretically predictable from wheel geometry and wheel weight. Conveniently, wheel weight is a separately measured output of the instrumented rail (reaction rail) segment.

Because of the potential diagnostic benefit to be realized by measuring the lateral forces described in case 3, a semi-conductor strain gage bridge was added to the reaction rail. This bridge was designed to allow the reaction rail to sense lateral wheel forces.

The full potential of lateral force measurements in diagnosing brake system malfunctions was not determined during field tests because:

1. The strain gage bridge and readout functioned erratically, finally breaking down.

2. Only one reaction rail was used in field tests. As stated previously, the decision to use only one instrumented reaction rail was made for reasons of cost. However, as Section 3 of this report points out, two reaction rails are necessary to fully characterize braking forces.

2.1.1.4 Effects of Car and Rail Dynamics

The reaction rail is capable of sensing vertical and longitudinal forces exerted by a passing wheel. In its present configuration, however, the reaction rail is used in only one rail of the track. It is therefore important to consider how railcar dynamics might introduce errors into indicated horizontal and vertical force outputs.

1. Car roll: As a passing car rolls about its longitudinal axis, its vertical reaction on the rail shifts from left to right. The frequency of roll depends on specific car parameters. The magnitude of weight shift depends on car speed.

If only one reaction rail is used, there is no way of knowing the passing axle right-to-left weight distribution, thus the axle weight. If two reaction rails are used, this problem is averted since the sum of right and left indicated wheel weights will equal the true axle weight.

2. Car pitch: Although a passing car is constrained somewhat by its leading and trailing couplers, it may pitch about the car center, thereby resulting in a periodic front-to-rear truck weight shift. Pitching motions may be excited, for example, when both wheels of an axle hit a pair of misaligned reaction rails, or other simultaneous rail joints.

Since the reaction rail is intended for use with partially braked cars on consists, a brake-induced pitching motion is also possible. If the forward truck braking is greater than on the rear truck, a pitching moment is generated which will cause a higher indicated weight on the front wheels.

These effects will not introduce significant errors into truck measurements but will result in errors in total car weight measurement. For example, if the car is undergoing periodic pitching, the passing front truck may weigh "heavy", but the passing rear truck may also weigh "heavy". The single axle reaction rail is not capable of averaging out pitching oscillations.

3. Car Bounce: The effect of car bounce on indicated wheel or axle weight will be very similar to that of car pitch. The vertical load will be alternately increased and decreased as the car passes by.

As was the case with pitching motion, there will be no fixed relation between bounce frequency and wheel weighing. The possibility for error exists here even between axles on the same truck. If the truck reaction force on the rail changes due to bounce before the second axle of a truck passes over the rail, then the sum of the two indicated axle weights will not equal the true truck weight.

4. Track Deformation Wave: As a loaded axle approaches and departs the reaction rail, the entire rail (including reaction rail) defects under the axle weight. Because the proposed reaction rail is a deflection sensitive device, it will sense approaching and leaving axles in addition to weighing them when they are directly on the rail.

This effect was clearly seen in field test data, but was subtracted from weight measurements to give true indicated weight.

Actual field tests using a single reaction rail were performed realizing that errors due to car dynamics were possible. Tests were planned for consist speeds ranging from 10 mph to 60 mph (16-96 kph) in order to identify a test speed for which dynamic errors were minimized.

2.1.1.5 Rail Reaction to Impact Loads

Reaction rail response to impact loads must be considered for two reasons. First, the reaction rail may be misaligned with the parent rail so as to create either a step-up or step-down joint. Secondly, a flat spot on a passing wheel will create an impact load on the rail.

The railcar-wheel-reaction rail system can be idealized as shown in Figure 7-a. It is assumed that the passing wheel has an undamped compliance of approximately 250,000 lbs/ft. Tse (7) uses this value as a freight car suspension stiffness for mathematical modeling purposes. No damping or friction is assumed for this analysis, so a "worst-case" response can be calculated. The suspension stiffness is represented in Figure 7 by a spring, K_1.

The reaction rail vertical stiffness, K_2, depends on the elastic properties of its rail cap support members and can be calculated by:

$$K_2 = \frac{W}{\Delta y} = \frac{AE}{L} \qquad (8)$$

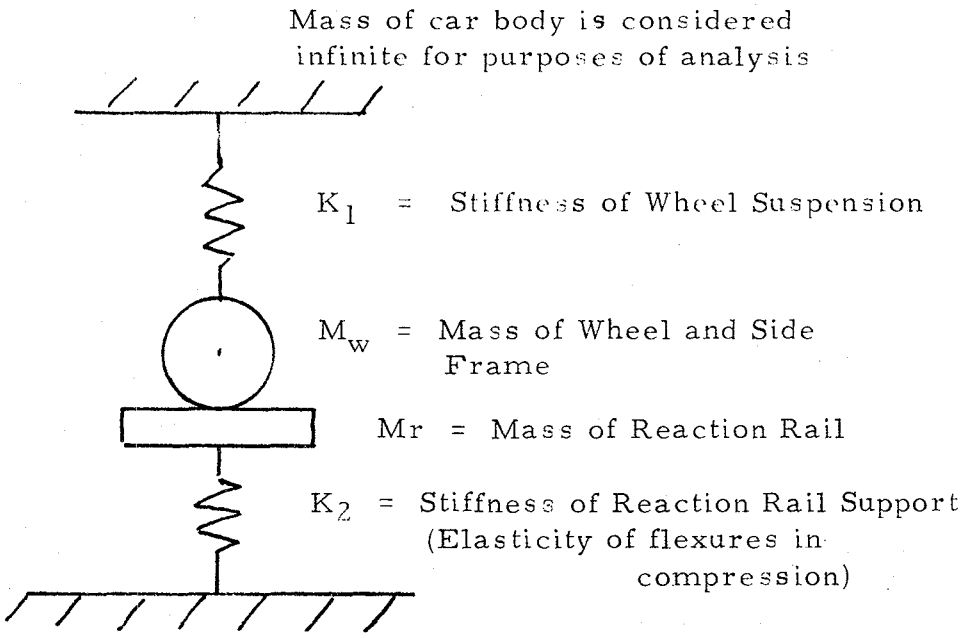

FIGURE 7a - Wheel/Rail Model for Impact Loading

FIGURE 7b - Equivalent Mass-Spring Model

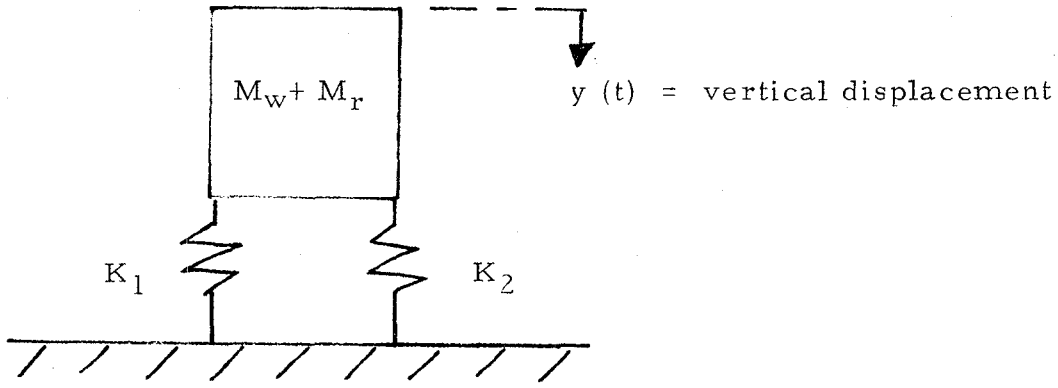

FIGURE 7

IMPACT LOADING OF THE REACTION RAIL

Where: W = Applied load (lbf)

Δy = Rail Vertical Deflection (in)

A = Total cross-sectional area of reaction rail cap support members = 3 in^2

E = Modulus of elasticity of rail supports = 30×10^6 lbs f/in^2

L = Length or rail cap support members = 2.5 inches.

Using the values for A, E, and L for the reaction rail as fabricated, the spring constant for the rail, $K_2 = 36 \times 10^6$ lbs f/in. = 432×10^6 lbs f/ft. Masses involved are:

M_w = 49.5 slugs = total mass of wheel set/side frame divided by 4 to represent equivalent mass of one wheel.

M_r = 0.74 slugs = mass of reaction rail head in 18 in. reaction rail. (136 lb rail weighs 136 lbs per yard, with 35% of its weight distributed in the head)

The unloaded natural frequency of the reaction rail is:

$$f = \frac{1}{2\pi}\sqrt{\frac{K_2}{M_r}} \quad \text{cycles/sec.} \qquad (9)$$

Using above values for K_1, M_r; the natural frequency of vibration in the vertical direction is 3845 cycles per second.

The measurement quantity of concern, however, is the natural frequency of the reaction rail with the railcar on it. If the railcar itself is considered to be virtually stationary in the vertical direction, with only the sprung wheel set free to move, the loaded natural frequency of the reaction rail be:

$$f = \frac{1}{2\pi}\sqrt{\frac{K_1 + K_2}{M_r + M_w}} \quad \text{cycles/sec.} \qquad (10)$$

Using the above values for stiffness and mass, the loaded natural frequency is found to be 467 cycles/sec.

The equivalent "passing frequency" of the wheel passing over the 18 inch (45.7 cm) reaction rail at 60 miles per hour (96Km/Hr.) is 9.3 cycles per second. Even in the loaded condition, the reaction rail natural frequency is 50 times greater than the rate at which wheels pass over the reaction rail.

It is therefore concluded that impact loads applied to the reaction rail will result in rail vibrations, but the frequency of those vibrations will be too high to significantly affect the measurement of vertical load.

2.1.2 Wheel Temperature Response to Braking Inputs

As the brake shoe is applied to the wheel tread, kinetic energy is dissipated as heat through the wheel and shoe. If the consist is maintained at a constant velocity, and if the wheels do not slip with respect to the rail, then heat will be generated at a rate, H (BTU/hr):

$$H = 6.79\ F_r\ V_c \quad \text{(BTU/hr)} \qquad (11)$$

Where: F_r = Horizontal braking reaction force measured at the rail (lb_f)

V_c = Consist velocity (mph)

The heat generated during braking is then dissipated in the following manner:

1. Conduction losses to the atmosphere and to adjacent structures depending on ambient temperature and initial temperatures of adjacent structures.

2. Convection losses to the atmosphere depending on ambient temperature, wheel emissivity, and wheel temperature.

3. Radiation losses to the atmosphere depending on ambient temperature, wheel emissivity, and wheel temperature.

Heat which has not been dissipated in one of the above ways will raise wheel temperature as equilibrium is approached. Wheel temperature alone then, is not an absolute measure of applied braking effort unless a number of initial and boundary conditions are given so that losses can be calculated.

If, however, the actual brake retarding force exerted on one wheel were known (as measured by the instrumented rail segment), and the relative temperatures of the right and left wheels known (as measured by two IR sensors), then it should be possible to deduce the brake retarding force on each wheel. One of the basic objectives of this program was to test this hypothesis. The design of the appropriate wheel temperature sensor required an estimate of the range of temperatures to be expected during a typical brake inspection.

Novak, et. al. (9) reports wheel temperature distribution in wheels braked by both composition and cast iron brake shoes. A consist velocity of 50 miles per hour (80 K_m/Hr.) and applied braking of 45 to 51 horsepower (33.6 - 38.0 Kw) resulted in wheel tread temperatures of 320°F (160°C) after five minutes and 500°F (260°C) after fifteen minutes. These results were obtained using composition brake shoes, and slightly lower temperatures were observed using cast iron brake shoes. The maximum temperatures attained during these tests were found in the brake shoe itself, and in some cases, this temperature exceeded 1000°F (538°C).

It was decided that a reasonable wheel temperature measurement capability would be 100°-1000°F (38°-538°C). A device capable of measuring wheel temperatures in this range should be sufficient, since the proposed brake inspection would be conducted at slightly less than full service braking. In addition, a certain degree of control over maximum wheel temperatures can be exercised by limiting the consist speed and time of brake application allowed during brake inspection.

2.1.3 Brake System Malfunction Analysis

An analysis of brake system component malfunctions which might possibly occur was performed and used to determine whether or not the malfunction could be detected by the prototype inspection system.

Figure 8 identifies the typical brake system components of a standard air brake system. Table I then presents results of the malfunction analysis and the expected measurement system outputs unique to each malfunction.

The analysis of the malfunctions was twofold. First, the results of this analysis might influence the design of the prototype sensor, if design modifications to the proposed system could be made within the time and cost constraints of the original program plan. Second, and more important, the results of the malfunction analysis were to be used as a basis for proposing second generation design improvements to the prototype wayside brake inspection system so that an advanced model would offer maximum diagnostic inspection capabilities.

It should be pointed out that design of the instrumented rail and IR sensors had already begun and were taking place in parallel with the malfunction analysis effort. Determination as to which malfunctions could be sensed with the inspection system under construction required a certain amount of subjective, qualitative judgment unsubstantiated by actual test data.

The determination as to whether or not the prototype system would be capable of sensing and diagnosing various brake component malfunctions is indicated in the "Problem" column of Table I. One, two or three asterisks follow the problem cause and should be interpreted as follows:

* A malfunction that is definitely detectable by brake performance measurements.

** A malfunction that <u>may</u> be detectable by brake performance measurements.

*** A malfunction that probably <u>cannot</u> be detected by brake performance measurements.

2.2 Design of the Instrumented Rail Sub-System

2.2.1 Design Criteria

The instrumented rail segment must be capable of measuring wheel reaction forces (discussed in Section 2.1.1), reasonably accurate and

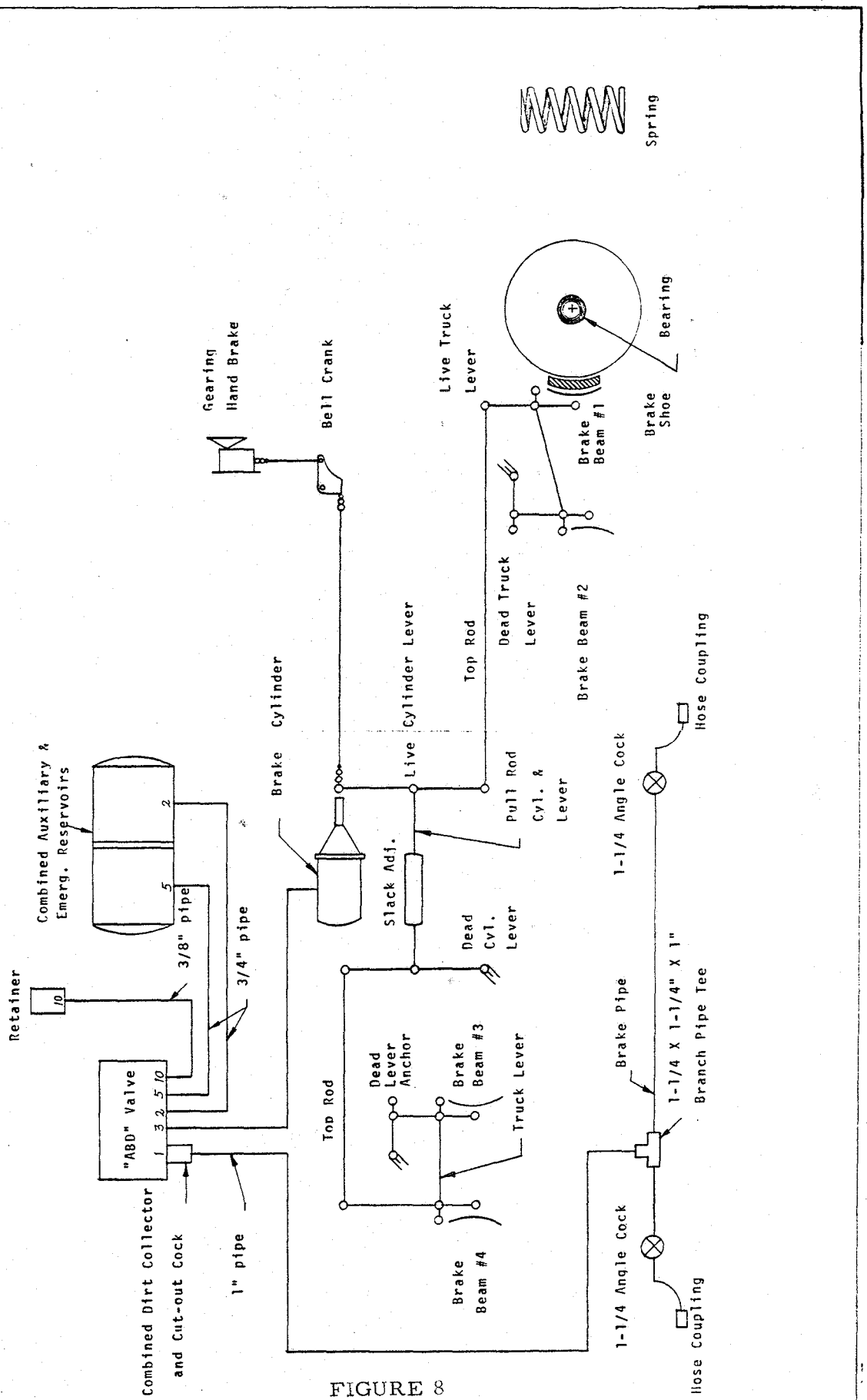

FIGURE 8

PRIMARY BRAKING COMPONENTS

TABLE 1. BRAKE COMPONENT MALFUNCTION ANALYSIS

			OUTPUT INDICATION	
	COMPONENT	PROBLEM	INFRARED	REACTION MEASUREMENT
I. Brake Rigging	Brake Cylinder	Leaking**	Low well balanced temperature rise all wheels	Low reaction force on all axles relative to values on other side of other cars
		Sticking or frozen**	Significant balanced temp. rise above nominal average on other wheels of other cars when brakes aren't applied	Low residual balanced reaction force on all axles of car when brakes are not applied
		Inoperative*	No temp. rise above ambient	No reaction measured
	Slack Adjuster	Improper Adjustment**	Low or no temperature rise. Possibility of unbalanced rise between axles on same car	Low or diminished reaction relative to other axles in consist. Possibility of variations in reaction from axle to asle on same car
		Broken**	Same as above with possibility of no rise above ambient	Same as above with possibility of no reaction on any axles
	Top Rods	Broken*	No temp rise	No reaction
		Bent**	Possibility of abnormal and uneven temp rise above values on other wheels of other cars	Possibility of uneven reaction with individually higher values than measured on other axles of other cars
	Truck Levers Cylinder Levers Dead Levers Aux. Levers	Broken, Bent or Frozen**	Same as above	Same as above
	Brake Beams	Broken or Badly Bent**	Normal, low or no temperature rise on one or both wheels of one axle of one truck. Other brakes may be subnormal	Reaction may be subnormal on one or all axles
II. Pneumatic Components	Control Valve	Cutout closed or valve completely inoperative*	No temperature rise on any wheels of car, other cars in consist operative	No reaction on any axle of car, other cars in consist operative
		Low output**	Low well balanced temperature rise on all wheels	Low reaction force on all axles relative to values on other axles of other cars
		High output**	High well balanced temperature rise on all wheels	High reaction force on all axles relative to values on other axles of other cars
		Sticking or Hysteresis**	Normal or somewhat subnormal temperature rise on all wheels relative to wheels on other cars as brakes are applied. After brake pipe pressure is increased, brakes tend to remain set and measured temp is higher	Normal or somewhat subnormal reaction on all axles relative to axles on other cars as brakes are applied. As brakes are released, measured reaction will be higher

KEY
* Malfunction definitely detectable by brake performance measurements.
** Malfunction may be detectable by brake performance measurements.
*** Malfunction probably not detectable by brake performance measurements

TABLE 1. BRAKE COMPONENT MALFUNCTION ANALYSIS (CONT.)

	COMPONENT	PROBLEM	OUTPUT INDICATION	
			INFRARED	REACTION MEASUREMENT
II. Pneumatic Components (continued)	Brake Pipe and Interconnecting Piping	Leaking**	Small leaks not detectable. Large leaks cause complete loss of brak-in or emergency stop if reservoirs are full	Same as IR
	Hose Couplings	Leaking**	Same as brake pipe	Same as brake pipe
		Open*	Very high wheel temperatures on all wheels	Very high reaction on all axles
	Auxilliary Reservoir	Low or Empty**	Low temperature rise on all wheels of car	Low reaction force on all axles of car
	Emergency Reservoir	Low or Empty**	Low or no temperature rise during emergency stop conditions	Low or no reaction force on all axles during emergency stop conditions
	Dirt Collector	Plugged**	Low or no temp rise on all wheels during normal operation	Low or no reaction on all axles during normal operations
III. Wheels & Shoes	Wheels	Cracked***	Normal output	Normal output
		Worn**	Normal output	Reaction may be below normal or unusually erratic depending on wear characteristics
		Buildup**	Normal output	High frequency irregular modulation in vertical axis
		Shelling**	Normal output	High frequency periodic modulation in vertical axis
		Spalling**	Normal output	High frequency periodic modulation in vertical axis
		Thermal Shelling**	Normal output	High frequency modulation in vertical axis
		Flat Spots**	Normal output	Large amplitude variation in vertical output if flat hits instrumented section
		Previously Overheated ***	Normal output	Normal output
	Shoes	Worn***	Normal output	Normal output
		Missing*	Higher than normal for other wheels on same car if brake head is bearing hard on wheel	Lower reaction
IV. Misc. Running Gear	Axle Journals	Hot Box***	No output	Very small reaction when brakes not applied

KEY

* Malfunction definitely detectable by brake performance measurements.

** Malfunction may be detectable by brake performance measurements.

*** Malfunction probably not detectable by brake performance measurement.

TABLE 1. BRAKE COMPONENT MALFUNCTION ANALYSIS (CONT.)

	COMPONENT	PROBLEM	OUTPUT INDICATION	
			INFRARED	REACTION MEASUREMENT
V. Misc. Running Gear (continued)	Springs	Broken**	No output	Abnormal, vertical transient when wheel encounters test unit
	Hand Brake or Retainer	Not released*	Possibility of a significant temp rise if long run preceeds measurement	A reaction will be seen that is proportional to degree of braking

KEY

* Malfunction definitely detectable by brake performance measurements.

** Malfunction may be detectable by brake performance measurements.

*** Malfunction probably not detectable by brake performance measurement

repeatable, reliable, and fail-safe in that failure of the instrumented segment must not present a safety hazard to passing railcars.

Design criteria for the instrumented rail segment as a measuring element were:

1. Capable of a 40,000 (18,144 kg) vertical wheel load.

2. Capable of measuring a 8,000 lb. (3,624 kg) horizontal brake load reaction.

3. Accurate and repeatable to 5% of full load capacity.

4. Element must have infinite fatigue life under expected loads.

5. Element must be capable of occasional overloads without permanent damage to the measurement ability or structural integrity.

6. Element must be temperature insensitive.

7. Element must be easily repairable and otherwise maintainable.

Design criteria necessary to preserve the structural integrity of the overall track include:

1. The reaction rail segment should exhibit minimum variation in effective rail strength as compared to the existing rail. If variations are unavoidable, then the reaction rail section must be stronger.

2. Failure of the reaction rail segment should not result in catastrophic failure of the rail's primary support function.

3. Critical areas within the reaction rail section must be protected from dirt, moisture and other contaminants.

4. For purposes of prototype testing, the reaction segment should be fabricated into a section of 136 lb. A.R.E.A. rail.

The instrumental rail (reaction rail) as finally designed consisted of a relatively rigid rail cap (136 lb. rail) supported by two relatively elastic flexible members or "flexures". Use of flexures, common in the design of multiple axis dynamometers, provides rigid support in one direction while allowing freedom of motion in other(s). To a first approximation, the flexures do not influence the deflection of the more rigid member (rail cap).

The dimensions of the flexures are such that a 40,000 lb (18,144 kg) vertical load on the center of the unit will theoretically produce a 0.005 in (0.127 mm) vertical deflection and an 8,000 lb (3,629 kg) horizontal load in the longitudinal direction will theoretically produce a 0.005 in (0.127 mm) horizontal deflection. This is accomplished in such a way that the maximum stress under combined loading does not exceed 50,000 psi (3.477×10^9 bar). A detailed analytical treatment of the reaction rail design is presented in Appendix A, "Structural Analysis of Rail Section". The need to have these relatively large deflections and linear behavior, in small volume, required that this part be fabricated as a monolithic, joint-free structure.

In order to attain a theoretically infinite fatigue life for the flexured supports, it was also necessary to use 4340 chrom-moly steel heat treated to 150,000 psi (1.034×10^{10} bar) ultimate tensile strength. In addition, a high polish to the flexure surfaces before and after heat treating was required.

The heat treat vendor provided certification of heat treatment of the section. Both the center of the flexure and the rail cap had a hardness of Rockwell C 37 indicating the uniformity of the section metallurgy.

There is evidence that high-speed train operation can induce loads many times greater than the usual design loads. To avoid any potential problem in this regard, the unit has been provided with "stops" that will limit the travel and thereby, the maximum stress in the flexure sections.

The design has also considered the unlikely possibility that a flexure section might fail completely. Should this happen, the horizontal section will drop 1/16 in. (1.5 mm) (the width of the saw cut) and rest on the base, secured between joint bars horizontally and by two caging pins vertically.

2.2.2 Instrumented Rail Segment Design

Figure 9 shows the reaction rail section designed to fulfill the criteria of Section 2.2.1. Dimensions of critical reaction rail elements are presented in Figure A-1 of Appendix A, "Structural Analysis of Rail Section".

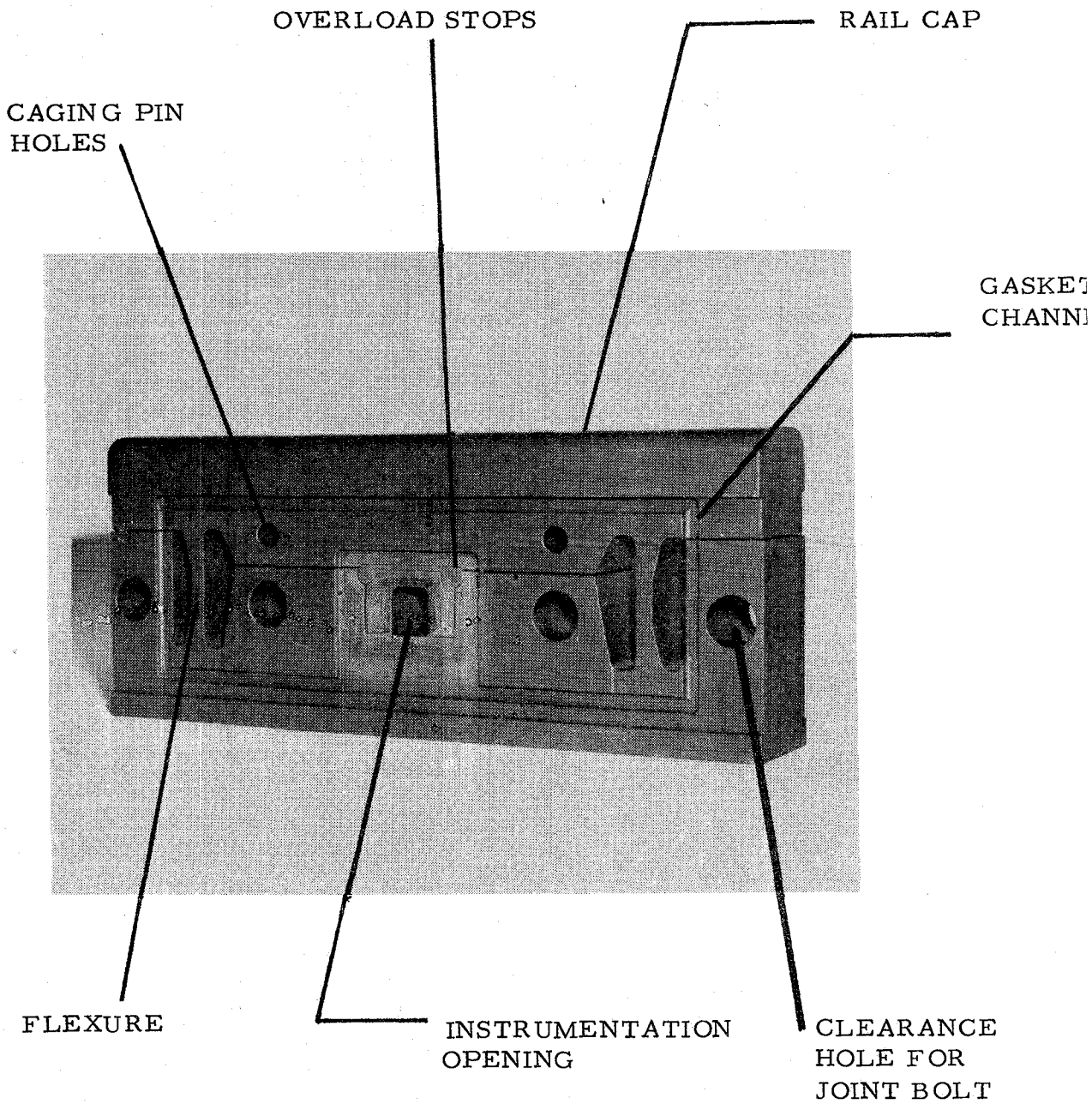

FIGURE 9

REACTION RAIL SECTION SHOWING MAJOR ELEMENTS

Mechanical elements of the instrumented rail section fall into three principal component categories:

1. A rail section which has measurable elastic deflection under applied wheel loads. (See Section 2.2.2.1).

2. A transducer unit that measures vertical and longitudinal deflections of the rail section. (See Section 2.2.2.2).

3. A support structure which connects rail ends and the instrumented section into a structurally sound, integral part of the rail system. (See Section 2.2.2.3).

Although the original design of the instrumented rail did not provide for measurement of transverse deflections due to side loads, it was possible to instrument the flexures with strain gages so that side forces could be measured. A strain gage bridge arrangement designed to cancel strains due to vertical and longitudinal loads was devised and applied to the rail segment after the prototype rail was fabricated.

A complete set of specifications for the instrumented rail section is provided in Appendix G.

2.2.2.1 Reaction Rail Section

The reaction rail section (See Figure 9) is sized to fit in line with a standard 136 lb. rail. It is basically a heavy, horizontal member 18 inches (45.7 cm) long that is secured on a mounting base by means of two vertical flexures. The flexures are flexible beams that provide elastic structural attachment between the relatively rigid top and bottom members.

2.2.2.2 Transducer Bolt

The active measuring elements that sense deflection of the flexure are contained in a bolt-like structure that is easily installed or replaced in the field (See Figure 10). The bolt is held in place by a 1/2-13 nut. It is self-keying for proper orientation and can be installed with a wrench. The power and signal leads are brought outside with a weather tight circular multi-pin connector. The actual measurement transducers are a pair of linear variable differential transformers (LVDT's) mounted

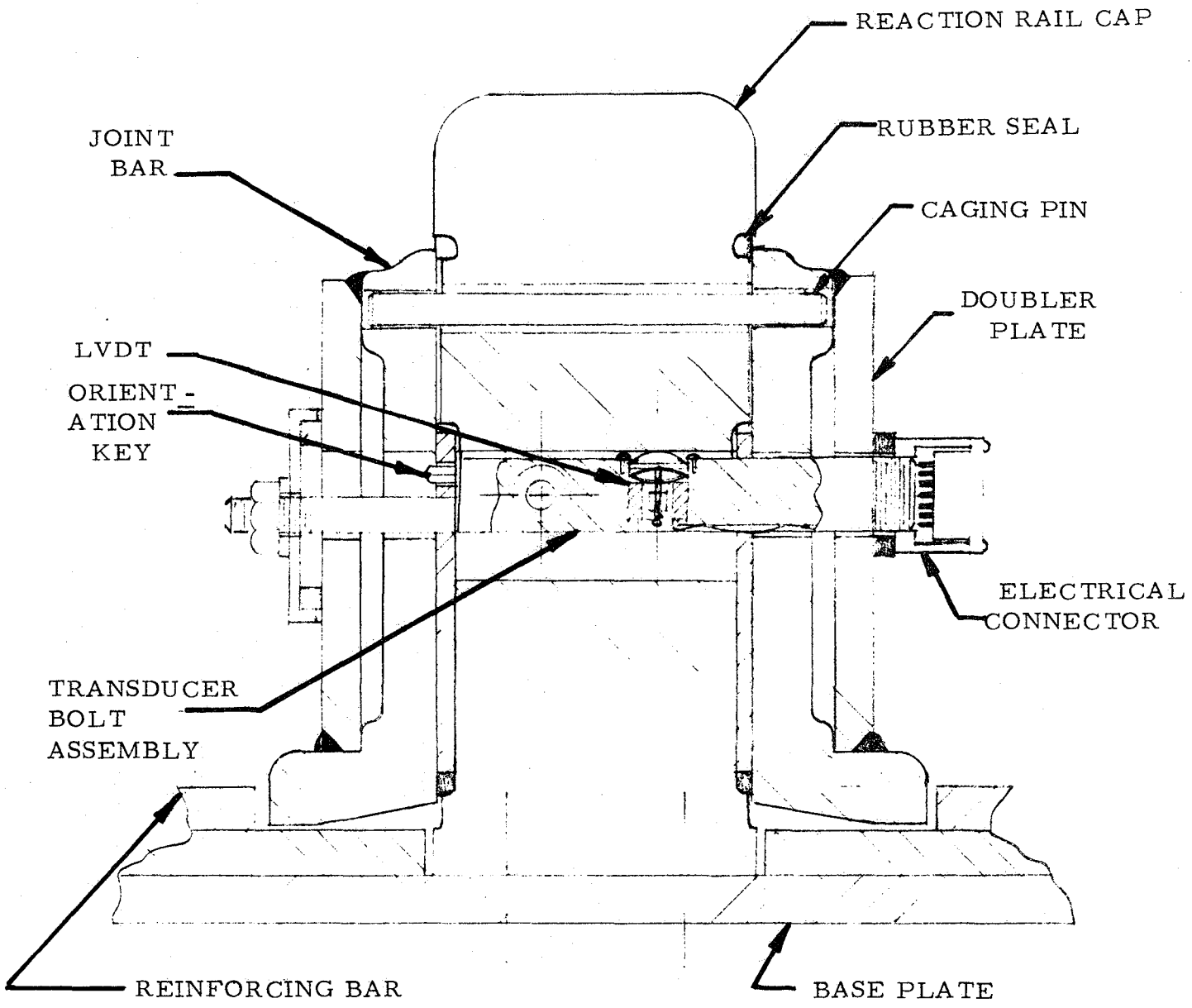

FIGURE 10

SECTION THROUGH TRANSDUCER BOLT

orthogonally to each other so as to read vertical and horizontal deflections independently. LVDT's were chosen for the measurement function because of their sensitivity and linearity and are unaffected by ambient temperatures over the range of -65°F to 300°F (-53°C to 140°C). The LVDT has a linear response to better than 1/2% of full range and it can be set up to reliably resolve down to 10 microinch (254 m).

2.2.2.3 Tie-in Structure

The structure that integrates the reaction rail section into an existing rail system is a mechanical assembly that spans three cross ties and is 54 inches (1.37m) long. It uses joint bars that have sufficient additional length so that the adjoining rails can use the standard hole pattern for a six bolt joint.

Additional strength is provided by doubler plates on the joint bars and 5/8 inch (1.58 cm) thick plates at the base of the rail. These compensate for the flexibility of the reaction rail and the material that is removed from the joint bars to provide clearance around the reaction rail. The resulting joint exceeds a standard joint in both strength and stiffness.

A rubber gasketing provides sealing to keep moisture and dirt from impairing reaction rail operation.

2.3 Design of Infrared Sensor System

2.3.1 General Considerations

The operational profiles of braking consists passing the infrared instrumentation site is assumed to fall within the following range of values:

Consist speed:	5 mps to 62 mps (8-120 km/hr)
Wheel diameter:	24 to 36 inch (61 to 91 cm)
Minimum wheel spacing:	4 feet (1.2 m)

Thermal range of wheels due to braking:	100° to 1000°F (37° to 538°C)
Maximum temperature one inch in from wheel circumference:	750°F (399°C)
Environmental temperature range:	-20°F to 125°F (-29° to 52°C)

From this assumed range of operational parameters, it was possible to derive the required IR sensor characteristics, and subsequently, to select appropriate IR sensor components. This analysis is presented in Appendix B, "Design Analysis of the Infrared Sensor".

First, it was arbitrarily decided that the sensor would focus on a one inch diameter spot, located one inch above the point of tangency at the wheel/rail interface. Such a target location is far enough inboard of the wheel circumference to allow a reasonable IR measurement time, yet is close enough to the braking surface to respond thermally to braking inputs.

As a 24 inch wheel passes at 60 miles per hour, the full one-inch target area located one inch above the rail remains in line of sight for approximately 7 milliseconds. Since the response of the sensor element should be roughly 10 times faster than this, a one millisecond or better response time was selected as a design requirement.

The next step in the design process was to determine the spectral response range for which a detector must be selected. The mid-wavelength of a blackbody at the maximum temperature of 750°F (399°C) is 6.1 microns. The mid-wavelength at the lower temperature limit of 100°F (38°C) is 13.2 microns. The range of wavelengths encompassing ±25% of the infrared energy above and below these values extend the range to 4.1 microns at the high temperature, and 21 microns at the low temperature.

The design criteria for the infrared sensor can be summarized as follows:

1. Spectral response in the range of 4 to 21 microns.

2. Response time of 1 millisecond or better.

3. Target size of 1 inch diameter located 2 to 4 feet (60-120 cm) from the sensor.

4. Target temperature of 100°F to 750°F (38°C-399°C).

5. Ambient temperature of -20°F to 125°F (-29°C to 52°C).

Commercially available infrared sensors meeting the above requirements were sought. Those sensors exhibiting the required spectral response did not possess fast enough response times. Conversely, those instruments with the required response times did not possess adequate spectral response ranges, unless a cooled instrument was used. Handling and use of liquid nitrogen in a wayside environment is impractical so cooled instruments were not considered as alternatives.

It was finally decided that the best compromise of instrument spectral response, response time, and cost would be attained by purchasing and assembling the appropriate components. Components to be selected, purchased and assembled included; detectors, optics, pre-amplifiers, amplifiers and supporting structures.

2.3.2 Detector Design

Infrared instrumentation vendors were contacted and given the measurement requirements described above. Vendor recommendations were evaluated and an indium antimonide photoconductive element was selected based on its maximum response wavelength (5 to 7 microns) and its low time constant (less than 0.1 microsecond). Details on the response characteristics of this detector element are discussed in Appendix B.

A vendor supplied set consisting of indium antimonide detector, lens system and amplifier was assembled into a custom-fabricated housing.

2.3.3 Optics Design

The optics chosen for this system consist of a three-inch Cassagrain lens system made from reflective plastic coupled through an infrared transmission lens of polycrystalline zinc sulfide.

The Cassagrain focusing lens provides a minimum spot size of 1.4 in. (6.25 mm) at an operating distance of 24 in. (61 cm) with a half angle of 3°. Thus, at a distance of 36 in. (91 cm), the spot size is 1.5 in. (3.8 cm).

The Irtran 2 infrared transmitting lens is cut in a planar circular shape of about 3 1/4 in. (8.2 cm) in diameter and .039 in. (1 mm) thick. This lens has maximum attenuation of approximately 10% over the spectrum of 4 to 9 mm. Its primary function is to block out air currents which cause spurious detector outputs and its secondary function is to seal the complete unit, thereby keeping out water, dust and other contaminants.

2.3.4 Circuit Design

A vendor-supplied amplifier could not be made operational with the matching detector element. An amplifier capable of doing the required job was designed and built.

The circuit employed for this detector consists of a discrete current source and five monolithic operational amplifiers interconnected to yield a total gain of 20,000 with a bandwidth extending from 2 Hz to 30 Hz (See Figure 11).

The current source supplies bias current to the IR detector which in turn is AC coupled to a low noise operational amplifier A·1, designed to have a voltage gain of 1,000 over the designed bandwidth. This amplifier is then followed by a current gain stage A·2. Because each of these two chips, A·1 and A·2 operate from a single voltage for increased stability, chip A·3 is employed to provide the necessary bias voltage for both.

The output of chip A·2 is AC coupled to a two-pole filter section, which has a "roll off" frequency of 30 Hz, and on the chip A·4. Amplifier A·4A provides additional gain and ground reference restoration while amplifier A·4B provides output buffering.

Chips A·1, A·2, and A·3 require + 18 VAC for operation while chips A4 and A4B require +18 VAC and -18 VAC, respectively.

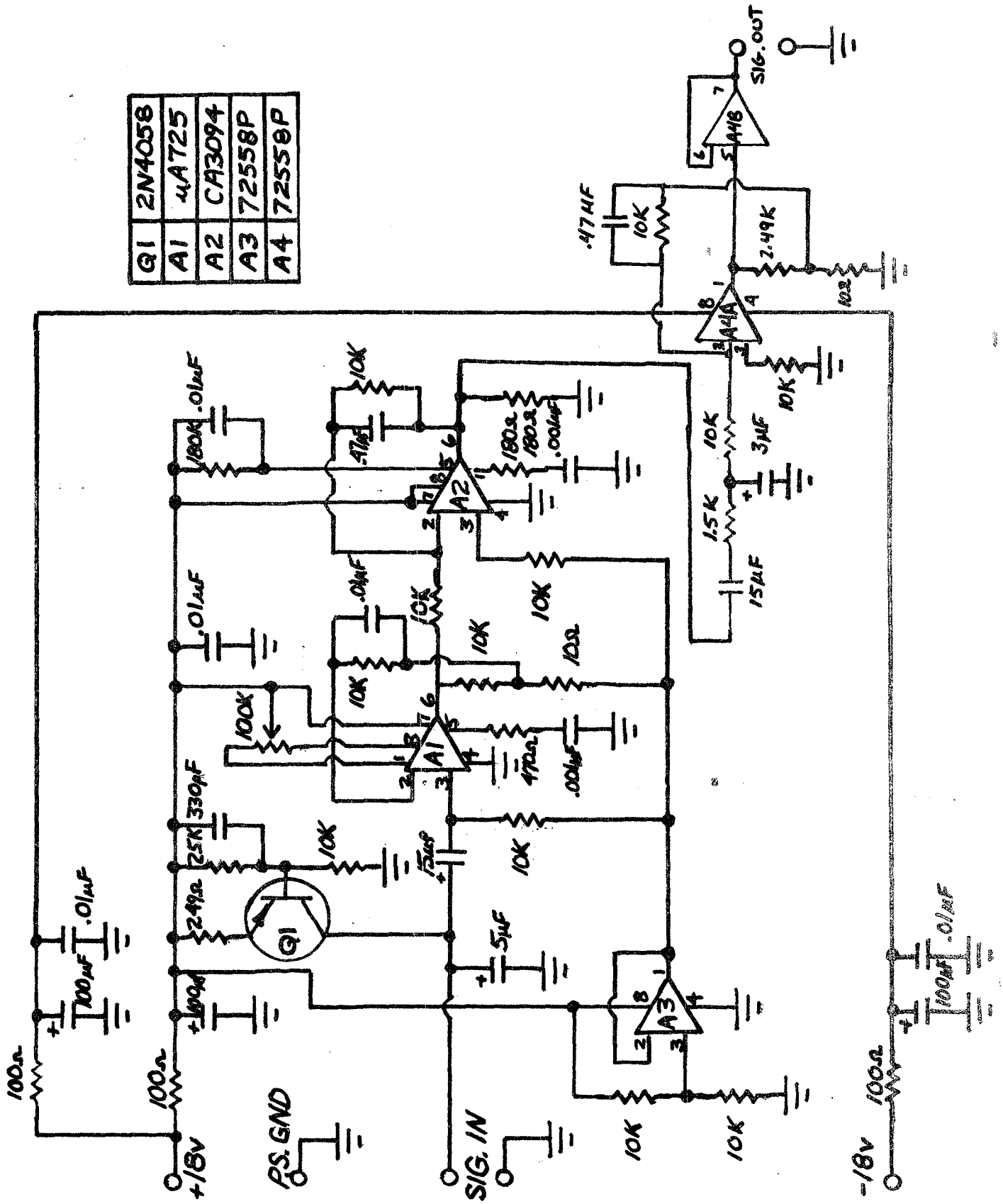

FIGURE 11

INFRA RED DETECTOR
AMPLIFIER CIRCUIT

The amplifier then exhibited the following operational characteristics:

Sensitivity:	0.2 μv
Gain:	20,000
Bandwidth:	2Hz to 30Hz
Dynamic input sensing range:	0.2 uV to 10 mV
Temperature sensing range (above ambient):	30° F to 1,000°F (-1.1 C to 538 C)
Operating temperature:	32° F to 158° F (0° C to 70° C).

2.3.5 Packaging

The packaging of this unit consists of an aluminum tube 3 1/4 in. (8.2 cm) diameter and 15 in. (38.1 cm) long. One end is fitted with a protective bezel for holding the Irtran 2 window, and the other end has a plate housing two connectors. One connector is provided for input power and another for output signals. Internal to this tube is the reflective Cassagrain lens and amplifier board. The detector is mounted at the focal point of the lens and signal wires are brought out through an appropriate strain relief.

This aluminum tube is suspended in a larger tube 5 in. (12.7 cm) diameter of cast steel which acts as an impact shield for the more delicate aluminum assembly. One end of this cast steel tube is fitted with a muffin fan that provides 35 CFM of air for cooling, while the other end is open for viewing (see Figures 12 and 13).

2.4 Laboratory Testing and Calibration

A laboratory test plan was prepared (see Appendix C) prior to fabrication of the prototype reaction rail and IR sensor. The test objectives were laboratory verification of the performance of the two main sub-systems - the instrumented rail section and the IR sensor. This section describes the results of those tests.

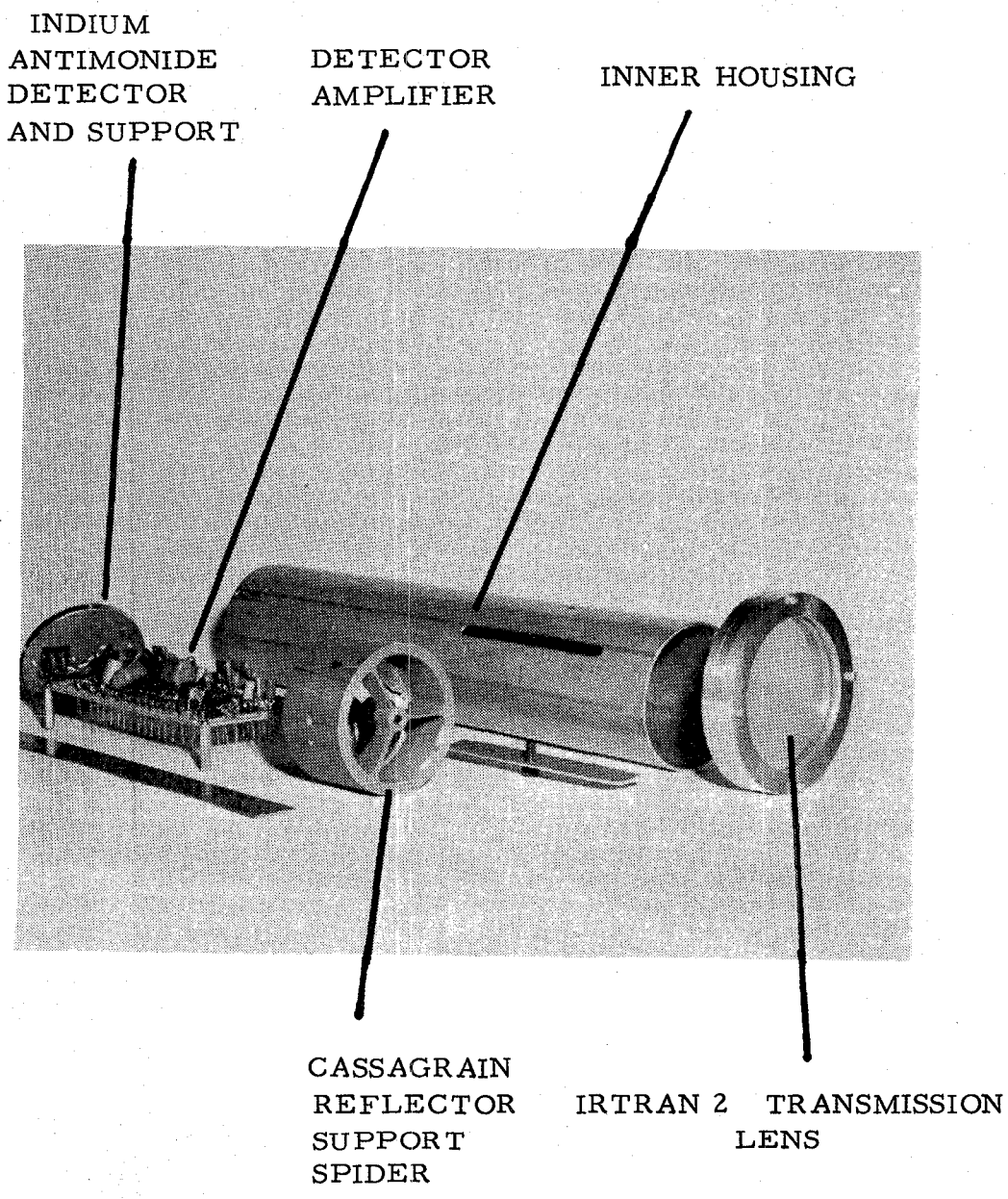

FIGURE 12

INFRARED DETECTOR UNIT DISASSEMBLED

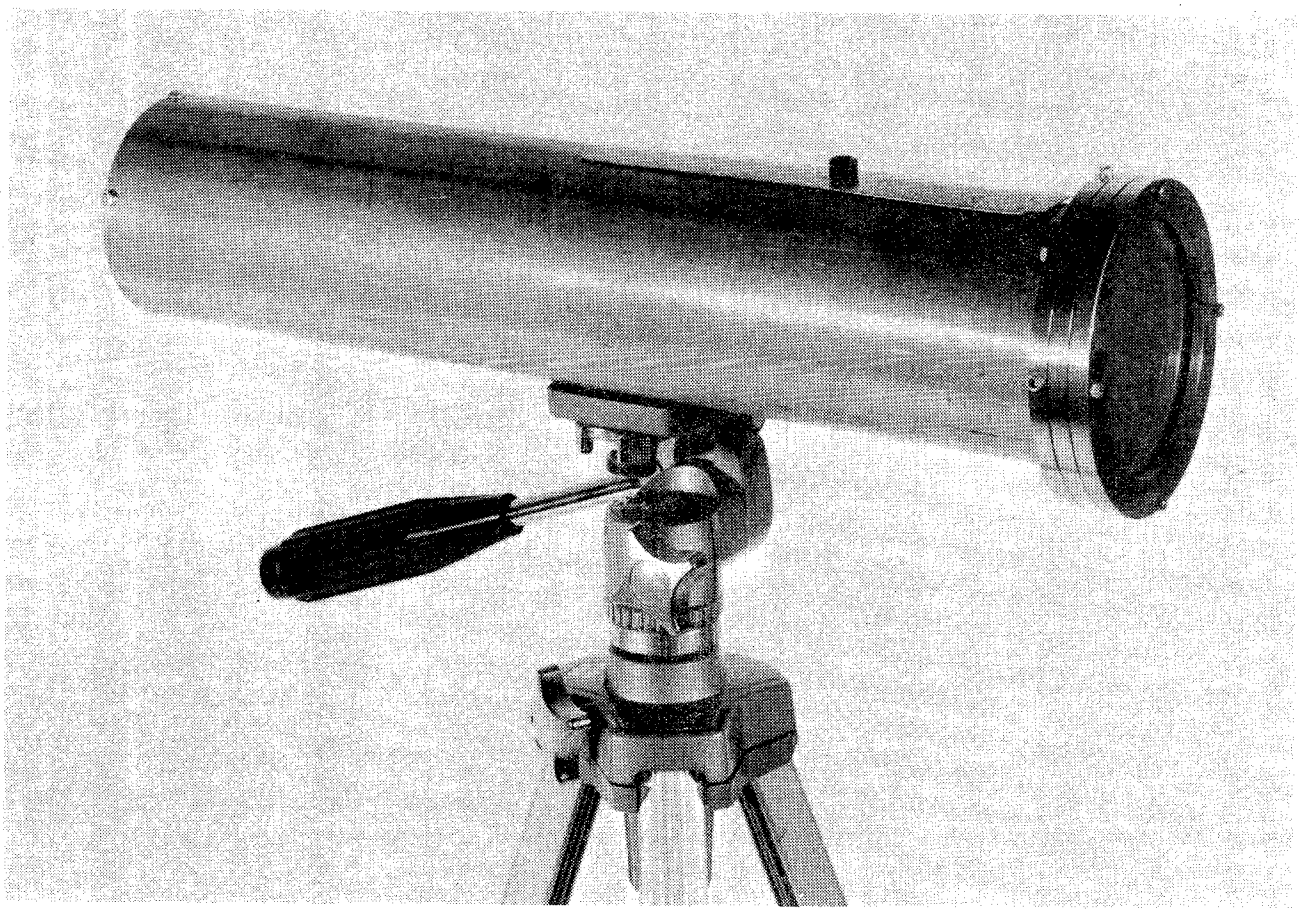

FIGURE 13

INFRARED DETECTOR UNIT ASSEMBLED WITHOUT
OUTSIDE PROTECTIVE TUBE

2.4.1 Laboratory Testing of the Instrumented Rail

The LVDTs were calibrated as assembled in the transducer bolt using a micrometer-driven fixture. This calibration yielded precise deflection versus LVDT voltage output correlations for both the vertical and longitudinal LVDTs. Vertical LVDT sensitivity was determined to be 63.83 millivolts (dc) per mil deflection. Longitudinal LVDT sensitivity was 68.18 millivolts per mil. This voltage versus deflection relationship is evident in the voltage and deflection scales of Figures 14 and 15. It should be noted that the LVDT sensitivity is variable and can be changed by adjusting the RANGE potentiometer of the LVDT demodulating circuitry. Even though the potentiometers have lock nuts, it will be necessary to calibrate both LVDTs upon system installation and periodically thereafter. There is no guarantee that the reaction can be reproduced in the field, particularly if individual LVDT sensitivities are re-adjusted.

When the above bench calibration was completed, the transducer bolt was inserted into the rail section. The entire reaction rail assembly was then mounted into and loaded by a hydraulic press as shown in Figure 16. Figure 14 shows system voltage output versus applied vertical load (at the center of the reaction rail). Figure 15 shows system voltage output versus applied longitudinal load, with no simultaneous vertical loading. The break point in both curves was determined to be due to contact with and subsequent stiffness contribution from the over-travel stop pins. Since the over-travel stop pins are set to limit reaction rail and flexure stresses to a safe level, it is not possible to re-adjust the stops to allow a continuous, linear calibration over the entire loading range.

Figure 14 also shows the effect on voltage output due to vertical loading of simultaneously applied horizontal forces. As evident in the Figure, the effect of horizontal loads is less than 5%.

Attempts to simulate the effect of vertical loads on measured horizontal loads were not successful since the vertical load application ram effectively "clamped" the reaction rail head section in place, thereby restricting its motion. In practice, this clamping effect would not exist since the downward force will be applied by a rolling wheel. Efforts to simulate the rolling wheel effect by using a solid steel roller between the vertical press ram and the rail section were successful at very low applied vertical loads, but failed when localized yielding began to occur at the roll/rail interface. This might be avoided by using much larger

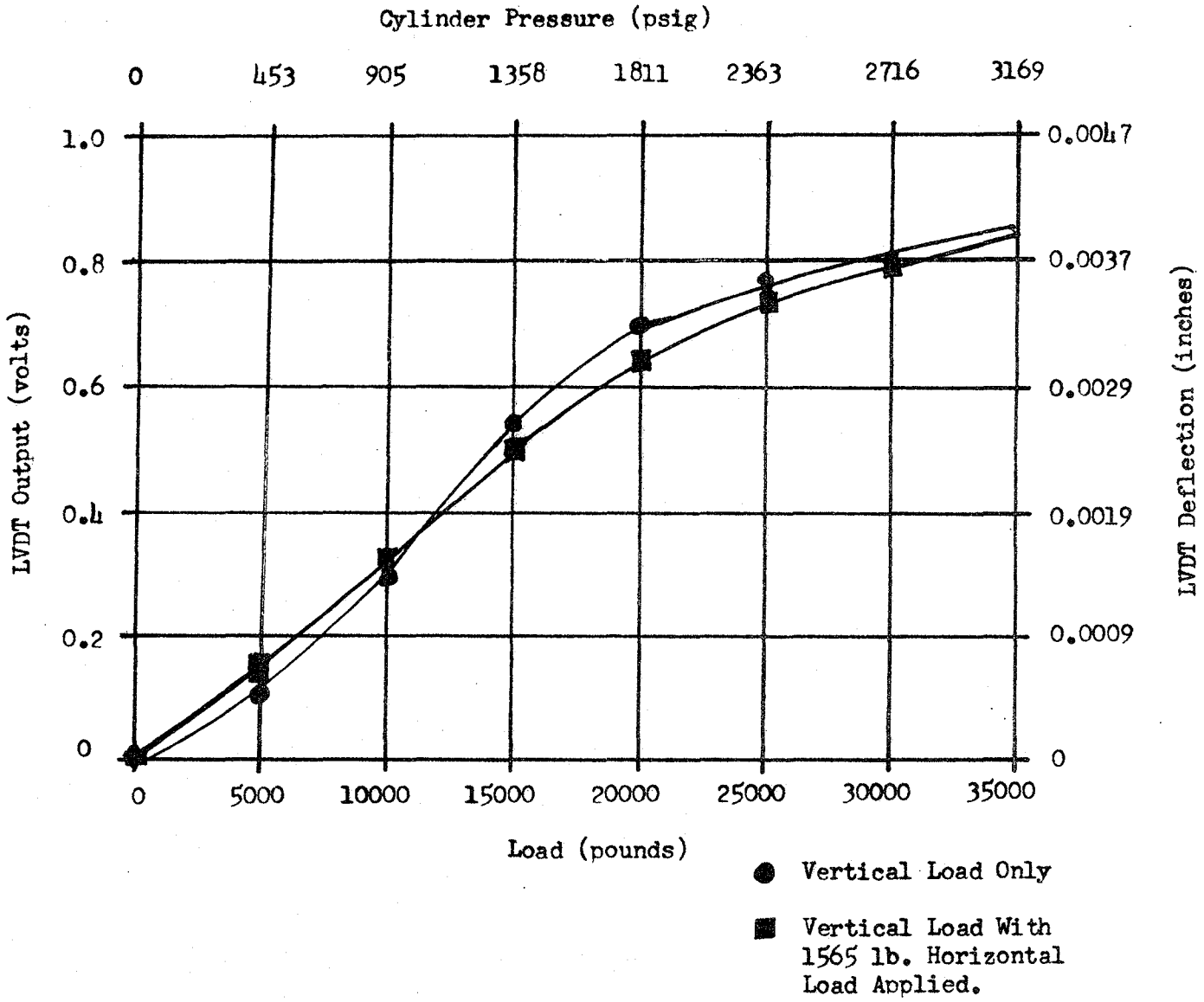

FIGURE 14

LABORATORY CALIBRATION OF VERTICAL FORCE MEASUREMENT CAPABILITY

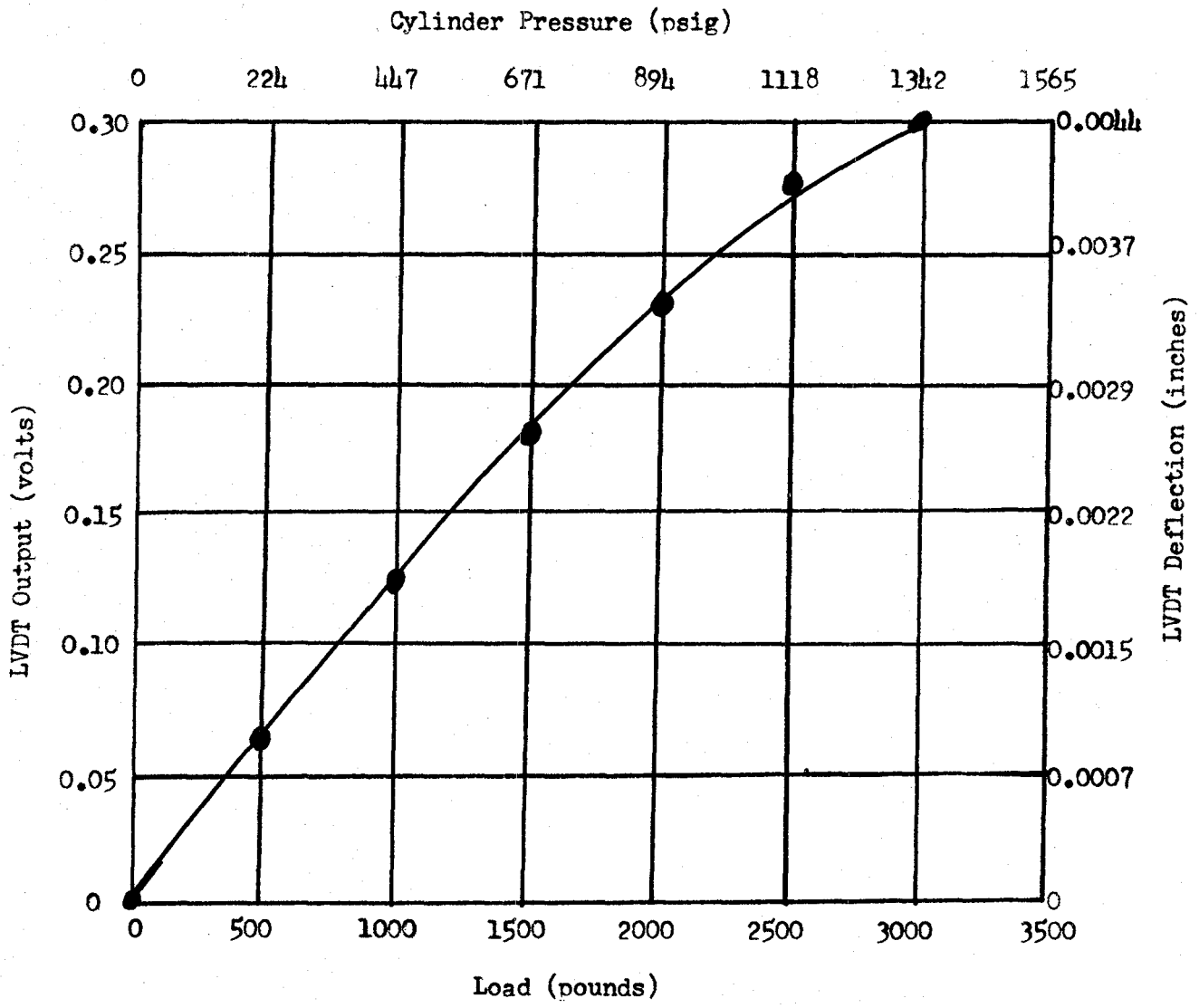

FIGURE 15

LABORATORY CALIBRATION OF HORIZONTAL FORCE MEASUREMENT CAPABILITY

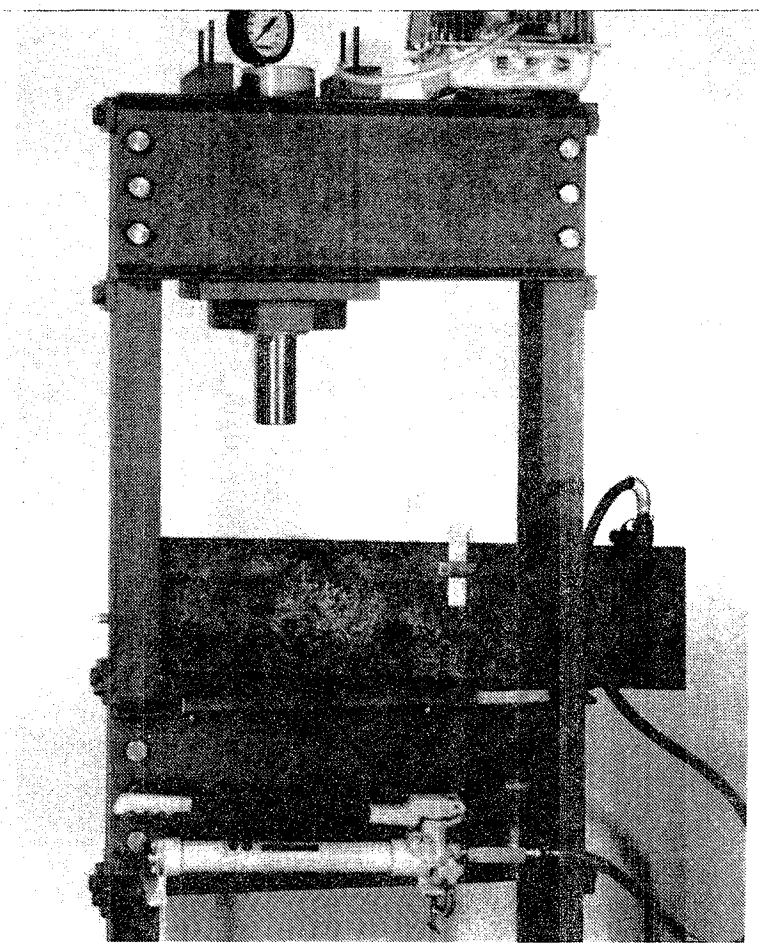

FIGURE 16

HYDRAULIC PRESS WITH TEST FIXTURE FOR CALIBRATING INSTRUMENTED RAIL SECTION

diameter rollers, but the cost of constructing special calibration fixtures discouraged further development efforts in this area. The most realistic simulation of combined loading will take place during field calibration.

In addition to system voltage output versus applied load calibration, stress levels in both flexures were monitored using strain gages. As stated previously, the overload stops were set to limit stress in the flexures, not necessarily to allow linear calibration over the entire load range.

2.4.2 Laboratory Testing of the Infrared Sensor

A series of laboratory tests were conducted on the completed IR sub-section to verify its dynamic performance. This was done using a heated target and a rotating chopping wheel moving between the target and the detector assembly. Polished aluminum and rusted steel were utilized as targets. With no change in the test setup, except for the target material, a variation in the signal output voltage of approximately 5 to 1 was observed. The tests were conducted with target temperatures ranging from 30° F (16.6° C) to 250° F (121° C) above ambient. Signal output when viewing the aluminum plate target resulted in a 4 mV output while the rusted iron target resulted in a 20 mV output.

The frequency response was tested and found to be flat within 5% over the 2 to 30 Hz range, although at the lower speed some small level noise (2 to 3 mV) was observed.

The completely assembled unit showed no short or long-term drift as viewed at the output.

The two assembled units were compared for sensitivity, gain and frequency response and found to be within 5% of each other throughout.

2.5 Preliminary Field Tests of the Infrared Sensor

A wayside field test of the infrared and car counter subsystem was conducted on June 24, 1977 at Fitchburg, Massachusetts. The test utilized the two infrared detectors of the type previously described and a photo-electric counting system consisting of a light

beam emitter and a photo-electric receiver. (Emitter portion shown in Figure 17). The passage of two relatively long freight trains was monitored at the bottom of a long downgrade. The tests were performed with the permission of the Boston and Maine Railroad.

The photo-counter elements were supported on two tripods about 6 ft. (1.88 m) high, one on either side of the railroad track. The receiver output was connected so as to produce a tick mark on the event channel of the chart recorder each time a car passed.

Initially, the IR detectors were also set up on tripods, however, because they had to be relatively close to the track, this made them vulnerable to damage by potential dragging equipment.

For the second run, the IR detectors were taken off the tripods and positioned on the ground in a bed of crushed stone. They were focused to a point of 1 in. (2.54 cm) above the rail by utilizing a portable heat source and were set back from this rail about 30 in. (76 cm).

The following train data were made available by the controller in a nearby tower:

Train length, cars:	79
Loaded Cars:	43
Empty cars:	36
Train speed at site:	30 mph (48.4 kmh)
Time of day:	12:27 PM
Weather conditions:	Clear and Sunny
Ambient temperature:	78°F (25°C)
Train number:	NE2.

The IR sensor-amplifier-recorder system functioned properly, indicating high temperatures as (some) wheels passed. In several cases, high indicated wheel temperatures were correlated visually with several smoking braked wheels. In other cases, no discernible recorder pen excursions were noted as wheels passed by. Although not verifiable, it was hypothesized that the brakes on these wheels were not functioning properly.

These tests, although qualitative in nature, demonstrated that the IR sensor portion of the prototype brake inspection system was capable of detecting "hot" wheels.

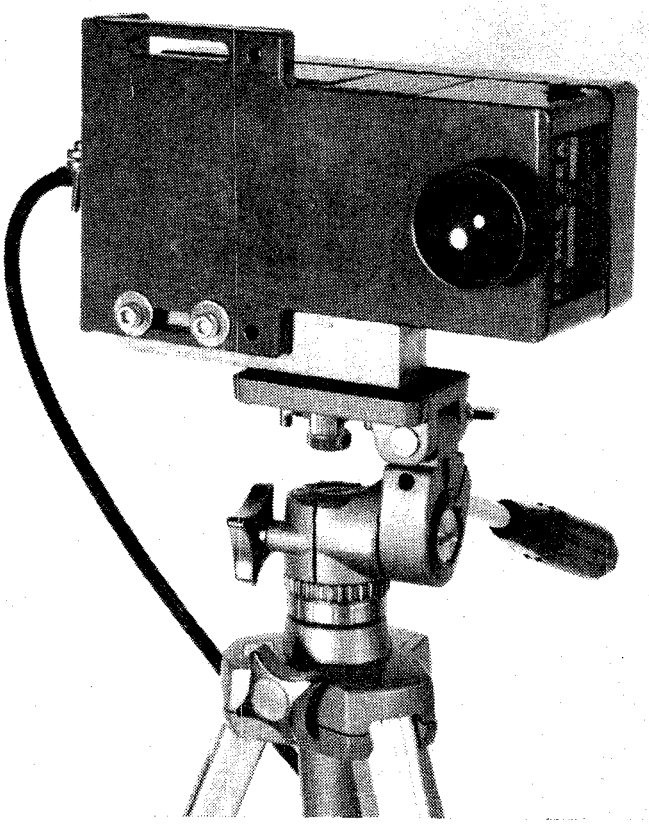

FIGURE 17

PHOTO-ELECTRIC UNIT USED FOR COUNTING CARS

3. PROTOTYPE BRAKE INSPECTION SYSTEM VERIFICATION TESTS

3.1 Verification Test Objectives

Overall Brake Inspection System performance test objectives were:

1. To demonstrate that the prototype Brake Inspection System hardware developed under Phase I would in fact indicate car weight and braking effort on a wheel-by-wheel basis.

2. To determine the accuracy and repeatability of the reaction rail in measuring vertical wheel forces (weight) and horizontal wheel forces (braking effort).

3. To determine the effectiveness of the infrared subsystem in proportioning total axle braking force between right and left wheel brakes.

4. To determine the effects of the following on indicated weight and indicated brake force:
   a. Consist velocity (mph).
   b. Normal air brake application (psi reduction).
   c. Orientation (forward or reverse).
   d. Type of brake shoe (composition or cast iron).
   e. Brake modifications (cutout, dragging hand brakes)

5. To identify measurements characteristic of brake system malfunctions as postulated in Section 2.1.3, thereby gaining a preliminary look at the diagnostic capability of the Prototype Brake Inspection System.

In order to achieve these objectives under actual field conditions, a detailed test plan was prepared. This plan called for the installation of the prototype Brake Inspection System hardware in a section of test track at the Transportation Test Center in Pueblo, Colorado. Runs would be made at speeds ranging from 5 mph to 60 mph under varying conditions of brake application.

3.2 Test Conduct

The prototype Brake Inspection System was set up at TTC at the location depicted in Figure 18. The reaction rail was inserted into the outside, westernmost rail of this section of track such that the left wheels of the test consist would cross over the sensor as the consist proceeded in a northerly direction. Figure 19 shows the reaction rail inserted in the parent rail. Figure 19b shows the reaction rail segment after tie-in to the parent rail with joint bars.

The test consist was made up of one locomotive and four test cars of the following description, and in the following order:

Locomotive DOT-001

Car I: DOTX-502, Loaded Box, Cast Iron Brake Pads.

Car II: DOTX-501, Empty Box, Composition Brake Pads.

Car III: USAF-42015, Loaded Gondola, Composition Brake Pads.

Car IV: USAF-42016, Empty Gondola, Cast Iron Brake Pads.

Figure 20 shows the test consist schematic identifying cars, truck designation, and wheel numbering scheme. All cars were initially connected with the "A" end toward locomotive. The only exception to this order occurred on the last day of testing (Runs 45 - 58) at which time the orientation of Car IV was reversed. Under this configuration, the "B" end of Car IV was connected to the "B" end of Car III. All other tests were made with the consist as shown in Figure 20.

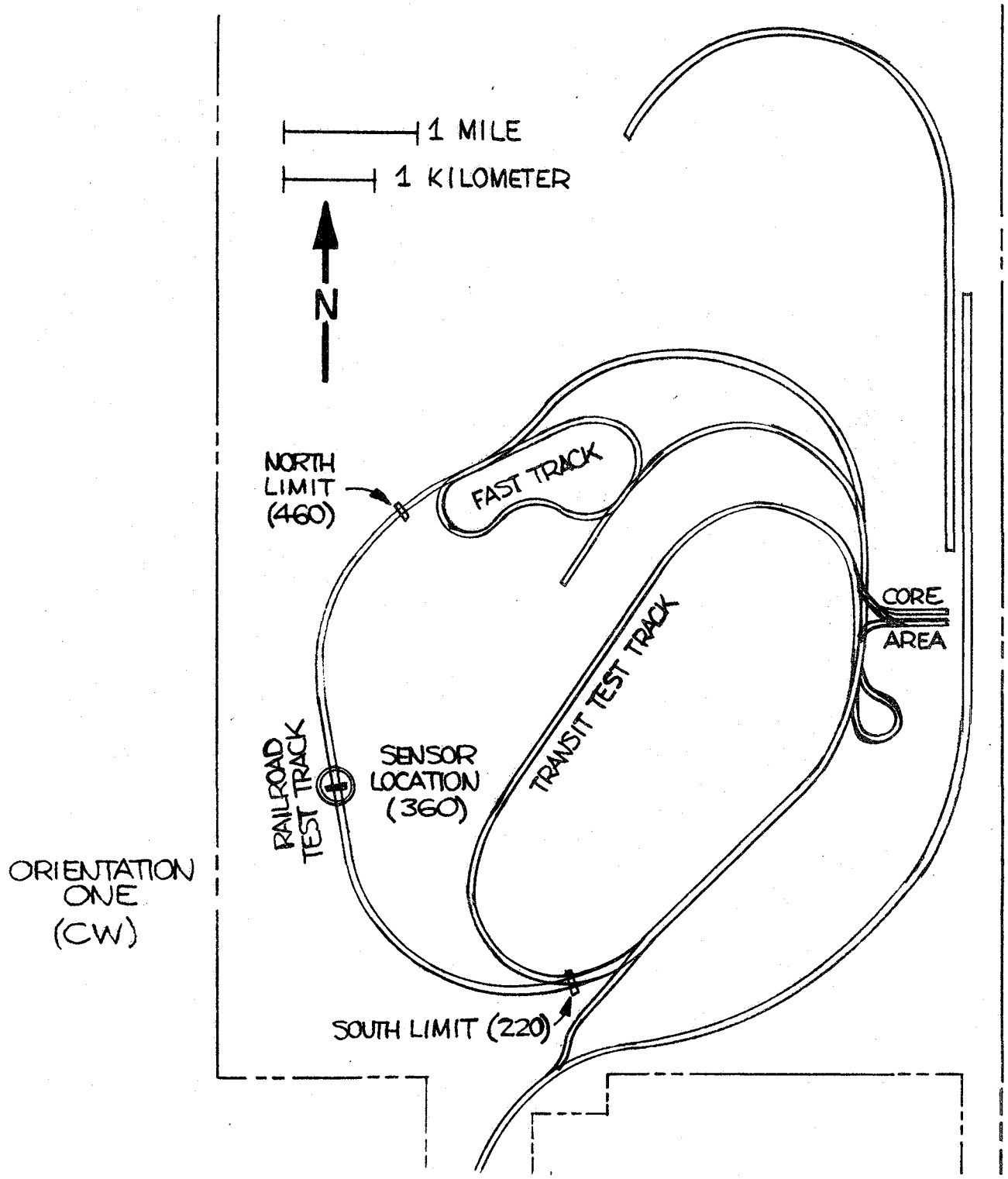

FIGURE 18

TEST SITE LOCATION

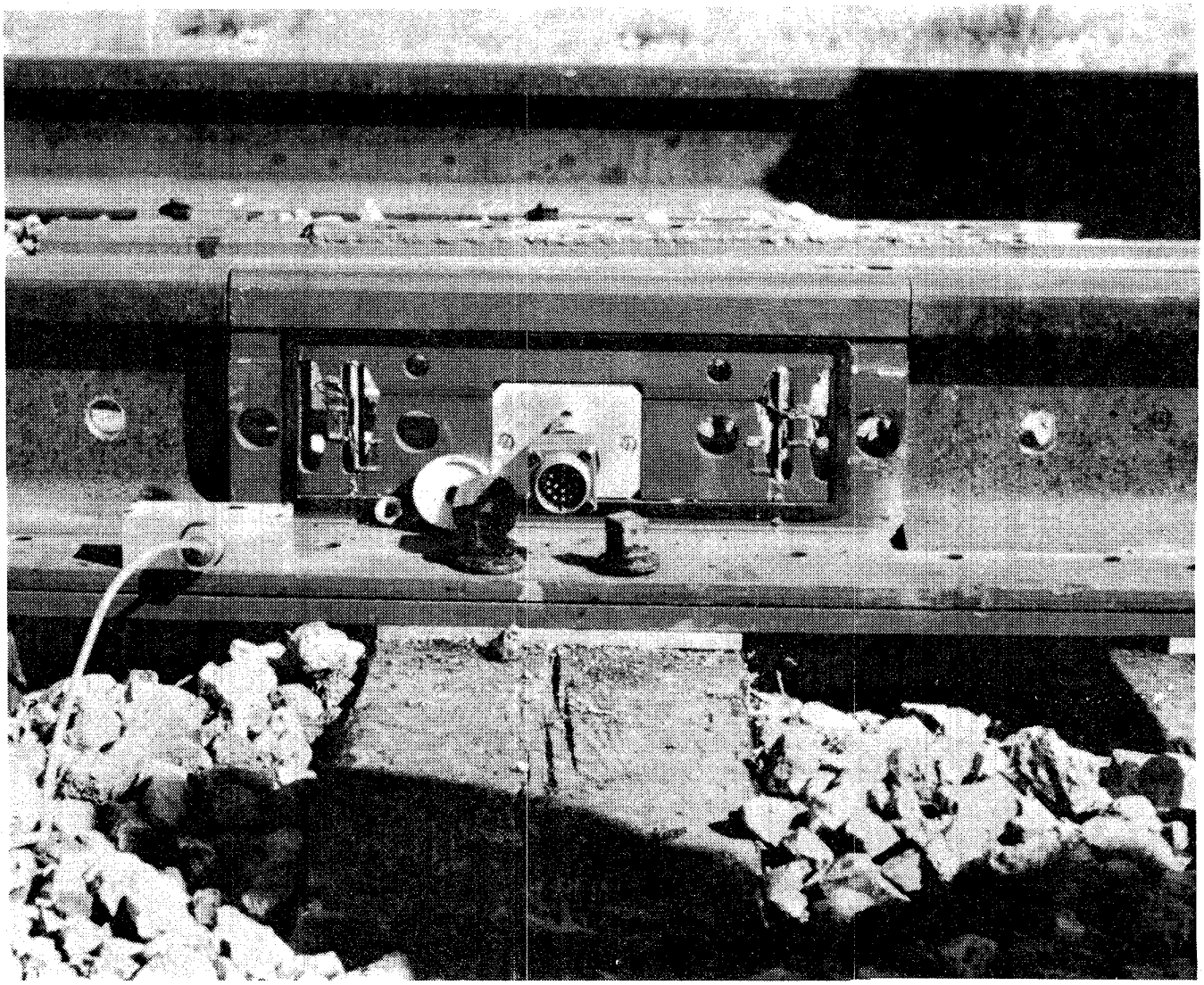

Figure 19a

REACTION RAIL INSTALLED IN PARENT TRACK BEFORE TIE-IN WITH JOINT BAR

FIGURE 19. REACTION RAIL INSTALLATION

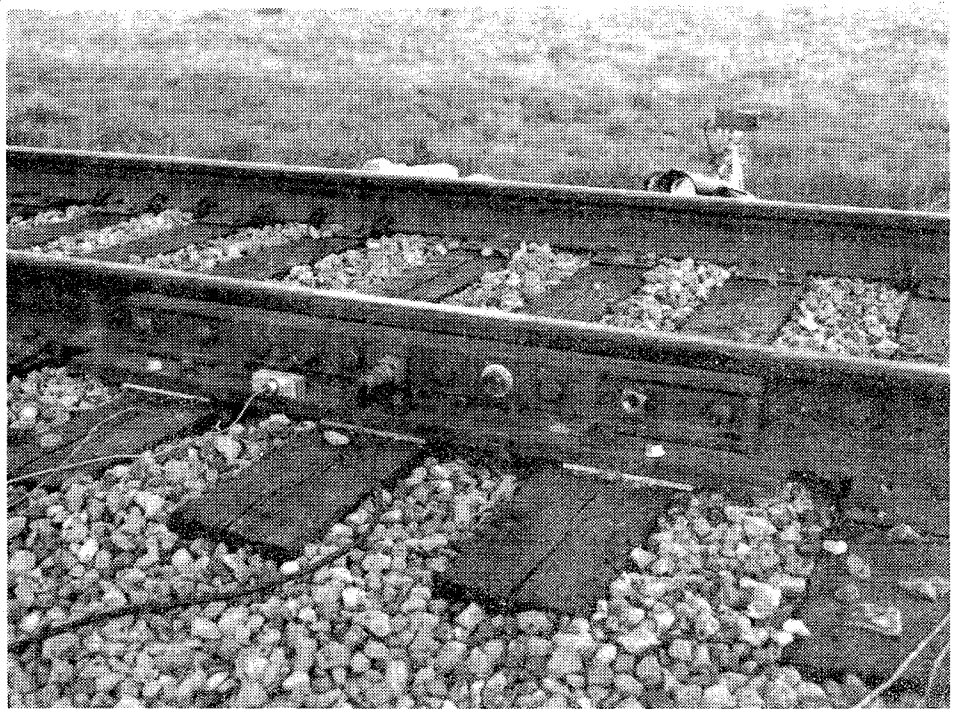

Figure 19b

REACTION RAIL INSTALLED IN PARENT TRACK
READY FOR FIELD TESTING

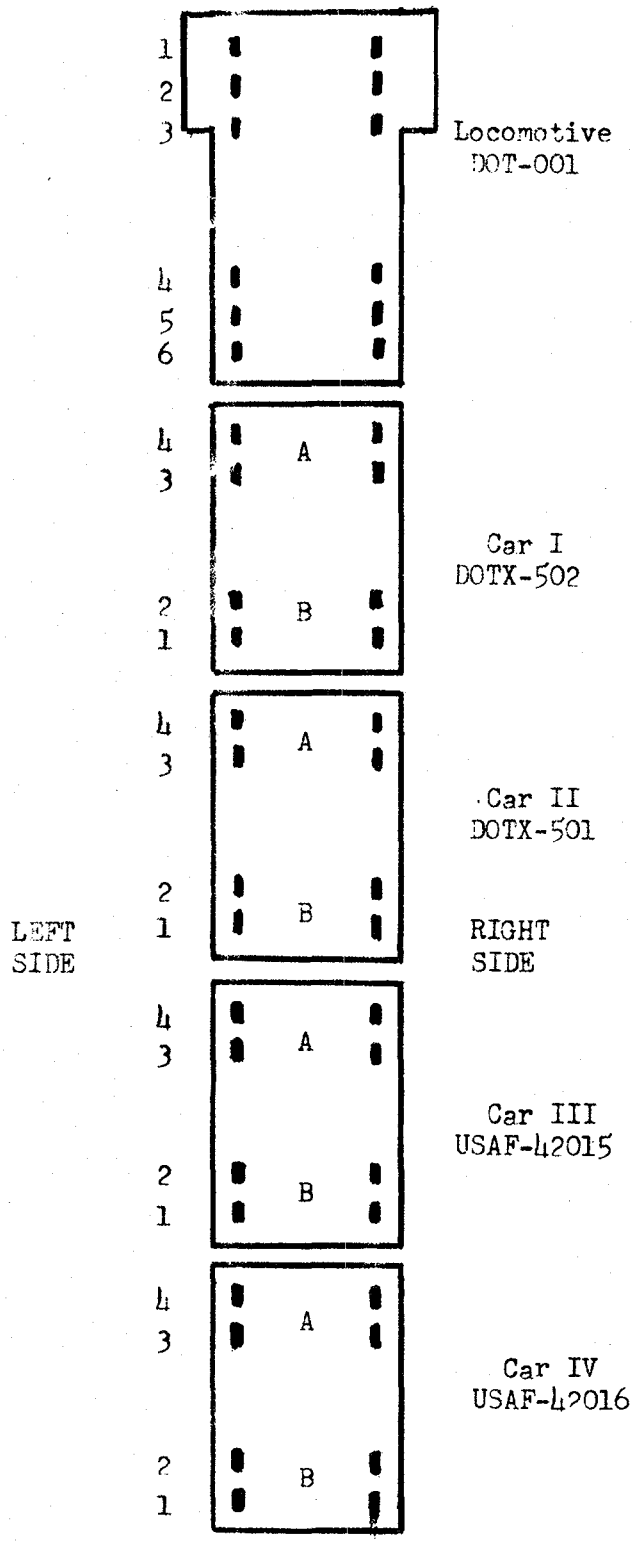

The "B" end of a car is defined as the end on which the hand brake is installed.

NOTE: Car IV was reversed for Runs 45 through 58.

FIGURE 20

TEST CONSIST MAKE-UP AND NUMBERING SYSTEM

Tests were conducted December 5-8, 1977, at Pueblo, Colorado. Table 2 is a master test schedule, showing actual test runs made, consist velocities, consist direction, orientation, brake pressure reduction, and comments on specific runs. Notice that Runs 1-24 and 45-58 were made with the locomotive heading south, thus the right wheels of the consist passed over, and were sensed by the reaction rail. Runs 25-55 were made with the locomotive heading north, thus the reaction rail measurements were made on the left side wheels.

Field observations of the data collected on horizontal (braking) forces as indicated by the reaction rail identified an unexpected phenomenon. Instead of all braked wheels registering a retarding force on the reaction rail, roughly one-half were indicating the opposite, or a "driving" force on the reaction rail. This effect was hypothesized to be due to small differences in wheel diameter which resulted in torque being transmitted by one wheel to the opposite wheel, thereby "driving" the measured wheel. To test this hypothesis, heavy grease was applied to the opposite rail prior to Run 52. Run 52, and all subsequent tests showed positive braking on all wheels, thereby proving the original hypothesis. An analysis of this effect is presented in Section 3.5.

Tables 3a - 3d illustrate the various conditions related to each run in matrix form for each car. These representations are helpful in visualizing exactly which runs were performed under identical conditions. The matrices of Table 3 also assist in the subsequent analysis of vertical and horizontal braking force sensitivity to the various test conditions.

3.3 Verification Test Results

3.3.1 Field Calibrations

Field calibrations were made for each of the following sub-systems or sub-system functions:

1. Reaction Rail, Vertical Force: Static weight calibrations were made by pulling the test consist onto the reaction rail on a wheel basis and recording the resulting vertical and horizontal LVDT output. These outputs were then correlated with known truck weights for each test car. Test car weights were obtained independently of these tests by weighing the A end, the B end, and the total car for each test car on a scale. Table 4 presents the results of this calibration.

TABLE 2

TEST RUN SUMMARY

Run	Date	Direction (a)	Orientation	Wheel Side (b)	Train Speed (mph)	Brake Red'n (psi)	Comments
1	12/6	S	Pull	R	5	0	Baseline run-no brakes
2	12/6	N	Push	R	4	0	" "
3	12/6	S	Pull	R	5	0	" "
4	12/6	N	Push	R	5	0	" "
5	12/6	S	Pull	R	10	0	" "
6	12/6	N	Push	R	10	0	" "
7	12/6	S	Pull	R	20	0	" "
8	12/6	N	Push	R	20	0	" "
9	12/6	S	Pull	R	40	0	" "
10	12/6	N	Push	R	40	0	" "
11	12/6	S	Pull	R	60	0	" "
12	12/6	N	Push	R	60	0	" "
13	12/6	S	Pull	R	10	6	Baseline runs - braked
14	12/6	N	Push	R	10	11	" "
15	12/6	S	Pull	R	10	15	" "
16	12/6	N	Push	R	20	6	" "
17	12/6	S	Pull	R	20	11	" "
18	12/6	N	Push	R	20	15	" "
19	12/6	S	Pull	R	40	6	" "
20	12/6	N	Push	R	40	11	" "
21	12/6	S	Pull	R	40	15	" "
22	12/6	N	Push	R	60	6	" "
23	12/6	S	Pull	R	60	11	" "
24	12/6	S	Pull	R	60	15	" "
25	12/7	N	Pull	L	10	11	Braked runs - See Note
26	12/7	S	Push	L	20	11	" (c)
27	12/7	N	Pull	L	40	11	" "
27A	12/7	S	Push	L	20	11	" "
28	12/7	N	Pull	L	60	11	" "
28A	12/7	S	Push	L	30	11	" "
29	12/7	N	Pull	L	10	11	Braked runs - See Note
30	12/7	S	Push	L	20	11	" (d)
31	12/7	N	Pull	L	40	11	" "
32	12/7	N	Pull	L	60	11	" "
33	12/7	N	Pull	L	10	11	Braked runs - See Note
34	12/7	S	Push	L	20	11	" (e)
35	12/7	N	Pull	L	40	11	" "
36	12/7	N	Pull	L	60	11	" "
41	12/7	N	Pull	L	60	0	No brakes - All Normal
42	12/7	S	Push	L	10	0	" "
43	12/7	N	Pull	L	40	0	" "
44	12/7	S	Push	L	20	0	" "

TABLE 2 (Cont.)

TEST RUN SUMMARY

Run	Date	Direc-tion (a)	Orien-tation	Wheel Side (b)	Train Speed (mph)	Brake Red'n (psi)	Comments
45	12/8	S	Pull	R(f)	40	0	No brakes - All Normal
46	12/8	N	Push	R	20	0	" "
47	12/8	S	Pull	R	60	0	" "
48	12/8	N	Push	R	10	0	" "
49	12/8	S	Pull	R	30	0	Traction run #1
50	12/8	N	Push	R	30	0	Traction run #2
51	12/8	S	Pull	R	30	0	Grease rail - Sensor
52	12/8	N	Push	R	10	11	Grease rail-Far side
53	12/8	S	Pull	R	10	15	" "
54	12/8	N	Push	R	40	11	" "
54A	12/8	S	Pull	R	40	11	" "
54B	12/8	N	Push	R	20	13	" "
54C	12/8	S	Pull	R	40	13	" "
55	12/8	S	Pull	R	40	13	" "
56	12/8	S	Pull	R	40	13	" "
57	12/8	N	Push	R	10	6	See Note (g)
58	12/8	S	Pull	R	40	13	See Note (h)

Notes:

a. Direction denoted by S = South; N = North.
b. Wheel side, right (R) or left (L) designates wheels passing over reaction rail. Refer to Figure 20 for convention.
c. For Runs 25-28A; Cars I and III with normal 11 psi reduction; Car II with 11 psi reduction plus hand brake drag; Car IV with brakes disconnected - no brakes.
d. Runs 29-32; Cars II and IV - 11 psi reduction; Car III - 11 psi reduction plus dragging hand brake; Car I - no brakes.
e. Runs 33-36; Cars I and III - 11 psi reduction; Car IV - 11 psi reduction plus hand brake drag; Car II - no brakes.
f. For Runs 45-58, Car IV was reversed, so data for that car will represent left (L) rather than right (R) side wheels.
g. Run 57 - Brakes dragged to R22 with 6 psi reduction at 20 mph, returned at 20 mph at 6 psi reduction; slow to 10 mph through test section. New cast iron brake shoes on Car III, all right side wheels.
h. Run 58 - Brakes dragged to R47 at 11 psi reduction, ahead through test zone at 40 mph, 13 psi reduction.
i. Letters after run numbers (27A, 28A, 54A, 54B, 54C) represent non-scheduled tests (as per the predetermined test plan) for which good data was taken.

TABLE 3a

TEST VARIABLE MATRIX FOR CAR I (DOTX-502)

Brake Red. (psi)	Orient-ation	Consist Velocity				
		10 mph*	20 mph	30 mph	40 mph	60 mph
0	Pull	R (1) (3) (5) L (29)	R (7)	R (49) (51)	R (9) (45) L (31) (43)	R (11) (47) L (32) (41)
	Push	R (2) (4) (6) (48) L (42)	R (8) (46) L (30) (44)	R (50)	R (10)	R (12)
6	Pull	R (13)			R (19)	
	Push	R (57)	R (16)			R (22)
11	Pull	L (25) (33)	R (17)		R (54A) L (27) (35)	R (23) L (28) (36)
	Push	R (14) (52)	L (34) L (26) (27A)	L (28A)	R (20) (54)	
13-15	Pull	R (15) (53)			R (21) (54C) R (55) (56) (58)	R (24)
	Push		R (18) (54B)			

* Including lower speeds

R = Data is from right side wheels passing over reaction rails.
L = Data is from left side wheels passing over reaction rail.
(N) = Run number. Refer to Figure 21.

Letters after run numbers (27A, 28A, 54A, 54B, 54C) represent non-scheduled tests (as per the predetermined test plan) for which good data was taken.

TABLE 3b

TEST VARIABLE MATRIX FOR CAR II (DOTX-501)

Brake Red. (psi)	Orientation	Consist Velocity				
		10 mph *	20 mph	30 mph	40 mph	60 mph
0	Pull	R (1) (3) (5) L (33)	R (7)	R (49) (51)	R (9) (45) L (35) (43)	R (11) (47) L (36) (41)
	Push	R (2) (4) (6) (48) L (42)	R (8) (46) L (34) (44)	R (50)	R (10)	R (12)
6	Pull	R (13)			R (19)	
	Push	R (57)	R (16)			R (22)
11	Pull	L (25) (29)	R (17)		R (54A) L (27) (31)	R (23) L (28) (32)
	Push	R (14) (52)	L (30) L (26) (27A)	L (28A)	R (20) (54)	
13-15	Pull	R (15) (53)			R (21) (54C) R (55) (56) (58)	R (24)
	Push		R (18) (54B)			

* Including lower speeds

R = Data is from right side wheels passing over reaction rail.
L = Data is from left side wheels passing over reaction rail.
(N) = Run number. Refer to Figure 21.

TABLE 3c

TEST VARIABLE MATRIX FOR CAR III (USAF-42015)

Brake Red. (psi)	Orient-ation	Consist Velocity				
		10 mph *	20 mph	30 mph	40 mph	60 mph
0	Pull	R (1) (3) (5)	R (7)	R (49) (51)	R (9) (45) L (43)	R (11) (47) L (41)
	Push	R (2) (4) (6) (48) L (42)	R (8) (46) L (44)	R (50)	R (10)	R (12)
6	Pull	R (13)			R (19)	
	Push	R (57)	R (16)			R (22)
11	Pull	L (25) (29) (33)	R (17)		R (54A) L (27) (31) (35)	R (23) L (28) (32) (36)
	Push	R (14) (52)	L (26) (27A) L (30) (34)	L (28A)	R (20) (54)	
13-15	Pull	R (15) (53)			R (21) (54C) R (55) (56) (58)	R (24)
	Push		R (18) (54B)			

* Including lower speeds

R = Data is from right side wheels passing over reaction rail.
L = Data is from left side wheels passing over reaction rail.
(N) = Run number. Refer to Figure 21.

TABLE 3d

TEST VARIABLE MATRIX FOR CAR IV (USAF-42016)

Brake Red. (psi)	Orient-ation	Consist Velocity				
		10 mph *	20 mph	30 mph	40 mph	60 mph
0	Pull	R (1) (3) (5) L (25)	R (7)	L (49) (51)	R (9) L (27) (43) (45)	R (11) L (28) (41) (47)
	Push	R (2) (4) (6) L (42) (48)	R (8) L (44) L (27A) (26) (46)	L (28A) (50)	R (10)	R (12)
6	Pull	R (13)			R (19)	
	Push	L (57)	R (16)			R (22)
11	Pull	L (29) (33)	R (17)		L (31) (35) (54A)	R (23) L (32) (36)
	Push	R (14) L (52)	L (30) (34)		R (20) L (54)	
13-15	Pull	R (15) L (53)			R (21) L (54C) L (55) (56) (58)	R (24)
	Push		R (18) L (54B)			

* Including lower speeds

R = Data is from right side wheels passing over reaction rail.
L = Data is from left side wheels passing over reaction rail.
(N) = Run number. Refer to Figure 21.

TABLE 4

STATIC WEIGHT CALIBRATION - FIELD

Car	Truck and Wheel	Indicated Wheel Weight [1] (mv)	Indicated Truck Weight [2] (mv)	Actual Truck Weight [3] (lbs)	Calibration Factor (lbs/mv)	Deviation From Average (%)
I	A 4	240				
	3	280	1040	50,000	48.08	+ 2.8
	B 2	360				
	1	320	1360	51,440	37.82	- 19.2
II	A 4	100				
	3	120	440	22,380	50.86	+ 8.8
	B 2	140				
	1	120	520	22,560	43.38	- 7.2
III	A 4	160				
	3	200	720	39,400	54.72	+ 16.9
	B 2	160				
	1	180	680	37,820	55.62	+ 18.9
IV	A 4	150				
	3	130	560	24,520	43.79	- 6.4
	B 2	150				
	1	160	680	24,780	39.97	- 14.5
				Mean Factor	46.78	
				Standard Deviation	6.62	

1. Millivolt output of vertical LVDT for each wheel approximately at center of reaction rail.

2. Sum of millivolt output for two wheels on each truck times 2 to approximate full (left and right side) truck weight.

3. Actual truck weight as weighed on scale.

As a result of wide variations in calibrated rail sensitivity, this method of calibration was considered inadequate. In order to try to get the wheel being measured directly over the center of the reaction rail segment, the consist had to be manually moved back and forth until the chart deflections were maximum. Chart deflection was monitored trackside and instructions passed to the locomotive operator by radio.

Since the actual mode of reaction rail operation is dynamic, rather than static, an alternative method of determining vertical force calibration was employed. The average vertical LVDT output for the first twelve test runs was taken to be indicative of wheel weight for each axle, and these outputs were correlated to known truck weights. All vertical force data reported herein is based on the calculated reaction rail sensitivity of 1.0 millivolts per 36.81 lbs. vertical force or .027 mv/lb (.060 mv/kg). This is the average dynamic calibration factor based on the first twelve test runs mean millivolt indication for each wheel.

As a consideration of the data thus reduced will show, this calibration may not be the best possible choice either. The first twelve test runs include various combinations of consist velocities, and push versus pull orientations. However, this calibration is used consistently for all subsequent data reduction and analysis so comparisons between the various axles, trucks, and cars are indeed valid. If a better correlative reaction rail vertical sensitivity can be derived, then all data reported here could be scaled by a constant multiplier.

Table 5 presents the calculated vertical sensitivities as derived from the first twelve runs for each axle and known truck weights.

2. Reaction Rail, Horizontal Force: Static horizontal force calibrations were initially attempted by placing a braked wheel on the reaction rail, and then hydraulically applying known horizontal loads to that axle. The problem encountered with this calibration setup was that all of the applied horizontal force was not transmitted to the reaction rail. Car/truck/axle compliances absorbed the applied load in a complex manner, resulting in a number of uncontrollable relative displacements and load distributions.

A simpler, more direct method was finally used to calibrate the horizontal reaction LVDT. A hydraulic load was applied to a C-clamp attached directly to the reaction rail. Figure 21 presents the results of this calibration.

TABLE 5

DYNAMIC WEIGHT CALIBRATION - FIELD

Car	Truck	Wheel	Indicated Weight [1] (mv)	Indicated Truck Weight [2] (mv)	Actual Weight [3] (lbs)	Calibration Factor (lbs/mv)	Deviation From Average (%)
I	A	4	336.7 (18.7)				
		3	350.0 (44.7)	1373.3	50,000	36.41	- 1.1
	B	2	388.3 (42.2)				
		1	351.7 (36.6)	1480.0	51,400	34.73	- 5.7
II	A	4	158.3 (32.4)				
		3	146.7 (19.7)	610.0	22,380	36.69	- 0.3
	B	2	141.7 (10.3)				
		1	155.0 (17.3)	593.3	22,560	38.02	+ 3.3
III	A	4	265.0 (17.3)				
		3	291.7 (37.6)	1113.3	39,400	35.39	- 3.9
	B	2	250.0 (27.6)				
		1	250.0 (32.5)	1000.0	37,820	37.82	+ 2.7
IV	A	4	158.3 (15.9)				
		3	168.3 (18.0)	653.3	24,520	37.53	+ 2.0
	B	2	163.6 (12.1)	654.6	24,780	37.86	+ 2.9
		1	163.6 (15.0)				
				Average Cal. Factor		36.81	
				Standard Deviation		1.23	

1. Mean millivolt output of vertical LVDT for first 12 test runs. Number in parentheses is the standard deviation of mv output for first 12 runs.
2. Sum of wheels on truck times 2 for right and left side.
3. Actual weight measured independently on scale.

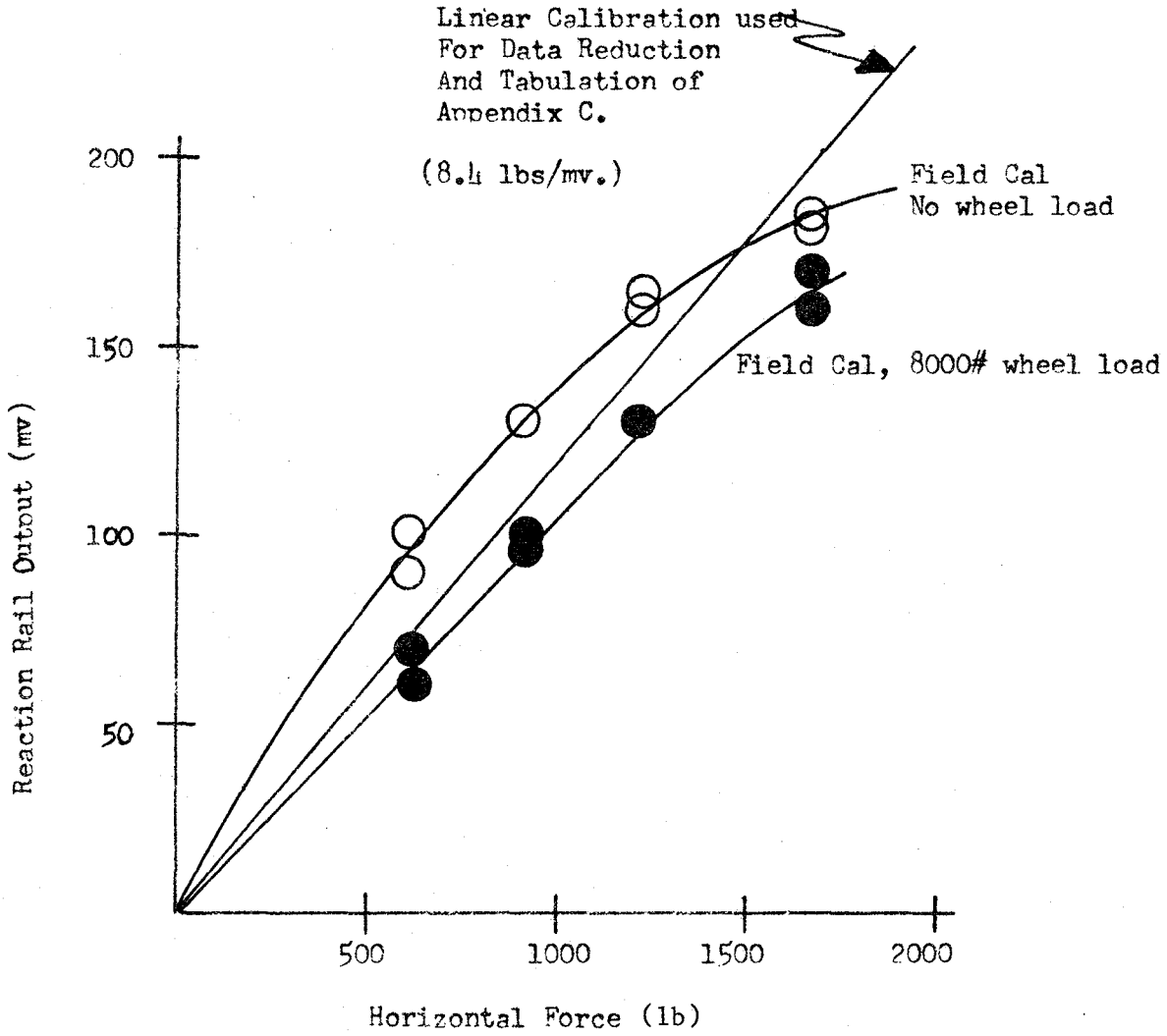

FIGURE 21

FIELD CALIBRATION OF HORIZONTAL FORCE CAPABILITY OF REACTION RAIL

Following calibration without accompanying vertical load, one wheel of the car (axle weight = 16,000 lbs.) was positioned on the rail. Horizontal loads were applied as before with the resulting LVDT outputs shown also in Figure 21. It should be noted that calibrations with the rail unloaded showed no cross-talk between horizontal and vertical LVDT's. With the rail under an 8,000 lb. (3,636 kg) vertical load, the applied horizontal load resulted in indicated changes in vertical output. Under a maximum applied horizontal of 3,000 lbs. (1,364 kg), the indicated vertical load changed by 2,100 lbs. (4,955 kg), or 26 per cent of its indicated value. It was later concluded that cross-sensitivity must have been induced by peculiarities of the calibration technique, since this magnitude of vertical deviation was not observed as a result of actual braking loads under dynamic test conditions.

3. IR Sub-System: Figure 22 shows the IR sensor calibration made in the laboratory. As can be seen in the Figure, the output curve is non-linear with target temperature, but has been approximated by two linear relations for each sensor. The temperature data of Appendix E is tabulated using the correlations shown in the Figure, and is tabulated as wheel temperature rise above ambient. From most test runs, the ambient temperature was approximately 30°F (-1°C), and to get actual temperature, add 30°F to each tabulated value.

Calibration checks were made in the field using an aluminum target, heated electrically to 300°F (149°C) which was slid back and forth on the rail past the sensor. These calibration checks correspond to within 5% of the laboratory calibration curve, thus that curve is used.

3.3.2 Test Data

All test data was recorded directly on a six-channel strip chart recorder. Channel 1 recorded side load indication as sensed by a strain gage bridge applied to the reaction rail flexures. Loading towards the outside of the track due to tapered railcar wheels was recorded positive while forces exerted towards the inside of the track due to cylindrical locomotive wheels indicated negative.

Channel 2 recorded vertical LVDT output (weight) with wheel weight recording in the positive direction. Channel 3 recorded horizontal or braking forces as indicated by the horizontal LVDT. Braking force indi-

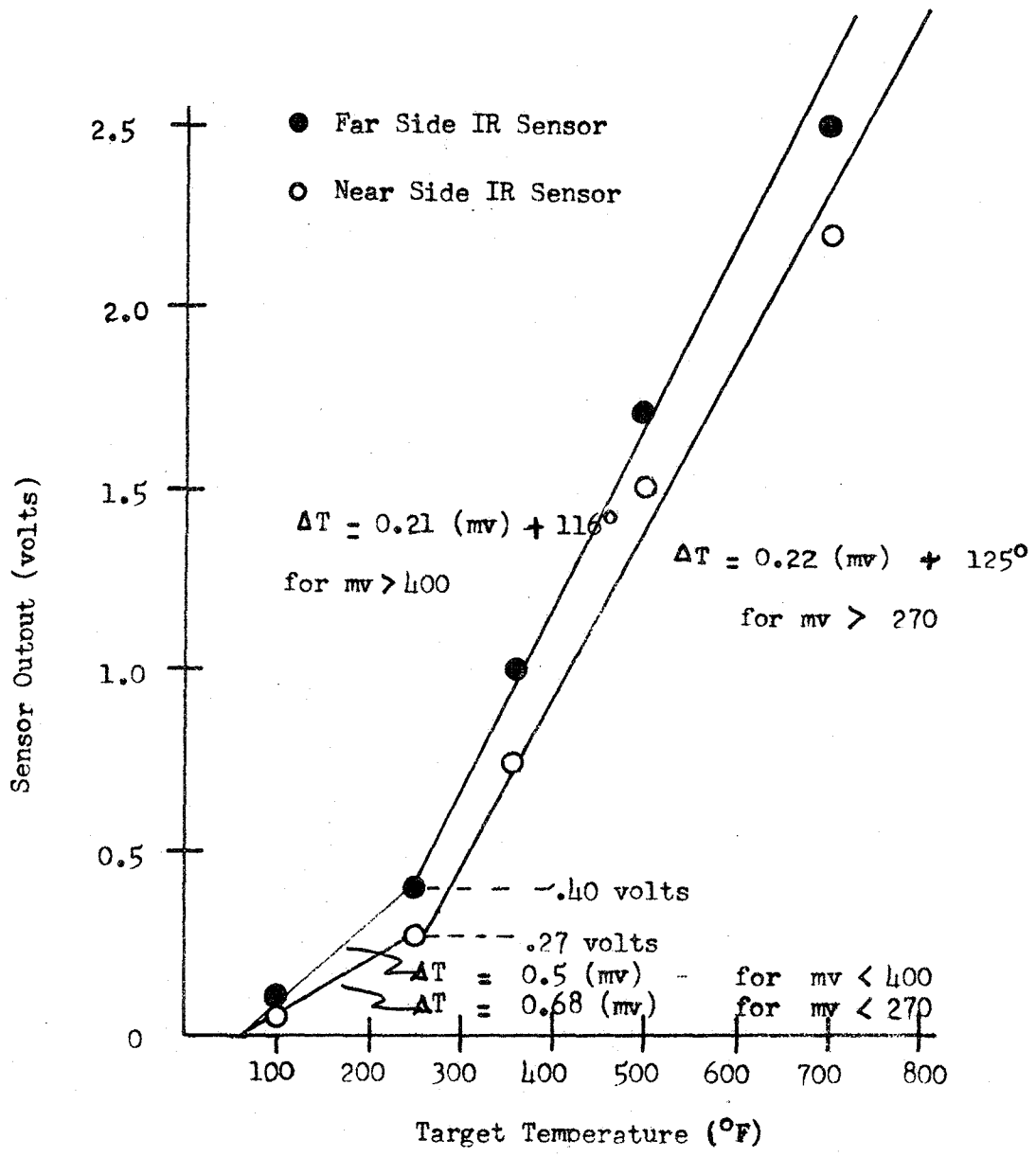

FIGURE 22

INFREARED SENSOR CALIBRATION

cated positive when the test consist was traversing the reaction rail traveling south, and negative while traversing to the north. Driving forces indicate positive while traveling north, negative while traveling south.

Channels 4 and 5 recorded IR sensor output, both indicating negative pen deflections for temperature increases.

Recorder channel sensitivities varied depending on channel, and often were changed between test runs so as to give optimum indications. Appendix E presents all data (in reduced form) with indications of chart speed and channel sensitivity for the quantities being measured.

Section 3.3.3 describes data interpretation and reduction methods used, and Section 3.5 discusses the nature of the raw data further.

3.3.3 Data Reduction

This section discusses the tabulation (3.3.3.1) and interpretation (3.3.3.2) of field test data. No attempt is made in this section to analyze or otherwise discuss the results.

3.3.3.1 Tabulation of Field Test Data

All field test data reported herein has been converted into units of force (lbs) or temperature (^{o}F) above ambient with the exception of reaction rail side loads which are reported as millivolt output. The side load outputs were generated by a strain gage bridge applied to the sides of the reaction rail flexures, but the rail was not field calibrated for side loads. The side load data in millivolts is useful in determining the direction of side loads due to the passing wheels, and in visualizing relative magnitudes of the side loading due to each wheel.

The conversion to units of force or temperature was made by first converting from chart recorder pen deflection (chart divisions) to millivolts as follows:

$$\begin{matrix}\text{Millivolt} \\ \text{Output}\end{matrix} = \begin{matrix}\text{Pen} \\ \text{Deflection}\end{matrix} \text{(div.)} \times \begin{matrix}\text{Channel} \\ \text{Sensitivity}\end{matrix} \text{(mv/div.)} \quad (12)$$

The following millivolt-to-force (or temperature) calibration factors were then applied to the indicated millivolt outputs:

1. Vertical Load (Channel 2):

$$S_v = 36.81 \text{ lbs/mv.}$$

2. Horizontal Load (Channel 3):

$$S_h = 8.40 \text{ lbs/mv.}$$

3. Near Side Wheel Temperature (Channel 4):

$$S_{T_n} = .68\ ^{o}\text{F/mv. for mv} < 270$$

$$= .22\ ^{o}\text{F/mv} + 125^{o}\text{F for mv} > 270$$

4. Far Side Wheel Temperature (Channel 5):

$$S_{Tf} = 0.5\ ^{o}\text{F/mv. for mv} < 400$$

$$= 0.21\ ^{o}\text{F/mv.} + 116^{o}\text{F for mv} > 400.$$

The force and temperature values thus derived are tabulated for reference as Appendix E of this report. Side load (in millivolts), vertical load, horizontal load, near side wheel temperature and far side wheel temperature are tabulated for all test runs (1-58) on a wheel by wheel basis. Note that force measurements apply to one side of the test consist only, depending on the direction in which the consist was headed. In all cases, the "Near Side Wheel Temperature" is the temperature rise above ambient of the wheel which passes over the reaction rail, and the "Far Side Wheel Temperature" is the temperature rise above ambient of the opposite wheel on that same axle.

No data (n.d.) entries in Appendix E represent points missing from the actual strip chart or pen deflections which are unintelligible. The strain gage bridge used for side load measurements became non-operational after the first 24 runs, thus no data was recorded for subsequent tests. No data (n.d.) entries usually occur for the last car (Car IV), and are a result of accidentally turning off or otherwise interrupting the chart recorder before all cars had passed over the reaction rail.

The near side IR detector exhibited highly erratic outputs throughout all tests. Since the only difference between the near and far side IR sensors was the lack of a sapphire window, the erratic output was attributed to this fact. The instrument was apparently affected significantly by wind and test consist induced air currents. For this reason, the strip chart recording was difficult to interpret, and data was extracted and tabulated only in a limited number of cases. The far side (Channel 5) IR sensor performed in a much more stable manner. An "a" designation was tabulated for all cases in which the IR sensor did not produce any output, therefore indicating ambient, or background temperature. A dash (-) indicates that the erratic behavior of the sensor resulted in an unintelligible temperature indication.

Field calibration checks were made periodically throughout the tests by bringing the test consist to a stop and measuring wheel tread temperatures with a pyrometer. These wheel temperature measurements are presented in parenthesis to the right of the last column of each wheel data set of Appendix E.

3.3.3.2 Interpretation of Field Test Data

Figure 23 shows typical chart recordings for vertical and horizontal forces recorded at a chart speed of 25 mm per second. The height of the vertical force peak was read at its maximum point. For cases where 60 cycle noise was present, the "zero" trace was taken to be the visual average of the noise and the peak value was also appropriately reduced by one-half of the average noise level. For cases where the vertical force peak did not return exactly to previous zero, the center of the imaginary line connecting the "before" and "after" zero level was taken to be the actual zero.

A scale calibrated in chart divisions was prepared on vellum and used as an overlay for each vertical peak. The overlay zero was visually

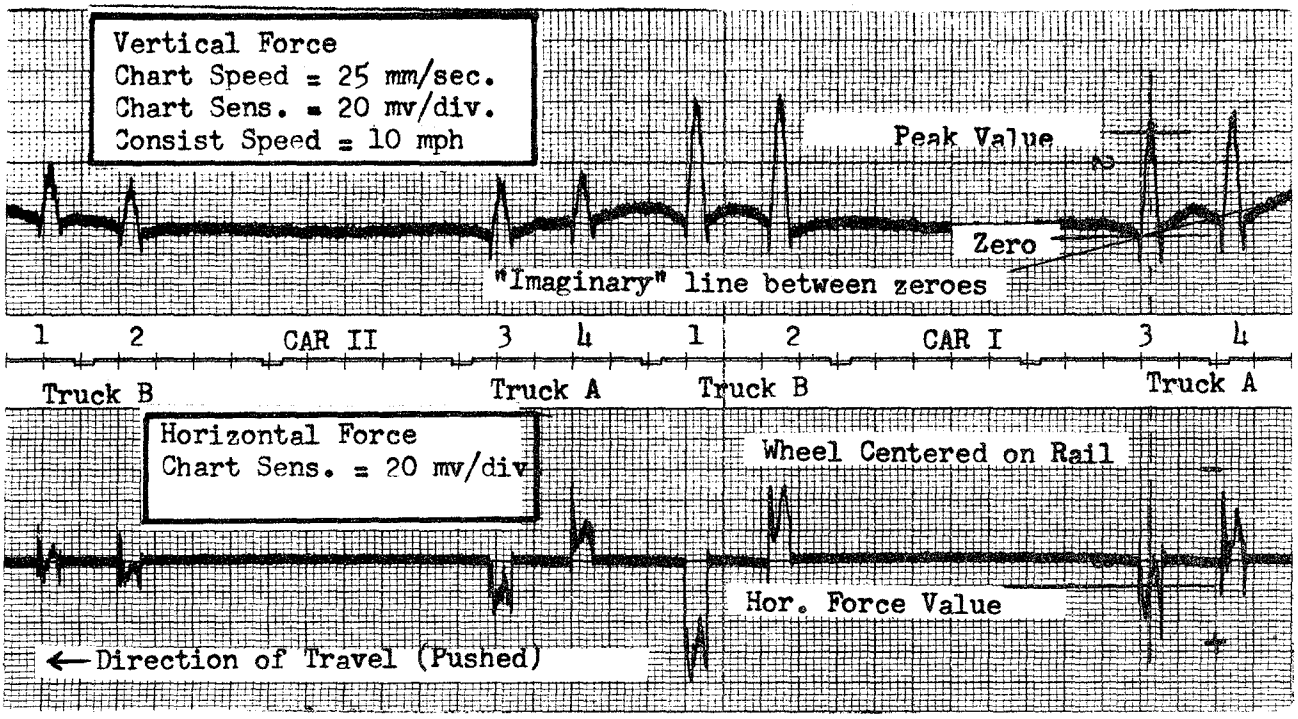

Interpretation Procedure:

1. Determine vertical force zero by drawing imaginary line between the center of the "before" and "after" zero trace. The actual zero is taken to be at the intersection of this line with the vertical peak center-line, which is the point at which the wheel is exactly centered on the reaction rail.

2. Determine the vertical force peak value by subtracting one-half of the 60 cycle noise superimposed on the zero trace (here it is a total of two chart divisions) from the indicated maximum value.

3. Extend the wheel/rail center-line from the well defined vertical force peak to the lesser defined horizontal trace. Determine horizontal force zero as in Step 1.

4. Determine horizontal force value at the point where center-line intersects the actual trace.

Note: The event trace between charts indicates a pulse every second. Chart speed can be deduced from this information.

FIGURE 23

ILLUSTRATION OF VERTICAL AND HORIZONTAL FORCE INTERPRETATION FROM RAW DATA

situated at the average chart zero and vertical force peak height read directly from the overlay. Appropriate visual compensation was made for noise superimposed on the trace at both its zero and peak. This overlay method allowed rapid determination and tabulation of indicated vertical forces for all wheels of all cars.

Vertical force indications were rounded to the nearest whole chart division (20 millivolts) and recorded directly as force by reference to a previously prepared chart division to force conversion table. The calibration constant used was 736.2 lbs/div., derived from the vertical transducer sensitivity of 36.81 lbs/mv. and the chart recorder sensitivity of 20 mv./div.

Considering the rounding process and the fact that visual interpolation of the indicated zero and peak height was necessary, the resulting reduced data is estimated to be accurate to ± 1 chart division, or ± 736 lbs. This interpretation error can be considered to be constant over the range of measured wheel weights, and independent of vertical force peak height.

Interpretation of the horizontal force values was made in a similar manner, but was more difficult because the point at which the car wheel passes directly over the rail section center is not well defined. In the previous case of vertical force, the indicated force is a maximum precisely at the point where the wheel passes over the rail center. For horizontal forces, there is a vertical-load-induced readout which is a maximum when the wheel just hits and leaves the reaction rail. The correct horizontal force readout occurs when the wheel is centered on the reaction rail, but at that point, the transducer output is changing rapidly.

In order to tabulate horizontal force data, the corresponding vertical force peak was used to identify the exact point at which the wheel passed reaction rail center. The horizontal force trace was then intersected at this point and the horizontal reaction taken to be the recorder pen deflection from zero to the intersection. Again, exact zero trace position was not always evident, so visual interpolation was required. Horizontal force pen deflection was rounded off to the nearest whole number of chart divisions and tabulated directly as force using a previously prepared chart division to force conversion table. Braking forces are tabulated as positive, and driving or tractive forces are tabulated as negative.

Because of the difficulty in precisely determining the horizontal force value at the reaction rail center, rounding of pen deflections to the nearest full division, and visual zero trace interpolation, the horizontal forces reported herein may be in error by as much as ± 2 chart divisions. As was the case with vertical force interpretation error, this error can be considered to be constant over the entire range of indicated horizontal forces, thus will be greatest (percentage-wise) at the lower force values.

Vertical force, horizontal force, near side wheel temperature and far side temperature were compiled separately for all wheels of the test consist on a run-by-run basis. The data were then tabulated on a wheel-by-wheel basis and presented in Appendix E.

3.3.4 Static Measurements Performed on Test Consist

Following prototype verification tests at Pueblo, TTC performed the following static measurements on the test consists:

1. Test car dimensions
2. Test car weights
3. Brake pad forces as a function of pressure reduction.

These measurements are presented in Appendix D. The test car weights were used to establish the dynamic vertical load calibration factor used in analyzing weight results (See Section 3.3.1).

3.4 Test Data Analysis Plan

The data obtained during field tests at TTC was analyzed to reach conclusions as to each of the five verification test objectives stated in Section 3.1. Sections 3.4.1 through 3.4.5 describe the analysis required to achieve each of the five objectives. Specific results of the analysis and discussion of the results are presented in Section 3.5.

Time and resource limitations precluded detailed analysis of each wheel to the degree possible with the existing data. As the data reduction and analysis proceeded, it became obvious that many factors influenced measured quantities and that sensitivity and second order effect analyses could be performed ad infinitum. So as not to discourage further investigations based on the results reported herein, all data for all test runs is presented in Appendix E. The data as tabulated in that Appendix is subject to the potential interpretation errors as described previously in Section 3.3.3.2.

There are some areas in which the desired analysis can not be carried out, at least quantitatively, as a result of inadequate data. Thus one important outcome of the current work is a clearer understanding of the type, quantity, and quality of data to be acquired in future testing and system evaluation.

3.4.1 Test Objective 1 - Data Analysis

Test Objective 1 was:

> To demonstrate that the Brake Inspection System hardware developed under Phase I of the program would in fact indicate car weight and braking effort on a wheel-by-wheel basis.

The purpose of this particular analysis is to evaluate the Brake Inspection System concept as a whole. The feasibility of the system as designed will be investigated without concern for the quantitative details of its performance (analyzed in depth in subsequent sections).

The procedure to be used for analyzing Objective 1 will be one of identifying overall system problems which were encountered, and describing alternate solutions to each. Analysis and results are discussed in Section 3.5.

3.4.2 Test Objective 2 - Data Analysis

Test Objective 2 was:

> To determine the accuracy and repeatability of the reaction rail sub-system in indicating vertical wheel force (weight) and horizontal wheel forces (braking effort).

Reaction rail accuracy is defined as the difference between indicated force values and actual force values expressed as a percentage of full scale sensor capacity. For weight measurements, the indicated weight is taken to be the mean value of all test data recorded for a particular wheel. The actual weight is taken to be one quarter of the actual truck weight as measured on a static scale.

The reaction rail evaluated during these tests has no provision for absolute calibration, thus it must be calibrated in place using known quantities as secondary standards. Since vertical force measurements are intended to be used as axle weight indication, it makes sense to calibrate the vertical force sensor using axles of known (static) weight. The output of the system under dynamic conditions can thus be related to the static weight as measured on an accurate scale. Vertical force or weight "accuracy" will then be a measure of how closely the reaction rail, once calibrated,

indicates the correct static weight of many different wheels (under similar test conditions). Vertical force (weight) "repeatability" will be a measure of how closely the indicated weight is repeated on the same wheel on subsequent passes, under similar conditions. Although data exists to make such a determination, detailed data on all factors which might have an effect on indicated weight (wind speed and direction, individual truck dynamic characteristics, etc.) does not exist.

The analysis methodology used to determine vertical force measurement accuracy and repeatability is as follows:

1. Using a derived calibration factor (36.81 lbs/mv as calculated in Section 3.3.1), wheel weights were determined based on vertical LVDT millivolt outputs. Appendix E presents the vertical force measurements calculated using this factor.

2. The indicated weights of each wheel were averaged over the first twelve (non-braked) test runs.

3. Absolute dynamic weighing accuracy was calculated as the percentage variation of the mean indicated weight from the actual (static) weight as measured on a scale.

4. Accuracy as a percentage of full scale was calculated as the difference between indicated and actual truck weights as a percentage of reaction rail full-scale rated vertical force capacity (40,000 lbs.).

5. Repeatability was determined as the standard deviation from the mean of indicated wheel weights for the various runs made.

Analysis of the horizontal force data was complicated by an unanticipated phenomenon which resulted in indicated driving forces on the rail even though braking was applied. An analysis of this effect is presented in Section 3.5.

Since roughly 50 percent of the horizontal force data appeared as driving rather than braking forces, the mean and standard deviation from the mean of horizontal forces exerted by a given wheel from run to run would have no significant physical meaning. Little quantitative analysis of horizontal force data is possible for Runs 1-51, but for Runs 52-58, the rail opposite the reaction rail was greased, which had the effect of eliminating the indicated driving force. For these runs it is possible to calculate horizontal braking reaction as a function of brake pressure reduction, and to look at the deviation of indicated forces for the same brake pressure reduction. These results are presented and discussed in Section 3.5.2.

3.4.3 Test Objective 3 - Data Analysis

Test Objective 3 was:

> To determine the effectiveness of the infrared subsystem in proportioning total axle braking force between right and left wheel brakes.

Since wheel temperature depends not only on how "hard" the brakes are applied, but also on how long they have been applied, ambient temperature, wind speed, and absolute wheel temperature alone are not reliable indicators of instantaneous brake performance. Recognizing this fact, the Brake Inspection System was designed with the thought that relative, rather than absolute, wheel temperatures could be used to differentiate between the right and left side brake effectiveness. The single reaction rail would measure the absolute braking effort at the wheel/rail interface, while the relative (right to left) wheel temperatures would be used to deduce the absolute braking effort of the other wheel. Since both wheels are assumed to have undergone identical braking and environmental histories, their relative temperatures should be an accurate indicator of instantaneous brake performance.

Existing field test data is not sufficient to directly evaluate this right-to-left wheel brake effort proportioning concept since there was only one reaction rail used. Furthermore, safety considerations precluded the "rigging" of the brake system such that the right side was braked while the left was not. One indirect comparison which can be made includes right versus left wheel temperatures for axles which show significantly different braking reactions from right to left as measured on runs when the consist is traveling in different directions. The runs to be compared will necessarily have been made on different days, thus a source of experimental uncertainty exists.

3.4.4 Test Objective 4 - Data Analysis

Test Objective 4 was:

> To demonstrate the effects on indicated weight and braking force of:
>
> a. Consist velocity
> b. Normal air brake application
> c. Consist orientation
> d. Type of brake shoe
> e. Brake modifications (cut out, dragging hand brake, etc.)

Investigation of the various effects of the many test variables on indicated weight and brake effort is an area in which much time can be spent searching for significant correlations. The analysis performed herein to determine measurement system sensitivity to test variables are only those which are really apparent. The railcar/track/environment interaction is an extremely complex one, and a complete analysis of this interaction based on test data obtained is beyond the scope of the present work.

The basic analysis plan was to calculate the mean and standard deviation of various combinations of test data obtained under different test conditions. It is here that a test variable matrix such as that presented in Table 3 is helpful in isolating similar combinations of test runs for comparison.

Variations in the mean value of a measurement (weight, braking, temperature) as a function of a single test variable (speed, brake reduction, orientation) define the effect of that variable on that measurement. The standard deviation of results within a single set of test conditions indicates how well all other variables are "held constant".

Analyses performed and discussed in more detail in Section 3.5 include:

1. Average wheel weight, all runs
2. Average wheel weight, push versus pull
3. Average wheel weight, left versus right
4. Average wheel weight, braked versus non-braked
5. Average wheel weight versus speed
6. Average horizontal force versus applied braking
7. Average horizontal force versus speed
8. Average horizontal force, push versus pull
9. Wheel temperatures versus applied braking
10. Wheel temperatures versus brake shoe type.

3.4.5 Test Objective 5 - Data Analysis

Test Objective 5 was:

> To identify measurements characteristic of brake system malfunction as postulated in Section 2.1.3, thereby gaining a preliminary look at the diagnostic capability of the Brake Inspection System.

The tests performed did not contain a great number of simulated brake system malfunctions. The single most important malfunction, total brake failure, was simulated by cutting out brake pressure to a car such that no braking could be applied to the wheels of that car.

Analysis of data toward the objective of diagnosing brake system malfunctions can be expressed only in terms of the system's capability to measure applied braking effort. Qualitative estimates of the effect of various malfunctions can be estimated, but actual simulations would be required to determine system outputs due to specific malfunctions.

3.5 Discussion of Field Test Data, Data Analysis and Results

3.5.1 Vertical Force Measurements

Vertical force measurements recorded during field tests were very consistent and easily interpreted. Figure 24a shows the vertical force trace for the entire consist pulled over the rail at 20 mph. The trace is compressed by using a relatively slow chart speed of 5 mm per second. Since the consist is pulled, the vertical force peaks for the locomotive are sensed by the rail first, thus the direction of motion is evident from the chart.

Inspection of Figure24a reveals that there is an indicated vertical force just prior to and just after a wheel passes over the reaction rail. This phenomenon can be explained by recalling that the base of the reaction rail is integrated very firmly with the existing rail. Furthermore, there is no special base preparation for the reaction rail (such as a concrete pad) so it is free to conform to any shape imposed upon it by the existing rail. Figure 23a depicts the case where a wheel load occurs both ahead of and just past the reaction rail, but no wheel is on the rail itself. Notice also that the same general situation will occur with a wheel on only one side of the reaction rail, as is the case when the rail is approached by the locomotive or left by the last car.

The span of track between adjacent wheels will tend to flex up as shown in the diagram. Since the base of the reaction rail is integrally tied into the main rail system, the base of the reaction rail will tend to flex upward to conform with the curvature of the main rail. As the reaction rail base flexes upward, the vertical force LVDT senses a relative deflection which is identical in direction to that sensed when a wheel is actually on the center of the reaction rail. Since the flexural stiffness of the instrumented rail base is greater than that of the instrumented rail sections the indicated vertical force is much less.

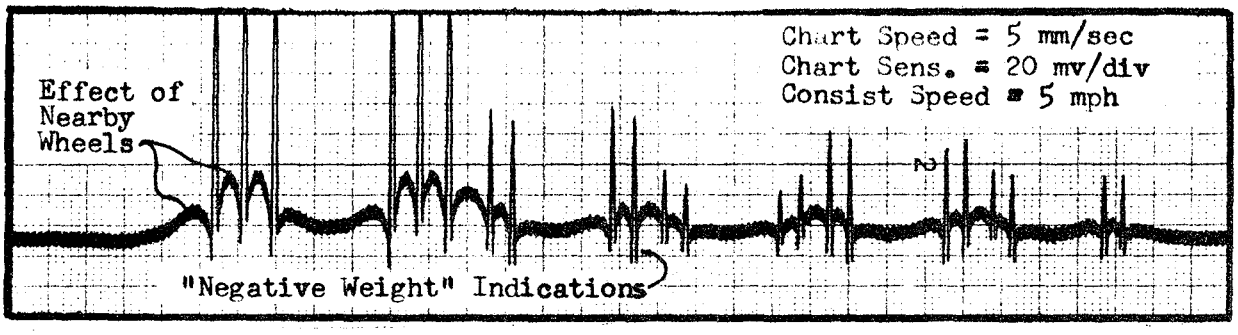

FIGURE 24a

TYPICAL VERTICAL FORCE TRACE FOR ENTIRE TEST CONSIST

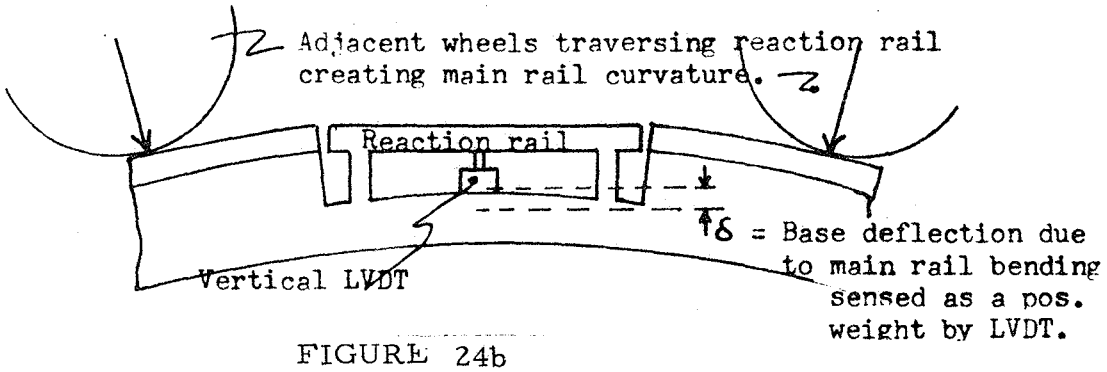

FIGURE 24b

INFLUENCE OF NEARBY WHEELS ON VERTICAL FORCE INDICATION

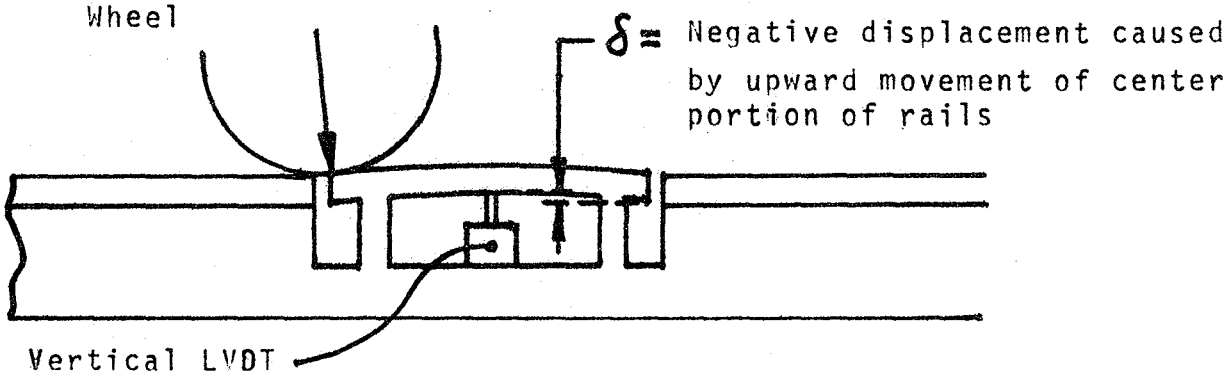

FIGURE 24c

NEGATIVE DISPLACEMENT EFFECT OF WHEEL ON END OF REACTION RAIL

Notice also that the vertical force output indicates negative weight just as the wheel contacts the reaction rail, and again just as the wheel leaves. Figure 24c shows (highly exaggerated) the case of a wheel just contacting the rail, before it has moved into the central span which is supported by the two flexure members. Here the bending moment applied to the reaction rail is opposite that applied when the wheel is centered. The resultant deflection as measured by the vertical LVDT is such that a negative force is indicated.

Several measures can be taken to eliminate the two spurious signals discussed above. The first method is to automate data acquisition in such a manner that both the "approaching wheel" and the "negative weight" phenomena are electronically suppressed. This is essentially what has been done in the manual data analysis and interpretation described in this report. An automated system would take the peak value for vertical force to be the average between upward and downward excursions. The initial and final "negative weight" peaks would be ignored.

Methods for physically eliminating the above phenomena would be expensive, and might possibly create more problems than they would solve. The effects of approaching and leaving wheels might be eliminated by building the reaction rail into a rigid (concrete) pad extending 15 feet before and after the rail. (Reference to Figure 24a shows that the locomotive influence shows up approximately 10 chart divisions prior to the first wheel actually contacting the instrumented rail. Since the chart speed is 5 mm per second and the consist velocity is 5 miles per hour, the calculated "influence" distance is 14.6 feet.) In addition to the expense of such an undertaking, reaction rail reliability might suffer because of the more intense load environment it would be subject to without a compliant base. The negative force peaks experienced as the wheel just contacts and just leaves the reaction rail could be eliminated by instrumented redesign, with no rail head overhang beyond the flexure members.

Because of the consistency of vertical force (weight) measurements and known car weights, "accuracy" of the vertical force measuring capability of the reaction rail can be determined. Table 6 compares the average indicated truck weights (average of the first twelve runs) with actual measured truck weights and shows accuracy both as a percentage of actual measurement, and as a percentage of reaction rail full scale (40,000 lbs/wheel). Absolute accuracy is seen to be within 6 percent for all trucks, and full-scale accuracy to be better than 2 percent. Table 7 compares actual weights (as weighed on scale) on each car to the indicated car weights which were calculated by adding the wheel weight for all four wheels and multiplying by two to account for the other (right or left) side. As might be expected,

TABLE 6

VERTICAL FORCE MEASUREMENT ACCURACY

Car	Truck	Average Indicated Weight (1) (lbs)	Actual Weight (lbs)	Absolute Accuracy (%)	Full-Scale Accuracy (2) (%)
I	A	50,553	50,000	1.1	0.35
	B	54,478	51,400	6.0	1.92
II	A	22,454	22,380	0.3	.05
	B	21,840	22,560	3.2	.45
III	A	40,982	39,400	4.0	.99
	B	36,810	37,820	2.7	.63
IV	A	24,048	24,520	1.9	.29
	B	24,094	24,780	2.8	.43

1. Sum of wheel weights indicated for truck times two to account for right and left sides. Calibration factor used was 36.81 lbs/mv. Indicated weight for each wheel is the average value for the first twelve test runs.

2. Full scale accuracy based on a rated vertical force capacity of 40,000 lbs/wheel.

TABLE 7

VERTICAL FORCE MEASUREMENT ACCURACY - ENTIRE CAR

Car	Average Indicated Weight (lbs) [1]	Actual Weight (lbs) [2]	Absolute Accuracy (%)	Full-Scale Accuracy (%) [3]
I	105,011	101,420	3.5	1.12
II	44,294	45,020	1.6	.23
III	77,792	77,140	0.8	.20
IV	48,142	48,068	0.2	.02

1. Sum of all four individual indicated wheel weights times two to account for right and left sides. Calibration factor used was 36.81 lb/mv. Indicated weight for each wheel is the average weight for the first twelve runs.

2. Actual weight obtained from independent scale measurements. Entire car weights are separate measurements from the individual truck weights shown in Figure 30, thus the sum of actual truck weights may not exactly equal actual car weights due to scale inaccuracies.

3. Full scale accuracy based on a rated vertical force capacity of 40,000 lbs/wheel.

the accuracy of total car weight measurement is better than individual truck weighing accuracy. This is so, because the total car weight (as measured dynamically) averages out any weight transfer from truck to truck which might be occurring as a result of car motion. Since data was not taken as to dynamic motions of the cars during test runs, the effects of dynamic truck-to-truck weight transfer cannot be quantified.

Repeatability of vertical force measurements is meaningful only when applied to data obtained under similar test conditions. For this reason, discussion of repeatability is deferred until after presentation of the various sensitivity analyses. Where mean values for vertical forces are presented, the standard deviations are listed in parentheses directly after or below those values. These standard deviations are themselves indicative of vertical force repeatability for the various test run conditions for which they are calculated.

Thus far vertical forces have been discussed in terms of the weight averaged over the first twelve runs. These test runs were all non-braked runs made at various consist speeds and alternated between forward (pull) and reverse (push) directions. Table 8 compares the mean wheel weight as calculated for the first twelve runs to the mean wheel weights calculated for all runs. Table 8 can be viewed as a braked versus non-braked comparison. There is no apparent pattern to the deviation of average wheel weight for all runs from that of the first twelve (non-braked) runs.

If it is assumed that consist dynamics are going to have a significant effect on wheel weights, then it might be hypothesized that indicated weights will vary with braking, with speed, and with whether or not the consist was pushed or pulled by the locomotive. Table 9 compares the "push" runs to the "pull" runs for wheel weight averages of all runs. Note that for 14 out of 16 wheels, the indicated weight is greater by up to 15 percent for the pushed cars. For the two wheels which show pulled weight to be greater than pushed weight, the difference is less than 1 percent. A check on the influence of the direction (north or south) in which the consist was being pulled or pushed was made on Wheel 3 of Car III. For the case in which the cars were pushed to the north (18 runs), the "pushed" wheel weight exceeded the "pulled" wheel weight by 14.7 percent. For the case in which the cars were pushed to the south (7 runs), the "pushed" wheel weight exceeded the "pulled" weight by 10.1 percent. It would appear that the observed phenomenon is in face due to pushing versus pulling, and that forces are transmitted through the couplings during "pushing" in such a manner as to increase the apparent weight of the cars.

TABLE 8

COMPARISON OF MEAN WHEEL WEIGHTS FOR FIRST TWELVE RUNS TO MEAN WHEEL WEIGHTS FOR ALL RUNS

Note: Standard deviations are shown in parentheses below each indicated wheel weight.

Car	Truck	Wheel	Mean Weight First 12 (lbs)	Mean Weight All Runs (lbs)	Deviation of First 12 from All Runs
I	A	4	12,393 (690)	11,888 (1884)	+ 4.2 %
		3	12,883 (1646)	12,087 (2057)	+ 6.6 %
	B	2	14,294 (1552)	14,212 (1653)	+ 0.6 %
		1	12,945 (1349)	12,815 (1103)	+ 1.0 %
II	A	4	5,828 (1194)	5,715 (921)	+ 2.0 %
		3	5,399 (725)	5,590 (672)	- 3.5 %
	B	2	5,214 (379)	5,528 (632)	- 5.7 %
		1	5,706 (637)	5,802 (821)	- 1.7 %
III	A	4	9,755 (637)	9,770 (1158)	- 0.2 %
		3	10,736 (1385)	10,544 (1519)	+ 1.8 %
	B	2	9,202 (1017)	9,692 (1166)	- 5.1 %
		1	9,202 (1195)	9,062 (1288)	+ 1.5 %
IV	A	4	5,828 (584)	6,199 (606)	- 6.0 %
		3	6,196 (663)	6,174 (664)	+ 0.4 %
	B	2	6,024 (444)	6,192 (726)	- 2.7 %
		1	6,024 (553)	6,192 (592)	- 2.7 %

TABLE 9

COMPARISON OF MEAN WHEEL WEIGHTS FOR ALL PULLED RUNS TO MEAN WHEEL WEIGHTS FOR ALL PUSHED RUNS

Note: Standard deviations are shown in parentheses below each indicated average wheel weight.

Car	Truck	Wheel	Mean Weight All Pulled Runs (lbs)	Mean Weight All Pushed Runs (lbs)	Relation of Pushed Weight to Pulled Wt.
I	A	4	11,628 (955)	12,679 (1406)	+ 9.0 %
		3	11,584 (1336)	13,193 (1123)	+ 13.8 %
	B	2	13,598 (1787)	15,048 (976)	+ 10.7 %
		1	12,299 (841)	13,517 (1039)	+ 9.9 %
II	A	4	5,404 (1252)	5,948 (924)	+ 10.1 %
		3	5,435 (628)	5,801 (683)	+ 6.7 %
	B	2	5,521 (684)	5,536 (567)	+ 0.3 %
		1	5,738 (902)	5,890 (705)	+ 2.6 %
III	A	4	9,775 (1199)	9,747 (1120)	- 0.3 %
		3	9,939 (1407)	11,367 (1277)	+ 14.4 %
	B	2	9,700 (1325)	9,688 (943)	- 0.1 %
		1	8,568 (1234)	9,877 (893)	+ 15.3 %
IV	A	4	6,068 (611)	6,380 (561)	+ 5.1 %
		3	5,912 (624)	6,534 (545)	+ 10.5 %
	B	2	6,063 (770)	6,392 (527)	+ 5.4 %
		1	5,998 (605)	6,492 (433)	+ 8.2 %

34 test runs were "pulled" 25 test runs were "pushed"

Table 10 presents indicated weights of Truck B of Car I as a function of consist velocity. Only non-braked runs are considered, and they are broken down into subsets of "pushed" weight versus "pulled" weight and test consist velocity. There is no apparent correlation of indicated weight to speed from these results.

Table 11 presents indicated weights as a function of brake pressure reduction for both ends A and B of Car I at one consist velocity, 10 mph. Again, there is no apparent relationship, but for the cases considered, the indicated weight seems to drop slightly under light braking (6 psi reduction) and rise again under moderate to heavy braking (11-15 psi reduction).

While the areas of indicated weight sensitivity to consist speed, orientation, and applied braking are necessary to understand the measurement dynamics of the instrumented rail, it was decided that the data obtained during these field tests was not sufficient to fully analyze any such dependency. In many cases there is only one test run for the conditions under investigation. The relation between consist dynamics and indicated reaction rail forces is clearly a complex one, and any data collected to validate this relationship should be preceded by a detailed dynamic analysis and modelling effort. Only in this manner will all relevant variables be identified and data collected.

3.5.2 Horizontal Force Measurements

Expected horizontal forces as a result of rolling resistance and applied braking were analyzed in Section 2.1.1. The analysis indicated that both rolling resistance, M_o, and braking retardation, F_R, would show up as positive horizontal force indications by the reaction rail. Recorded field test data showed a completely unexpected result in that a great number of the indicated horizontal force peaks were negative, indicating not a braking force, but a "driving" force. Figure 23 shows this effect where horizontal force peaks below the zero line indicate braking and force peaks above the zero line indicate tractive, or driving reactions. One of the peaks appears right on the zero line and would have to be considered a net zero horizontal force.

Reference to the horizontal reaction data of Appendix C shows that 55 percent of the indicated wheel horizontal reactions for the first twelve (non-braked) test runs were "braking" reactions, 41 percent were "driving" reactions, and 4 percent were net zero reactions. For the second twelve (braked) test runs, the braked reactions increased to 60 percent with 40 percent driving reactions and 10 percent net zero reactions. The phenomenon of apparent driving reaction even though brakes were applied was clearly a significant occurrence.

TABLE 10

INDICATED WEIGHT SENSITIVITY TO SPEED

Car I (DOTX-502)
Truck B; Wheels 1,2; Right Side
No applied braking

CASE I: PULLED RUNS

Run No.	Indicated Weight 2	Indicated Weight 1	Truck Weight	Consist Speed
1	13,988	11,779	25,767	10 mph
3	13,988	12,410	26,398	or
5	13,988	13,252	27,240	less
Ave.	13,988	12,480	26,468	
7	15,460	11,779	27,239	20 mph
49	13,988	12,515	26,503	
51	15,460	12,515	27,975	30 mph
Ave.	14,724	12,515	27,239	
9	11,043	10,307	21,350	
45	12,515	12,515	25,030	40 mph
Ave.	11,779	11,411	23,190	
11	13,252	13,988	27,240	
47	14,724	12,515	27,239	60 mph
Ave.	13,988	13,252	27,240	

CASE II : PUSHED RUNS

2	14,724	13,988	28,712	
4	14,724	13,252	27,976	10 mph
6	15,460	14,724	30,184	or
48	14,724	13,988	28,712	less
Ave.	14,908	13,988	28,896	
8	15,460	11,779	27,239	
46	16,196	13,988	30,184	20 mph
Ave.	15,828	12,884	28,712	
50	13,988	13,988	27,976	30 mph
10	15,460	13,252	28,712	40 mph
12	14,724	11,779	26,503	60 mph

TABLE 11

INDICATED WEIGHT SENSITIVITY TO BRAKING

Car I (DOTX-502)
Truck B; Wheels 1,2 ; Right Side ; Consist Velocity 10 mph

Run No.	Indicated Weight 2	Indicated Weight 1	Truck Weight	Brake Reduction
CASE I : PULLED RUNS				
5	13,988	13,252	27,240	0 psig
13	14,724	11,569	26,293	6 psig
15	14,724	12,515	27,239	
53	14,724	11,779	26,503	15 psig
Ave.	14,724	12,147	26,871	
CASE II : PUSHED RUNS				
6	15,460	14,724	30,184	
48	14,724	13,988	28,712	0 psig
Ave.	15,092	14,356	29,448	
57	14,724	13,988	28,712	6 psig
14	16,196	13,988	30,184	
52	14,724	14,724	29,448	11 psig
Ave.	15,460	14,356	29,816	
Truck A; Wheels 3,4 ; Right Side ; Consist Velocity 10 mph				
CASE I : PULLED RUNS				
5	13,252	13,252	26,504	0 psig
13	11,043	11,779	22,822	6 psig
15	11,779	13,988	25,767	
53	11,779	13,254	25,033	15 psig
Ave.	11,779	13,621	25,400	
CASE II : PUSHED RUNS				
6	12,515	13,252	25,767	
48	13,252	12,515	25,767	0 psig
Ave.	12,884	12,884	25,767	
57	13,252	12,515	25,767	6 psig
14	12,515	12,515	25,030	
52	13,252	13,252	26,504	11 psig
Ave.	12,884	12,884	25,768	

It was postulated from preliminary recorded data that this effect was due to torque build-up in the axle in such a manner as to re-distribute the braking reaction between the two wheels on that axle. In many cases, the torque build-up would be such that a negative, or driving, reaction would occur at one wheel. Since there was only one reaction rail, it would see both braking and driving force indications as the wheels passed. To test this hypothesis, heavy grease was applied to the rail opposite the reaction rail for Test Runs 52-58. The hypothesis was confirmed when all subsequent horizontal force reactions indicated braking rather than driving. The torque build-up in the axle could not take place because wheels opposite the reaction rail would slip. Therefore the entire axle braking effort showed up as braking on the reaction rail.

Torque build-up in the axle can be explained in terms of right-to-left differences in effective wheel tread diameters. The "effective" wheel tread diameter is the diameter at which the adhesive force, F_A, between the rail and the wheel acts. Since railcar wheels are tapered, this effective diameter may vary as the truck moves laterally, or as the wheel flange comes into contact with the inner side of the rail. Figure 24 depicts the case where two wheels on the same axle are of different (highly exaggerated) effective radii. The radius of wheel 1 is greater than the radius of wheel 2.

Assume that both wheels roll without slipping as they are pulled at constant velocity, V, in the direction shown in the diagram. Under these conditions, wheel 1 will tend to rotate with an angular velocity $w_1 = V/R_1$; and wheel 2 will tend to rotate at angular velocity $w_2 = V/R_2$. As Equation 13 shows, this difference in angular velocity from wheel to wheel causes wheel 2 to rotate through a greater angle $\Delta\theta_2$, in a given period of time than does wheel 1.

$$\frac{W_1}{W_2} = \frac{\Delta\theta 1/\ t}{\Delta\theta_2/\ t} = \frac{\Delta\theta 1}{\Delta\theta_2} = \frac{V/R_1}{V/R_2} = \frac{R_2}{R_1} \qquad (13)$$

If the consist velocity, V, is written as $\Delta x/\Delta t$, then the net difference in angle traversed by wheels 1 and 2, $(\Delta\theta_2 - \theta_1)$, can be expressed as a function of wheel radii and linear distance travelled down the track by the wheel.

$$W_2 - W_1 = V\left(\frac{1}{R_2} - \frac{1}{R_1}\right) = \frac{\Delta x}{\Delta t}\left(\frac{1}{R_2} - \frac{1}{R_1}\right) = \frac{\Delta\theta 2 - \Delta\theta 1}{\Delta t} \qquad (14)$$

$$\Delta\theta_2 - \Delta\theta_1 = \Delta x \left(\frac{1}{R_2} - \frac{1}{R_1}\right) = \Delta\phi \qquad (15)$$

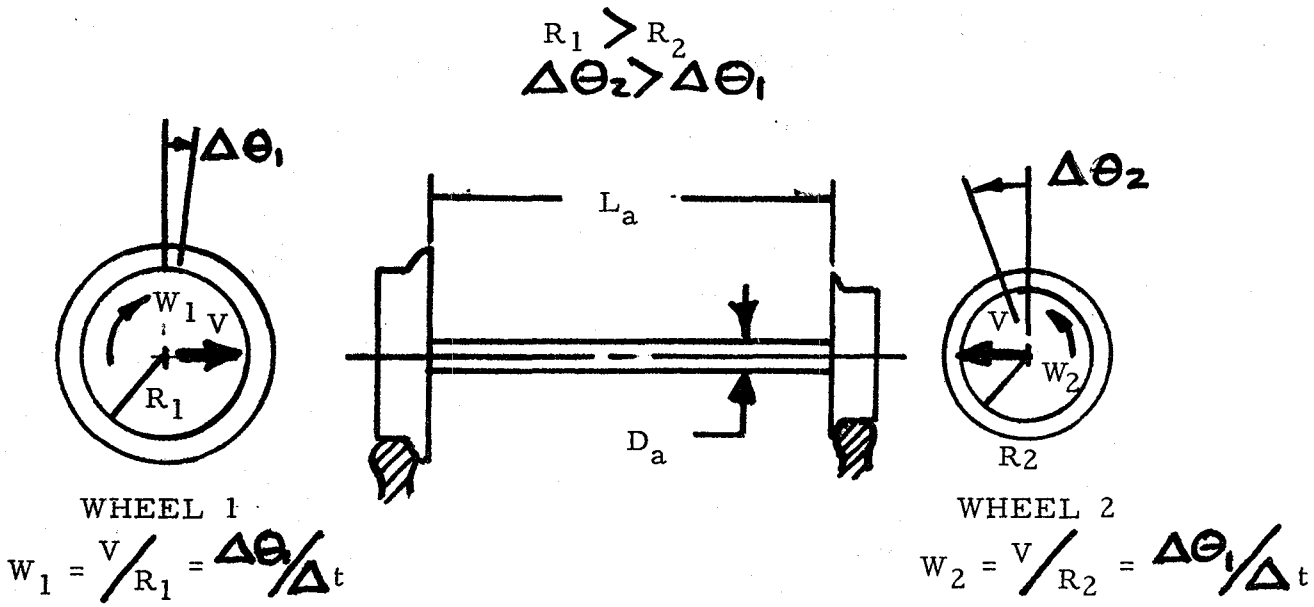

FIGURE 25

WHEEL AND AXLE NOMENCLATURE

F_R = Retarding Force of Brake

F_A = Adhesive Force at Wheel/Rail Interface.

M_o = Initial Rolling Resistance

T = Torque Build-up in Axle

NOTE: All forces passing through the axle center are omitted.

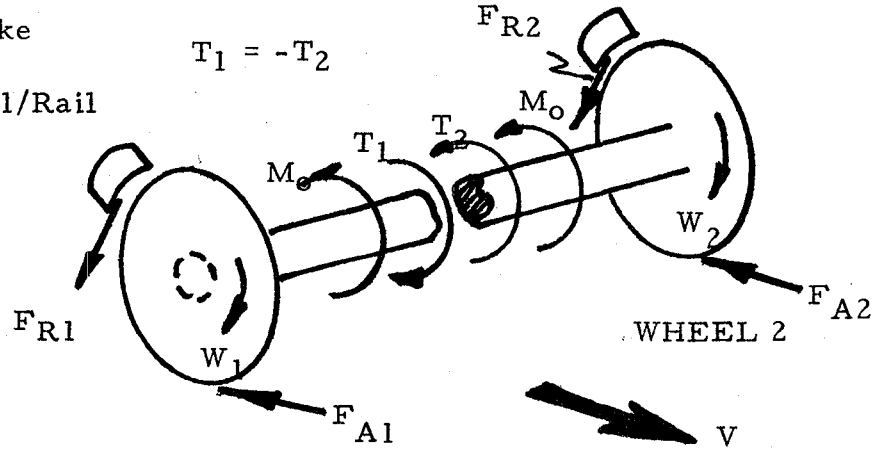

FIGURE 26

FREE-BODY DIAGRAM OF AXLE

The difference in angular traverse between wheels is defined as and is the angle which must be taken up by twist in the axle. The torque build-up due to this imposed angular twist can be written as:

$$T = \frac{GJ}{L_a} \Delta\phi = \frac{GJ}{L_a} \left(\frac{1}{R_2} - \frac{1}{R_1} \right) \tag{16}$$

where: T = Torque in axle, (in-lbs)

L_a = Axle length (in)

G = Shear modulus for axle material (lbs/in^2)

J = Polar moment of inertia for axle cross-section (in^4)

($\frac{\pi D_a^4}{32}$ for solid axle, where D_a = axle diameter).

The analysis of Section 2.1.1 must then be modified to account for this additional torque imposed by one wheel of an axle upon the other. In order to do this, both wheels must be considered simultaneously. Figure 26 is a free body diagram of both wheels of a single axle. All forces not contributing to moments about the axle are omitted, since they do not figure in the braking reaction force.

A summation of moments about the center of each wheel in the same manner as Equation 1, and subsequent re-arrangement of terms yields the following expressions for the adhesive force, F_a, at the wheel/rail interface. The horizontal reaction force, F_h, measured by the reaction rail will then be the negative of F_A, i.e. $F_h = -F_A$.

$$\sum_{\text{wheel 1}} M = M_o + R_1 F_R - R_1 F_{A1} - T = 0 \tag{17a}$$

$$F_{A1} = F_{R_1} + \frac{M_o}{R_1} - \frac{T}{R_1} = F_{h1} \tag{17b}$$

$$\sum_{\text{wheel 2}} M = M_o + R_2 F_{R2} - R_2 F_{A2} + T = 0 \tag{18a}$$

$$F_{A2} = F_{R2} + \frac{M_o}{R_2} \quad \frac{T}{R_2} = -F_{h_2} \tag{18b}$$

Equations 17 and 18 show the following:

1. The smaller effective diameter wheel (wheel 2) will transmit a torque, T, through the axle to wheel 1, causing the adhesive force, F_{A1}, to decrease by the amount T/R_1. When this moment, T, becomes great enough, F_{A1} will actually become negative, thereby appearing as a driving, rather than braking force at the wheel/rail interface.

2. The sum of horizontal reaction forces, F_h, of both wheel 1 and wheel 2 results in a cancellation of T, thus is an accurate indicator of the total brake retarding force acting on that axle.

3. Since the magnitude of T depends on distance travelled, and because it will drop to zero if F_A or F_A reaches the maximum available adhesion on that rail ($F_{Amax} = W \times f_a$), there is no way of telling from reaction rail data only, what fraction of T is showing up on wheel 1 and what fraction is showing up on wheel 2.

4. If two reaction rails were used simultaneously, the total measured brake reaction would be correct, but independent means of determining wheel 1 braking and wheel 2 braking would be necessary. This, of course, is the reason for employing the IR sensor sub-system.

For the car weights used in these tests, typical maximum values for braking or driving forces can be calculated. Car I was the heaviest car, weighing 101,420 lbs (46,100 kg) or roughly 12,500 lbs (5682 kg) per wheel. Using a typical adhesion of 20 percent (good rail at 10 mph), the maximum expected braking (or driving) force would be 2500 lbs (1136 kg). Depending upon the distance from the reaction rail to the point where the axle to be measured last relaxed itself (by slipping), the measured value of horizontal force will fall somewhere between $\pm$ 2500 lbs (1136 kg). The values recorded for horizontal force during these tests cannot be related to actual braking effort because this distance is not known.

Test Runs 52-58 were made with heavy grease placed on the rail opposite the reaction rail. For those runs, it can be assumed that the torque build up in the axle is minimal since the opposite wheel will slip at very low values of applied moment tending to resist rolling. Table 12 shows indicated horizontal (braking) forces for Runs 52-58 broken down by applied brake system pressure reduction. There appears to be a general increase of brake force with pressure reduction. Because of the effects of other variables such as speed and orientation, these results cannot be considered conclusive. Further tests should be made to eliminate uncertainty due to "averaging" in the effects of these variables.

Two general strategies for horizontal brake force measurement using the reaction rail concept appear possible:

1. Use two reaction rails to measure total axle braking force and use another means (IR) of distinguishing brake capability from right side to left side.

2. Use a single reaction rail with a low adhesion opposing rail-segment to relax built-up axle torque by slipping the opposite wheel. This strategy might also be implemented by increasing the adhesion of the reaction rail (e.g., by roughening up the surface), if a permanent method of obtaining that adhesion could be found.

3.5.3 Infrared Measurements

Attempts to correlate the infrared field test data with specific brake performance were not completely successful. The indicated wheel temperatures ranged from ambient (30° F) to approximately 450° F. While there was no close correlation between indicated IR output and applied brake pressure reduction, there were several qualitative observations which indicated that the IR technique used was viable for brake inspection:

1. The sensors indicated no temperature rise above ambient for non-braked wheels. (First twelve test runs)

2. In general, small reductions in brake pipe pressure resulted in a low wheel temperature rise while higher pressure reductions produced greater heating.

TABLE 12

HORIZONTAL BRAKING FORCE AS A FUNCTION OF BRAKE PRESSURE REDUCTION FOR RUNS 52-58

Runs at each reduction level: 6 psig : 57
11 psig : 52 , 54 , 54A
13 psig : 54B , 54C , 55 , 56 , 58
15 psig : 53

Car	Wheel	Indicated Braking @ 6 psi (lbs)	Indicated Braking @ 11 psi (lbs)	Indicated Braking @ 13 psi (lb)	Indicated Braking @ 15 psi (lb)
I	4	252	616	537	504
	3	168	336	504	504
	2	85	448	520	1008
	1	252	952	504	504
II	4	0	451	633	1176
	3	85	784	605	1344
	2	85	563	504	1008
	1	85	952	739	1176
III	4	252	840	807	1680
	3	252	896	723	1176
	2	252	896	840	1344
	1	252	1120	740	1176
IV	4	- 85	168	286	840
	3	252	616	168	672
	2	- 85	124	105	336
	1	252	336	189	504

3. Increasing the distance traveled, with any given brake pipe pressure reduction, caused an increase in wheel temperature.

4. Heavier cars (I and III) showed generally higher wheel temperatures than the lighter cars (II and IV) for a given test run speed and brake reduction. One would expect more energy dissipation (thus higher temperatures) in the wheels of the heavier cars.

The relationship which was sought, but not evident from the field test data, was a close correlation between:

1. Indicated wheel temperature and brake pressure reduction at similar consist speeds.

2. Indicated wheel temperature and consist speed at similar brake pressure reductions.

The infrared sensors were re-checked in the laboratory after field tests and a significant sensitivity of the sensor amplifier to target speed was found. At higher frequencies (speeds), output was lower. This explains in part why many indicated wheel temperatures appeared to drop, even though the consist speed was increased with brake reduction held constant.

A number of problems with the IR sensors were experienced which introduced considerable uncertainty as to the validity of the IR field test data. To summarize:

1. At ambient temperatures below 40° F(°C) the IR amplifiers developed a parasitic oscillation in the power supply. This condition was corrected with the addition of an electric heater.

2. The near side IR sensor (focused on the wheels passing over the reaction rail) exhibited highly erratic behavior, later attributed to the lack of a quartz window to protect the sensor element from the environment (wind, consist induced on currents, etc..).

3. As stated above, the sensor amplifiers exhibited a previously undetected sensitivity to target speed. If this condition was in existence during field tests, then indicated outputs are not simply temperature dependent, but temperature and speed dependent.

These problems can all be overcome by minor equipment re-design, thus the IR sensing technique still appears, conceptually, to be a viable brake inspection method. Although not directly a problem with the IR detectors, conditions at the test site were far from favorable. Ambient temperatures were at times below freezing with occasional snow and high winds. This, in addition to working after dark, made outside measurements and adjustments difficult to accomplish precisely.

4. CONCLUSIONS

4.1 Overall Brake Inspection System

The concepts tested during this project appear to be adequate to measure railcar braking capability on a wheel by wheel basis. Electrical outputs are generated which are proportional to wheel weight, wheel reaction along the track direction, and wheel IR radiation.

Both analysis and testing have shown that a single reaction rail is not capable of providing the brake force indication required, but that two reaction rails would provide an indication of total axle braking. This total axle brake force indication, along with IR information on both wheels should provide sufficient data to determine the quality and extent of braking for each individual wheel.

The test program conducted with the brake inspection hardware was not extensive enough to determine the system diagnostic capabilities beyond the first order ability to sense brake reactions at the rail. Indications are that the reaction rail sub-system, coupled with electronic logic, could diagnose brake system and truck suspension system malfunctions. The apparent sensitivity of the rail to consist dynamics presents the potential for a greater diagnostic capability than originally expected.

A program to determine system sensitivity to, and ability to diagnose specific malfunctions will require an in-depth test program in which the specific malfunctions are simulated and all other test conditions held constant.

4.2 Instrumented Rail Sub-System

The full-scale accuracy of the vertical force measuring transducer was determined to be approximately 2 percent, in spite of a great number of highly influential, uncontrollable, and variable test conditions. The sensitivity of the reaction rail to these conditions (e.g.: consist speed, dynamic characteristics, orientation, etc.) was found to be high standard deviation of indicated measurements about their mean. In some cases, these approached 10% of the measured value.

Absolute accuracy of the horizontal, or braking force measurement could not be determined because of the unexpected result that not all braked wheels exert a braking reaction on the adjacent rail. Because the nature of the horizontal force measuring system is identical to that of the vertical force measuring system (i.e., an LVDT sensed elastic deflection) it would not be expected that the accuracy of that capability would be different from that of the vertical sensor.

Exact determination of the system's accuracy and repeatability was further complicated by the necessity to visually interpret and interpolate test data in which small fixed errors are a significant percentage of the quantity measured. It is believed that automatic data acquisition and manipulation can be implemented at reasonable cost and with a marked increase in system accuracy.

4.3 Infrared Sensor Sub-System

The IR sensor designed, built and tested here performed as expected, and indicated relative wheel temperatures of wheels passing at speeds up to 60 mph. The ability of the device to sense temperatures over such a wide speed range introduced some dynamic problems which detracted from absolute IR measurement accuracy.

The detector used to sense temperatures of wheels passing over the reaction rail experienced stability problems due to the lack of a sapphire window. For this reason, a meaningful correlation between wheel temperatures and brake force measurements by the reaction rail could not be made.

5. RECOMMENDATIONS

The following recommendations are made to both improve the Wayside Brake Inspection design and to better understand the design as it exists today.

1. A comprehensive dynamic analysis of the effects of railcar and consist dynamics on reaction forces transmitted to the rail by the wheels should be made.

2. The reaction rail in its current configuration should be used to assist in developing the analytical model of (1) above, and finally in verifying that model. Such a test program would result not only in a better understanding of the measurement system, but also of train dynamics in general.

3. Further tests should be performed using a two reaction rail inspection system. These tests should be planned to yield statistically significant results in each of the following areas:

   a. Correlation of horizontal and vertical forces and wheel temperatures to specific brake malfunctions, simulated one at a time on the test consist.

   b. Determination of the specific inspection procedures which result in the most consistent and accurate determinations.

4. The reaction rail design should be refined to eliminate some unwanted characteristics (such as the indicated "negative" weight resulting from reaction rail overhanging the flexure members).

5. The infrared detector sub-system design should be refined to eliminate sensor dependency on wheel emissivity and to filter out all other unwanted thermal effects.

6. REFERENCES

1. Federal Railroad Administration, Part 232.1, "Power Brakes, Minimum Percentages." Title 49, Code of Federal Regulations, January 1, 1971.

2. Association of American Railroads, Interchange Rules, 1971.

3. David G. Blaine and Mark F. Hengen, "Brake-System Operation and Testing Procedures and Their Effects on Train Performance," ASME paper No. 71-WA/RT-9, presented November 1971.

4. Franklin G. Fisher, Anthony J. Maiale and Edward L. Rogers, "Computerized Weighing of Railroad Freight Cars Coupled In-Motion," ASME paper No. 66-RR-2, presented May 1966.

5. The Air Brake Association, Engineering and Design of Railway Brake Systems, September 1975.

6. S. Timoshenko and B.F. Langer, "Stresses in Railroad Track," Transactions, ASME, Applied Mechanics, Vol. 54, p. 277, 1932.

7. Y.H. Tse and G.C. Martin, "Flexible Body Railroad Freight Car - Mathematical Model," Technical Documentation, International Government-Industry Research Program on Track-Train Dynamics, 1975, IIRI, Chicago, IL.

8. Marks' Standard Handbook for Mechanical Engineers, Seventh Edition, Edited by Theodore Baumeister, McGraw Hill Book Company, New York, 1967.

9. G.E. Novak, G.E. Dahlman, B.J. Eck and W.J. Kucera, "Thermal Patterns in 36 Inch Freight Car Wheels During Service Tests," presented Dec. 5, 1976 at ASME Winter Annual Meeting, New York.

10. R.J. Roark and W.C. Young, Formulas for Stress and Strain, 5th edition, 1975, McGraw Hill, Inc., New York.

7. BIBLIOGRAPHY

P. W. Abbott, G. Morosow, J. Macpherson; "Track-Train Dynamics," SAE paper 751058, 1975.

Abex Corporation (for Assoc. of Amer. Railroads); "Comparative Performance Test of High-Phosphorus Type and Standard Metal Brake Shoes" Greenville, PA, September-October 1973.

D. R. Ahlbeck, H. D. Harrison, S. L. Noble; "An Investigation of Factors Contributing to Wide Gage on Tangent Railroad Track," ASME Paper No. 75-WA/RT-1, presented at Winter Annual Meeting, Houston, TX, November 1975.

D. R. Ahlbeck, H. D. Harrison, R. H. Prause; "Evaluation of Analytical and Experimental Methodologies for the Characterization of Wheel/Rail Loads," Interim Report, Nov. 1976, for U. S. Dept. of Trans., Fed. Railroad Admin., Report No. FRA-OR&D-76-276.

D. R. Ahlbeck, H. D. Harrison; "Techniques for Measuring Wheel Rail Forces with Trackside Instrumentation," ASME Paper No. 77-WA/RT-9, 1977.

J. R. Anderes; "Analysis of Kansas Test Track Beam Response," Contract No. DOT-FR-54090, PB-271412/9ST.

Association of American Railroads; Track Train Dynamics - Harmonic Roll Series, Volumes 1-4, International Government - Industry Research Program on Truck-Train Dynamics, 1973-74.

Association of American Railroads; Track Train Dynamics - To Improve Freight Train Performance; Report R-122, 1973, Int. Gov.-Industry Research Program on Track Train Dynamics.

Association of American Railroads; Track-Train Dynamics: Phase I, Report No. AAR R-180, 1975.

Association of American Railroads; Instrumentation for Measurement of Forces on Wheels of Rail Vehicles, FRA-ORD&D-85-11; May 1974.

Association of American Railroads; Track Train Dynamics Interaction, Second Conference; Volumes 1,2; 1975.

W.A. Berg, R.H. Alber; "Tread Braking Versus the Wheel," presented at The Air Brake Association Annual Meeting, Chicago, Sep. 18, 1972.

F.B. Blader, E.F. Kurtz, Jr.; "Dynamic Stability of Cars in Long Freight Trains," ASME Paper No. 73-WA/RT-2, presented at Winter Annual Mtg., Nov. 1973, Detroit, MI.

F.B. Blader; "Direct Recording of Wheel-Rail Parameters," Final Report C1GGT-75-13, Oct. 1975, Canadian Institute of Guided Ground Support.

T.P. Brown, J.B. Loach; "Measurement of Dynamic Forces on Track," Railway Gazette, Vol. 120, 10/64, p. 938-940.

R. Byrne; "Performance Characteristics of Freight Car Trucks Determined Through Road Testing," ASME Paper No. 76-WA/RT-4; December 1976.

R. Cass; "Dynamic Measurement of Absolute Track Properties," ASME Paper No. 69-RR-6, April 1969

C.W. Clarke; "Track Loading Fundamentals, Parts 1-7"; Railway Gazette; 1/11/57, 1/25/57, 2/8/57, 2/22/57, 3/8/57, 3/22/57, 4/26/57.

N.K. Cooperrider; "Railway Truck Response to Random Rail Irregularities,"ASME Paper No. 74-WA/RT-2, presented at Winter Annual Mtg. New York, Nov. 1974.

G.R. Doyle, Jr., R.H. Prause; "Hunting Stability of Rail Vehicles With Torsionally Flexible Wheelsets," ASME Paper No. 75-WA/RT-2, presented at Winter Annual Mtg. Houston, Nov. 1975

L.P. Greenfield, R.N. Hodges; "An Investigation of Container Flat Car Ride Quality," ASME Paper No. 75-WA/RT-7, presented at Winter Annual Mtg. Houston, Nov. 1975.

Griffin Wheel Company; "Properties and Structure of Steel Wheels," Internal Report, September 1972.

J.E. Hart, F.J. Grejda; "Computer Simulation of Rail Vehicle Braking Performance," ASME Paper No. 72-WA/RT-5, presented at Winter Annual Mtg, New York, Nov. 1972.

W.W. Hay; Railroad Engineering, Vol. 1, John Wiley & Sons, Inc; New York, 1953.

International Union of Railways; "Braking and Acceleration Forces on Bridges. Magnitude and Distribution of Braking and Starting Forces in the Track"; Report D101/RP1/E, Oct. 1969.

International Union of Railways; "Interaction Between Vehicles and Track. Equations of Motion for a Railway Vehicle"; Report C116/RP4/E, Oct. 1974.

International Union of Railways; "Interaction Between Vehicles and Track. A Survey of Current Practice Concerning Track Parameters and Views on Their Influence onVehicle Riding"; Report C116/RP7/E, Oct. 1976.

International Union of Railways; "Braking and Acceleration Forces on Bridges and Interaction Between Track and Structure. Braking Forces on Prestressed Reinforced Concrete Bridge with Neoprene Bearings," Report D101/RP11/E, Apr. 1977.

W.D. Kaiser, G.L. Nessler, P.C. Meacham; "A Review of Measurement Techniques, Requirements and Available Data on the Dynamic Compliance of Railroad Track," Interim Report FRA-ORD&D-76-70, May 1975. Contract No. DOT-FR-30051.

A.D. Kerr; Symposium on Railroad Track Mechanics, Princeton University, 1975; Final Report 76-TR-1, Oct. 1975 under Contract No. DOT-FR-40017.

A.D. Kerr; "On the Stress Analysis of Rails and Ties" from Design and Analysis of Railroad Track, a Princeton University Continuing Education Course, Oct 1976.

E.H. Law; "Literature Survey of Railway Vehicle Dynamics Research," ASME Winter Annual Mtg, 1973; AMD-Vol. 5; Surveys of Research in Transportation Technology.

E. F. Lind; "Track/Train Dynamics Bibliography," Association of American Railroads Report, Chicago, IL, February 1973.

E. F. Lind; "Track/Train Dynamics Research and Progress: Phase One," ASME Paper No. 75-WA/RT-9, presented at Winter Annual Mtg., Houston, Nov. 1975.

N. W. Luttrell, J. A. Andersen, R. A. Bardwell; " Computer Oriented Data Collection and Reduction System for Analysis of Railroad Freight Car Truck Behavior," ASME Paper No. 75-WA/RT-4, presented at Winter Annual Mtg., Houston, Nov. 1975.

W. H. Maraghy; "Coupled Vehicle/Track Dynamics," Vehicle System Dynamics, Vo. 4, No. 2-3, p. 203-207, 1975.

H. A. Marta, K. D. Mels; "Wheel-Rail Adhesion," ASME Paper No. 68-WA/RR-1, presented at Winter Annual Mtg, New York, Dec. 1968.

G. C. Martin, Y. H. Tse; "Parametric Studies on a Railroad Freight Car Mathematical Model," ASME Paper No. 75-WA/RT-11, presented at Winter Annual Mtg, Houston, Nov. 1975.

P. Matic, S. Kimar; "Moire Analysis of Planar Elastic Contact For Understanding Wheel-Rail Traction,"FRA Interim Report IIT-TRANS-77-1, WO. 6, Apr. 1977 under Contract No. DOT-OS-40103. PB-270639/8ST.

L. A. McLean, W. E. Mims; "Performance of Freight Car Brake Regulators During Static and Dynamic Conditions," ASME Paper No. 68-WA/RR-4, presented at Winter Annual Mtg., N. Y., Dec. 1968.

M. C. Meacham, D. R. Ahlbeck; "A Computer Study of Dynamic Loads Caused by Vehicle-Track Interaction," ASME Paper No. 69-RR-1, presented at IEEE-ASME Joint Railroad Conference, Montreal, Apr. 1969.

E. T. Myers, "S. P. Scale Weighs 3 1/2 Cars a Minute," Modern Railroads, Nov. 1970, p. 82.

L. A. Peterson, W. H. Freeman, J. M. Wandrisco; "Measurement and Analysis of Wheel-Rail Forces" ASME Paper No. 71-WA/RT-4, 1971.

A. R. Pockington, R. A. Allen; "Improved Data from Load Measuring Wheels," Railway Engineer, Vol. 2, No. 4, Aug. 1977, pg. 37-43.

J.B. Raidt, W.P. Manos, B. Johnstone; "Vertical Motions During Railcar Impacts,"ASME Paper No. 75-WA/RT-10, presented at Winter Annual Mtg., Houston, Nov. 1975.

L. Rus; "The Stability and Transfer Functions of Rail Vehicles," Vehicle System Dynamics, No. 2-3, 1975, pg. 159-165.

Y. Sato; "Measurement of Track Spring Constant and Attenuation Coefficient," Permanent Way, Vol. 18, No. 69, June 1977, p. 9-17.

A.H. Wickins; "The Dynamics of Railway Vehicles on Straight Track: Fundamental Considerations of Lateral Stability," Proc. of Inst. of Mech. Eng., Vo. 180, Pt 3F, 1965-66.

A.H. Wickens; "General Aspects of the Lateral Dynamics of Railway Vehicles,"ASME Paper No. 68-WA/RR-3, presented at Winter Annual Mtg., Dec. 1968, New York.

A.H. Wickens, A.O. Gilchrist; "Vehicle Dynamics - A Practical Theory," Railway Engineer, Vo. 2, No. 4, Aug. 1977, p.26-34.

C.D. Wright; "Contribution of Empty and Load Brake Equipment to Increased Braking Level," presented at the Air Brake Association Annual Meeting, Sep. 14, 1971.

APPENDIX A

STRUCTURAL ANALYSIS OF THE INSTRUMENTED RAIL SECTION

1. INTRODUCTION

The following analysis was performed to determine the stresses and deflections in the instrumented rail (reaction rail) section in response to applied vertical (weight) and horizontal (braking) loads. Vertical and horizontal deflections of the rail section would be measured by appropriate sensors, and the output of those sensors would be an indication of applied load.

The instrumented rail structural design problem was two-fold. First, the rail must deflect enough under load to be accurately measured, but not so much that the resultant stresses exceed the fatigue strength of the rail material. Second, the rail must be designed such that the measured vertical deflection is independent of the measured horizontal reaction.

The analysis of this Appendix is performed on a rail design of configuration and dimensions finally selected for the instrumented rail portion of the prototype wayside brake inspection system. It shows that the actual instrumented rail does produce measurable deflections without exceeding material fatigue strength, and that both horizontal and vertical forces can be measured independently of each other.

2. RAIL SECTION CONFIGURATION

Figure A-1a shows the basic rail section and its dimensions. The section is a horizontal rail cap (136 lb rail) of the dimensions shown, supported by two narrow vertical flexures. The measurement concept embodied in this design is illustrated by Figure A-1b. Vertical loads are measured by sensing the total vertical deflection of the rail section under the weight of a passing railcar wheel. The total vertical deflection will occur as a result of rail cap bending (as shown) and axial deflection of the flexures as they shorten in compression. Horizontal loads are sensed by measuring the total horizontal movement of the rail cap as the flexures bend as shown in the lower diagram of Figure A-1b. The analysis which follows uses elementary beam theory to calculate expected vertical and horizontal rail cap deflections as a result of applied loads.

The center rail section is 3 inches (7.6 cm) wide, 3.25 inches (8.2 cm) deep and is 12 inches (30 cm) long between flexure centers. The flexures are 3 inches (7.5 cm) wide, 0.5 inches (1.3 cm) thick and 2.5 inches (6.3 cm) long.

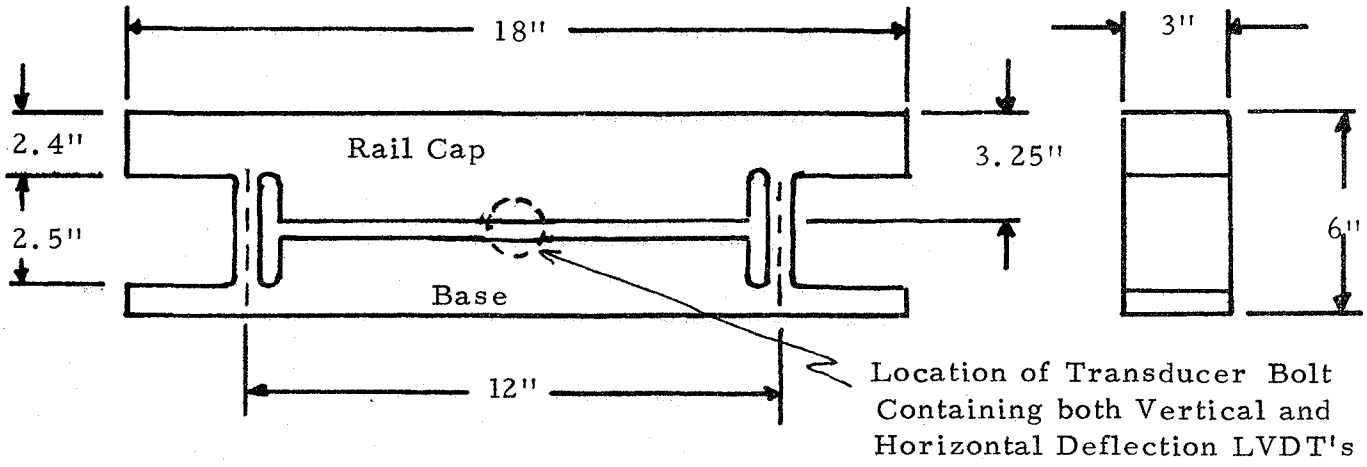

FIGURE A-1a

PRINCIPAL REACTION RAIL DIMENSIONS

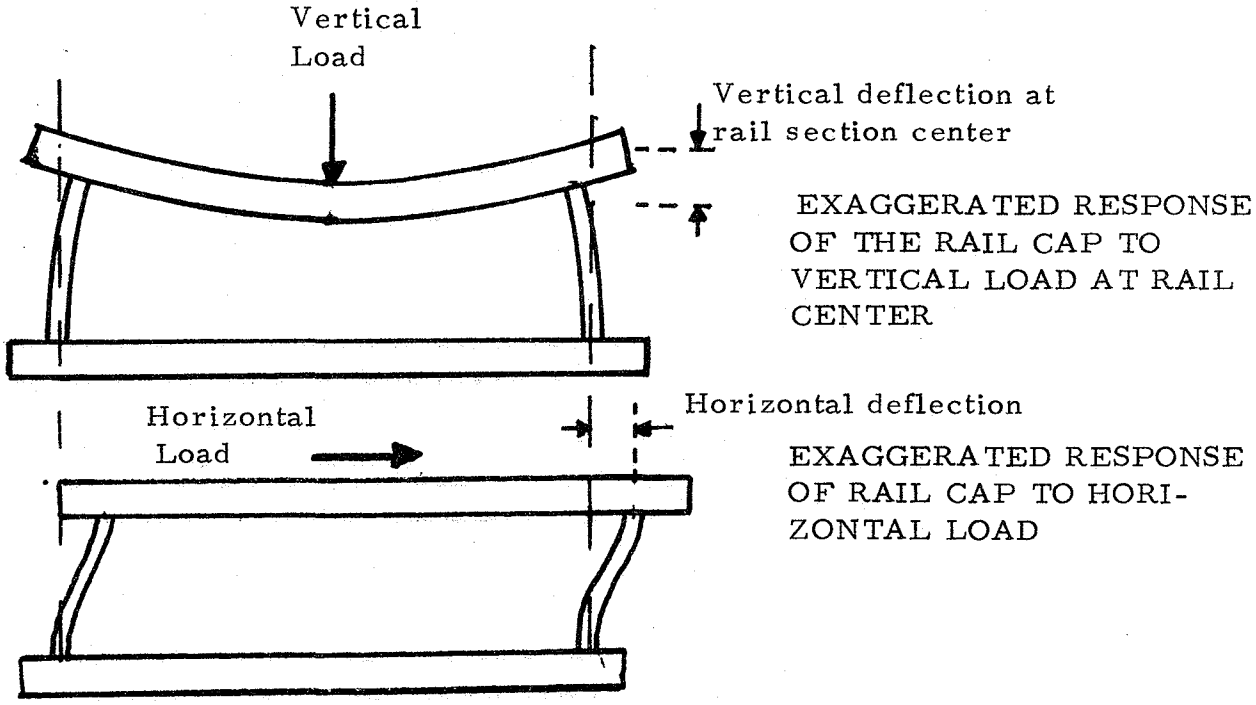

FIGURE A-1b

ASSUMED RESPONSE OF REACTION RAIL TO
VERTICAL AND HORIZONTAL FORCE INPUT

3. LOADS

The track is currently designed to withstand the maximum concentrated load seen in American service - 40,000 lbs. The rail section is also designed to withstand a horizontal (brake) load of 10,000 lbs. which corresponds to an adhesion level (coefficient of friction) of 25% in conjunction with a 40,000 lb. vertical load. These maximum loads are not expected to be seen very frequently, since many roads do not allow even this heavy a load.

For the purposes of analysis, the following commonly experienced loads are considered typical and are used to design for essentially infinite fatigue life for the section:

Maximum vertical load: 35,000 lbs., experienced as locomotives pass over the section.

Maximum horizontal load: 7,700 lbs., anticipated as a result of 35,000 lb. wheel load and maximum zero speed normal rail adhesion of 22%. (See Figure 3 and Reference 5).

4. DEFLECTIONS

Transducers are used to measure both the vertical and horizontal deflection of the center of the rail section.

The total vertical deflection of the center of the rail section, Y_T, can be written:

$$Y_T = Y_B + Y_S + Y_C \qquad \text{(A-1)}$$

Where: Y_T = Total vertical deflection (inches).

Y_B = Deflection due to rail cap bending (inches).

Y_S = Deflection due to rail cap shear (inches).

Y_C = Deflection due to axial compression of the support flexures (inches).

To calculate deflection due to bending (Y_B), the rail cap is idealized as a simply supported beam with a concentrated load at its center as shown in Figure A-2a. This model neglects the reaction moments exerted on the rail cap by the flexures as they bend, but these moments are small compared to the bending moment due to wheel weight. A 40,000 lb vertical load results in a bending moment of 120,000 inch-lbs in the rail, while the reaction

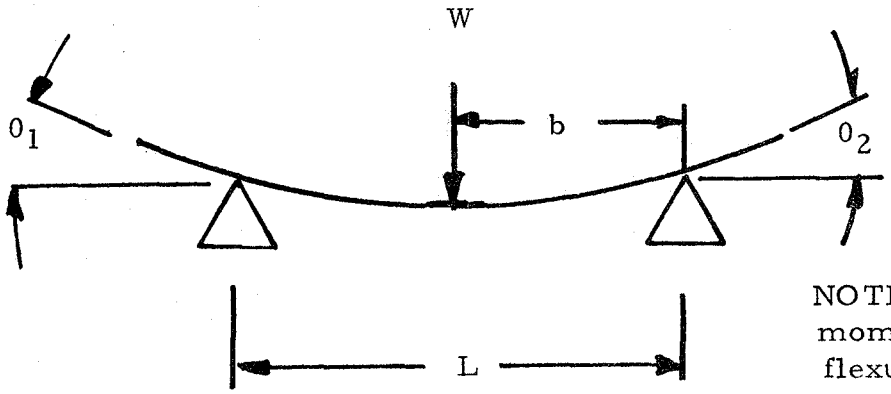

NOTE: Reaction moments due to flexure bending are neglected.

FIGURE A-2a

IDEALIZED RAIL CAP SECTION

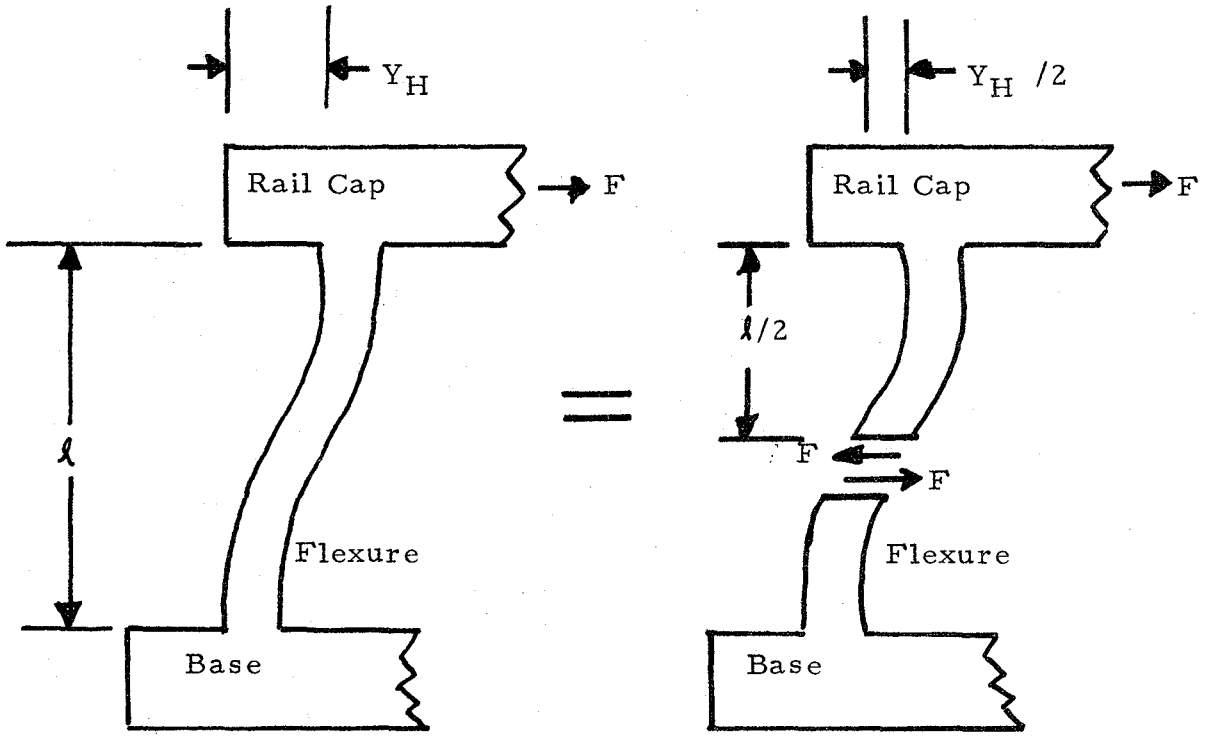

FIGURE A-2b

IDEALIZED FLEXURE UNDER HORIZONTAL LOAD (F)
MODELLED AS TWO SIMPLE CANTILEVER BEAMS
FOR PURPOSES OF ANALYSIS

moment due to flexure bending under that load is only 1765 inch-lbs. (See Section 5.2 of this Appendix for calculation of these moments).

Under these assumptions, the maximum rail section bending deflection occurs when the wheel is at the beam center and can be written as: (Ref. 10, page 97, Case 1e)

$$Y_B = \frac{WL^3}{48\,EI} \qquad \text{(A-2)}$$

where: Y_B = Deflection due to bending (inches).

W = Concentrated load at beam center. Maximum assumed to be 40,000 lbs (18,160 Kg).

L = Beam supported length. For reaction rail, L = 12 inches (30.5 cm.).

E = Modulus of Elasticity = 30×10^6 lbs/in^2 for Chrome-Moly steel. (2.1×10^6 Kg/cm^2.)

I = Area moment of inertia of beam cross section = 8.6 in^4 (358 cm^4).

Evaluation of Equation A-2 yields:

$$Y_B = 5.6 \times 10^{-3} \text{ in (.14mm).} \qquad \text{(A-2a)}$$

The vertical deflection due to compression of the flexures can be written as:

$$Y_C = \frac{W\ell}{2A_f E} \qquad \text{(A-3)}$$

Where:

Y_C = Deflection of reaction rail due to compression of the supporting flexures (inches).

ℓ = Length of the flextures = 2.5 inches (6.4 cm.).

$2A_f$ = Total cross-sectional area of the two flexures = 1.5 in^2 (9.7 cm^2).

Equation A-3 assumes that the flexures are subject to pure axial, compressive loads and that they do not buckle. Solving Equation A-3 yields:

$$Y_C = 1.1 \times 10^{-3} \text{ inches } (.03 \text{ mm.}). \quad \text{(A-3a)}$$

Because the beam is deep relative to its span (L/D = 4) shear stresses and resulting deflections are not negligible. The deflection due to shear deflection, Y_S, can be written for an end supported, centrally loaded beam as: (Ref. 10, page 185)

$$Y_S = \frac{1}{4} F \frac{WL}{A_r G} \quad \text{(A-4)}$$

Where:

Y_S = Deflection due to shear force in beam (inches).

F = Factor depending on form of beam cross section = 1.2 for a rectangular section.

W = Center load = 40,000 lbs (18,160 Kg).

L = Beam length = 12 inches (30.5 cm.).

A_r = Cross-sectional area of reaction rail head = 9.75 in^2 (63 cm^2).

G = Modulus of Rigidity = 11.5×10^6 lbs/in^2 ($.8 \times 10^6$ Kg/cm^2).

Solving Equation A-4 yields:

$$Y_S = 1.3 \times 10^{-3} \text{ inches } (.03 \text{ mm.}). \quad \text{(A-4a)}$$

The total vertical deflection of the rail section under a 40,000 lb. load at the rail midpoint is then:

$$Y_T = Y_B + Y_C + Y_S = 8.0 \times 10^{-3} \text{ inches } (.2\text{mm}). \quad \text{(A-1a)}$$

Horizontal rail deflection due to applied braking inputs can be calculated by assuming that the support flexures bend as two cantilever beams, attached end to end. Both beams are subject to the constraint that the cantilever ends are maintained parallel, so the total deflection can be calculated by "cutting" the flexure at its center (Figure A-2b) and assuming that each flexure half bends as a simple cantilever.

The deflection relationship for "one-half" of a flexure is then: (Ref. 10, page 96, Case 1a)

$$\left(\frac{Y_H}{2}\right) = \frac{F\left(\frac{\ell}{2}^3\right)}{3EI_f} \qquad \text{(A-5)}$$

Where:

Y_H = Total Horizontal deflection (inches).

F = Applied load = Total load/2 since there are two flexures = 5,000 lbs. (2,270 Kg.).

ℓ = Total Flexure length = 2.5 inches (6.4 cm.).

E = Modulus of Elasticity = 30×10^6 lbs/in^2

I_f = Flexure area moment of inertia = 0.0313 in^4 (1.3 cm^4).

The above values yield a value for Y_H:

$$Y_H = 6.0 \times 10^{-3} \text{inches } (.15 \text{ mm.}). \qquad \text{(A-5a)}$$

It should be noted that even without braking, the rail section will deflect horizontally when the wheel is at any location other than the rail ends or rail center. The magnitude of this deflection is a second-order result of stress in the flexure. The magnitude is small as is calculated in Section 5.2, Equations A-9a and A-9b.

5. STRESSES IN RAIL MEMBERS

5.1 Rail Cap

The most significant stress in the rail segment cap occurs due to bending when the wheel is in the center of the section. The maximum bending moment in the center, assuming the beam is free to rotate at the end is 1.2×10^5 inch-lbs. A comparable, but lower bending moment occurs in the overhanging part of the track: 1.0×10^5 inch-lbs.

The stress in the reaction rail due to bending is calculated using the classical beam equation:

$$S_{max} = \frac{M\,C}{I_r} \qquad \text{(A-6)}$$

Where:

S_{max} = Maximum fiber stress in the rail at the surface. Under wheel loading, the top surface of the rail will be in compression, the bottom of the rail in tension. (lbs/in^2)

M = Bending moment in beam
= 1.2×10^5 in-lbs in rail section.

C = Distance from neutral axis of rail to rail surface. (inches)
= 1.63 inches (4.1 cm) in rail section.
= 1.2 inches (3.0 cm) in overhang section.

I_r = Area moment of inertia of rail (in^4).
= 8.6 in^4 (358 cm^4) in rail section.
= 3.5 in^4 (146 cm^4) in overhang.

The maximum stress is 22,700 lbs/in^2 (1599 Kg/cm^2) in the reaction rail section, and 34,300 lbs/in^2 (2410 Kg/cm^2) in the overhang section.

5.2 Straight Flexures

The reaction rail flexures experience a complex stress distribution as a result of the applied loads shown schematically in Figure A-3.

1. A bending moment is applied to the flexures as a result the braking force, F, creating the moment distribution in Figure A-4.

2. A moment (M_1 or M_2) is impressed upon each flexure when the rail bends under wheel weight, and the flexures accommodate the resulting deflection.

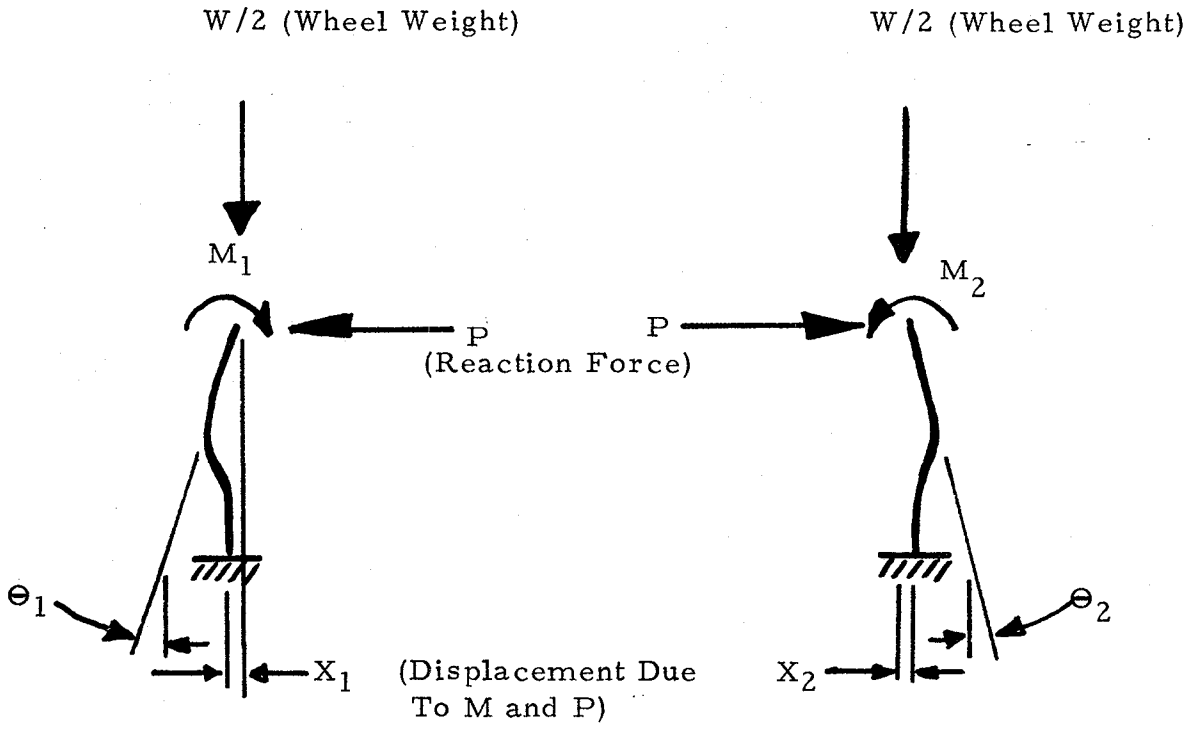

FIGURE A-3

LOADS AND DEFLECTIONS OF THE FLEXURES AS A RESULT OF APPLIED VERTICAL LOAD ONLY

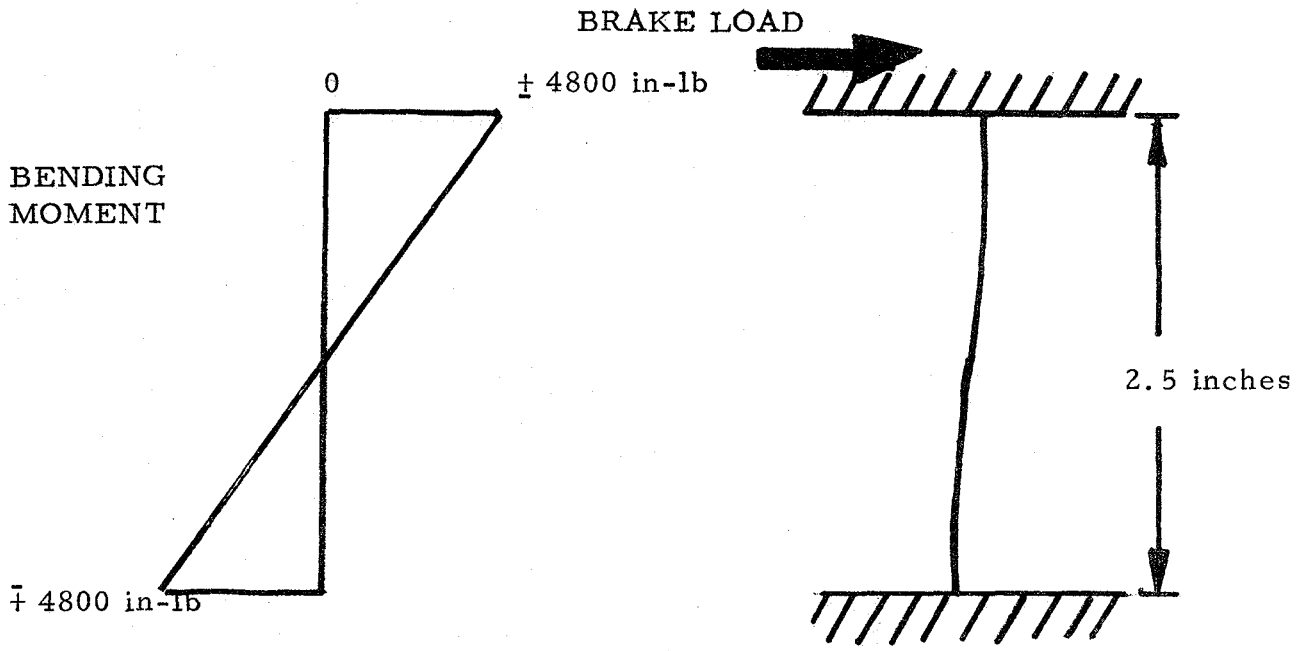

FIGURE A-4

BENDING MOMENT DISTRIBUTION IN

FLEXURE DUE TO BRAKE LOAD ONLY

3. Each flexure undergoes compression from the weight of the wheel.

4. The equal and opposite horizontal reaction force, P, of the rail section, tending to "straighten" out the flexures.

The stresses resulting from each of those loads is considered in the analysis that follows. The 35,000 lb. (15,890 Kg.) vertical load is used in the calculations that follow, as that is the load that may be seen with a frequency that will determine fatigue life.

Bending moment due only to the braking force is a maximum of 4,800 in.-lbs. It is distributed in the flexures as indicated in Figure A-4. To this must be added the bending moment distribution due to flexure accommodation of the deflection of the main reaction rail.

To calculate the applied bending moments, M_1 and M_2, it is assumed that the main rail section bends under wheel weight W, resulting in angles θ_1 and θ_2 as shown in Figure A-1b. These angles are then impressed upon the flexures as indicated in Figure A-3, since the rail and the flexures are rigidly connected. These angles are: (Ref. 10 page 97, Case 1e)

$$\theta_1 = \frac{1}{6} \frac{W}{E I_r} \left(bL \frac{b^3}{L} \right) \qquad \text{(A-7a)}$$

$$\theta_2 = \frac{1}{6} \frac{W}{E I_r} \left(2bL + \frac{b^3}{L} - 3b \right) \qquad \text{(A-7b)}$$

Where

θ_1 = Angle of bend at left end of beam in Figure A-1b. (radians)

θ_2 = Angle of bend at right end of beam in Figure A-1b. (radians)

b = Distance of applied load, W, from right end of beam in Figure A-1b. (inches)

E, I_r, and L are defined after Equation A-2.

The forces and moments (M_1 and M_2) applied to flexures (See Figure A-3) result in flexure angles which must match those of the rail section described by Equations A-7. These flexure angles are due to both the unknown moments (M_1 and M_2) and the horizontal Force P.

The horizontal force is equal and opposite on each flexure, as required by equilibrium.

Superposing the relations between applied moment (M), and applied force (P), and flexure angle (θ) yields: (Ref. 10, p. 96 and 101, Case 1a and Case 3a)

$$\theta_1 = \frac{M_1}{EI_f} - \frac{P\ell^2}{2EI_f} \qquad \text{(A-8a)}$$

$$\theta_2 = \frac{M_2}{EI_f} - \frac{P\ell^2}{2EI_f} \qquad \text{(A-8b)}$$

Where the geometric variables are defined in Figure A-3, and where:

I_f = Flexure cross section moment of inertia (in^4)

= .0313 in^4 (1.3 cm^4)

The horizontal deflection of each flexure as a function of applied moment, M, and reaction force, P, can also be written as a superposition of simpler equations: (Ref. 10, p. 96 and 101, Case 1a and Case 3a)

$$X_1 = \frac{M_1\ell^2}{2EI_f} - \frac{P\ell^3}{3EI_f} \qquad \text{(A-9a)}$$

$$X_2 = X_1 = \frac{P\ell^3}{3EI_f} - \frac{M_2\ell^2}{2EI_f} \qquad \text{(A-9b)}$$

Where X_1 and X_2 are defined in Figure A-3.

The four equations; A-8a, A-8b, A-9a, and A-9b can be solved for the four unknowns; M_1, M_2, P, and X_1 ($=X_2$) to satisfy θ_1 and θ_2 as imposed by the main rail section. The results of this analysis for several wheel positions along the rail are summarized in Table A-1.

TABLE A-1

SUMMARIZED FLEXURE CALCULATIONS
FOR 0.5 INCH THICK STRAIGHT FLEXTURES

Wheel Position, b	θ_1	θ_2	M_1	M_2	P	X
0	0	0	0	0	0	0
2	+.53	+.83	930	1040	591	-1.8×10^{-4}
4	+.97	+1.21	1531	1620	945	-1.5×10^{-4}
6	+1.22	+1.22	1765	1765	1060	0
8	+1.21	+.97	1620	1530	945	1.5×10^{-4}
10	+.83	+.53	1040	930	591	1.8×10^{-4}
0	0	0	0	0	0	0
	(Milliradian)		(Inch-lb)		(Lb)	(Inches)

Refer to Figure A-3 for graphical description of variables.

Θ_1 , Θ_2 , = Flexure deflection angles imposed by bending main rail. Calculated by Equations A-8a and A-8b. (milliradians)

M_1 , M_2 = Moments resulting from imposed angles Θ_1 , Θ_2. (inch-lbs)

P = Horizontal reaction force tending to "straighten" flexures. (lb)

X_1 , X_2 = Horizontal displacements resulting from M_1, M_2, and P. (inches) Calculated by Equations A-9a and A-9b.

Figure A-5 shows graphically the bending moment distribution in the flexures for different wheel locations. The maximum value of 1765 in-lb must be added to the moment due to braking along to give the maximum bending moment of 6565 in-lb. This applied to the beam stress equation yields the maximum bending stress, $\pm$ 58,000 psi. Combining this with the stresses resulting from vertical loads (+5,000-28,500 psi) shows that the stresses in the flexure can range from -86,500 psi to +63,000 psi. This maximum stress occurs only at the top, cantilevered end of the flexure, leaving the remainder of the flexure length relatively unstressed.

If the conditions of a + 74,700 lbs/in^2 alternating stress about a mean stress of -11,700 lb/in^2 are plotted on a Goodman diagram, it is found that a fatigue life of less than 10^6 cycles exists (Figure A-6). This fact leads to consideration of a tapered flexure which has comparable overall flexibility and is more uniformly stressed over its length.

5.3 Tapered Flexures

A design with more balanced stress distribution was obtained by tapering the flexures to have a minimum thickness of 0.400 inches (1.0 cm) with a profile shown in Figure A-7. This design resulted in a flexure with stiffness comparable to the straight 0.5 inch (1.3 cm) thick flexure but with a much lower bending stress and slightly higher axial stresses. This was obtained at slight additional cost to produce the tapered flexure.

The stiffness characteristics of the tapered flexure were obtained by a numerical integration of the beam equation:

$$\frac{d^2y}{dx^2} = \frac{M(x)}{EI_f(x)} \qquad \text{(A-10)}$$

This resulted in derivatives that can be used in the four simultaneous equations applied earlier to the straight flexures. Values of these factors are listed below and compared with those for the straight flexure:

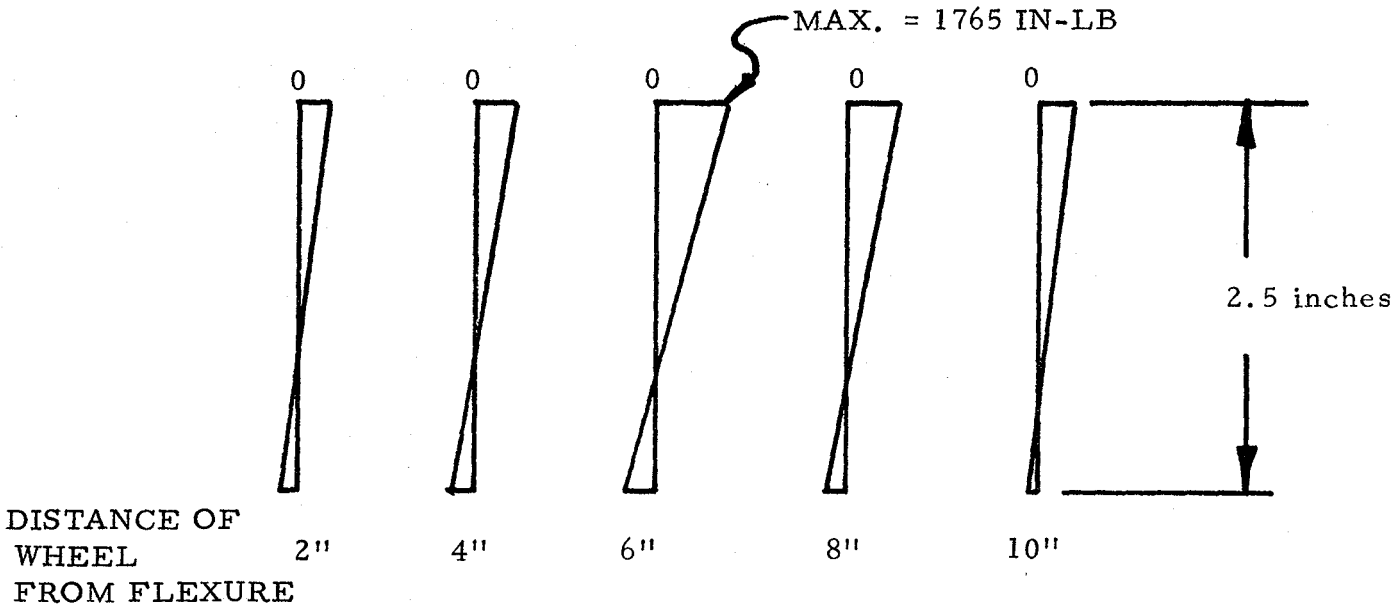

FIGURE A-5

DISTRIBUTION OF BENDING MOMENT IN FLEXURE DUE TO MAIN RAIL DEFLECTION UNDER WHEEL LOAD

AISI 4340 Chrome-Moly Steel

Tensile Strength = 160 ksi
Endurance Limit = 70 ksi

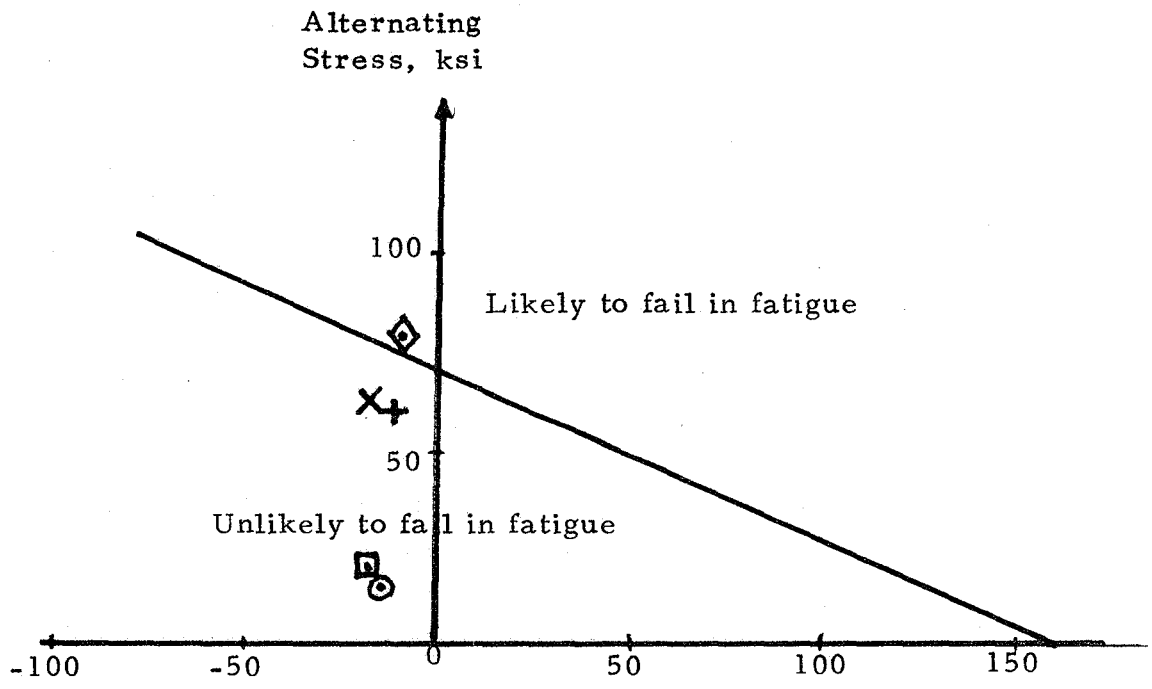

KEY:

- ⊙ Central Rail Cap section, 40,000 lb. wheel load
- ⊡ Overhanging Rail Section, 40,000 lb. wheel load
- × Tapered Flexure, 40,000 lb. wheel load
- ◈ Straight Flexure, 35,000 lb. wheel load
- + Tapered Flexure, 35,000 lb. wheel load

FIGURE A-6
GOODMAN FATIGUE DIAGRAM FOR AISI 4340

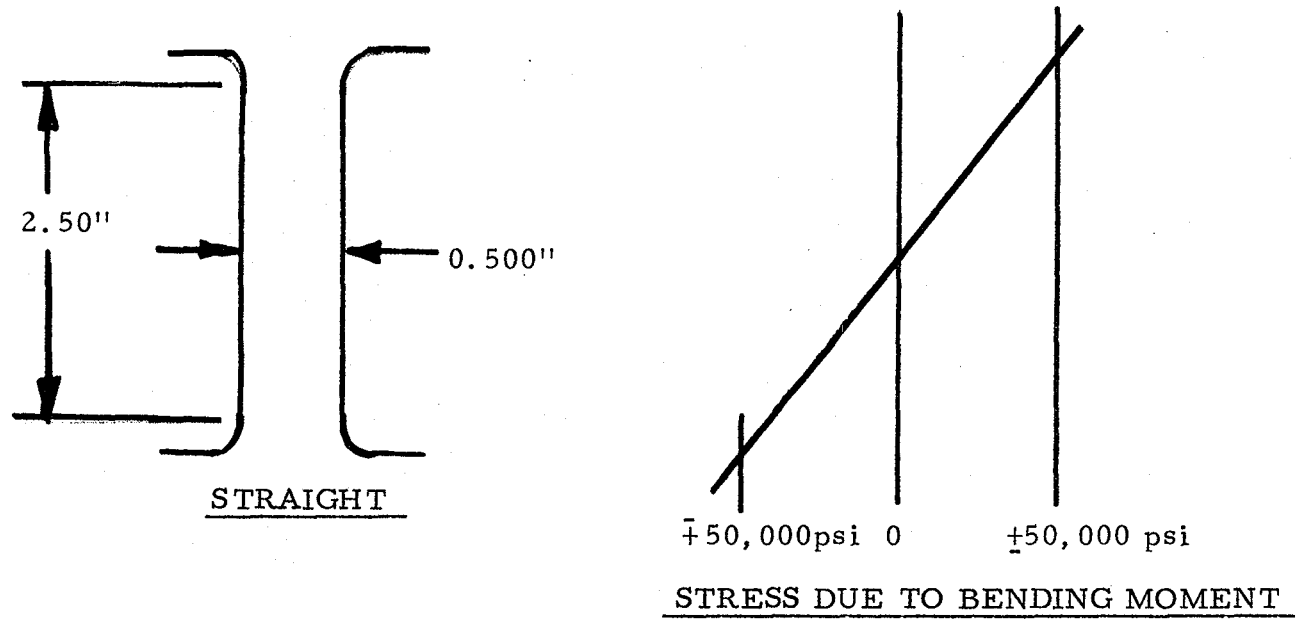

FIGURE A-7

COMPARISON OF BENDING STRESSES
IN STRAIGHT AND TAPERED SURFACES

	Tapered Flexure	Straight Flexure
$d\delta/dF$	-7.64×10^{-6} in/ b	-5.60×10^{-6} in/lb
$d\theta/dF$	5.52×10^{-6} rad/lb	3.36×10^{-6} rad/lb
$d\delta/dM$	4.88×10^{-6} in/in-lb	3.36×10^{-6} in/in-lb
$d\theta/dM$	-3.91×10^{-6} rad/in-lb	-2.69×10^{-6} rad/in-lb

All coefficients for the tapered flexure are approximately 1.4 times more compliant than the straight flexure. It can then be estimated to satisfy the θ_1 and θ_2 constraints will be 1/1.4 or .71 times those calculated for the straight flexure (Table A-1). The maximum bending moment experienced by the flexure will then be 6060 inch-lbs. instead of 6565 inch-lbs. The tapered flexure is thus shaped to give essentially constant (maximum) bending stresses of $\pm$ 35,000 lbs/in^2. In combination with the stresses from vertical loads, the stresses in the flexures are found to range from -70,600 lbs lbs/in^2 to 41,300 lbs/in^2.

6. FATIGUE SUMMARY

If the rail section were made from AISI 4340 chrom-moly steel, heat treated to $\geqslant$158,000 psi ultimate tensile strength, the system should have infinite fatigue life. Various points are shown on the Goodman diagram, Figure A-6 to indicate the safety of the section. The sizeable compression load causes the flexure data to fall outside normal test data; it seems reasonable, however, to extrapolate the curves to enclose our points. The points shown are:

Central rail cap section due to 40,000 lb load:

mean stress = $\pm$ 11,500 psi;

alternating stress = 11,500 psi.

Overhanging rail cap section due to 40,000 lb load:

mean stress = $\pm$ 17,500 psi;

alternating stress = 17,500 psi.

Straight flexure under 35,000 lb load:

mean stress = -11,700 psi;

alternating stress = 74,700 psi.

Tapered flexure under 35,000 lb load:

mean stress = -14,600 psi;

alternating stress = 56,000 psi.

Tapered flexure under 40,000 lb load:

mean stress = - 16,700 psi;

alternating stress = 64,000 psi.

By looking at Figure A-6 it can be seen that under any circumstances the track section is safe. The flexure is safe only as long as the flexure is carefully made and is free from notches and other surface imperfections. (It will be necessary to manufacture the flexures with reasonable care and to protect them from damage in service).

APPENDIX B

DESIGN ANALYSIS OF THE INFRARED SENSOR SYSTEM

1. INTRODUCTION

This Appendix describes the procedure by which IR Sensor speed and wavelength response were derived. The physical properties of the selected detector (Indium Antimonide) are presented.

2. SENSOR RESPONSE TIME REQUIREMENTS

Figure B-1 represents a wheel of diameter D. It is required to sense wheel temperature at a point one inch inboard of the wheel circumference as the wheel passes at velocity V. The distance over which the target travels as the wheel passes by is L. By geometrical considerations:

$$L = D \sin \theta \tag{B-1}$$

and,

$$\theta = \cos^{-1} \frac{D-2}{D} \tag{B-2}$$

where L and D are in inches. The distance over which the entire area of a one-inch diameter focal point is on the passing wheel is (L-1) inches.

As a wheel passes at a speed, V (in/sec), the length of time that the entire one inch focal point "sees" the wheel is:

$$t = \frac{L-1}{V} \text{ (sec)}, \tag{B-3}$$

For purposes of selecting an infrared detector, the minimum possible time, t, to be expected should be calculated, and a detector chosen accordingly. The smallest diameter wheels to be considered are 24 inch (61 cm.) wheels, and the maximum expected velocity is 60 miles per hour (96 Km/Hr.) or 1056 inches per sec. (2682 cm/sec). Equations B-2 and B-1 yield:

$$L = 9.6 \text{ inches } (24.4 \text{ cm}) \tag{B-4}$$

for D = 24 inches (61 cm).

t = Passing time = (L - 1)/V Seconds

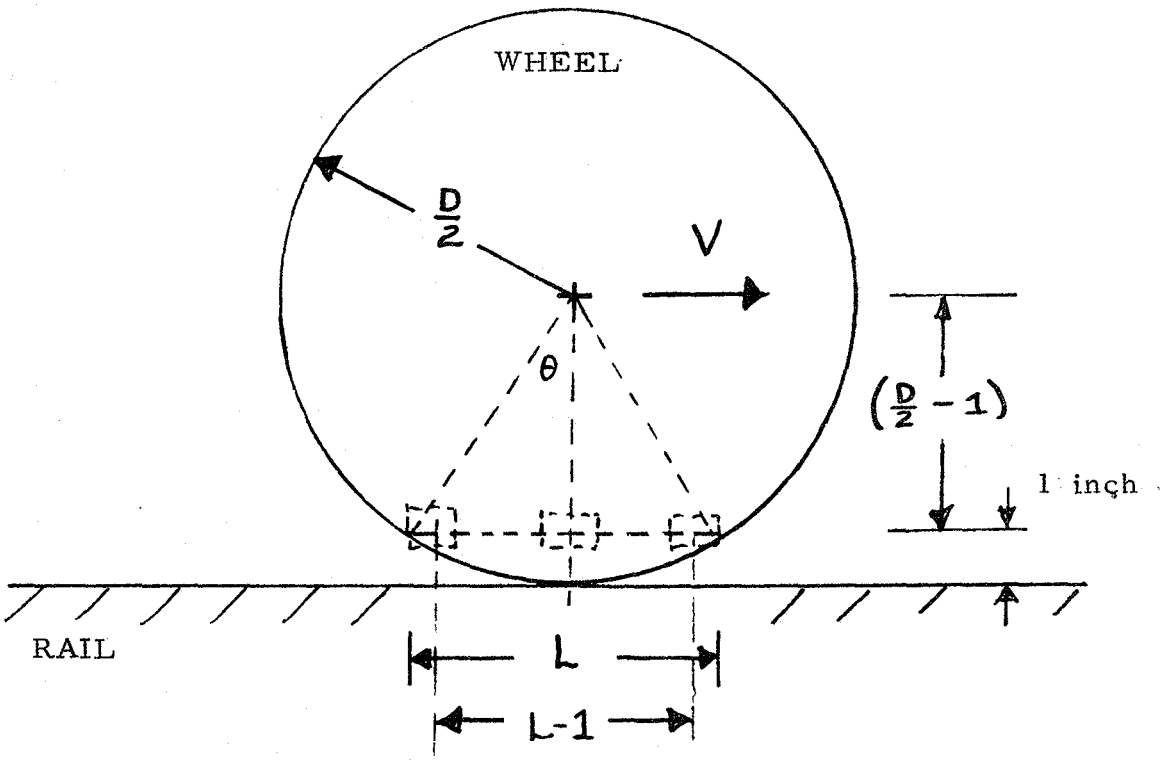

V = Consist Velocity (Inches/Second)
D = Wheel Diameter (Inches)
L - 1 = Available Target Length (Inches)

FIGURE B-1

SCHEMATIC FOR
CALCULATION OF REQUIRED TIME RESPONSE

Equation B-3 then yields:

$$t = 8.1 \times 10^{-3} \text{ sec} \qquad \text{(B-5)}$$

The time response of the IR sensor (detector plus associated amplification) should be at least 10 times faster, or 0.8 milliseconds.

3. SENSOR BANDWIDTH REQUIREMENTS

The anticipated maximum temperature of the braked wheels at a point one inch in from its circumference was 750° F (399° C). This value was derived from published results (9) describing temperature profiles in braked wheels.

At the 750° F temperature, the black body radiation midpoint (50% of the energy lies on either side) is at a wavelength of 6.1 microns. At this temperature, 1210° R (672 K), 55% of the energy lies between the wavelength of 4.2 microns and 9.7 microns.

At a lower temperature, 100° F (38° C), the mid-band wavelength is 13.2 microns. The range 9.0 to 20.9 microns encompasses 55% of the total radiant energy.

The ideal detector bandwidth would then be from 4.2 to 20.9 microns with a maximum response in the range of 6 to 13 microns. In addition, the ideal detector response time would be less than 0.8 milliseconds (in conjunction with its associated electronics).

4. SURVEY OF AVAILABLE COMMERCIAL INFRA-RED SENSORS

A survey of IR sensor manufacturers was made. A tire defect sensor appeared to be the most suitable device capable of measuring at the required speed and over the required range. Typical specifications were:

Minimum temperature resolution:	1° F(.5° C)
Sensitivity:	10 mV/° F
Response:	50 μsec.
Temperature Range:	100° F - 800° F

The complete instrument was determined to be too costly for the project, however, the manufacturer agreed to sell the critical internal components. These components were assembled into a system suitable for use as part of the prototype wayside brake inspection system. Components purchased included an indium antimonide detector, a Cassagrain lens system and amplifier.

5. THE INDIUM ANTIMONIDE DETECTOR

The detector chosen for this system was an indium antimonide (InSb) photo conductive element. This device is sensitive to radiation extending from visible to 7.5 μm and is intended for use with modulated or pulsed radiation.

The device is packaged in a modified, square, semiconductor flatpack measuring .267 in. (6.8 mm) on a side and .078 in. (2.0 mm) thick. The radiation sensitive area on the device is also square and measures .078 in. (2.0 mm) on a side with a field of view of 120 in each dimension.

Typical characteristics of the device at 72°F(20°C) are:

Wavelength at maximum response:	5.0 to 7.0 μm
Spectral response:	visible to 7.5 μm
Cell resistance:	650 Ω
Time constant:	0.1 μs
Responsivity (6.0 m):	5.0 V/W
Operating temperature:	-55 F to + 70 F (-48° C to -21° C)
Maximum bias current:	25 mA

D^* (6.0 μm) 15 cm ($Hz^{-1/2}/W$)

Note: $D^* = \frac{V_s}{V_n} \times \left(A_d \ \Delta f\right)^{1/2}$ (B-6)

where:

D^*	=	"Detectivity", an index of signal-to-noise per watt of incident radiation cm ($Hz^{-1/2}/W$)
V_s	=	Signal (volts)
V_n	=	Noise (volts)
Δf	=	Bandwidth (Hz)
W	=	Incident radiative power (Watts)
A_d	=	Area of detector (mm^2).

The above indium antimonide detector is the same device used in a commercial instrument used to detect "hot spots" on high speed tire testers.

Figure B-2 shows the InSb detector relative responsivity to incident radiation wavelength. Also shown are peak output black body temperatures as a function of wavelength and the black body power as a function of wavelength at 600°, 400°, and 300°K.

FiguresB-3 and B-4 show the InSb detector relative responsivity as a function of applied detector bias current, for the short circuit and open circuit conditions respectively. Relative responsivity is the ratio of detector output (volts) to radiation input (watts). Maximum detector bias current is 25 mA.

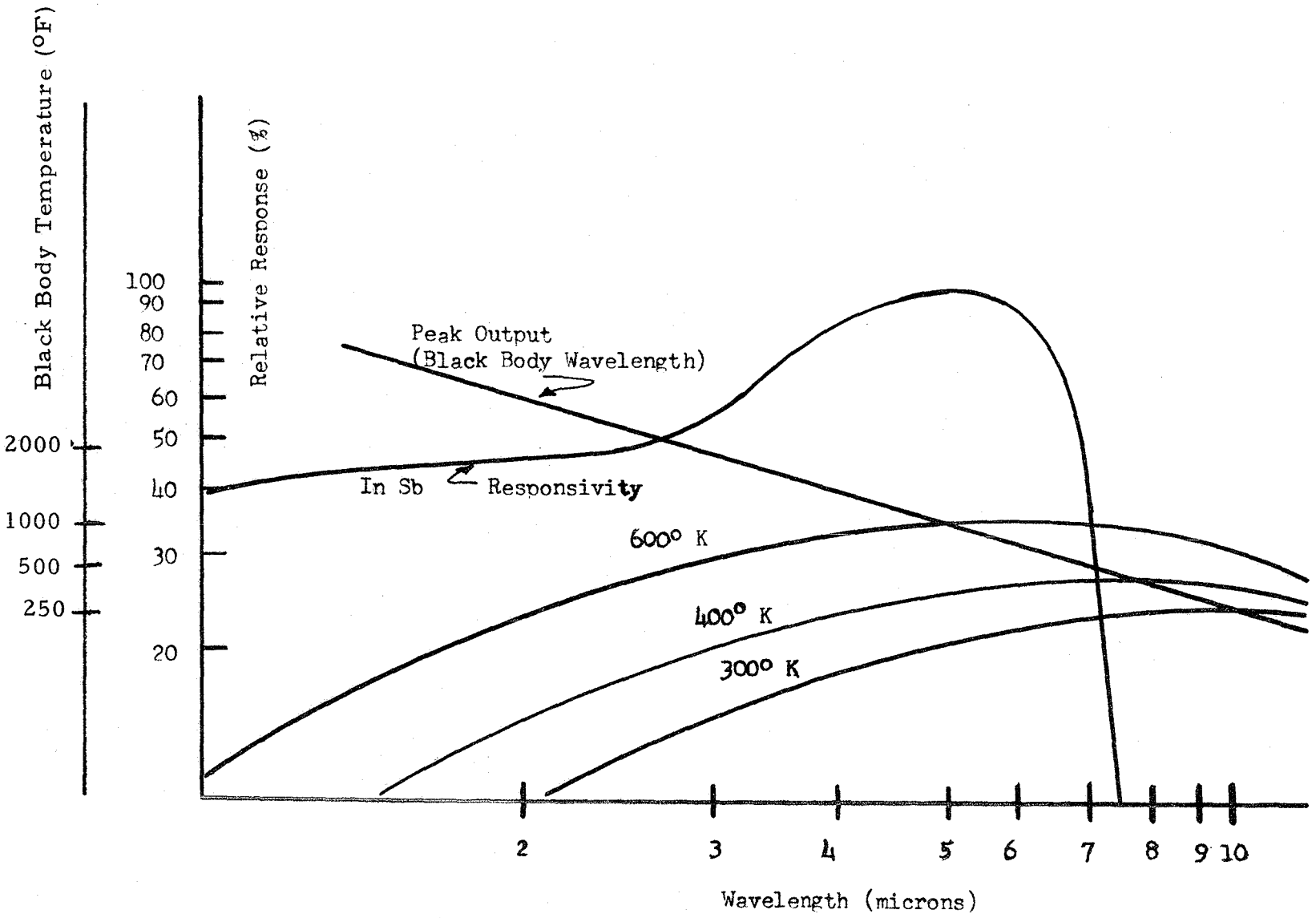

FIGURE B-2

INDIUM ANTIMONIDE DETECTOR WAVELENGTH RESPONSE
AND BLACK BODY PEAK OUTPUT

OPEN CIRCUIT CHARACTERISTICS

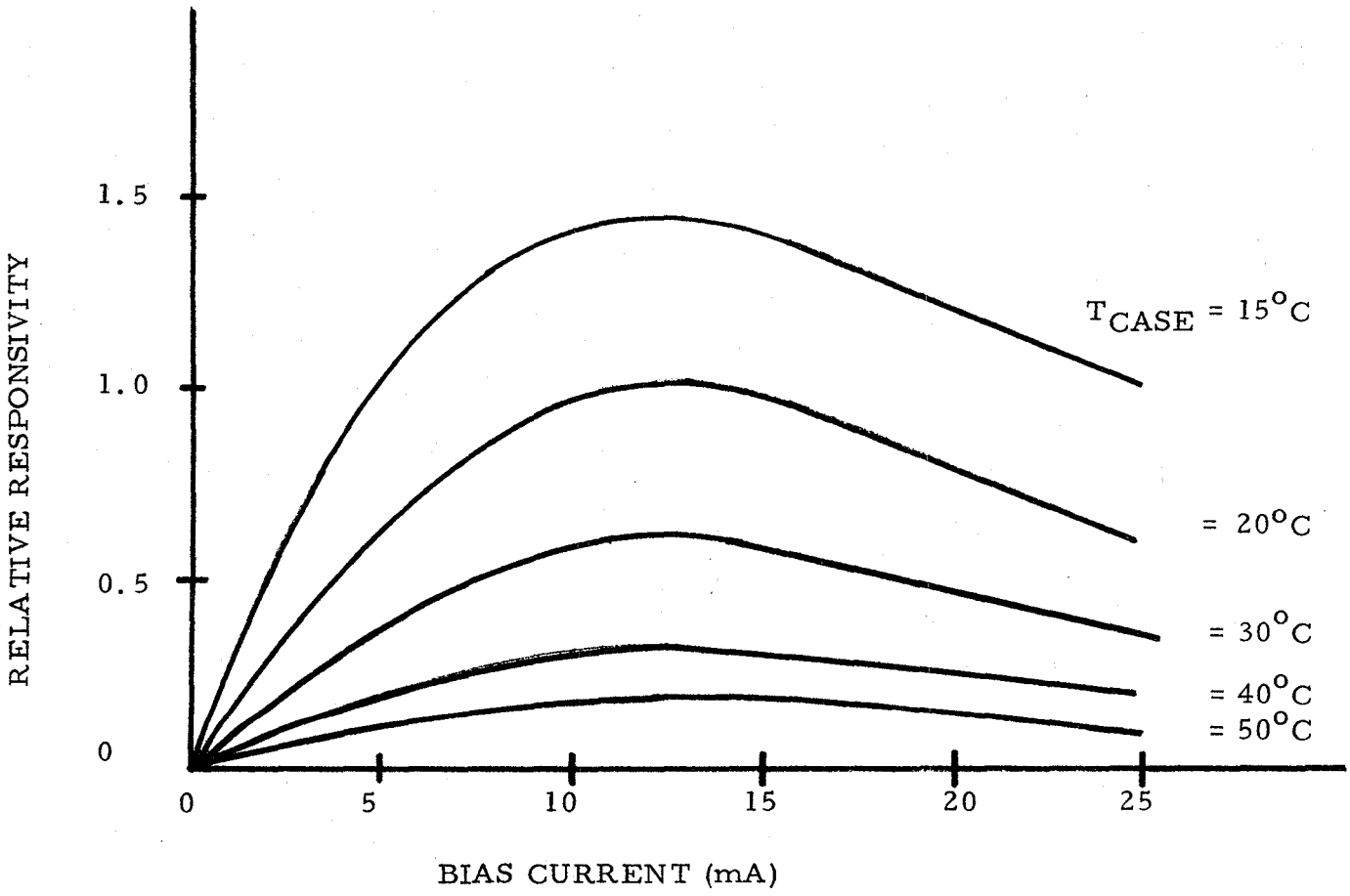

FIGURE B-3

DETECTOR SHORT CIRCUIT
CHARACTERISTICS

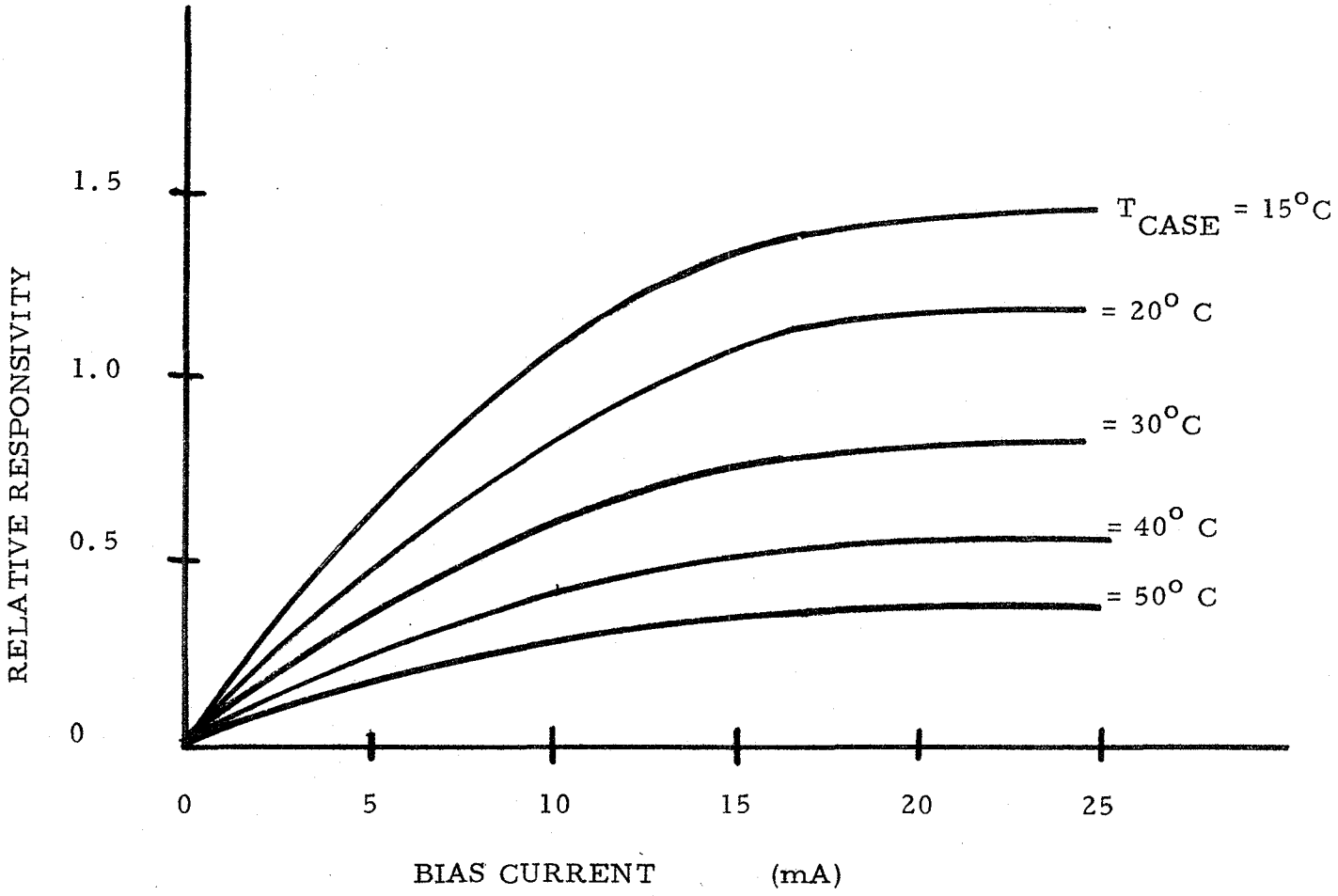

FIGURE B-4

DETECTOR OPEN CIRCUIT
CHARACTERISTICS

APPENDIX C

LABORATORY TEST PLAN

1. INTRODUCTION

The laboratory tests which were conducted carried out as part of Task I of this project had as their objective the establishment of the operating characteristics of the two major system subassemblies. These are the infrared scanning system and the instrumented rail section.

2. INFRARED SCANNING SYSTEM

The infrared scanning system to be used in the prototype brake inspection system will consist of two detectors, one on each side of the track. They will be positioned so that each unit focuses on the same area on each wheel of a single axle. Two major areas relating to the performance of the hardware are to be examined during the course of the laboratory program. They are:

- effect of wheel speed vs. detector sensitivity
- effect of variations in thermal emissivity of the wheel's surface.

In order to obtain data on these effects, a single detector was set up in the laboratory. It was positioned so that it could view a target mounted on a large rotating disc. This target was fabricated from the same type of material that is used in railroad wheels and was equipped with a heater to bring it to different temperatures above room temperature. The wheel was constructed so that the response of the system when viewing a wheel on a car moving at speeds up to 60 mph could be established.

These tests were conducted in the following format. First, a heated segment was used which had surface sharacteristics typical of wheels in use. Sensor output was measured for speeds of 10, 20, 30, 40, 50 and 60 miles per hour, and for temperature differences of 10, 50, 100, and 300 ^{o}F above ambient. Sensor sensitivity to speed appeared to be negligible. Sensor output as a function of temperature difference is reported in Section 2.4.2.

These data showed the sensitivity of the infrared detector under the types of temperature increases and differences which may be expected as shown by the Analysis of Malfunctions (Section 2.1.3) to predict system performance.

A similar series of tests was performed with the surface condition of the metal segment modified as it might be in actual use by

- Dirt
- Water
- Grease
- Overheating

to obtain an indication of how minimal system performance may be effected by these factors.

3. INSTRUMENTED RAIL SECTION

The laboratory tests which were carried out on the instrumented rail section had an objective somewhat different from that of the infrared detector tests. In this case, static tests were conducted by loading the instrumented section with a hydraulic press. These tests produced calibration curves which give strain gage and LVDT output as a function of loading. Loads were applied vertically and horizontally. Results were analyzed to verify that:

- Angular loadings are properly resolved into horizontal and vertical components.
- Strains from maximum loadings are acceptable.
- Calibration curves show acceptable sensitivity and stability.

4. CONCLUSION

After these tests were completed, data was collected which was used to predict system performance in the field. Section 2.4 describes the results of laboratory testing and calibration.

APPENDIX D

FIELD TEST RESULTS - STATIC MEASUREMENTS

The following static measurements were made on the four test consist cars in preparation for dynamic testing of the prototype wayside brake inspection system. Measurements were made December 1, 1977.

CAR ID#		WEIGHT LBS. Individual Truck	Whole Car
USAF 42016	B	24,780	48,680
Empty Gondola	A	24,520	
	Total	49,300	
USAF 42015	B	37,820	77,140
Empty Gondola	A	39,400	
	Total	77,220	
DOTX 501	B	22,560	45,020
Empty Boxcar	A	22,380	
	Total	44,940	
DOTX 502	B	51,440	101,420
Loaded Boxcar	A	50,000	
	Total	101,440	

Measurement Site - Pueblo Depot Activity

SCALE	Range	300,000 lbs.
	Resolution	20 lbs.
	Accuracy	0.2%
	Date of Last Calibration	October 4, 1977

CAR DIMENSIONS

MEASUREMENT	BOXCAR DOTX 502	GONDOLA USAF 42015
a. Wheel Diameter	33 (nominal)	33 in.
b. Axle Separation Center to Center	66 1/16 in.	66 3/16 in.
c. Center pin separation Center to Center	30 ft. 8 in.	32 ft. 7 in.
d. Height of coupler Center Line	33 1/4 in.	33 7/8 in.
e. Brake Cylinder Piston Diameter	10 in. (nominal)	10 in.
f. Brake rigging levers, Dist. from Center pivot	8" x 16"	6"x11" & 7 1/2x14 in.

Brake Shoe Definition

Composition type Cobra V-183,
Used on DOTX 501 Empty Boxcar
USAF 42015, Loaded gondola

Cast Iron type, High Phosphorus, used on DOTX 502, Loaded boxcar
USAF 42016, Empty gondola

Post Test Wheel Examination
Non-condemnable tread build up on wheels: R2, L2, R3, L3, R4, L4. of DOTX 501
No defects were reported on other cars.

"GOLDEN SHOE" MEASUREMENT

DEFINITION OF MEASUREMENT METHOD:

The "Golden Shoe" measures the normal force between the brake beam brake shoe holder and the vehicle wheel. It consists of a hydraulic load cell which replaces the brake shoe and readout gauge. The force generates hydrostatic pressure which is read out on the calibrated gauge. The gauge calibration curve accompanies the data and was used to produce the "calibration curve corrected " values listed on the typed sheets. A copy of the original gauge data is also included.

The rail car pneumatic brake system was actuated by using a compressed air source and controlled by a valve manifold which simulated the locomotive brake control. The system was charged to 70 psi and re-charged after each brake line pressure reduction. Pressure reduction was monitored by a gauge on the manifold for each car. The L-4 wheel was measured at least twice to establish repeatability. A second wheel, which varies from car to car, was measured to determine any variation of forces due to the brake rigging configuration.

The data is plotted on the accompanying graphs. The data is reduced to a linear equation by the method of least squares using a calculator. The data points for 3 and 20 psi were excluded from this calculation.

MEASURE ACCURACY:

	HYDRA CELL	AIR LINE PRESSURE
Range	500 - 20,000 lb.	0 - 90 psi
Resolution	100 lb.	1 psi
Correction Factor	Accompanying Calibration Curve	

"GOLDEN SHOE" MEASUREMENT

CALIBRATION CURVE CORRECTED DATA

Car Identification ID#: USAF 42016 * Car Type: Empty Gondola

Wheel Identification: L-4

('B' end axle is Number 1)

R - Air Line Pressure Reduction, PSI
F - Brake Shoe Normal Force, LBS

Equation of Data Curve:

F lbs = 191 lb / psi X R psi - 768 lbs.

R	F 1	F 2
3	200	200
6	300	400
9	950	1000
11	1350	1400
15	2100	2050
20	2300	2300

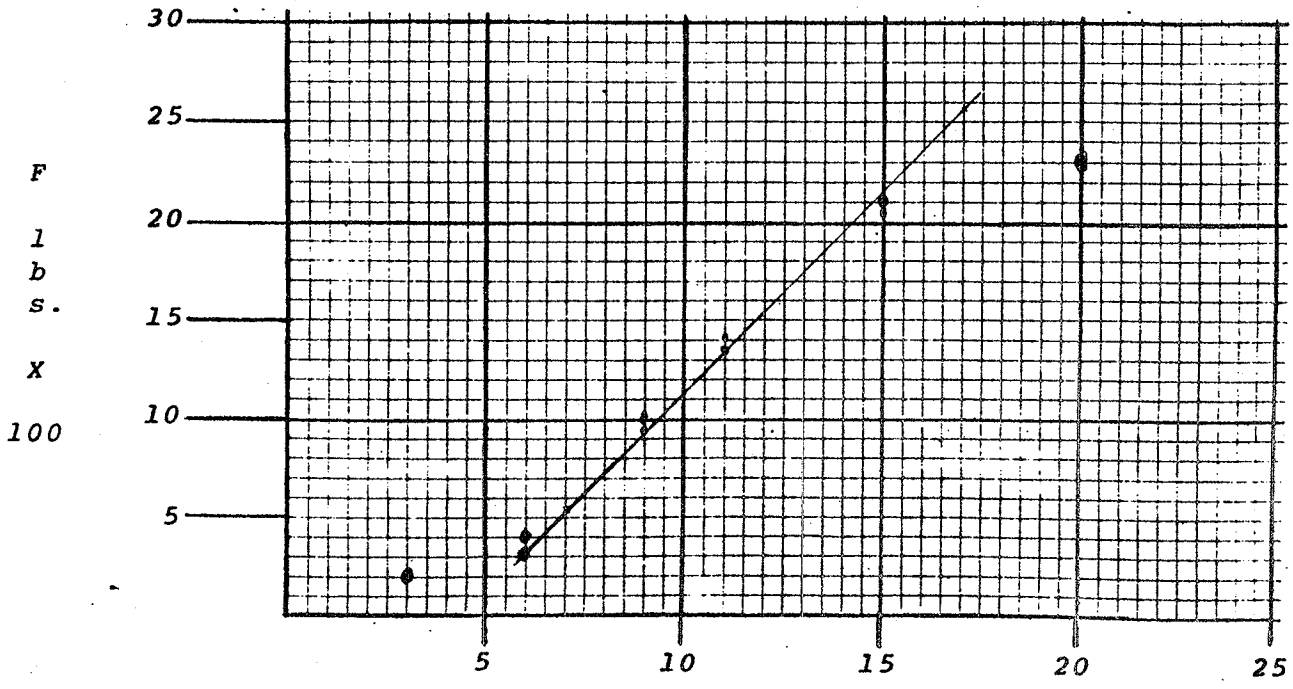

"GOLDEN SHOE" MEASUREMENT

CALIBRATION CURVE CORRECTED DATA

Car Identification ID#: USAF 42016 Car Type: Empty Gondola

Wheel Identification: L-2

('B' end axle is Number 1)

R - Air Line Pressure Reduction, PSI
F - Brake Shoe Normal Force, LBS

Equation of Data Curve:

F lbs = 177 lb / psi X R psi - 676 lbs.

R	F 1	F 2
3		
6	400	
9		
11	1250	
15	2000	
20		

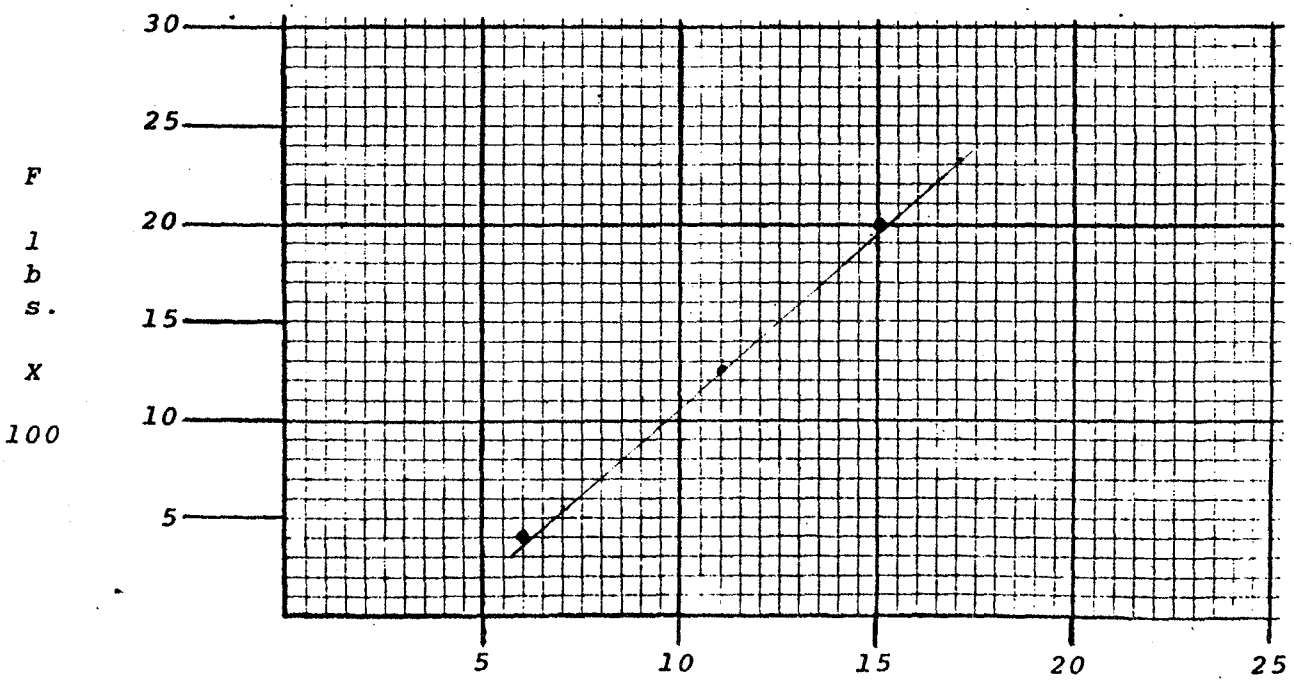

"GOLDEN SHOE" MEASUREMENT

CALIBRATION CURVE CORRECTED DATA

Car Identification ID#: USAF 42015 Car Type: Loaded Gondola

Wheel Identification: L-1
('B' end axle is Number 1)

R - Air Line Pressure Reduction, PSI
F - Brake Shoe Normal Force, LBS

Equation of Data Curve:

F lbs = 195 lb / psi X R psi - 409 lbs.

R	F 1	F 2
3	350	500
6	650	800
9	1400	1400
11	1700	1800
15	2500	2500
20	2700	2600

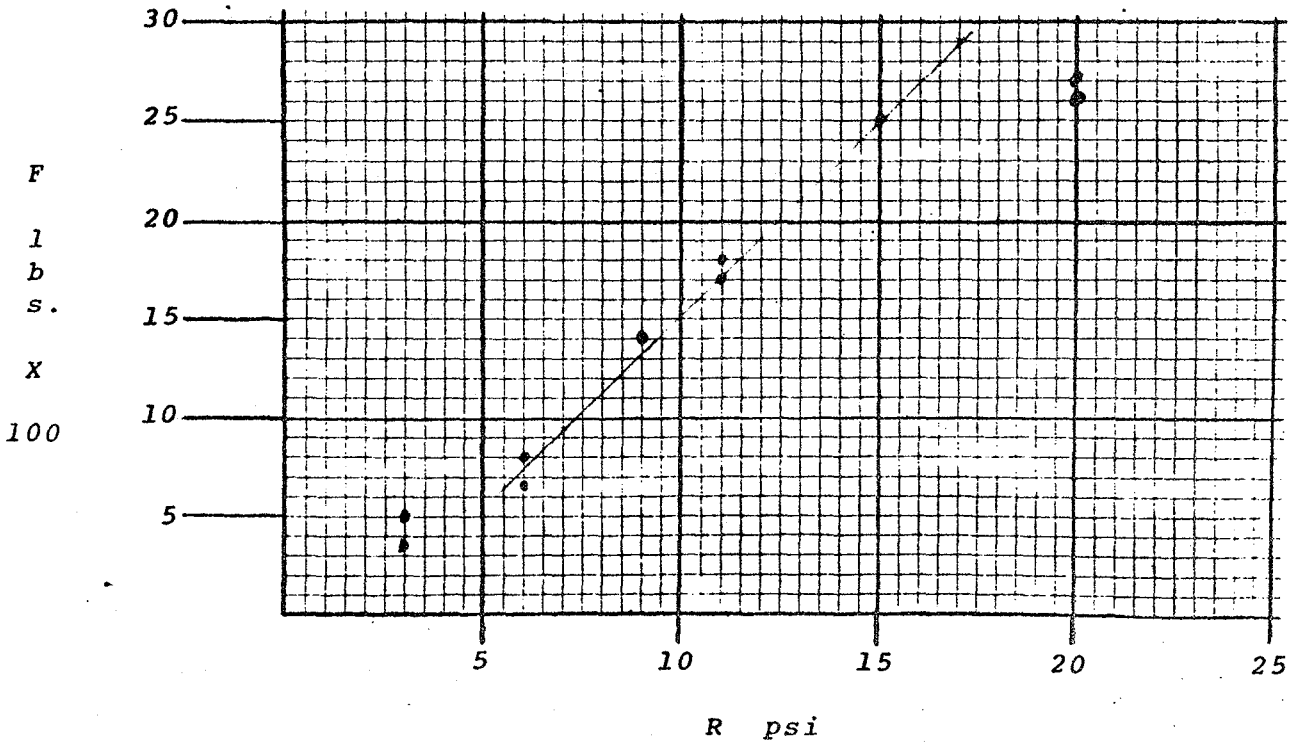

"GOLDEN SHOE" MEASUREMENT

CALIBRATION CURVE CORRECTED DATA

Car Identification ID#: USAF 42015 Car Type: Loaded Gondola

Wheel Identification: L-4

('B' end axle is Number 1)

R - Air Line Pressure Reduction, PSI
F - Brake Shoe Normal Force, LBS

Equation of Data Curve:

F lbs = 195 lb / psi X R psi - 717 lbs.

R	F 1	2
3	250	
6	500	
9	1000	
11	1400	
15	2250	
20	2250	

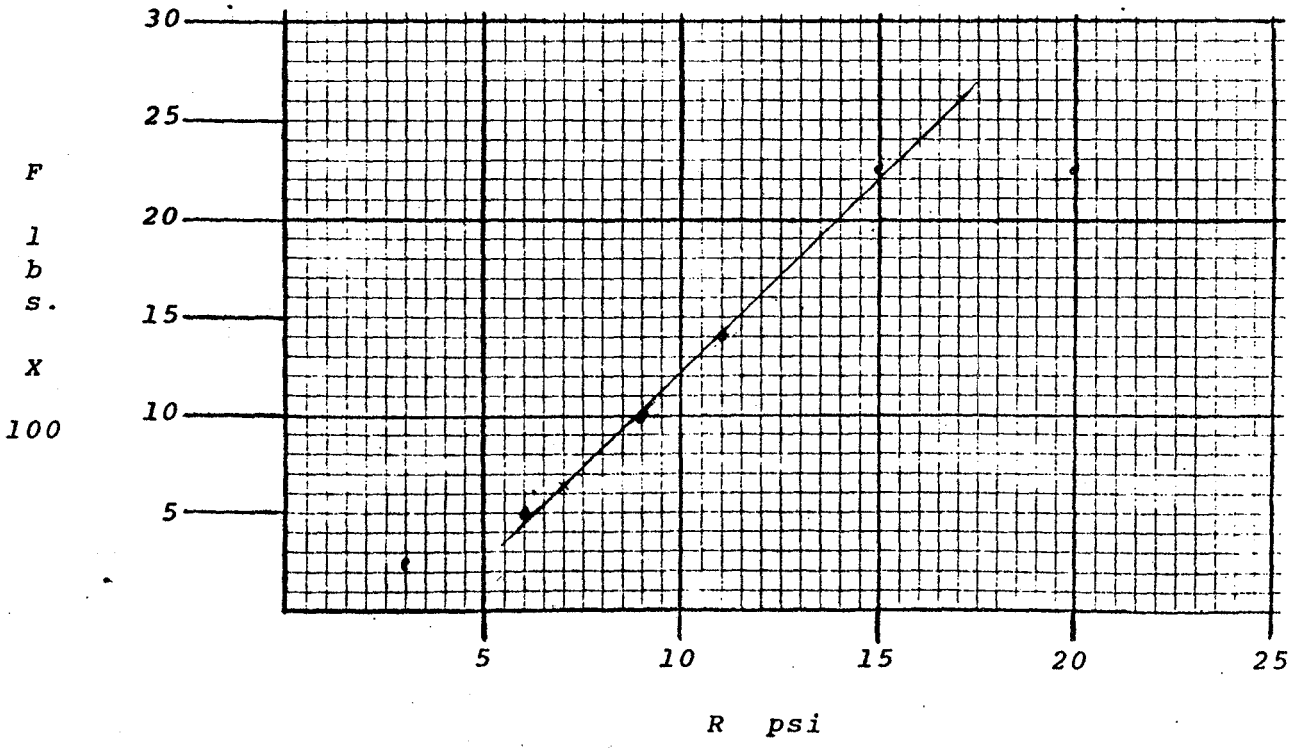

"GOLDEN SHOE" MEASUREMENT

CALIBRATION CURVE CORRECTED DATA

Car Identification ID#: DOTX 501 Car Type: Empty Boxcar

Wheel Identification: L-3

('B' end axle is Number 1)

R - Air Line Pressure Reduction, PSI
F - Brake Shoe Normal Force, LBS

Equation of Data Curve:

F lbs = 182 lb / psi X R psi - 339 lbs.

R	F 1	2
3		
6	800	
9	1200	
11	1700	
15	2400	
20	2800	

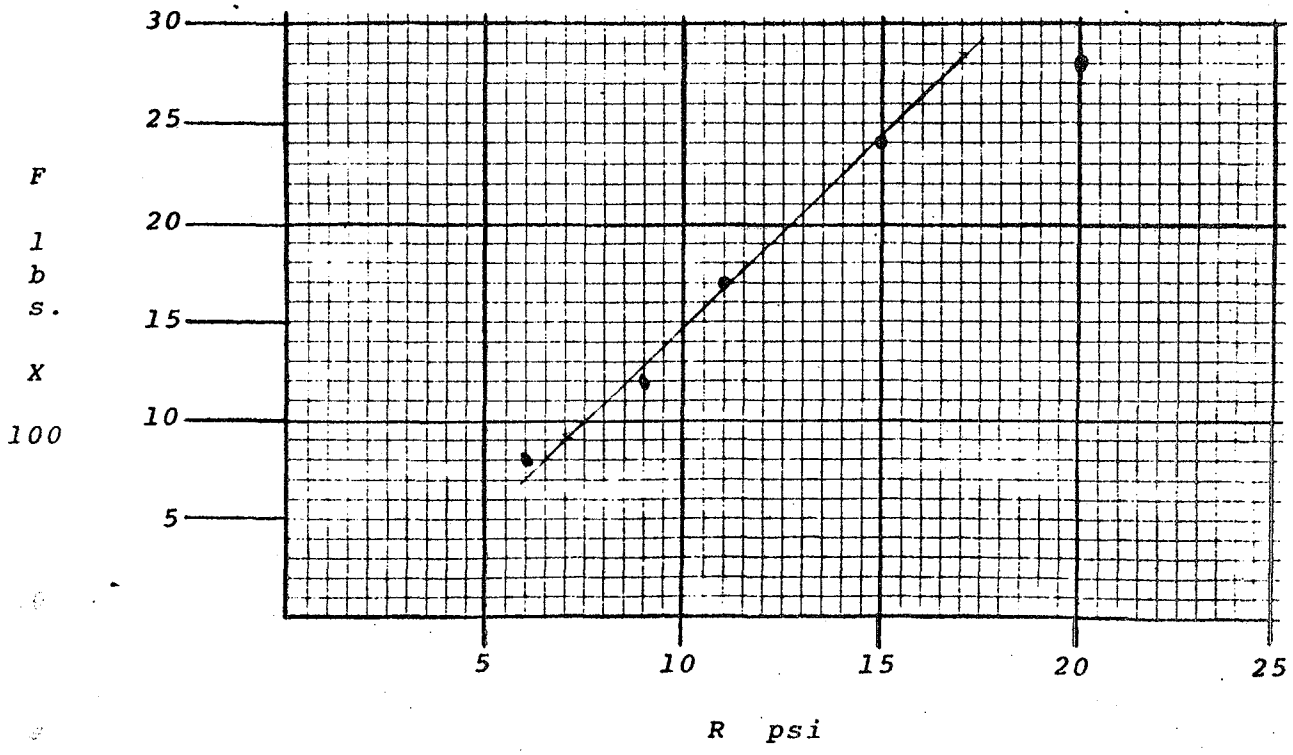

"GOLDEN SHOE" MEASUREMENT

CALIBRATION CURVE CORRECTED DATA

Car Identification ID#: DOTX 501 Car Type: Empty Boxcar

Wheel Identification: L-4

('B' end axle is Number 1)

R - Air Line Pressure Reduction, PSI
F - Brake Shoe Normal Force, LBS

Equation of Data Curve:

F lbs = 176 lb / psi X R psi - 646 lbs.

R	F 1	F 2
3		
6	400	400
9	900	850
11	1250	1550
15	1900	2000
20	2250	2300

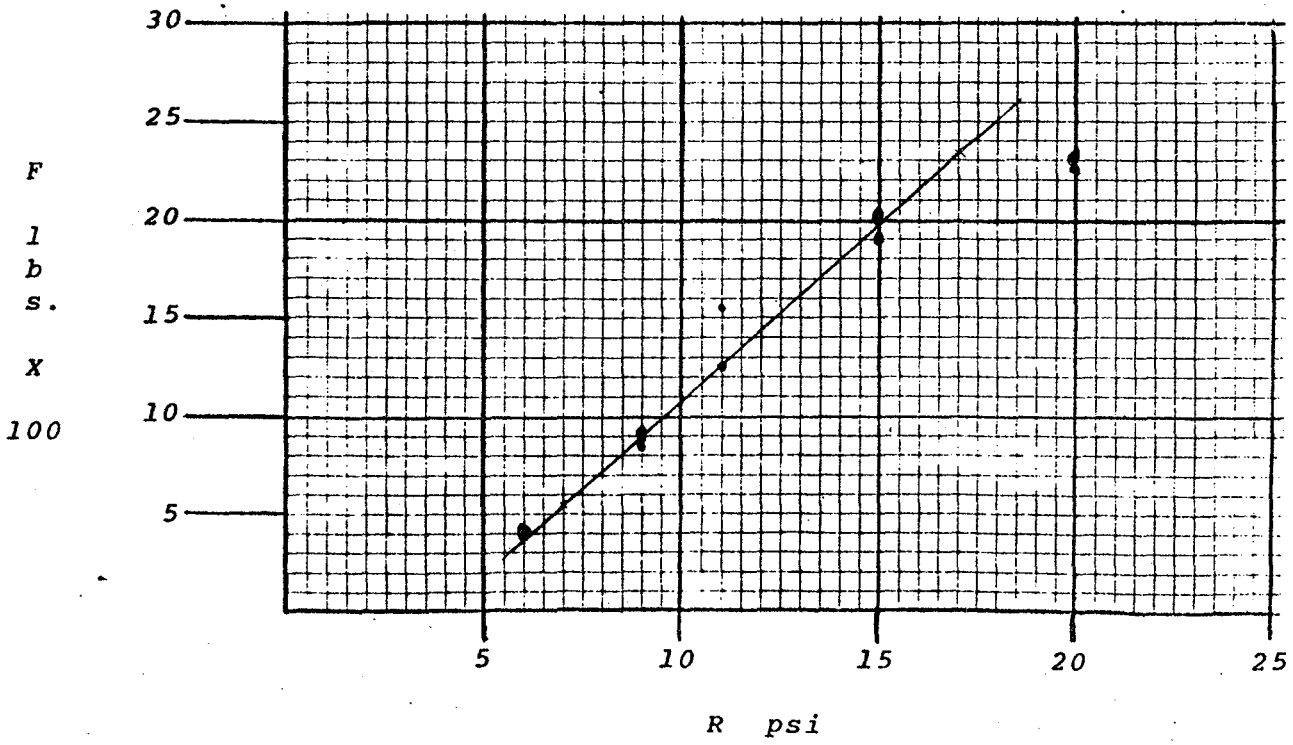

"GOLDEN SHOE" MEASUREMENT

CALIBRATION CURVE CORRECTED DATA

Car Identification ID#: DOTX 502 Car Type: Loaded Boxcar

Wheel Identification: R-4

('B' end axle is Number 1)

R - Air Line Pressure Reduction, PSI
F - Brake Shoe Normal Force, LBS

Equation of Data Curve:

F lbs = 171 lb / psi X R psi - 289 lbs.

R	F 1	F 2
3	500	600
6	650	800
9	1200	1350
11	1600	1600
15	2200	2350
20	2700	2800

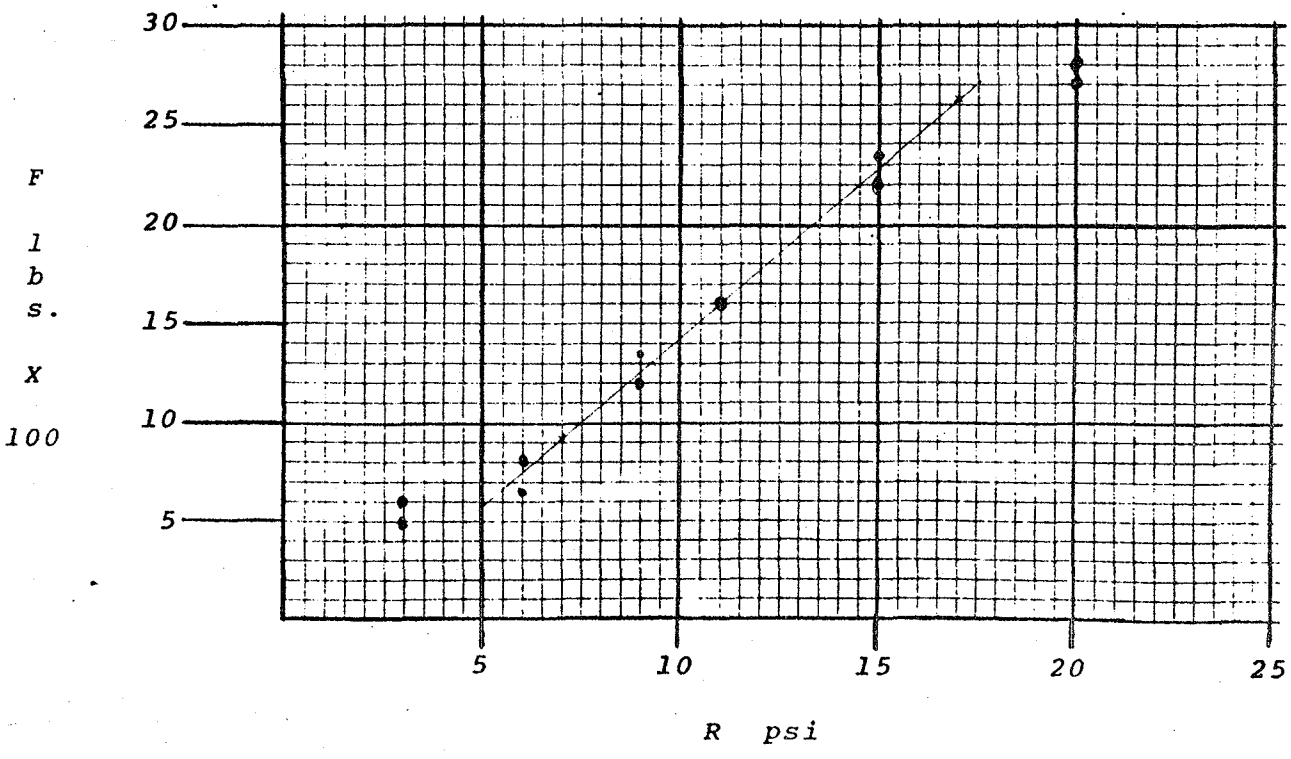

APPENDIX E

FIELD TEST RESULTS - DYNAMIC MEASUREMENTS

Description of Data:

Each test run was characterized by a prescribed consist speed and brake pressure reduction. In general, the test consist was alternately pulled and pushed over the instrumented rail at the appropriate speed.

Five runs; 27A, 28A, 54A, 54B, and 54C were not called for in the test plan, but represent documented runs made to prepare the test consist for the scheduled test runs to follow. The data is included because they represent perfectly valid measurements made on the test consist.

Negative horizontal loads are traction, or driving, forces. Positive horizontal loads represent **braking forces.**

Side load forces are positive towards the outside of the track, negative towards the center of the track. The side load measuring strain gages were damaged, thus inoperative, for test runs 27-58. This is designated as "n.d." (no data).

Temperatures are recorded as temperature (^{o}F) rise above ambient. Ambient temperature during all tests ranged from 26 to 32^{o}F.

When a passing axle did not result in a perceptable I.R. sensor output, indicated temperature is recorded as "a"(ambient). That is, the sensor did not distinguish between a p. ssing axle and the ambient background.

A dash (-) in either temperature column indicates that the recorded I.R. sensor data was unintelligible. A temperature indication was present, but could not be interpreted.

A star (*) beside a temperature indication means that the chart pen went off the recorder scale. The value recorded in the data sheet is therefore lower than that which actually occurred. The maximum indicated chart range varies because chart recorder sensitivity was adjusted as required between 20, 50 and 100 millivolts per division.

Wheel temperatures in the last column were measured with a pyrometer after the consist had been brought to a stop. Measurements were made on the near side wheels only, and only for runs 12, 15, 18, 20, 23, and 27.

TABLE E-1
Field Test Data for Car I
Loaded Box DOTX-502
Truck A Axle 4
Actual Truck Weight = 50,000 lbs.

Run	Orien-tation	Wheel Side	Train Speed (mph)	Brake Red'n (psi)	Vertical Load (lb)	Horzntl Load (lb)	Side Load (mv)	Near Side Temp (°F)	Far Side Temp (°F)	Wheel Temp (°F)
1	Pull	R	5	0	12,515	- 336	2600	a	a	
2	Push	R	4	0	11,779	- 672	2400	a	a	
3	Pull	R	5	0	12,515	- 336	3000	a	a	
4	Push	R	5	0	11,779	- 840	2400	a	a	
5	Pull	R	10	0	13,252	336	2600	a	a	
6	Push	R	10	0	12,515	- 504	2600	a	a	
7	Pull	R	20	0	11,779	- 336	3600	a	a	
8	Push	R	20	0	12,515	- 840	3800	a	a	
9	Pull	R	40	0	11,779	840	n.d.	a	a	
10	Push	R	40	0	12,515	- 504	3200	a	a	
11	Pull	R	60	0	11,779	1176	1200	a	a	
12	Push	R	60	0	13,988	0	2000	a	a	(35)
13	Pull	R	10	6	11,043	- 672	3000	a	a	
14	Push	R	10	11	12,515	336	2000	41	10	
15	Pull	R	10	15	11,779	- 336	4000	109	30	(95)
16	Push	R	20	6	13,252	- 504	3200	27	10	
17	Pull	R	20	11	12,515	-1512	4000	54	20	
18	Push	R	20	15	15,460	3024	1400	-	50	(140)
19	Pull	R	40	6	10,307	- 840	4000	-	20	
20	Push	R	40	11	13,988	2016	2200	-	30	(120)
21	Pull	R	40	15	11,043	-1512	5000	-	100	
22	Push	R	60	6	13,252	- 672	3000	-	25	
23	Pull	R	60	11	10,307	-1344	4400	-	50	(110)
24	Pull	R	60	15	10,307	-2184	5000	-	50	
25	Pull	L	10	11	13,252	1848	1000	-	10	
26	Push	L	20	11	9,571	- 672	2000	136	75	
27	Pull	L	40	11	11,779	1176	n.d.	-	75	(210)
27A	Push	L	20	11	11,779	- 168	"	170	25	
28	Pull	L	60	11	10,307	2184	"	257	25	
28A	Push	L	30	11	11,779	0	"	213	50	
29	Pull	L	10	0	11,043	1848	"	-	20	
30	Push	L	20	0	11,043	504	"	-	15	
31	Pull	L	40	0	11,043	1176	"	a	a	
32	Pull	L	60	0	11,043	1680	"	a	a	
33	Pull	L	10	11	13,252	1848	"	163	50	
34	Push	L	20	11	11,779	- 840	"	41	125	
35	Pull	L	40	11	11,779	1512	"	-	75	
36	Pull	L	60	11	11,779	2016	"	-	38	

TABLE E-2 (Cont'd)

Field Test Data for Car I
Loaded Box DOTX-502
Truck A Axle 3
Actual Truck Weight = 50,000

Run	Orien-tation	Wheel Side	Train Speed (mph)	Brake Red'n (psi)	Vertical Load (lb)	Horzntl Load (lb)	Side Load (mv)	Near Side Temp (°F)	Far Side Temp (°F)
41	Pull	L	60	0	12,515	- 840	n.d.	a	a
42	Push	L	10	0	12,515	- 504	"	a	25
43	Pull	L	40	0	10,307	- 840	"	a	25
44	Push	L	20	0	12,515	- 840	"	a	25
45	Pull	R	40	0	10,307	- 336	"	-	a
46	Push	R	20	0	14,724	840	"	-	a
47	Pull	R	60	0	11,779	672	"	-	a
48	Push	R	10	0	12,515	504	"	-	a
49	Pull	R	30	0	11,779	- 672	"	-	a
50	Push	R	30	0	14,724	840	"	-	a
51	Pull	R	30	0	12,515	- 168	"	-	a
52	Push	R	10	11	13,252	504	"	-	a
53	Pull	R	10	15	13,252	504	"	-	25
54	Push	R	40	11	13,988	336	"	-	a
54A	Pull	R	40	11	13,988	168	"	-	a
54B	Push	R	20	13	13,988	672	"	a	38
54C	Pull	R	40	13	8,834	1008	"	34	-
55	Pull	R	40	13	9,571	336	"	-	-
56	Pull	R	40	13	10,307	168	"	-	10
57	Push	R	10	6	12,515	168	"	-	20
58	Pull	R	40	13	9,571	336	"	-	a

Letters (A,B,C) after Run Number designate non-scheduled tests for which data was taken.

N.D. indicates that no data was taken. For Side loads, strain gages were inoperative for Runs 27-58.

A dash (-) indicates that temperature data existed, but was unintelligible.

A star (*) indicates that the temperature recorder went off scale. The recorded value is therefore less than the actual temperature.

All temperature readings are in °F above ambient. Ambient for all tests ranged from 26 to 32°F. The designation "a" means that no temperature rise occurred as the wheel passed, thus the wheel temperature was the same as ambient.

Horizontal traction forces are negative; braking forces are positive.

TABLE E-3
Field Test Data for Car I
Loaded Box DOTX-502
Truck B Axle 2
Actual Truck Weight = 51,440

Run	Orien-tation	Wheel Side	Train Speed (mph)	Brake Red'n (psi)	Vertical Load (lb)	Horzntl Load (lb)	Side Load (mv)	Near Side Temp (°F)	Far Side Temp (°F)	Wheel Temp (°F)
1	Pull	R	5	0	13,988	1512	- 600	a	a	
2	Push	R	4	0	14,724	-1680	- 600	a	a	
3	Pull	R	5	0	13,988	1008	- 600	a	a	
4	Push	R	5	0	14,724	-1512	- 400	a	a	
5	Pull	R	10	0	13,988	840	- 800	a	a	
6	Push	R	10	0	15,460	-1176	-1200	a	a	
7	Pull	R	20	0	15,460	1512	-1800	a	a	
8	Push	R	20	0	16,933	-1848	-1400	a	a	
9	Pull	R	40	0	11,043	1176	-1500	a	a	
10	Push	R	40	0	15,460	-1176	-1600	a	a	
11	Pull	R	60	0	13,252	840	-1500	a	a	
12	Push	R	60	0	12,515	- 672	0	a	a	(35)
13	Pull	R	10	6	14,724	1512	-1500	a	a	
14	Push	R	10	11	16,196	-1008	-2000	14	15	
15	Pull	R	10	15	14,724	2352	-1000	122	50	(130)
16	Push	R	20	6	16,196	-1680	-1600	54	10	
17	Pull	R	20	11	13,252	1848	-1000	82	50	
18	Push	R	20	15	16,196	- 840	-1600	-	70	(200)
19	Pull	R	40	6	11,779	1512	-1000	-	30	
20	Push	R	40	11	13,988	-1008	-1200	-	60	(165)
21	Pull	R	40	15	12,515	1680	- 800	-	274	
22	Push	R	60	6	14,724	-1512	-2000	-	10	
23	Pull	R	60	11	13,252	2688	-2000	-	125	(125)
24	Pull	R	60	15	10,307	1848	-1000	-	175	
25	Pull	L	10	11	14,724	672	-1000	-	40	
26	Push	L	20	11	13,988	840	-1000	290	221	
27	Pull	L	40	11	13,252	0	n.d.	-	221	(300)
27A	Push	L	20	11	14,724	504	"	-	100	
28	Pull	L	60	11	13,252	- 336	"	235	75	
28A	Push	L	30	11	15,460	1008	"	301	38	
29	Pull	L	10	0	13,988	840	"	-	30	
30	Push	L	20	0	13,988	- 168	"	-	a	
31	Pull	L	40	0	16,933	- 168	"	a	a	
32	Pull	L	60	0	14,724	336	"	a	a	
33	Pull	L	10	11	15,460	672	"	82	90	
34	Push	L	20	11	14,724	336	"	102	200	
35	Pull	L	40	11	15,460	0	"	-	175	
36	Pull	L	60	11	15,460	840	"	-	75	

TABLE E-3 (Cont'd)

Field Test Data for Car I
Loaded Box DOTX-502
Truck B Axle 2
Actual Truck Weight = 51,440

Run	Orientation	Wheel Side	Train Speed (mph)	Brake Red'n (psi)	Vertical Load (lb)	Horzntl Load (lb)	Side Load (mv)	Near Side Temp (°F)	Far Side Temp (°F)
41	Pull	L	60	0	13,988	336	n.d.	a	a
42	Push	L	10	0	16,196	- 336	"	a	25
43	Pull	L	40	0	15,460	0	"	a	25
44	Push	L	20	0	14,724	336	"	a	25
45	Pull	R	40	0	12,515	840	"	a	a
46	Push	R	20	0	16,196	- 504	"	a	a
47	Pull	R	60	0	14,724	1008	"	a	a
48	Push	R	10	0	14,724	504	"	a	a
49	Pull	R	30	0	13,988	0	"	a	a
50	Push	R	30	0	13,988	- 840	"	a	a
51	Pull	R	30	0	15,460	168	"	a	a
52	Push	R	10	11	14,724	336	"	a	a
53	Pull	R	10	15	14,724	1008	"	a	25
54	Push	R	40	11	15,460	336	"	a	a
54A	Pull	R	40	11	11,779	672	"	a	a
54B	Push	R	20	13	15,460	840	"	a	50
54C	Pull	R	40	13	12,515	672	"	68	75
55	Pull	R	40	13	8,098	415	"	-	30
56	Pull	R	40	13	11,779	252	"	54	30
57	Push	R	10	6	14,724	85	"	-	20
58	Pull	R	40	13	11,779	420	"	-	a

Letters (A,B,C) after Run Number designate non-scheduled tests for which data was taken.

N.D. indicates that no data was taken. For Side loads, strain gages were inoperative for Runs 27-58.

A dash (-) indicates that temperature data existed, but was unintelligible.

A star (*) indicates that the temperature recorder went off scale. The recorded value is therefore less than the actual temperature.

All temperature readings are in °F above ambient. Ambient for all tests ranged from 26 to 32°F. The designation "a" means that no temperature rise occurred as the wheel passed, thus the wheel temperature was the same as ambient.

Horizontal traction forces are negative; braking forces are positive.

TABLE E-4
Field Test Data for Car I
Loaded Box DOTX-502
Truck B Axle 1
Actual Truck Weight = 51,440

Run	Orien-tation	Wheel Side	Train Speed (mph)	Brake Red'n (psi)	Vertical Load (lb)	Horzntl Load (lb)	Side Load (mv)	Near Side Temp (°F)	Far Side Temp (°F)	Wheel Temp (°F)
1	Pull	R	5	0	11,779	-1008	3600	a	a	
2	Push	R	4	0	13,988	2352	0	a	a	
3	Pull	R	5	0	12,515	- 840	3400	a	a	
4	Push	R	5	0	13,252	2352	-1200	a	a	
5	Pull	R	10	0	13,252	- 672	3000	a	a	
6	Push	R	10	0	14,724	2856	- 400	a	a	
7	Pull	R	20	0	11,779	- 672	4000	a	a	
8	Push	R	20	0	14,724	2520	400	a	a	
9	Pull	R	40	0	10,307	-1344	n.d.	a	a	
10	Push	R	40	0	13,252	2352	1800	a	a	
11	Pull	R	60	0	13,988	504	1500	a	a	
12	Push	R	60	0	11,779	2352	0	a	a	(35)
13	Pull	R	10	6	11,779	-1680	4000	a	a	
14	Push	R	10	11	13,988	3024	500	41	20	
15	Pull	R	10	15	12,515	-1008	2500	54	30	(125)
16	Push	R	20	6	13,988	2016	- 200	7	20	
17	Pull	R	20	11	13,252	-2016	4000	27	40	
18	Push	R	20	15	13,252	3024	1400	-	100	(110)
19	Pull	R	40	6	11,779	-2016	5000	-	20	
20	Push	R	40	11	12,515	3024	1000	-	50	(115)
21	Pull	R	40	15	12,515	-1512	4800	-	125	
22	Push	R	60	6	13,252	3360	-1800	-	19	
23	Pull	R	60	11	11,043	-1344	3600	-	50	(100)
24	Pull	R	60	15	10,307	-1008	3000	-	100	
25	Pull	L	10	11	12,515	840	1500	-	10	
26	Push	L	20	11	12,515	- 672	3000	290	25	
27	Pull	L	40	11	13,252	672	n.d.	-	75	(280)
27A	Push	L	20	11	12,515	- 840	"	-	13	
28	Pull	L	60	11	12,515	504	"	290	25	
28A	Push	L	30	11	11,043	-1680	"	323	-	
29	Pull	L	10	0	11,779	336	"	-	a	
30	Push	L	20	0	14,724	-1008	"	-	a	
31	Pull	L	40	0	11,779	672	"	a	a	
32	Pull	L	60	0	12,515	672	"	a	a	
33	Pull	L	10	11	13,252	336	"	82	30	
34	Push	L	20	11	13,252	-1344	"	109	50	
35	Pull	L	40	11	11,779	0	"	-	100	
36	Pull	L	60	11	12,515	1008	"	-	38	

TABLE E-4 (Cont'd)

Field Test Data for Car I
Loaded Box DOTX-502
Truck B Axle 1
Actual Truck Weight = 51,440

Run	Orientation	Wheel Side	Train Speed (mph)	Brake Red'n (psi)	Vertical Load (lb)	Horsntl Load (lb)	Side Load (mv)	Near Side Temp (°F)	Far Side Temp (°F)
41	Pull	L	60	0	13,252	1008	n.d.	a	a
42	Push	L	10	0	12,515	-1008	"	a	25
43	Pull	L	40	0	13,988	168	"	a	25
44	Push	L	20	0	15,460	-1176	"	a	25
45	Pull	R	40	0	12,515	- 168	"	-	a
46	Push	R	20	0	13,988	1344	"	-	a
47	Pull	R	60	0	12,515	0	"	-	a
48	Push	R	10	0	13,988	840	"	-	a
49	Pull	R	30	0	12,515	-1008	"	-	a
50	Push	R	30	0	13,988	1680	"	-	a
51	Pull	R	30	0	12,515	0	"	-	a
52	Push	R	10	11	14,724	1176	"	-	a
53	Pull	R	10	15	11,779	504	"	-	a
54	Push	R	40	11	13,988	840	"	-	a
54A	Pull	R	40	11	11.779	840	"	-	a
54B	Push	R	20	13	12,515	840	"	-	25
54C	Pull	R	40	13	11,779	672	"	34	50
55	Pull	R	40	13	12,515	336	"	-	20
56	Pull	R	40	13	12,515	252	"	41	20
57	Push	R	10	6	13,988	252	"	-	10
58	Pull	R	40	13	11,779	420	"	-	a

Letters (A,B,C) after Run Number designate non-scheduled tests for which data was taken.

N.D. indicates that no data was taken. For Side loads, strain gages were inoperative for Runs 27-58.

A dash (-) indicates that temperature data existed, but was unintelligible.

A star (*) indicates that the temperature recorder went off scale. The recorded value is therefore less than the actual temperature.

All temperature readings are in °F above ambient. Ambient for all tests ranged from 26 to 32°F. The designation "a" means that no temperature rise occurred as the wheel passed, thus the wheel temperature was the same as ambient.

Horizontal traction forces are negative; braking forces are positive.

TABLE E-5
Field Test Data for Car II
Empty Box DOTX-501
Truck A Axle 4
Actual Truck Weight = 22,380

Run	Orien-tation	Wheel Side	Train Speed (mph)	Brake Red'n (psi)	Vertical Load (lb)	Horzntl Load (lb)	Side Load (mv)	Near Side Temp (°F)	Far Side Temp (°F)	Wheel Temp (°F)
1	Pull	R	5	0	5,153	504	1200	a	a	
2	Push	R	4	0	5,153	- 672	1800	a	a	
3	Pull	R	5	0	5,153	504	1200	a	a	
4	Push	R	5	0	5,153	- 672	1800	a	a	
5	Pull	R	10	0	5,153	504	1400	a	a	
6	Push	R	10	0	5,153	- 504	1800	a	a	
7	Pull	R	20	0	5,153	1008	1600	a	a	
8	Push	R	20	0	7,362	- 504	1400	a	a	
9	Pull	R	40	0	5,153	840	n.d.	a	a	
10	Push	R	40	0	5,890	336	0	a	a	
11	Pull	R	60	0	6,626	504	1800	a	a	
12	Push	R	60	0	8,834	- 840	500	a	a	(35)
13	Pull	R	10	6	5,153	336	3500	a	a	
14	Push	R	10	11	5,890	- 672	1500	27	10	
15	Pull	R	10	15	5,153	336	1500	54	10	(120)
16	Push	R	20	6	5,890	- 504	1600	14	10	
17	Pull	R	20	11	5,890	504	2600	54	10	
18	Push	R	20	15	5,890	- 504	1800	82	90	(165)
19	Pull	R	40	6	4,417	1008	1400	41	50	
20	Push	R	40	11	5,890	336	1000	163	150	(175)
21	Pull	R	40	15	5,153	1008	1200	-	50	
22	Push	R	60	6	5,153	0	-1200	-	50	
23	Pull	R	60	11	6,626	1848	-1200	-	200	(185)
24	Pull	R	60	15	5,153	840	1800	-	150	
25	Pull	L	10	11	5,153	504	500	-	10	
26	Push	L	20	11	5,153	0	1000	102	75	
27	Pull	L	40	11	4,417	0	n.d.	301	358	(250)
27A	Push	L	20	11	5,153	0	"	334	40	
28	Pull	L	60	11	5,890	504	"	334	200	
28A	Push	L	30	11	7,362	168	"	400	100	
29	Pull	L	10	11	5,153	672	"	-	50	
30	Push	L	20	11	5,153	0	"	-	110	
31	Pull	L	40	11	4,417	672	"	61	160	
32	Pull	L	60	11	5,153	336	"	41	160	
33	Pull	L	10	0	5,153	504	"	14	40	
34	Push	L	20	0	5,153	- 168	"	a	-	
35	Pull	L	40	0	5,153	504	"	a	-	
36	Pull	L	60	0	7,362	0	"	a	-	

TABLE E-1 (Cont'd)

Field Test Data for Car I

Loaded Box DOTX-502

Truck A Axle 4

Actual Truck Weight = 50,000 lbs.

Run	Orien-tation	Wheel Side	Train Speed (mph)	Brake Red'n (psi)	Vertical Load (lb)	Horzntl Load (lb)	Side Load (mv)	Near Side Temp (°F)	Far Side Temp (°F)
41	Pull	L	60	0	11,779	1176	N.D.	a	a
42	Push	L	10	0	11,043	336	"	a	25
43	Pull	L	40	0	9,571	1008	"	a	25
44	Push	L	20	0	10,307	672	"	a	25
45	Pull	R	40	0	10,307	0	"	-	a
46	Push	R	20	0	13,988	0	"	-	a
47	Pull	R	60	0	12,515	- 504	"	-	a
48	Push	R	10	0	13,252	840	"	-	a
49	Pull	R	30	0	11,043	- 840	"	-	a
50	Push	R	30	0	13,988	- 336	"	-	a
51	Pull	R	30	0	12,515	168	"	-	a
52	Push	R	10	11	13,252	336	"	-	a
53	Pull	R	10	15	11,779	504	"	-	50
54	Push	R	40	11	14,724	672	"	-	a
54A	Pull	R	40	11	11,043	840	"	-	a
54B	Push	R	20	13	13,252	504	"	a	25
54C	Pull	R	40	13	11,043	1176	"	34	-
55	Pull	R	40	13	12,515	415	"	-	-
56	Pull	R	40	13	12,515	252	"	-	10
57	Push	R	10	6	13,252	252	"	-	20
58	Pull	R	40	13	12,515	336	"	-	a

Letters (A,B,C) after Run Number designate non-scheduled tests for which data was taken.

N.D. indicates that no data was taken. For Side loads, strain gages were inoperative for Runs 27-58.

A dash (-) indicates that temperature data existed, but was unintelligible.

A star (*) indicates that the temperature recorder went off scale. The recorded value is therefore less than the actual temperature.

All temperature readings are in °F above ambient. Ambient for all tests ranged from 26 to 32°F. The designation "a" means that no temperature rise occurred as the wheel passed, thus the wheel temperature was the same as ambient.

Horizontal traction forces are negative; braking forces are positive.

TABLE E-2
Field Test Data for Car I
Loaded Box DOTX-502
Truck A Axle 3
Actual Truck Weight - 50,000

Run	Orien-tation	Wheel Side	Train Speed (mph)	Brake Red'n (psi)	Vertical Load (lb)	Horzntl Load (lb)	Side Load (mv)	Near Side Temp (°F)	Far Side Temp (°F)	Wheel Temp (°F)
1	Pull	R	5	0	12,515	- 672	2600	a	a	
2	Push	R	4	0	12,515	672	2000	a	a	
3	Pull	R	5	0	12,515	-1008	2800	a	a	
4	Push	R	5	0	12,515	1008	2000	a	a	
5	Pull	R	10	0	13,252	- 504	2600	a	a	
6	Push	R	10	0	13,252	1008	2200	a	a	
7	Pull	R	20	0	11,779	-1512	2400	a	a	
8	Push	R	20	0	14,724	840	2600	a	a	
9	Pull	R	40	0	8,834	-1008	n.d.	a	a	
10	Push	R	40	0	13,252	1512	3000	a	a	
11	Pull	R	60	0	13,988	- 168	1500	a	a	
12	Push	R	60	0	15,460	1344	1000	a	a	(35)
13	Pull	R	10	6	11,779	- 336	3500	a	a	
14	Push	R	10	11	12,515	168	2500	27	20	
15	Pull	R	10	15	13,988	1176	1000	95	30	(95)
16	Push	R	20	6	14,724	- 672	2800	41	15	
17	Pull	R	20	11	11,779	168	2000	82	30	
18	Push	R	20	15	13,988	-1848	4000	-	60	(150)
19	Pull	R	40	6	11,043	- 672	2400	-	10	
20	Push	R	40	11	11,779	-2016	4000	-	30	(115)
21	Pull	R	40	15	11,043	2352	- 400	-	75	
22	Push	R	60	6	13,988	2520	2000	-	50	
23	Pull	R	60	11	11,779	2688	600	-	10	(110)
24	Pull	R	60	15	10,307	2184	-1400	-	100	
25	Pull	L	10	11	11,779	-1008	2500	-	10	
26	Push	L	20	11	11,043	672	2800	213	50	
27	Pull	L	40	11	11,779	-1008	n.d.	-	38	(220)
27A	Push	L	20	11	12,515	168	"	235	25	
28	Pull	L	60	11	11,779	- 840	"	246	25	
28A	Push	L	30	11	11,779	0	"	312	38	
29	Pull	L	10	0	11,779	- 840	"	-	10	
30	Push	L	20	0	12,515	-1008	"	-	10	
31	Pull	L	40	0	11,043	- 168	"	a	a	
32	Pull	L	60	0	11,043	-1176	"	a	a	
33	Pull	L	10	11	12,515	- 504	"	82	50	
34	Push	L	20	11	12,515	672	"	54	100	
35	Pull	L	40	11	11,043	-1176	"	-	75	
36	Pull	L	60	11	11,779	- 336	"	-	38	

TABLE E-2 (Cont'd)

Field Test Data for Car I
Loaded Box DOTX-502
Truck A Axle 3
Actual Truck Weight = 50,000

Run	Orien-tation	Wheel Side	Train Speed (mph)	Brake Red'n (psi)	Vertical Load (lb)	Horzntl Load (lb)	Side Load (mv)	Near Side Temp (°F)	Far Side Temp (°F)
41	Pull	L	60	0	12,515	- 840	n.d.	a	a
42	Push	L	10	0	12,515	- 504	"	a	25
43	Pull	L	40	0	10,307	- 840	"	a	25
44	Push	L	20	0	12,515	- 840	"	a	25
45	Pull	R	40	0	10,307	- 336	"	-	a
46	Push	R	20	0	14,724	840	"	-	a
47	Pull	R	60	0	11,779	672	"	-	a
48	Push	R	10	0	12,515	504	"	-	a
49	Pull	R	30	0	11,779	- 672	"	-	a
50	Push	R	30	0	14,724	840	"	-	a
51	Pull	R	30	0	12,515	- 168	"	-	a
52	Push	R	10	11	13,252	504	"	-	a
53	Pull	R	10	15	13,252	504	"	-	25
54	Push	R	40	11	13,988	336	"	-	a
54A	Pull	R	40	11	13,988	168	"	-	a
54B	Push	R	20	13	13,988	672	"	a	38
54C	Pull	R	40	13	8,834	1008	"	34	-
55	Pull	R	40	13	9,571	336	"	-	-
56	Pull	R	40	13	10,307	168	"	-	10
57	Push	R	10	6	12,515	168	"	-	20
58	Pull	R	40	13	9,571	336	"	-	a

Letters (A,B,C) after Run Number designate non-scheduled tests for which data was taken.

N.D. indicates that no data was taken. For Side loads, strain gages were inoperative for Runs 27-58.

A dash (-) indicates that temperature data existed, but was unintelligible.

A star (*) indicates that the temperature recorder went off scale. The recorded value is therefore less than the actual temperature.

All temperature readings are in °F above ambient. Ambient for all tests ranged from 26 to 32°F. The designation "a" means that no temperature rise occurred as the wheel passed, thus the wheel temperature was the same as ambient.

Horizontal traction forces are negative; braking forces are positive.

TABLE E-3
Field Test Data for Car I
Loaded Box DOTX-502
Truck B Axle 2
Actual Truck Weight = 51,440

Run	Orien-tation	Wheel Side	Train Speed (mph)	Brake Red'n (psi)	Vertical Load (lb)	Horzntl Load (lb)	Side Load (mv)	Near Side Temp (°F)	Far Side Temp (°F)	Wheel Temp (°F)
1	Pull	R	5	0	13,988	1512	- 600	a	a	
2	Push	R	4	0	14,724	-1680	- 600	a	a	
3	Pull	R	5	0	13,988	1008	- 600	a	a	
4	Push	R	5	0	14,724	-1512	- 400	a	a	
5	Pull	R	10	0	13,988	840	- 800	a	a	
6	Push	R	10	0	15,460	-1176	-1200	a	a	
7	Pull	R	20	0	15,460	1512	-1800	a	a	
8	Push	R	20	0	16,933	-1848	-1400	a	a	
9	Pull	R	40	0	11,043	1176	-1500	a	a	
10	Push	R	40	0	15,460	-1176	-1600	a	a	
11	Pull	R	60	0	13,252	840	-1500	a	a	
12	Push	R	60	0	12,515	- 672	0	a	a	(35)
13	Pull	R	10	6	14,724	1512	-1500	a	a	
14	Push	R	10	11	16,196	-1008	-2000	14	15	
15	Pull	R	10	15	14,724	2352	-1000	122	50	(130)
16	Push	R	20	6	16,196	-1680	-1600	54	10	
17	Pull	R	20	11	13,252	1848	-1000	82	50	
18	Push	R	20	15	16,196	- 840	-1600	-	70	(200)
19	Pull	R	40	6	11,779	1512	-1000	-	30	
20	Push	R	40	11	13,988	-1008	-1200	-	60	(165)
21	Pull	R	40	15	12,515	1680	- 800	-	274	
22	Push	R	60	6	14,724	-1512	-2000	-	10	
23	Pull	R	60	11	13,252	2688	-2000	-	125	(125)
24	Pull	R	60	15	10,307	1848	-1000	-	175	
25	Pull	L	10	11	14,724	672	-1000	-	40	
26	Push	L	20	11	13,988	840	-1000	290	221	
27	Pull	L	40	11	13,252	0	n.d.	-	221	(300)
27A	Push	L	20	11	14,724	504	"	-	100	
28	Pull	L	60	11	13,252	- 336	"	235	75	
28A	Push	L	30	11	15,460	1008	"	301	38	
29	Pull	L	10	0	13,988	840	"	-	30	
30	Push	L	20	0	13,988	- 168	"	-	a	
31	Pull	L	40	0	16,933	- 168	"	a	a	
32	Pull	L	60	0	14,724	336	"	a	a	
33	Pull	L	10	11	15,460	672	"	82	90	
34	Push	L	20	11	14,724	336	"	102	200	
35	Pull	L	40	11	15,460	0	"	-	175	
36	Pull	L	60	11	15,460	840	"	-	75	

TABLE E-3 (Cont'd)

Field Test Data for Car I
Loaded Box DOTX-502
Truck B Axle 2
Actual Truck Weight = 51,440

Run	Orientation	Wheel Side	Train Speed (mph)	Brake Red'n (psi)	Vertical Load (lb)	Horzntl Load (lb)	Side Load (mv)	Near Side Temp (°F)	Far Side Temp (°F)
41	Pull	L	60	0	13,988	336	n.d.	a	a
42	Push	L	10	0	16,196	- 336	"	a	25
43	Pull	L	40	0	15,460	0	"	a	25
44	Push	L	20	0	14,724	336	"	a	25
45	Pull	R	40	0	12,515	840	"	a	a
46	Push	R	20	0	16,196	- 504	"	a	a
47	Pull	R	60	0	14,724	1008	"	a	a
48	Push	R	10	0	14,724	504	"	a	a
49	Pull	R	30	0	13,988	0	"	a	a
50	Push	R	30	0	13,988	- 840	"	a	a
51	Pull	R	30	0	15,460	168	"	a	a
52	Push	R	10	11	14,724	336	"	a	a
53	Pull	R	10	15	14,724	1008	"	a	25
54	Push	R	40	11	15,460	336	"	a	a
54A	Pull	R	40	11	11,779	672	"	a	a
54B	Push	R	20	13	15,460	840	"	a	50
54C	Pull	R	40	13	12,515	672	"	68	75
55	Pull	R	40	13	8,098	415	"	-	30
56	Pull	R	40	13	11,779	252	"	54	30
57	Push	R	10	6	14,724	85	"	-	20
58	Pull	R	40	13	11,779	420	"	-	a

Letters (A,B,C) after Run Number designate non-scheduled tests for which data was taken.

N.D. indicates that no data was taken. For Side loads, strain gages were inoperative for Runs 27-58.

A dash (-) indicates that temperature data existed, but was unintelligible.

A star (*) indicates that the temperature recorder went off scale. The recorded value is therefore less than the actual temperature.

All temperature readings are in °F above ambient. Ambient for all tests ranged from 26 to 32°F. The designation "a" means that no temperature rise occurred as the wheel passed, thus the wheel temperature was the same as ambient.

Horizontal traction forces are negative; braking forces are positive.

TABLE E-4
Field Test Data for Car I
Loaded Box DOTX-502
Truck B Axle 1
Actual Truck Weight = 51,440

Run	Orien-tation	Wheel Side	Train Speed (mph)	Brake Red'n (psi)	Vertical Load (lb)	Horzntl Load (lb)	Side Load (mv)	Near Side Temp (°F)	Far Side Temp (°F)	Wheel Temp (°F)
1	Pull	R	5	0	11,779	-1008	3600	a	a	
2	Push	R	4	0	13,988	2352	0	a	a	
3	Pull	R	5	0	12,515	- 840	3400	a	a	
4	Push	R	5	0	13,252	2352	-1200	a	a	
5	Pull	R	10	0	13,252	- 672	3000	a	a	
6	Push	R	10	0	14,724	2856	- 400	a	a	
7	Pull	R	20	0	11,779	- 672	4000	a	a	
8	Push	R	20	0	14,724	2520	400	a	a	
9	Pull	R	40	0	10,307	-1344	n.d.	a	a	
10	Push	R	40	0	13,252	2352	1800	a	a	
11	Pull	R	60	0	13,988	504	1500	a	a	
12	Push	R	60	0	11,779	2352	0	a	a	(35)
13	Pull	R	10	6	11,779	-1680	4000	a	a	
14	Push	R	10	11	13,988	3024	500	41	20	
15	Pull	R	10	15	12,515	-1008	2500	54	30	(125)
16	Push	R	20	6	13,988	2016	- 200	7	20	
17	Pull	R	20	11	13,252	-2016	4000	27	40	
18	Push	R	20	15	13,252	3024	1400	-	100	(110)
19	Pull	R	40	6	11,779	-2016	5000	-	20	
20	Push	R	40	11	12,515	3024	1000	-	50	(115)
21	Pull	R	40	15	12,515	-1512	4800	-	125	
22	Push	R	60	6	13,252	3360	-1800	-	10	
23	Pull	R	60	11	11,043	-1344	3600	-	50	(100)
24	Pull	R	60	15	10,307	-1008	3000	-	100	
25	Pull	L	10	11	12,515	840	1500	-	10	
26	Push	L	20	11	12,515	- 672	3000	290	25	
27	Pull	L	40	11	13,252	672	n.d.	-	75	(280)
27A	Push	L	20	11	12,515	- 840	"	-	13	
28	Pull	L	60	11	12,515	504	"	290	25	
28A	Push	L	30	11	11,043	-1680	"	323	-	
29	Pull	L	10	0	11,779	336	"	-	a	
30	Push	L	20	0	14,724	-1008	"	-	a	
31	Pull	L	40	0	11,779	672	"	a	a	
32	Pull	L	60	0	12,515	672	"	a	a	
33	Pull	L	10	11	13,252	336	"	82	30	
34	Push	L	20	11	13,252	-1344	"	109	50	
35	Pull	L	40	11	11,779	0	"	-	100	
36	Pull	L	60	11	12,515	1008	"	-	38	

TABLE E-4 (Cont'd)

Field Test Data for Car I
Loaded Box DOTX-502
Truck B Axle 1
Actual Truck Weight = 51,440

Run	Orien-tation	Wheel Side	Train Speed (mph)	Brake Red'n (psi)	Vertical Load (lb)	Horzntl Load (lb)	Side Load (mv)	Near Side Temp (°F)	Far Side Temp (°F)
41	Pull	L	60	0	13,252	1008	n.d.	a	a
42	Push	L	10	0	12,515	-1008	"	a	25
43	Pull	L	40	0	13,988	168	"	a	25
44	Push	L	20	0	15,460	-1176	"	a	25
45	Pull	R	40	0	12,515	- 168	"	-	a
46	Push	R	20	0	13,988	1344	"	-	a
47	Pull	R	60	0	12,515	0	"	-	a
48	Push	R	10	0	13,988	840	"	-	a
49	Pull	R	30	0	12,515	-1008	"	-	a
50	Push	R	30	0	13,988	1680	"	-	a
51	Pull	R	30	0	12,515	0	"	-	a
52	Push	R	10	11	14,724	1176	"	-	a
53	Pull	R	10	15	11,779	504	"	-	a
54	Push	R	40	11	13,988	840	"	-	a
54A	Pull	R	40	11	11.779	840	"	-	a
54B	Push	R	20	13	12,515	840	"	-	25
54C	Pull	R	40	13	11,779	672	"	34	50
55	Pull	R	40	13	12,515	336	"	-	20
56	Pull	R	40	13	12,515	252	"	41	20
57	Push	R	10	6	13,988	252	"	-	10
58	Pull	R	40	13	11,779	420	"	-	a

Letters (A,B,C) after Run Number designate non-scheduled tests for which data was taken.

N.D. indicates that no data was taken. For Side loads, strain gages were inoperative for Runs 27-58.

A dash (-) indicates that temperature data existed, but was unintelligible.

A star (*) indicated that the temperature recorder went off scale. The recorded value is therefore less than the actual temperature.

All temperature readings are in °F above ambient. Ambient for all tests ranged from 26 to 32°F. The designation "a" means that no temperature rise occurred as the wheel passed, thus the wheel temperature was the same as ambient.

Horizontal traction forces are negative; braking forces are positive.

TABLE E-5
Field Test Data for Car II
Empty Box DOTX-501
Truck A Axle 4
Actual Truck Weight = 22,380

Run	Orien-tation	Wheel Side	Train Speed (mph)	Brake Red'n (psi)	Vertical Load (lb)	Horzntl Load (lb)	Side Load (mv)	Near Side Temp (°F)	Far Side Temp (°F)	Wheel Temp (°F)
1	Pull	R	5	0	5,153	504	1200	a	a	
2	Push	R	4	0	5,153	- 672	1800	a	a	
3	Pull	R	5	0	5,153	504	1200	a	a	
4	Push	R	5	0	5,153	- 672	1800	a	a	
5	Pull	R	10	0	5,153	504	1400	a	a	
6	Push	R	10	0	5,153	- 504	1800	a	a	
7	Pull	R	20	0	5,153	1008	1600	a	a	
8	Push	R	20	0	7,362	- 504	1400	a	a	
9	Pull	R	40	0	5,153	840	n.d.	a	a	
10	Push	R	40	0	5,890	336	0	a	a	
11	Pull	R	60	0	6,626	504	1800	a	a	
12	Push	R	60	0	8,834	- 840	500	a	a	(35)
13	Pull	R	10	6	5,153	336	3500	a	a	
14	Push	R	10	11	5,890	- 672	1500	27	10	
15	Pull	R	10	15	5,153	336	1500	54	10	(120)
16	Push	R	20	6	5,890	- 504	1600	14	10	
17	Pull	R	20	11	5,890	504	2600	54	10	
18	Push	R	20	15	5,890	- 504	1800	82	90	(165)
19	Pull	R	40	6	4,417	1008	1400	41	50	
20	Push	R	40	11	5,890	336	1000	163	150	(175)
21	Pull	R	40	15	5,153	1008	1200	-	50	
22	Push	R	60	6	5,153	0	-1200	-	50	
23	Pull	R	60	11	6,626	1848	-1200	-	200	(185)
24	Pull	R	60	15	5,153	840	1800	-	150	
25	Pull	L	10	11	5,153	504	500	-	10	
26	Push	L	20	11	5,153	0	1000	102	75	
27	Pull	L	40	11	4,417	0	n.d.	301	358	(250)
27A	Push	L	20	11	5,153	0	"	334	40	
28	Pull	L	60	11	5,890	504	"	334	200	
28A	Push	L	30	11	7,362	168	"	400	100	
29	Pull	L	10	11	5,153	672	"	-	50	
30	Push	L	20	11	5,153	0	"	-	110	
31	Pull	L	40	11	4,417	672	"	61	160	
32	Pull	L	60	11	5,153	336	"	41	160	
33	Pull	L	10	0	5,153	504	"	14	40	
34	Push	L	20	0	5,153	- 168	"	a	-	
35	Pull	L	40	0	5,153	504	"	a	-	
36	Pull	L	60	0	7,362	0	"	a	-	

TABLE E-5 (Cont'd)

Field Test Data for Car II
Empty Box DOTX-501
Truck A Axle 4
Actual Truck Weight = 22,380

Run	Orientation	Wheel Side	Train Speed (mph)	Brake Red'n (psi)	Vertical Load (lb)	Horsntl Load (lb)	Side Load (mv)	Near Side Temp (°F)	Far Side Temp (°F)
41	Pull	L	60	0	6,626	504	n.d.	a	a
42	Push	L	10	0	5,153	0	"	-	a
43	Pull	L	40	0	5,153	336	"	a	a
44	Push	L	20	0	5,153	- 336	"	a	a
45	Pull	R	40	0	5,890	0	"	-	a
46	Push	R	20	0	6,626	- 672	"	-	a
47	Pull	R	60	0	8,098	1008	"	-	a
48	Push	R	10	0	5,890	- 336	"	-	a
49	Pull	R	30	0	3,681	168	"	-	a
50	Push	R	30	0	5,890	- 168	"	-	a
51	Pull	R	30	0	6,626	168	"	-	a
52	Push	R	10	11	6,626	840	"	-	a
53	Pull	R	10	15	6,626	1176	"	-	a
54	Push	R	40	11	6,626	504	"	-	a
54A	Pull	R	40	11	5,890	1008	"	279	200
54B	Push	R	20	13	5,890	1176	"	-	75
54C	Pull	R	40	13	5,153	336	"	34	50
55	Pull	R	40	13	5,153	590	"	54	80
56	Pull	R	40	13	5,890	504	"	136	70
57	Push	R	10	6	6,626	0	"	-	30
58	Pull	R	40	13	5,890	560	"	-	100

Letters (A,B,C) after Run Number designate non-scheduled tests for which data was taken.

N.D. indicates that no data was taken. For Side loads, strain gages were inoperative for Runs 27-58.

A dash (-) indicates that temperature data existed, but was unintelligible.

A star (*) indicates that the temperature recorder went off scale. The recorded value is therefore less than the actual temperature.

All temperature readings are in °F above ambient. Ambient for all tests ranged from 26 to 32°F. The designation "a" means that no temperature rise occurred as the wheel passed, thus the wheel temperature was the same as ambient.

Horizontal traction forces are negative; braking forces are positive.

TABLE E-6
Field Test Data for Car II
Empty Box DOTX-501
Truck A Axle 3
Actual Truck Weight = 22,380

Run	Orien-tation	Wheel Side	Train Speed (mph)	Brake Red'n (psi)	Vertical Load (lb)	Horzntl Load (lb)	Side Load (mv)	Near Side Temp (°F)	Far Side Temp (°F)	Wheel Temp (°F)
1	Pull	R	5	0	5,890	- 336	1400	a	a	
2	Push	R	4	0	5,153	840	800	a	a	
3	Pull	R	5	0	4,417	- 336	1000	a	a	
4	Push	R	5	0	5,153	840	600	a	a	
5	Pull	R	10	0	5,153	- 504	1000	a	a	
6	Push	R	10	0	5,153	672	800	a	a	
7	Pull	R	20	0	5,890	- 504	1600	a	a	
8	Push	R	20	0	6,626	672	1000	a	a	
9	Pull	R	40	0	5,153	0	n.d.	a	a	
10	Push	R	40	0	6,626	1344	1200	a	a	
11	Pull	R	60	0	5,153	- 168	2000	a	a	
12	Push	R	60	0	4,417	336	-1000	a	a	(35)
13	Pull	R	10	6	5,153	504	1500	a	a	
14	Push	R	10	11	6,626	1008	1000	41	10	
15	Pull	R	10	15	5,890	0	1000	41	10	(125)
16	Push	R	20	6	6,626	672	1500	14	10	
17	Pull	R	20	11	5,890	- 504	1400	68	40	
18	Push	R	20	15	5,890	840	800	136	90	(170)
19	Pull	R	40	6	4,417	- 672	1000	41	50	
20	Push	R	40	11	5,890	1176	1000	68	190	(230)
21	Pull	R	40	15	5,890	672	-3000	-	389	
22	Push	R	60	6	5,153	1344	- 800	-	221	
23	Pull	R	60	11	5,890	840	-1600	-	284	(240)
24	Pull	R	60	15	4,417	336	- 800	-	284	
25	Pull	L	10	11	5,153	- 168	-1000	-	30	
26	Push	L	20	11	5,153	0	800	246	50	
27	Pull	L	40	11	4,417	672	n.d.	279	326	(200)
27A	Push	L	20	11	5,153	- 168	"	345	30	
28	Pull	L	60	11	5,890	672	"	301	75	
28A	Push	L	30	11	6,626	168	"	400	100	
29	Pull	L	10	11	5,890	- 336	"	-	40	
30	Push	L	20	11	5,890	- 168	"	-	130	
31	Pull	L	40	11	6,626	- 168	"	54	208	
32	Pull	L	60	11	5,890	672	"	27	50	
33	Pull	L	10	0	5,153	- 336	"	a	30	
34	Push	L	20	0	5,153	0	"	a	-	
35	Pull	L	40	0	5,153	- 168	"	a	-	
36	Pull	L	60	0	5,890	672	"	a	-	

TABLE E-6 (Cont'd)

Field Test Data for Car II
Empty Box DOTX-501
Truck A Axle 3
Actual Truck Weight = 22,380

Run	Orien-tation	Wheel Side	Train Speed (mph)	Brake Red'n (psi)	Vertical Load (lb)	Horzntl Load (lb)	Side Load (mv)	Near Side Temp (°F)	Far Side Temp (°F)
41	Pull	L	60	0	6,626	- 336	n.d.	a	a
42	Push	L	10	0	5,153	0	"	-	a
43	Pull	L	40	0	5,153	0	"	a	a
44	Push	L	20	0	5,153	- 168	"	a	a
45	Pull	R	40	0	5,153	- 168	"	-	a
46	Push	R	20	0	5,890	336	"	-	a
47	Pull	R	60	0	6,626	0	"	-	a
48	Push	R	10	0	5,890	672	"	-	a
49	Pull	R	30	0	4,417	168	"	-	a
50	Push	R	30	0	6,626	504	"	-	a
51	Pull	R	30	0	5,890	0	"	-	a
52	Push	R	10	11	5,890	840	"	-	a
53	Pull	R	10	15	5,890	1344	"	-	a
54	Push	R	40	11	6,626	504	"	-	a
54A	Pull	R	40	11	5,153	1008	"	136	50
54B	Push	R	20	13	5,890	1176	"	-	75
54C	Pull	R	40	13	5,153	1176	"	136	75
55	Pull	R	40	13	5,153	255	"	27	20
56	Pull	R	40	13	5,153	168	"	82	20
57	Push	R	10	6	6,626	85	"	-	10
58	Pull	R	40	13	5,153	252	"	-	a

Letters (A,B,C) after Run Number designate non-scheduled tests for which data was taken.

N.D. indicates that no data was taken. For Side loads, strain gages were inoperative for Runs 27-58.

A dash (-) indicates that temperature data existed, but was unintelligible.

A star (*) indicates that the temperature recorder went off scale. The recorded value is therefore less than the actual temperature.

All temperature readings are in °F above ambient. Ambient for all tests ranged from 26 to 32°F. The designation "a" means that no temperature rise occurred as the wheel passed, thus the wheel temperature was the same as ambient.

Horizontal traction forces are negative; braking forces are positive.

TABLE E-7
Field Test Data for Car II
Empty Box DOTX-501
Truck B Axle 2
Actual Truck Weight = 22,560

Run	Orien-tation	Wheel Side	Train Speed (mph)	Brake Red'n (psi)	Vertical Load (lb)	Horzntl Load (lb)	Side Load (mv)	Near Side Temp (°F)	Far Side Temp (°F)	Wheel Temp (°F)
1	Pull	R	5	0	5,153	- 336	1400	a	a	
2	Push	R	4	0	5,153	336	1400	a	a	
3	Pull	R	5	0	4,417	- 336	1600	a	a	
4	Push	R	5	0	5,153	0	1200	a	a	
5	Pull	R	10	0	5,153	- 336	1600	a	a	
6	Push	R	10	0	5,153	- 168	1400	a	a	
7	Pull	R	20	0	5,153	- 336	1600	a	a	
8	Push	R	20	0	5,890	- 336	1600	a	a	
9	Pull	R	40	0	5,153	- 168	n.d.	a	a	
10	Push	R	40	0	5,153	840	0	a	a	
11	Pull	R	60	0	5,153	168	2000	a	a	
12	Push	R	60	0	5,890	1176	500	a	a	(35)
13	Pull	R	10	6	5,153	0	3500	a	a	
14	Push	R	10	11	5,890	0	1500	27	10	
15	Pull	R	10	15	5,153	- 336	1200	68	20	(105)
16	Push	R	20	6	5,153	0	1500	27	10	
17	Pull	R	20	11	5,890	- 168	2600	82	40	
18	Push	R	20	15	5,153	168	1800	54	30	(130)
19	Pull	R	40	6	6,626	- 504	3200	54	20	
20	Push	R	40	11	5,890	504	800	95	90	(135)
21	Pull	R	40	15	5,890	840	1200	-	50	
22	Push	R	60	6	5,153	1176	- 400	-	50	
23	Pull	R	60	11	5,153	1344	1600	-	150	(170)
24	Pull	R	60	15	3,681	1008	1000	-	50	
25	Pull	L	10	11	6,626	336	0	-	a	
26	Push	L	20	11	5,153	336	800	68	75	
27	Pull	L	40	11	6,626	1176	n.d.	400*	284	(240)
27A	Push	L	20	11	5,153	168	"	257	60	
28	Pull	L	60	11	6,626	1008	"	367	150	
28A	Push	L	30	11	5,153	168	"	367	125	
29	Pull	L	10	11	5,890	672	"	-	60	
30	Push	L	20	11	5,153	168	"	-	60	
31	Pull	L	40	11	5,890	672	"	27	110	
32	Pull	L	60	11	5,890	672	"	41	90	
33	Pull	L	10	0	5,890	504	"	54	40	
34	Push	L	20	0	5,890	504	"	a	-	
35	Pull	L	40	0	5,890	336	"	a	-	
36	Pull	L	60	0	6,626	504	"	a	-	

TABLE E-7 (Cont'd)

Field Test Data for Car II
Empty Box DOTX-501
Truck B Axle 2
Actual Truck Weight = 22,560

Run	Orien-tation	Wheel Side	Train Speed (mph)	Brake Red'n (psi)	Vertical Load (lb)	Horzntl Load (lb)	Side Load (mv)	Near Side Temp (°F)	Far Side Temp (°F)
41	Pull	L	60	0	5,153	504	n.d.	a	a
42	Push	L	10	0	6,626	336	"	-	a
43	Pull	L	40	0	5,890	336	"	a	a
44	Push	L	20	0	5,153	336	"	a	a
45	Pull	R	40	0	5,890	0	"	-	a
46	Push	R	20	0	5,153	504	"	-	a
47	Pull	R	60	0	5,153	0	"	-	a
48	Push	R	10	0	5,890	504	"	-	a
49	Pull	R	30	0	4,417	- 168	"	-	a
50	Push	R	30	0	5,153	504	"	-	a
51	Pull	R	30	0	5,153	0	"	-	a
52	Push	R	10	11	5,153	1008	"	-	a
53	Pull	R	10	15	5,890	1008	"	-	a
54	Push	R	40	11	7,362	504	"	-	a
54A	Pull	R	40	11	5,890	1176	"	191	125
54B	Push	R	20	13	5,890	1176	"	-	100
54C	Pull	R	40	13	5,153	504	"	68	25
55	Pull	R	40	13	5,153	252	"	41	10
56	Pull	R	40	13	5,153	252	"	54	20
57	Push	R	10	6	5,890	85	"	68	10
58	Pull	R	40	13	5,153	336	"	a	10

Letters (A,B,C) after Run Number designate non-scheduled tests for which data was taken.

N.D. indicates that no data was taken. For Side loads, strain gages were inoperative for Runs 27-58.

A dash (-) indicates that temperature data existed, but was unintelligible.

A star (*) indicates that the temperature recorder went off scale. The recorded value is therefore less than the actual temperature.

All temperature readings are in °F above ambient. Ambient for all tests ranged from 26 to 32°F. The designation "a" means that no temperature rise occurred as the wheel passed, thus the wheel temperature was the same as ambient.

Horizontal traction forces are negative; braking forces are positive.

TABLE E-8
Field Test Data for Car II
Empty Box DOTX-501
Truck B Axle 1
Actual Truck Weight = 22,560

Run	Orien-tation	Wheel Side	Train Speed (mph)	Brake Red'n (psi)	Vertical Load (lb)	Horzntl Load (lb)	Side Load (mv)	Near Side Temp (°F)	Far Side Temp (°F)	Wheel Temp (°F)
1	Pull	R	5	0	5,890	- 336	1000	a	a	
2	Push	R	4	0	5,153	0	1400	a	a	
3	Pull	R	5	0	5,890	- 336	1200	a	a	
4	Push	R	5	0	5,153	840	800	a	a	
5	Pull	R	10	0	5,890	- 336	1200	a	a	
6	Push	R	10	0	5,890	672	600	a	a	
7	Pull	R	20	0	5,890	- 336	1600	a	a	
8	Push	R	20	0	7,362	504	800	a	a	
9	Pull	R	40	0	5,890	- 504	n.d.	a	a	
10	Push	R	40	0	5,153	672	1800	a	a	
11	Pull	R	60	0	5,153	0	500	a	a	
12	Push	R	60	0	5,153	504	500	a	a	(35)
13	Pull	R	10	6	5,890	- 504	1500	a	a	
14	Push	R	10	11	5,890	840	500	27	10	
15	Pull	R	10	15	5,890	- 504	500	41	10	(100)
16	Push	R	20	6	5,890	336	800	27	5	
17	Pull	R	20	11	6,626	- 168	1400	68	30	
18	Push	R	20	15	5,153	672	0	41	30	(130)
19	Pull	R	40	6	4,417	- 336	1800	54	15	
20	Push	R	40	11	5,153	840	800	109	20	(230)
21	Pull	R	40	15	5,890	1512	- 800	102	347	
22	Push	R	60	6	6,626	- 672	600	191	150	
23	Pull	R	60	11	5,890	1008	0	-	150	(230)
24	Pull	R	60	15	6,626	1512	- 800	-	242	
25	Pull	L	10	11	6,626	- 336	1500	-	10	
26	Push	L	20	11	5,153	- 168	800	68	100	
27	Pull	L	40	11	4,417	0	n.d.	202	368	(230)
27A	Push	L	20	11	5,153	168	"	279	30	
28	Pull	L	60	11	5,153	672	"	213	100	
28A	Push	L	30	11	5,890	168	"	367	150	
29	Pull	L	10	11	5,890	- 504	"	-	80	
30	Push	L	20	11	5,890	168	"	-	30	
31	Pull	L	40	11	4,417	0	"	14	90	
32	Pull	L	60	11	5,890	672	"	27	80	
33	Pull	L	10	0	5,890	- 504	"	41	40	
34	Push	L	20	0	5,890	0	"	a	-	
35	Pull	L	40	0	4,417	0	"	a	-	
36	Pull	L	60	0	5,153	- 672	"	a	-	

TABLE E-8 (Cont'd)

Field Test Data for Car II
Empty Box DOTX-501
Truck B Axle 1
Actual Truck Weight = 22,560

Run	Orien-tation	Wheel Side	Train Speed (mph)	Brake Red'n (psi)	Vertical Load (lb)	Horzntl Load (lb)	Side Load (mv)	Near Side Temp (°F)	Far Side Temp (°F)
41	Pull	L	60	0	5,890	- 168	n.d.	a	a
42	Push	L	10	0	7,362	- 336	"	-	a
43	Pull	L	40	0	5,153	- 504	"	a	a
44	Push	L	20	0	5,890	- 336	"	a	a
45	Pull	R	40	0	5,153	- 168	"	-	a
46	Push	R	20	0	5,890	0	"	-	a
47	Pull	R	60	0	4,417	336	"	-	a
48	Push	R	10	0	5,153	- 168	"	-	a
49	Pull	R	30	0	5,153	- 168	"	-	a
50	Push	R	30	0	6,626	- 168	"	-	a
51	Pull	R	30	0	5,890	0	"	-	a
52	Push	R	10	11	5,890	1008	"	-	a
53	Pull	R	10	15	5,890	1176	"	-	a
54	Push	R	40	11	6,626	672	"	-	a
54A	Pull	R	40	11	6,626	1176	"	202	175
54B	Push	R	20	13	6,626	1344	"	-	75
54C	Pull	R	40	13	5,890	840	"	191	100
55	Pull	R	40	13	5,153	415	"	54	50
56	Pull	R	40	13	8,834	504	"	95	80
57	Push	R	10	6	6,626	85	"	83	15
58	Pull	R	40	13	7,362	590	"	136	80

Letters (A,B,C) after Run Number designate non-scheduled tests for which data was taken.

N.D. indicates that no data was taken. For Side loads, strain gages were inoperative for Runs 27-58.

A dash (-) indicates that temperature data existed, but was unintelligible.

A star (*) indicates that the temperature recorder went off scale. The recorded value is therefore less than the actual temperature.

All temperature readings are in °F above ambient. Ambient for all tests ranged from 26 to 32°F. The designation "a" means that no temperature rise occurred as the wheel passed, thus the wheel temperature was the same as ambient.

Horizontal traction forces are negative; braking forces are positive.

TABLE E-9
Field Test Data for Car III
Loaded Gondola USAF-42015
Truck A Axle 4
Actual Truck Weight = 39,400

Run	Orien-tation	Wheel Side	Train Speed (mph)	Brake Red'n (psi)	Vertical Load (lb)	Horzntl Load (lb)	Side Load (mv)	Near Side Temp (°F)	Far Side Temp (°F)	Wheel Temp (°F)
1	Pull	R	5	0	10,307	840	1400	a	a	
2	Push	R	4	0	9,571	672	2200	a	a	
3	Pull	R	5	0	9,571	1008	1600	a	a	
4	Push	R	5	0	10,307	1680	1400	a	a	
5	Pull	R	10	0	10,307	1344	2200	a	a	
6	Push	R	10	0	9,571	1008	2000	a	a	
7	Pull	R	20	0	9,571	1680	1800	a	a	
8	Push	R	20	0	9,571	504	3600	a	a	
9	Pull	R	40	0	8,834	1176	n.d.	a	a	
10	Push	R	40	0	9,571	1176	3800	a	a	
11	Pull	R	60	0	11,043	504	2500	a	a	
12	Push	R	60	0	8,834	1008	1000	a	a	(35)
13	Pull	R	10	6	11,043	2184	1500	a	a	
14	Push	R	10	11	10,307	0	1500	41	30	
15	Pull	R	10	15	11,043	2352	2000	200	130	(250)
16	Push	R	20	6	11,043	504	2200	41	20	
17	Pull	R	20	11	11,043	168	2800	82	50	
18	Push	R	20	15	9,571	840	2600	217	190	(330)
19	Pull	R	40	6	10,307	168	2400	68	70	
20	Push	R	40	11	8,098	- 672	2800	163	100	(330)
21	Pull	R	40	15	8,834	2016	3000	102	263	
22	Push	R	60	6	11,779	0	1200	-	221	
23	Pull	R	60	11	10,307	1848	1800	-	221	(260)
24	Pull	R	60	15	11,779	1848	3400	136	305	
25	Pull	L	10	11	8,834	336	1500	217	30	
26	Push	L	20	11	7,362	0	600	246	150	
27	Pull	L	40	11	8,834	- 168	n.d.	400*	25	(375)
27A	Push	L	20	11	8,834	840	"	246	50	
28	Pull	L	60	11	8,834	840	"	334	50	
28A	Push	L	30	11	10,307	- 168	"	356	75	
29	Pull	L	10	11	8,834	1848	"	235*	204	
30	Push	L	20	11	8,098	840	"	257	221*	
31	Pull	L	40	11	9,571	168	"	61	200	
32	Pull	L	60	11	10,307	- 168	"	136	208	
33	Pull	L	10	11	9,571	1176	"	122	221*	
34	Push	L	20	11	8,834	0	"	177	253	
35	Pull	L	40	11	8,098	0	"	235	253	
36	Pull	L	60	11	7,362	1008	"	150	200	

TABLE E-9 (Cont'd)

Field Test Data for Car III
Loaded Gondola USAF-42015
Truck A Axle 4
Actual Truck Weight = 39,400

Run	Orientation	Wheel Side	Train Speed (mph)	Brake Red'n (psi)	Vertical Load (lb)	Horzntl Load (lb)	Side Load (mv)	Near Side Temp (°F)	Far Side Temp (°F)
41	Pull	L	60	0	11,779	1344	n.d.	a	50
42	Push	L	10	0	9,571	- 168	"	a	75
43	Pull	L	40	0	8,834	672	"	a	50
44	Push	L	20	0	8,834	840	"	41	a
45	Pull	R	40	0	8,098	840	"	-	a
46	Push	R	20	0	11,779	840	"	-	a
47	Pull	R	60	0	10,307	336	"	-	a
48	Push	R	10	0	10,307	840	"	-	a
49	Pull	R	30	0	8,834	- 336	"	-	a
50	Push	R	30	0	11,043	840	"	-	a
51	Pull	R	30	0	10,307	0	"	-	a
52	Push	R	10	11	10,307	1008	"	-	a
53	Pull	R	10	15	11,779	1680	"	-	a
54	Push	R	40	11	11,043	504	"	-	a
54A	Pull	R	40	11	8,098	1008	"	136	50
54B	Push	R	20	13	8,834	1512	"	-	75
54C	Pull	R	40	13	8,834	1176	"	191	100
55	Pull	R	40	13	10,307	590	"	54	40
56	Pull	R	40	13	11,779	504	"	82	70
57	Push	R	10	6	10,307	252	"	82	40
58	Pull	R	40	13	9,571	252	"	136	45

Letters (A,B,C) after Run Number designate non-scheduled tests for which data was taken.

N.D. indicates that no data was taken. For Side loads, strain gages were inoperative for Runs 27-58.

A dash (-) indicates that temperature data existed, but was unintelligible.

A star (*) indicates that the temperature recorder went off scale. The recorded value is therefore less than the actual temperature.

All temperature readings are in °F above ambient. Ambient for all tests ranged from 26 to 32°F. The designation "a" means that no temperature rise occurred as the wheel passed, thus the wheel temperature was the same as ambient.

Horizontal traction forces are negative; braking forces are positive.

TABLE E-10
Field Test Data for Car III
Loaded Gondola USAF-42015
Truck A Axle 3
Actual Truck Weight = 39,400

Run	Orien-tation	Wheel Side	Train Speed (mph)	Brake Red'n (psi)	Vertical Load (lb)	Horzntl Load (lb)	Side Load (mv)	Near Side Temp (°F)	Far Side Temp (°F)	Wheel Temp (°F)
1	Pull	R	5	0	11,779	-1008	1200	a	a	
2	Push	R	4	0	10,307	- 840	1400	a	a	
3	Pull	R	5	0	10,307	-1344	1400	a	a	
4	Push	R	5	0	10,307	-1512	1400	a	a	
5	Pull	R	10	0	11,043	-1344	1600	a	a	
6	Push	R	10	0	10,307	- 672	1600	a	a	
7	Pull	R	20	0	9,571	-1176	1800	a	a	
8	Push	R	20	0	12,515	-1008	2000	a	a	
9	Pull	R	40	0	8,098	-1344	n.d.	a	a	
10	Push	R	40	0	12,515	-1680	3000	a	a	
11	Pull	R	60	0	9,571	504	1000	a	a	
12	Push	R	60	0	12,515	-1008	1000	a	a	(35)
13	Pull	R	10	6	11,043	-1344	1800	a	a	
14	Push	R	10	11	13,252	2184	-1000	82	30	
15	Pull	R	10	15	11,779	1680	500	213	110	(275)
16	Push	R	20	6	12,515	-1008	2000	54	30	
17	Pull	R	20	11	10,307	- 672	2600	82	60	
18	Push	R	20	15	11,779	840	1800	235*	204	(350)
19	Pull	R	40	6	12,515	-1512	0	68	60	
20	Push	R	40	11	11,043	1344	2000	163	150	(325)
21	Pull	R	40	15	9,571	- 336	1600	102	347	
22	Push	R	60	6	13,988	1680	-1400	-	221	
23	Pull	R	60	11	13,988	- 840	0	-	100	(260)
24	Pull	R	60	15	10,307	- 672	1200	136	253	
25	Pull	L	10	11	9,571	336	500	204	50	
26	Push	L	20	11	11,043	1008	400	290	200	
27	Pull	L	40	11	8,098	672	n.d.	301	377*	(360)
27A	Push	L	20	11	9,571	336	"	356	75	
28	Pull	L	60	11	9,571	0	"	268	75	
28A	Push	L	30	11	10,307	336	"	345	100	
29	Pull	L	10	11	9,571	672	"	235*	204	
30	Push	L	20	11	10,307	336	"	290	221*	
31	Pull	L	40	11	8,834	672	"	61	221*	
32	Pull	L	60	11	9,571	336	"	122	190	
33	Pull	L	10	11	9,571	504	"	82	221*	
34	Push	L	20	11	11,043	840	"	191	274	
35	Pull	L	40	11	9,571	168	"	204	305	
36	Pull	L	60	11	8,834	840	"	163	200	

TABLE E-10 (Cont'd)

Field Test Data for Car III
Loaded Gondola USAF-42015
Truck A Axle 3
Actual Truck Weight = 39,400

Run	Orientation	Wheel Side	Train Speed (mph)	Brake Red'n (psi)	Vertical Load (lb)	Horsntl Load (lb)	Side Load (mv)	Near Side Temp (°F)	Far Side Temp (°F)
41	Pull	L	60	0	8,834	- 840	n.d.	a	50
42	Push	L	10	0	8,834	672	"	a	90
43	Pull	L	40	0	8,098	- 840	"	a	50
44	Push	L	20	0	9,571	336	"	27	a
45	Pull	R	40	0	9,571	-1008	"	-	a
46	Push	R	20	0	11,779	- 504	"	-	a
47	Pull	R	60	0	10,307	- 504	"	-	a
48	Push	R	10	0	11,043	- 504	"	-	a
49	Pull	R	30	0	11,043	-1008	"	-	a
50	Push	R	30	0	11,779	- 336	"	-	a
51	Pull	R	30	0	11,043	0	"	-	a
52	Push	R	10	11	11,043	1008	"	-	a
53	Pull	R	10	15	11,779	1176	"	-	a
54	Push	R	40	11	11,779	504	"	-	a
54A	Pull	R	40	11	7,362	1176	"	213	60
54B	Push	R	20	13	13,252	840	"	-	100
54C	Pull	R	40	13	10,307	1176	"	191	125
55	Pull	R	40	13	8,098	760	"	54	40
56	Pull	R	40	13	9,571	504	"	68	90
57	Push	R	10	6	11,779	252	"	82	20
58	Pull	R	40	13	8,834	336	"	68	45

Letters (A,B,C) after Run Number designate non-scheduled tests for which data was taken.

N.D. indicates that no data was taken. For Side loads, strain gages were inoperative for Runs 27-58.

A dash (-) indicates that temperature data existed, but was unintelligible.

A star (*) indicates that the temperature recorder went off scale. The recorded value is therefore less than the actual temperature.

All temperature readings are in °F above ambient. Ambient for all tests ranged from 26 to 32°F. The designation "a" means that no temperature rise occurred as the wheel passed, thus the wheel temperature was the same as ambient.

Horizontal traction forces are negative; braking forces are positive.

TABLE E-11
Field Test Data for Car III
Loaded Gondola USAF-42015
Truck B Axle 2
Actual Truck Weight = 37,820

Run	Orien-tation	Wheel Side	Train Speed (mph)	Brake Red'n (psi)	Vertical Load (lb)	Horzntl Load (lb)	Side Load (mv)	Near Side Temp (°F)	Far Side Temp (°F)	Wheel Temp (°F)
1	Pull	R	5	0	8,834	672	1400	a	a	
2	Push	R	4	0	8,834	168	1600	a	a	
3	Pull	R	5	0	8,098	504	1400	a	a	
4	Push	R	5	0	8,834	504	1400	a	a	
5	Pull	R	10	0	9,571	672	1400	a	a	
6	Push	R	10	0	10,307	168	1600	a	a	
7	Pull	R	20	0	8,834	1008	600	a	a	
8	Push	R	20	0	9,571	336	2000	a	a	
9	Pull	R	40	0	7,362	840	n.d.	a	a	
10	Push	R	40	0	10,307	504	1600	a	a	
11	Pull	R	60	0	8,834	840	2500	a	a	
12	Push	R	60	0	11,043	504	1000	a	a	(35)
13	Pull	R	10	6	9,571	2016	1500	a	a	
14	Push	R	10	11	9,571	672	1000	41	30	
15	Pull	R	10	15	9,571	2352	1500	209	110	(300)
16	Push	R	20	6	9,571	168	2000	41	20	
17	Pull	R	20	11	8,834	504	2800	109	60	
18	Push	R	20	15	10,307	1008	1000	222	221	(400)
19	Pull	R	40	6	8,834	0	3000	82	50	
20	Push	R	40	11	8,098	1344	2000	n.d.	213	(355)
21	Pull	R	40	15	8,098	1848	2800	102	326	
22	Push	R	60	6	10,307	672	800	-	150	
23	Pull	R	60	11	8,834	2856	1200	-	200	(260)
24	Pull	R	60	15	8,834	2184	3000	170	284	
25	Pull	L	10	11	10,307	672	1500	226	30	
26	Push	L	20	11	9,571	672	1000	246	284	
27	Pull	L	40	11	11,043	0	n.d.	400*	284	(370)
27A	Push	L	20	11	9,571	0	"	279	90	
28	Pull	L	60	11	11,043	168	"	257*	75	
28A	Push	L	30	11	12,515	168	"	367	63	
29	Pull	L	10	11	10,307	1176	"	235*	208	
30	Push	L	20	11	9,571	504	"	68	221*	
31	Pull	L	40	11	11,043	168	"	68	208	
32	Pull	L	60	11	11,779	1008	"	150	180	
33	Pull	L	10	11	9,571	840	"	122	213	
34	Push	L	20	11	10,307	1344	"	163	242	
35	Pull	L	40	11	11,043	168	"	187	211	
36	Pull	L	60	11	10,307	- 336	"	187	200	

TABLE E-11 (Cont'd)

Field Test Data for Car III
Loaded Gondola USAF-42015
Truck B Axle 2
Actual Truck Weight = 37,820

Run	Orientation	Wheel Side	Train Speed (mph)	Brake Red'n (psi)	Vertical Load (lb)	Horzntl Load (lb)	Side Load (mv)	Near Side Temp (°F)	Far Side Temp (°F)
41	Pull	L	60	0	12,515	1512	n.d.	a	25
42	Push	L	10	0	10,307	0	"	a	50
43	Pull	L	40	0	10,307	840	"	a	25
44	Push	L	20	0	9,571	336	"	41	a
45	Pull	R	40	0	9,571	504	"	-	a
46	Push	R	20	0	10,307	672	"	-	a
47	Pull	R	60	0	8,834	0	"	-	a
48	Push	R	10	0	9,571	840	"	-	a
49	Pull	R	30	0	8,834	- 672	"	-	a
50	Push	R	30	0	8,834	672	"	-	a
51	Pull	R	30	0	9,571	0	"	-	a
52	Push	R	10	11	8,834	1008	"	-	a
53	Pull	R	10	15	8,098	1344	"	-	a
54	Push	R	40	11	9,571	504	"	--	a
54A	Pull	R	40	11	8,098	1176	"	246	125
54B	Push	R	20	13	8,098	1176	"	-	100
54C	Pull	R	40	13	9,571	1512	"	202	125
55	Pull	R	40	13	11,043	590	"	41	40
56	Pull	R	40	13	13,252	504	"	82	70
57	Push	R	10	6	8,834	252	"	150	40
58	Pull	R	40	13	9,571	420	"	82	40

Letters (A,B,C) after Run Number designate non-scheduled tests for which data was taken.

N.D. indicates that no data was taken. For Side loads, strain gages were inoperative for Runs 27-58.

A dash (-) indicates that temperature data existed, but was unintelligible.

A star (*) indicates that the temperature recorder went off scale. The recorded value is therefore less than the actual temperature.

All temperature readings are in °F above ambient. Ambient for all tests ranged from 26 to 32°F. The designation "a" means that no temperature rise occurred as the wheel passed, thus the wheel temperature was the same as ambient.

Horizontal traction forces are negative; braking forces are positive.

TABLE E-12
Field Test Data for Car III
Loaded Gondola USAF-42015
Truck B Axle 1
Actual Truck Weight = 37,820

Run	Orien-tation	Wheel Side	Train Speed (mph)	Brake Red'n (psi)	Vertical Load (lb)	Horzntl Load (lb)	Side Load (mv)	Near Side Temp (°F)	Far Side Temp (°F)	Wheel Temp (°F)
1	Pull	R	5	0	9,571	-1008	1400	a	a	
2	Push	R	4	0	9,571	1008	1400	a	a	
3	Pull	R	5	0	8,834	-1008	1600	a	a	
4	Push	R	5	0	8,834	672	1400	a	a	
5	Pull	R	10	0	10,307	-1176	1600	a	a	
6	Push	R	10	0	10,307	672	1400	a	a	
7	Pull	R	20	0	8,834	-1008	2000	a	a	
8	Push	R	20	0	11,043	672	1800	a	a	
9	Pull	R	40	0	8,098	-1512	n.d.	a	a	
10	Push	R	40	0	10,307	840	1800	a	a	
11	Pull	R	60	0	7,362	-1176	2000	a	a	
12	Push	R	60	0	7,362	1176	1000	a	a	(35)
13	Pull	R	10	6	8,834	-1176	1800	a	a	
14	Push	R	10	11	10,307	840	800	109	30	
15	Pull	R	10	15	8,834	2352	500	209	120	(310)
16	Push	R	20	6	11,043	336	1400	68	30	
17	Pull	R	20	11	10,307	0	600	109	60	
18	Push	R	20	15	11,779	1176	1400	235*	221	(350)
19	Pull	R	40	6	9,571	0	0	82	60	
20	Push	R	40	11	n.d.	n.d.	n.d.	n.d.	160	
21	Pull	R	40	15	10,307	1008	- 800	136	326	
22	Push	R	60	6	10,307	168	1000	-	221	
23	Pull	R	60	11	5,153	504	0	-	175	(260)
24	Pull	R	60	15	8,834	0	- 600	136	263	
25	Pull	L	10	11	9,571	- 336	1000	226	50	
26	Push	L	20	11	9,571	1008	2600	334	316	
27	Pull	L	40	11	7,362	0	n.d.	290	377*	(350)
27A	Push	L	20	11	9,571	504	"	400*	125	
28	Pull	L	60	11	8,098	- 336	"	235	75	
28A	Push	L	30	11	8,834	336	"	400*	100	
29	Pull	L	10	11	8,834	168	"	235*	217	
30	Push	L	20	11	9,571	0	"	204	221*	
31	Pull	L	40	11	8,834	- 168	"	27	213	
32	Pull	L	60	11	8,098	- 840	"	136	208	
33	Pull	L	10	11	8,834	0	"	82	204	
34	Push	L	20	11	9,571	1008	"	150	242	
35	Pull	L	40	11	7,362	0	"	187	284	
36	Pull	L	60	11	9,571	- 504	"	187	200	

TABLE E-12 (Cont'd)
Field Test Data for Car III
Loaded Gondola USAF-42015
Truck B Axle 1
Actual Truck Weight = 37,820

Run	Orien-tation	Wheel Side	Train Speed (mph)	Brake Red'n (psi)	Vertical Load (lb)	Horzntl Load (lb)	Side Load (mv)	Near Side Temp (°F)	Far Side Temp (°F)
41	Pull	L	60	0	8,834	- 840	n.d.	a	50
42	Push	L	10	0	9,571	504	"	a	75
43	Pull	L	40	0	8,834	- 840	"	a	25
44	Push	L	20	0	9,571	168	"	41	a
45	Pull	R	40	0	8,834	- 336	"	-	a
46	Push	R	20	0	10,307	0	"	-	a
47	Pull	R	60	0	8,098	0	"	-	a
48	Push	R	10	0	9,571	- 168	"	-	a
49	Pull	R	30	0	9,571	- 672	"	-	a
50	Push	R	30	0	10,307	- 168	"	-	a
51	Pull	R	30	0	9,571	- 168	"	-	a
52	Push	R	10	11	9,571	1176	"	-	a
53	Pull	R	10	15	8,834	1176	"	-	a
54	Push	R	40	11	9,571	1008	"	-	a
54A	Pull	R	40	11	7,362	1176	"	191	100
54B	Push	R	20	13	11,043	672	"	180	125
54C	Pull	R	40	13	6,626	1344	"	41	125
55	Pull	R	40	13	6,626	672	"	82	40
56	Pull	R	40	13	5,890	590	"	95	70
57	Push	R	10	6	9,571	252	"	68	30
58	Pull	R	40	13	8,098	420	"		35

Letters (A,B,C) after Run Number designate non-scheduled tests for which data was taken.

N.D. indicates that no data was taken. For Side loads, strain gages were inoperative for Runs 27-58.

A dash (-) indicates that temperature data existed, but was unintelligible.

A star (*) indicates that the temperature recorder went off scale. The recorded value is therefore less than the actual temperature.

All temperature readings are in °F above ambient. Ambient for all tests ranged from 26 to 32°F. The designation "a" means that no temperature rise occurred as the wheel passed, thus the wheel temperature was the same as ambient.

Horizontal traction forces are negative; braking forces are positive.

TABLE E-13
Field Test Data for Car IV
Empty Gondola USAF-42016
Truck A Axle 4
Actual Truck Weight = 24,520

Run	Orien-tation	Wheel Side	Train Speed (mph)	Brake Red'n (psi)	Vertical Load (lb)	Horzntl Load (lb)	Side Load (mv)	Near Side Temp (°F)	Far Side Temp (°F)	Wheel Temp (°F)
1	Pull	R	5	0	5,890	672	600	a	a	
2	Push	R	4	0	5,890	- 336	1200	a	a	
3	Pull	R	5	0	5,890	- 168	1000	a	a	
4	Push	R	5	0	5,153	0	1200	a	a	
5	Pull	R	10	0	5,890	672	800	a	a	
6	Push	R	10	0	5,890	- 336	1000	a	a	
7	Pull	R	20	0	5,153	840	1000	a	a	
8	Push	R	20	0	7,362	336	1500	a	a	
9	Pull	R	40	0	5,153	504	n.d.	a	a	
10	Push	R	40	0	5,890	336	1000	a	a	
11	Pull	R	60	0	5,890	840	- 500	a	a	
12	Push	R	60	0	5,890	1008	500	a	a	(35)
13	Pull	R	10	6	5,890	840	800	a	a	
14	Push	R	10	11	5,890	0	800	14	a	
15	Pull	R	10	15	6,626	168	1000	a	a	(35)
16	Push	R	20	6	6,626	0	800	21	a	
17	Pull	R	20	11	5,890	672	1000	a	a	
18	Push	R	20	15	5,890	336	1600	a	10	(35)
19	Pull	R	40	6	5,153	336	1600	a	a	
20	Push	R	40	11	n.d.	n.d.	n.d.	n.d.	a	
21	Pull	R	40	15	6,626	0	1400	a	50	
22	Push	R	60	6	7,362	168	2000	a	50	
23	Pull	R	60	11	8,098	1008	3000	-	50	(90)
24	Pull	R	60	15	5,890	672	2200	-	a	
25	Pull	L	10	0	6,626	840	1000	a	a	
26	Push	L	20	0	5,890	- 336	2000	a	a	
27	Pull	L	40	0	5,153	0	n.d.	a	a	(85)
27A	Push	L	20	0	6,626	- 336	"	a	a	
28	Pull	L	60	0	5,890	168	"	a	a	
28A	Push	L	30	0	6,626	- 336	"	-	a	
29	Pull	L	10	11	5,890	1344	"	-	a	
30	Push	L	20	11	6,626	168	"	a	60	
31	Pull	L	40	11	5,890	504	"	a	30	
32	Pull	L	60	11	5,890	840	"	a	10	
33	Pull	L	10	11	6,626	1008	"	54	70	
34	Push	L	20	11	5,890	504	"	54	100	
35	Pull	L	40	11	5,890	336	"	-	100	
36	Pull	L	60	11	5,890	504	"	14	50	

TABLE E-13 (Cont'd)
Field Test Data for Car IV
Empty Gondola USAF-42016
Truck A Axle 4
Actual Truck Weight = 24,520

Run	Orien-tation	Wheel Side	Train Speed (mph)	Brake Red'n (psi)	Vertical Load (lb)	Horzntl Load (lb)	Side Load (mv)	Near Side Temp (°F)	Far Side Temp (°F)
41	Pull	L	60	0	6,626	0	n.d.	a	10
42	Push	L	10	0	6,626	0	"	a	25
43	Pull	L	40	0	5,890	168	"	a	a
44	Push	L	20	0	6,626	- 504	"	a	a
45	Pull	L	40	0	5,890	0	"	-	a
46	Push	L	20	0	6,626	504	"	-	a
47	Pull	L	60	0	5,153	672	"	-	a
48	Push	L	10	0	5,890	840	"	-	a
49	Pull	L	30	0	5,890	168	"	-	a
50	Push	L	30	0	6,626	840	"	-	a
51	Pull	L	30	0	6,626	0	"	-	a
52	Push	L	10	11	6,626	672	"	-	a
53	Pull	L	10	15	6,626	504	"	-	a
54	Push	L	40	11	6,626	504	"	-	a
54A	Pull	L	40	11	5,890	- 168	"	a	a
54B	Push	L	20	13	6,626	336	"	a	a
54C	Pull	L	40	13	6,626	336	"	a	a
55	Pull	L	40	13	6,626	85	"	a	a
56	Pull	L	40	13	6,626	0	"	a	a
57	Push	L	10	6	7,362	252	"	a	a
58	Pull	L	40	13	n.d.	n.d.	"	a	a

Letters (A,B,C) after Run Number designate non-scheduled tests for which data was taken.

N.D. indicates that no data was taken. For Side loads, strain gages were inoperative for Runs 27-58.

A dash (-) indicates that temperature data existed, but was unintelligible.

A star (*) indicates that the temperature recorder went off scale. The recorded value is therefore less than the actual temperature.

All temperature readings are in °F above ambient. Ambient for all tests ranged from 26 to 32°F. The designation "a" means that no temperature rise occurred as the wheel passed, thus the wheel temperature was the same as ambient.

Horizontal traction forces are negative; braking forces are positive.

TABLE E-14
Field Test Data for Car IV
Empty Gondola USAF-42016
Truck A Axle 3
Actual Truck Weight = 24,520

Run	Orien-tation	Wheel Side	Train Speed (mph)	Brake Red'n (psi)	Vertical Load (lb)	Horzntl Load (lb)	Side Load (mv)	Near Side Temp (°F)	Far Side Temp (°F)	Wheel Temp (°F)
1	Pull	R	5	0	5,890	- 336	1000	a	a	
2	Push	R	4	0	5,890	840	1200	a	a	
3	Pull	R	5	0	6,626	- 336	1000	a	a	
4	Push	R	5	0	5,890	672	1200	a	a	
5	Pull	R	10	0	6,626	- 336	1200	a	a	
6	Push	R	10	0	6,626	504	1000	a	a	
7	Pull	R	20	0	5,890	- 336	1000	a	a	
8	Push	R	20	0	6,626	336	1400	a	a	
9	Pull	R	40	0	5,153	336	n.d.	a	a	
10	Push	R	40	0	7,362	336	1200	a	a	
11	Pull	R	60	0	5,153	- 504	0	a	a	
12	Push	R	60	0	6,626	672	800	a	a	(35)
13	Pull	R	10	6	6,626	- 840	800	a	a	
14	Push	R	10	11	6,626	336	800	14	a	
15	Pull	R	10	15	6,626	- 504	1000	a	a	(35)
16	Push	R	20	6	6,626	168	800	14	a	
17	Pull	R	20	11	6,626	- 504	800	a	a	
18	Push	R	20	15	6,626	504	1200	a	10	(50)
19	Pull	R	40	6	5,153	168	1500	a	a	
20	Push	R	40	11	n.d.	n.d.	n.d.	n.d.	a	
21	Pull	R	40	15	6,626	- 168	- 600	a	50	
22	Push	R	60	6	6,626	336	1000	a	25	
23	Pull	R	60	11	5,890	672	-1800	-	25	(80)
24	Pull	R	60	15	5,890	1008	0	-	a	
25	Pull	L	10	0	5,890	- 504	1000	a	a	
26	Push	L	20	0	5,890	0	800	a	a	
27	Pull	L	40	0	5,890	0	n.d.	a	a	(80)
27A	Push	L	20	0	6,626	0	"	a	a	
28	Pull	L	60	0	5,153	0	"	a	-	
28A	Push	L	30	0	5,890	336	"	-	a	
29	Pull	L	10	11	5,890	- 840	"	-	30	
30	Push	L	20	11	7,362	504	"	a	80	
31	Pull	L	40	11	6,626	- 504	"	a	30	
32	Pull	L	60	11	5,153	0	"	a	20	
33	Pull	L	10	11	5,890	- 672	"	27	60	
34	Push	L	20	11	5,890	336	"	54	100	
35	Pull	L	40	11	5,153	- 504	"	-	100	
36	Pull	L	60	11	4,417	- 168	"	14	50	

TABLE E-14 (Cont'd)

Field Test Data for Car IV
Empty Gondola USAF-42016
Truck A Axle 3
Actual Truck Weight = 24,520

Run	Orien-tation	Wheel Side	Train Speed (mph)	Brake Red'n (psi)	Vertical Load (lb)	Horzntl Load (lb)	Side Load (mv)	Near Side Temp (°F)	Far Side Temp (°F)
41	Pull	L	60	0	5,890	- 168	n.d.	a	10
42	Push	L	10	0	6,626	0	"	a	25
43	Pull	L	40	0	6,626	0	"	a	a
44	Push	L	20	0	8,098	- 168	"	a	a
45	Pull	L	40	0	5,890	0	"	-	a
46	Push	L	20	0	6,626	672	"	-	a
47	Pull	L	60	0	5,153	840	"	-	a
48	Push	L	10	0	5,890	- 336	"	-	a
49	Pull	L	30	0	5,153	168	"	-	a
50	Push	L	30	0	5,890	0	"	-	a
51	Pull	L	30	0	6,626	168	"	-	a
52	Push	L	10	11	6,626	540	"	-	a
53	Pull	L	10	15	6,626	336	"	-	a
54	Push	L	40	11	6,626	- 168	"	-	a
54A	Pull	L	40	11	6,626	0	"	a	a
54B	Push	L	20	13	6,626	504	"	a	a
54C	Pull	L	40	13	5,890	0	"	a	a
55	Pull	L	40	13	5,890	0	"	a	a
56	Pull	L	40	13	5,890	- 85	"	a	a
57	Push	L	10	6	6,626	- 85	"	a	a
58	Pull	L	40	13	n.d.	n.d.	"	a	a

Letters (A,B,C) after Run Number designate non-scheduled tests for which data was taken.

N.D. indicates that no data was taken. For Side loads, strain gages were inoperative for Runs 27-58.

A dash (-) indicates that temperature data existed, but was unintelligible.

A star (*) indicates that the temperature recorder went off scale. The recorded value is therefore less than the actual temperature.

All temperature readings are in °F above ambient. Ambient for all tests ranged from 26 to 32°F. The designation "a" means that no temperature rise occurred as the wheel passed, thus the wheel temperature was the same as ambient.

Horizontal traction forces are negative; braking forces are positive.

TABLE E-15
Field Test Data for Car IV
Empty Gondola USAF-42016
Truck B Axle 2
Actual Truck Weight = 24,780

Run	Orien-tation	Wheel Side	Train Speed (mph)	Brake Red'n (psi)	Vertical Load (lb)	Horzntl Load (lb)	Side Load (mv)	Near Side Temp (°F)	Far Side Temp (°F)	Wheel Temp (°F)
1	Pull	R	5	0	5,890	672	1000	a	a	
2	Push	R	4	0	6,626	0	1200	a	a	
3	Pull	R	5	0	5,890	504	1000	a	a	
4	Push	R	5	0	5,890	0	1000	a	a	
5	Pull	R	10	0	6,626	504	800	a	a	
6	Push	R	10	0	5,890	168	1000	a	a	
7	Pull	R	20	0	5,890	504	1400	a	a	
8	Push	R	20	0	6,626	336	1400	a	a	
9	Pull	R	40	0	5,890	672	n.d.	a	a	
10	Push	R	40	0	5,153	- 504	600	a	a	
11	Pull	R	60	0	5,890	504	0	a	a	
12	Push	R	60	0	n.d.	n.d.	n.d.	n.d.	n.d.	
13	Pull	R	10	6	5,890	504	1000	a	a	
14	Push	R	10	11	6,626	0	800	14	a	
15	Pull	R	10	15	5,890	168	1000	34	a	(40)
16	Push	R	20	6	6,626	336	800	a	a	
17	Pull	R	20	11	6,626	672	800	a	a	
18	Push	R	20	15	6,626	504	1000	a	10	(40)
19	Pull	R	40	6	5,153	0	1000	a	a	
20	Push	R	40	11	n.d.	n.d.	n.d.	n.d.	a	
21	Pull	R	40	15	4,417	840	1000	a	200	
22	Push	R	60	6	6,626	0	1400	a	a	
23	Pull	R	60	11	4,417	- 504	1800	-	13	(80)
24	Pull	R	60	15	5,153	1008	0	-	a	
25	Pull	L	10	0	5,890	840	0	a	a	
26	Push	L	20	0	5,890	- 336	1000	a	a	
27	Pull	L	40	0	5,153	0	n.d.	a	a	(65)
27A	Push	L	20	0	n.d.	n.d.	"	a	a	
28	Pull	L	60	0	6,626	840	"	a	-	
28A	Push	L	30	0	5,890	0	"	-	a	
29	Pull	L	10	11	7,362	1512	"	-	50	
30	Push	L	20	11	5,890	168	"	a	40	
31	Pull	L	40	11	7,362	672	"	a	30	
32	Pull	L	60	11	7,362	840	"	a	20	
33	Pull	L	10	11	6,626	1176	"	68	60	
34	Push	L	20	11	6,626	0	"	82	125	
35	Pull	L	40	11	6,626	672	"	14	75	
36	Pull	L	60	11	6,626	1008	"	a	50	

TABLE E-15 (Cont'd)
Field Test Data for Car IV
Empty Gondola USAF-42016
Truck B Axle 2
Actual Truck Weight = 24,780

Run	Orien-tation	Wheel Side	Train Speed (mph)	Brake Red'n (psi)	Vertical Load (lb)	Horzntl Load (lb)	Side Load (mv)	Near Side Temp (°F)	Far Side Temp (°F)
41	Pull	L	60	0	6,626	504	n.d.	a	10
42	Push	L	10	0	6,626	0	"	a	25
43	Pull	L	40	0	6,626	672	"	a	a
44	Push	L	20	0	5,890	0	"	a	a
45	Pull	L	40	0	5,153	168	"	-	a
46	Push	L	20	0	6,626	672	"	-	a
47	Pull	L	60	0	5,153	336	"	-	a
48	Push	L	10	0	7,362	840	"	-	a
49	Pull	L	30	0	5,153	0	"	-	a
50	Push	L	30	0	7,362	840	"	-	a
51	Pull	L	30	0	6,626	0	"	-	a
52	Push	L	10	11	6,626	1008	"	-	a
53	Pull	L	10	15	5,890	672	"	-	a
54	Push	L	40	11	6,626	504	"	-	a
54A	Pull	L	40	11	5,890	336	"	a	a
54B	Push	L	20	13	5,890	672	"	a	a
54C	Pull	L	40	13	6,626	0	"	a	a
55	Pull	L	40	13	5,890	0	"	a	a
56	Pull	L	40	13	6,626	0	"	a	a
57	Push	L	10	6	6,626	252	"	a	a
58	Pull	L	40	13	6,626	168	"	a	a

Letters (A,B,C) after Run Number designate non-scheduled tests for which data was taken.

N.D. indicates that no data was taken. For Side loads, strain gages were inoperative for Runs 27-58.

A dash (-) indicates that temperature data existed, but was unintelligible.

A star (*) indicates that the temperature recorder went off scale. The recorded value is therefore less than the actual temperature.

All temperature readings are in °F above ambient. Ambient for all tests ranged from 26 to 32°F. The designation "a" means that no temperature rise occurred as the wheel passed, thus the wheel temperature was the same as ambient.

Horizontal traction forces are negative; braking forces are positive.

TABLE E-16
Field Test Data for Car IV
Empty Gondola USAF-42016
Truck B Axle 1
Actual Truck Weight = 24, 780

Run	Orien-tation	Wheel Side	Train Speed (mph)	Brake Red'n (psi)	Vertical Load (lb)	Horzntl Load (lb)	Side Load (mv)	Near Side Temp (°F)	Far Side Temp (°F)	Wheel Temp (°F)
1	Pull	R	5	0	6,626	- 336	1000	a	a	
2	Push	R	4	0	5,890	336	1200	a	a	
3	Pull	R	5	0	5,890	- 336	1000	a	a	
4	Push	R	5	0	5,890	504	1000	a	a	
5	Pull	R	10	0	6,626	- 336	800	a	a	
6	Push	R	10	0	5,890	504	1000	a	a	
7	Pull	R	20	0	5,153	- 168	1400	a	a	
8	Push	R	20	0	6,626	336	1400	a	a	
9	Pull	R	40	0	5,153	336	n.d.	a	a	
10	Push	R	40	0	6,626	168	600	a	a	
11	Pull	R	60	0	5,890	- 840	2500	a	a	
12	Push	R	60	0	n.d.	n.d.	n.d.	n.d.	n.d.	
13	Pull	R	10	6	5,890	- 504	1000	a	a	
14	Push	R	10	11	6,626	504	800	14	a	
15	Pull	R	10	15	6,626	- 336	1000	21	a	(35)
16	Push	R	20	6	6,626	504	600	a	a	
17	Pull	R	20	11	6,626	- 504	800	a	a	
18	Push	R	20	15	5,890	168	1400	a	10	(40)
19	Pull	R	40	6	5,153	0	2400	a	a	
20	Push	R	40	11	n.d.	n.d.	n.d.	n.d.	a	
21	Pull	R	40	15	5,890	1512	- 200	a	a	
22	Push	R	60	6	6,626	336	600	a	a	
23	Pull	R	60	11	6,626	1008	-2600	"	13	(60)
24	Pull	R	60	15	5,153	1344	- 800	-	a	
25	Pull	L	10	0	5,890	- 504	1500	a	a	
26	Push	L	20	0	5,890	504	600	a	a	
27	Pull	L	40	0	5,890	0	n.d.	a	a	(65)
27A	Push	L	20	0	n.d.	n.d.	"	a	a	
28	Pull	L	60	0	5,890	- 168	"	a	-	
28A	Push	L	30	0	6,626	168	"	-	a	
29	Pull	L	10	11	5,890	- 504	"	-	20	
30	Push	L	20	11	7,362	840	"	a	100	
31	Pull	L	40	11	5,890	- 672	"	a	20	
32	Pull	L	60	11	5,153	- 504	"	a	10	
33	Pull	L	10	11	5,890	- 504	"	27	60	
34	Push	L	20	11	6,626	1008	"	54	100	
35	Pull	L	40	11	5,890	- 672	"	a	75	
36	Pull	L	60	11	5,153	-1008	"	14	50	

TABLE E-16 (Cont'd)

Field Test Data for Car IV

Empty Gondola USAF-42016

Truck B Axle 1

Actual Truck Weight = 24, 780

Run	Orien-tation	Wheel Side	Train Speed (mph)	Brake Red'n (psi)	Vertical Load (lb)	Horzntl Load (lb)	Side Load (mv)	Near Side Temp (°F)	Far Side Temp (°F)
41	Pull	L	60	0	5,890	840	n.d.	a	10
42	Push	L	10	0	5,890	504	"	a	25
43	Pull	L	40	0	5,890	0	"	a	a
44	Push	L	20	0	6,626	0	"	a	a
45	Pull	L	40	0	6,626	1008	"	-	a
46	Push	L	20	0	6,626	336	"	-	a
47	Pull	L	60	0	7,362	840	"	-	a
48	Push	L	10	0	7,362	- 336	"	-	a
49	Pull	L	30	0	5,890	840	"	-	a
50	Push	L	30	0	6,626	- 504	"	-	a
51	Pull	L	30	0	7,362	168	"	-	a
52	Push	L	10	11	6,626	168	"	-	a
53	Pull	L	10	15	6,626	840	"	-	a
54	Push	L	40	11	6,626	- 168	"	-	a
54A	Pull	L	40	11	5,890	504	"	a	a
54B	Push	L	20	13	6,626	504	"	a	a
54C	Pull	L	40	13	5,890	168	"	a	a
55	Pull	L	40	13	5,153	336	"	a	a
56	Pull	L	40	13	6,626	0	"	a	a
57	Push	L	10	6	6,626	- 85	"	a	a
58	Pull	L	40	13	5,890	420	"	a	a

Letters (A,B,C) after Run Number designate non-scheduled tests for which data was taken.

N.D. indicates that no data was taken. For Side loads, strain gages were inoperative for Runs 27-58.

A dash (-) indicates that temperature data existed, but was unintelligible.

A star (*) indicates that the temperature recorder went off scale. The recorded value is therefore less than the actual temperature.

All temperature readings are in °F above ambient. Ambient for all tests ranged from 26 to 32°F. The designation "a" means that no temperature rise occurred as the wheel passed, thus the wheel temperature was the same as ambient.

Horizontal traction forces are negative; braking forces are positive.

APPENDIX F

DEFINITION OF AN IMPROVED SYSTEM FOR DETECTION AND IDENTIFICATION OF FAULTS IN RAILCAR BRAKING SYSTEMS

1. INTRODUCTION

A project is currently being conducted whose principal objective is the first phase development of equipment and methods for detecting malfunctioning brakes on moving railcars. The major components of this system include infrared detectors for sensing wheel temperatures, and rail mounted transducers for measuring the weight and braking reaction in each wheel passing through the test section. This initial project will carry development of the system through preliminary hardware design and fabrication, installation of equipment at the Pueblo test site, execution of a field test program and a review of data obtained to determine what correlations exist between recorded data and specific malfunctions. The purpose of this report is to present an outline of what additional development work is required as the next logical steps in bringing the system to a functional prototype stage.

After the completion of the first phase of the project, it is anticipated that work will continue along three major paths. The first of these will carry hardware development to the point where the various sensors can be specified, replicated and operated in the field with confidence that they will perform as required. The second major area of effort will involve development of a data processor section capable of accepting outputs from the track-side sensors and from them generating brake malfunction reports. The third major activity will provide one complete prototype system suitable for installation at Pueblo. In the following sections, the tasks and costs associated with these primary areas will be identified.

2. SENSOR DEVELOPMENT

2.1 Wheel Temperature Measurement Subsystem

The function performed by this section is to provide a measurement of wheel heating caused by the application of the brakes. This is accomplished by infrared detectors focused on the wheel rim areas that sense the radiation given off by each passing wheel. Relative braking effectiveness is expected to show corresponding changes in energy absorbed by the wheels, which should in turn be reflected in measurable wheel temperatures. During the initial phase of this project, these basic assumptions will be tested.

In later project stage, it will be necessary to carry the development forward with the following tasks.

. Stability and Calibration

Provide for extended, accurate field operations by refinement, redesign as may be required, and testing of the selected IR system. The objectives of this task will be to assure that the equipment supplied will dependably fulfill the required transducing function under the expected ambient conditions during extended periods of operation. Procedures to allow for efficient on-site functional testing, calibration and replacement of the instrument should be provided.

. Installation Development

Prepare designs for mounting hardware that will allow rapid installation of the detector assemblies. The results of this effort will provide a set of equipment that is fully compatible with the established requirements for equipment to be used in railroad environments.

. Interface Compatibility

Develop output line drivers capable of providing a 0 to +10V, 20 ma signal source. This capability will enable the physical separation of sensors from the data processing components.

. Refinement of the Thermal Fault Detection Algorithm

Perform analyses needed to relate measured thermal data with faults in the braking components. This effort may involve extensive testing and interative modification of the correlation algorithm.

2.2 Car Counting Subsystem

The car counting subsystem utilizes an interrupted light beam photodetector to sense the beginning and end of each car. The major task requirement for this element will be to provide a total physical package that allows the functional circuits and support elements to be installed in a manner that is fully compatible with railway equipment requirements.

2.3 Reaction Rail Subsystem

The reaction rail subsystem includes a specially configured length of rail consisting of a flexural support equipped with strain sensors that provide electrical outputs corresponding to wheel weight and to the reaction force in the direction parallel to the direction of train motion. The present design has been executed with few compromises. Nevertheless, some evolutionary modifications and tests may be desirable including the following:

- Installation Development

  Redesign of the mounting attachment provisions to allow for "drop in" installation.

- Improved Data Capture

  Investigate optimizing the length of the instrumented section. This may prove useful in obtaining a longer period of time in which to collect data.

- Calibration Unit

  Construct a test for use in periodically recalibrating the vertical and horizontal load sensing elements.

- Fabrication and Test of Improved Section

  Based on earlier results, fabricate, install and test a revised reaction rail. The tests should include evaluations of rail end battering, moisture/freezing effects and verification of accuracy with time and rail usage. Tests will also be required to verify continued structural integrity of the section. This may involve the use of X-rays, ultrasonics and magnaflux techniques.

- Refinement of the Reaction Fault Detection Algorithm

  Perform analyses needed to relate reaction and wheel weight measurement data to faults in the car's braking components. This effort may involve extensive testing and interative modification of the correlation algorithm.

3. SIGNAL PROCESSING

In the initial phase of the project, data reduction and interpretation were being accomplished by manual methods. An improved and more intensively used version of the system will generate such vast amounts of data that manual methods may cause excessive delays and expenditures of manpower. For this reason, it will be essential to have some means for automatically interpreting the data and presenting it in a format that will be timely and informative. In order to accomplish this, the additional system elements shown below will be required. In presenting this summary, only a qualitative identification of system components will be given since it is beyond the scope of this preliminary definition effort to design and specify in detail the hardware and software elements needed for actual implementation.

- Input Interface

  Design and fabricate line receivers to terminate incoming data lines from the drivers located at each remote sensor location. These elements provide the proper data processing bus impedance match in addition to filtering out higher frequency signals that may be picked up as noise. The system should be configured to accept up to ten analog and two digital inputs. This capacity will accomodate two reaction rail sections (4 analog inputs), four IR sensors (analog), one car counter (digital), plus two spare analog and one spare digital inputs for system growth and ancillary functions. This latter category may include inputs for train speed, ambient temperature or other system variables.

- Data Processing Hardware

  Provide a data processing hardware consisting of a real time clock and an analog to digital converter. An appropriate system will include 4K of core memory, 4K of semiconductor memory, a floppy disc for program development and a hard copy terminal. This equipment is to be used to accept raw signal data originating in the various sensors, digitize it, perform defined mathematical operations and print the results on a hard copy printer.

. System Software

Prepare a complete operating software package that will convert raw signal data into printed output identifying suspected brake component problems. This effort will involve creating an algorithm capable of performing the required correlations and presenting the results in a meaningful printed format.

4. FABRICATION AND TEST OF PROTOTYPE SYSTEM

Following the development of the items identified above, it will be necessary to fabricate, install and test one complete prototype system. This effort will have as its prime objective, verification of the basic diagnostic principles in a hardware/software form suitable for later wide scale field usage. Specific tasks to be accomplished include the following:

. Hardware Fabrication

Fabricate one complete rail brake diagnostic system consisting of infrared wheel temperature detectors, car counter, reaction rail section, interconnecting cables and data processing section.

. Installation

Install one prototype system at Pueblo and operate it in conjunction with railcars having known problems in their braking systems.

. Test Plan

Develop test plans for the site.

. Test Program

Conduct test programs and refine hardware and software portions of the system as may be indicated by the test results.

. Documentation

Prepare complete project report and documentation of all hardware developed.

APPENDIX G

SPECIFICATIONS FOR THE INSTRUMENTED RAIL

1. GENERAL CONFIGURATION

The general configuration at the un-mounted reaction rail is shown in the photograph of Figure 9. Figure A-1 (See Appendix A) shows the actual dimensions of several of the important rail features.

The reaction rail segment consists of a single, 18-inch (45.7 cm) mass of 4340 chromium-molybdenum steel, machined in an annealed state to the configuration and dimensions described above. The two vertical flexures are thus an integral part of the rail cap section and the base member. The flexure surfaces were polished to remove all surface irregularities from which fatigue cracks might originate.

The rail segment assembly was heat treated to a minimum ultimate tensile strength of 150,000 lbs/in^2 (10,545 Kg/cm^2). The reaction rail without associated joint bars weighs approximately 88 lbs. (40 Kg.).

2. MATERIAL

The rail material is AISI 4340 chromium molybdenum steel heat treated to greater than 150,000 lbs/in^2 (10,545 Kg/cm^2) Ultimate tensile strength and Rockwell Hardness of C37.

Properties of AISI 4340 in general are:

Density:	0.283 lbs/in^3 (7.8 gms/cc)
Tensile Strength: (Range depends on heat treat)	142,000-284,000 lbs/in^2 (9997-19,994 Kg/cm^2)
Yield Strength:	130,000-228,000 lbs/in^2 (9152-16,051 Kg/cm^2)
Hardness:	Rockwell C-19 to C-39

Based on measured hardness, the following properties are estimated for the reaction rail steel in its heat treated condition:

Tensile Strength:	268,000 lbs/in^2 (18,870 Kg/cm^2)
Yield Strength:	218,000 lbs/in^2 (15,350 Kg/cm^2)

3. TRANSDUCER BOLT

The transducer bolt is designed to facilitate insertion of the rail displacement transducers (Linear Variable Differential Transformers) into the instrumented rail section as it is installed in a parent rail.

Two type 010 MHR miniature LVDTs with the following characteristics were used:

Input Voltage:	3 V. rms
Frequency Range:	400 - 20,000 Hz
Temperature Range:	-65° F to +300° F (-54° C to 149° C)
Wall Voltage:	Less than 0.5% of full scale output
Shock Survival:	1000g for 11msec.
Vibration Tolerance:	20g up to 2 KHz
Input Impedance: (5,000 Hz excitation)	120 Ω
Output Impedance: (5,000 Hz excitation)	275 Ω
Sensitivity:	4.2 mv/0,001 in/v. input
Linearity @ 100% f.s.	.25%
Weight:	3.2 grams
Length:	0.54 inches (13.7 mm)

4. LVDT SIGNAL CONDITIONER

The LVDT signal conditioners used were self-contained power supply and conditioner made for use with the 010 MHR LVDT.

The CAS-050 Specifications follow:

Power Requirements:	115 VAC + 10% 50/400 Hz
Line Voltage Regulation:	± 10% line fluctuation results in less than ± 0.1% change in output
Transducer Excitation Voltage:	2 to 5 V rms (Internally adjustable)
Transducer Excitation Frequency:	5,000 Hz
Frequency Response	-3 db at 500 Hz
Noise and Ripple	15 mv rms max.
Impedance into Conditioner:	100,000 Ω
Stability:	± .05%
Non-linearity and Hysteresis:	.05% f.s. max.
Thermal Sensitivity:	.02%/ F max.
Dimensions:	
Length	13.5 inches (34 cm)
Width	2.0 inches (5 cm)
Height	4.0 inches (10 cm)
Output:	±10 VDC @ 20 ma. max.
Output Impedance:	100Ω max.
Operating Temperature:	0° F to 130° F
Weight:	3 lbs, 4 oz.

5. RECORDER

LVDT outputs were recorded on two channels of a six-channel general purpose recorder. Specifications for the recorder were:

Frequency Response	Flat within 2% to 40 Hz. 3 db down at 125 Hz
Measurement Range:	1 mV per chart division to 500 V dc full scale
Attenuator Steps:	1, 2, 5, 10, 20, 50, 100, 200, 500 mV/div. 1, 2, 5, 10 V/div.
Max. Input Voltage:	500 VDC
Input Impedance:	10 meg ohms
In Phase Rejection:	60 dB @ 60 Hz
Chart Speeds:	1, 5, 25, 125 mm/sec 1, 5, 25, 125 mm/min
Power Requirement	115 VAC $\pm$ 10% 60 Hz, 250 W
Dimensions:	
Width	17.5 inches (44.5 cm)
Height	16.9 inches (42.9 cm)
Depth	11.3 inches (28.7 cm)
Weight:	65 lbs (29.5 Kg)

6. REACTION RAIL SYSTEM - OPERATIONAL LIMITS

Maximum Weight per wheel	40,000 lbs 16,160 Kg)
Installed Clearance with parent rail	0.060 inches (15.2 mm)

APPENDIX H

SPECIFICATIONS FOR THE INFRARED SENSOR

1. GENERAL

The infrared sensor used in the wayside brake inspection system was custom built from components. Figures 12 and 13 show the sensor disassembled and assembled respectively. The sensor consists basically of the following components:

1. Indium Antimonide Detector and supporting structure
2. Detector Amplifier
3. Cassagrain reflective lens and supporting spider
4. Inner and outer protective cylinders
5. Irtran IR transmission lens.

2. INDIUM ANTIMONIDE DETECTOR

An indium antimonide detector was used for the IR sensor. The device is packaged in a modified, square, semiconductor flatpack measuring .267 in. (6.8 mm) on a side and .078 in. (2.0 mm) thick. The radiation sensitive area on the device is also square and measures .078 in. (2.0 mm) on a side with a field of view of 120°in each dimension.

Typical characteristics of the device at 72° F(20° C) are:

Wavelength at maximum response:	5.0 to 7.0 μm
Spectral response:	visible to 7.5 μm
Cell resistance:	650 Ω
Time constant:	0.1 μs

Responsivity (6.0 m):	5.0 V/W
Operating temperature:	-55° F to + 70° F (-48° C to -21° C)
Maximum bias current	25 mA
D^* (6.0 m)	15 cm ($Hz^{-1/2}$ / W)

Figure B-2 shows the spectral response curve for the detector. Figures B-3 and B-4 show the InSb detector relative responsivity as a function of applied detector bias current, for the short circuit and open circuit conditions respectively. Relative responsivity is the ratio of detector output (volts) to radiation input (watts). Maximum detector bias current is 25 mA.

3. OPTICS

The optics chosen for this system consist of a three inch Cassagrain lens system made from reflective plastic coupled through an infrared transmission lens of Irtran (Polycrystalline zinc sulfide).

Cassagrain Lens:

Focal length	36 inches (91 cm)
Target size:	1.5 inch diameter (3.8 cm)

Irtran Transmission Lens:

Material:	Irtran 2 (ZnS)
Diameter:	3.25 inches (8.2 cm)
Thickness:	0.039 inches (1 mm)
Transmission Losses:	<10% over range 4 to 9 microns

Density:	4.09 gms/cc.
Index of Refraction:	2.22
Harness, Knoop:	355
Modulus of Elasticity:	14×10^6 lbs/in (1×10^6 Kg/cm^2)

4. DETECTOR AMPLIFIER

The vendor supplied amplifier could not be made functional, so a detector amplifier was custom-built for use with the InSb detector. Figure 11 is a circuit diagram of the amplifier.

The amplifier exhibited the following operational characteristics:

Sensitivity:	0.2 v
Gain:	20,000
Bandwidth:	2 Hz to 30 Hz
Dynamic input sensing range:	0.2 μV to 10 mV
Temperature sensing range: (above ambient)	30° F to 1,000° F (-1.1° C to 538° C)
Operating temperature:	32° F to 158° F (0° C to 70° C)

5. SENSOR HOUSING

The packaging of this unit consists of an aluminum tube 3 1/4 in. (8.2 cm) diameter and 15 in. (38.1 cm) long. One end is fitted with a protective bezel for holding the Irtran window, and the other end has a plate housing two connectors. One connector is provided for input power and another for output signals. Internal to this tube is the reflective Cassagrain lens and amplifier board. The detector is mounted at the focal point of the lens and signal wires are brought out through an appropriate strain relief.

This aluminum tube is suspended in a larger tube 5 in. (12.7 cm) diameter of cast steel which acts as an impact shield for the more delicate aluminum assembly. One end of this cast steel tube is fitted with a muffin fan that provides 35 CFM of air for cooling, while the other end is open for viewing (see Figures 12 and 13).

6. RECORDER

The d.c. voltage output of the detector amplifier was fed directly into the Gould six channel recorded described in Appendix G, Section 5.0.

APPENDIX I

REPORT OF NEW TECHNOLOGY

The prototype wayside brake inspection system developed under this contract represents basically two new railway engineering concepts.

1. A single wheel reaction rail, capable of measuring dynamic wheel weight and braking force.

2. A brake system diagnostic analyzer comprised of one or two reaction rails and two remote infrared wheel temperature sensors.

A review of the literature (see References and Bibliography) indicates that devices similar to the reaction rail developed here have not been used for either weighing or for brake force analysis. There are complete truck weigh-in-motion scales which use strain gaged structural members to indicate vertical loads, but these devices are relatively large, complex installations. The reaction rail designed under this project offers the advantages of low component cost, low installation cost, and maintenance of structural integrity and continuity of the parent rail.

Wheel/rail interactions have been studied in the past by instrumenting the parent rail (strain gages); measuring rail deflections with respect to ground; and by measuring strain or deflections in supporting members (bridges). The general concept is not unlike that employed in design of the reaction rail, but these methods are not specifically designed to de-couple and sense vertical forces (weight) and horizontal forces (braking).

Unique features of the reaction rail design include:

1. Use of precisely designed flexures to result in a pre-determined horizontal deflection in response to a horizontal (braking) load component.

2. Use of a "transducer bolt" into which both the horizontal and vertical LVDTs are mounted and which can be inserted into and removed from the reaction rail after the rail is installed in the parent track.

It is the opinion of the designers that the reaction rail is in itself a patentable device, capable of being used for weighing-in-motion and/or horizontal reaction force measurement.

The infrared portion of the brake inspection system is not in itself a unique concept, since many companies manufacture and market remote temperature measuring devices and infrared sensors. Many are used in railway applications. It is believed, however, that the overall inspection system, of which the IR sensors are an integral part, is a unique and new measurement and diagnostic system.

Unique features of the overall system include:

1. Use of wheel temperatures to determine proportional right-to-left wheel braking on a single axle.

2. The ability to simultaneously weigh passing wheels, measure total braking forces, determine relative wheel temperatures, and identify and diagnose braking system malfunctions.

It is the opinion of the designers that the overall wayside inspection system is patentable and this patentability is currently under investigation.

In conclusion, it can be said that two new technologies have emerged from the current research:

1. Reaction Rail
2. Overall System

110 Copies